

Deciphering the role of *P. falciparum* Autophagy in Mechanisms of ER Homeostasis and Artemisinin Resistance

A thesis submitted for the degree of

DOCTOR OF PHILOSOPHY

by

ANANYA RAY



Molecular Biology and Genetics Unit

Jawaharlal Nehru Centre for Advanced Scientific Research

Bangalore- 560 064

February, 2022

To my mother

DECLARATION

I hereby declare that the matter embodied in the thesis entitled “**Deciphering the role of *P. falciparum* Autophagy in Mechanisms of ER Homeostasis and Artemisinin Resistance**” is the result of investigations carried out by me at the Molecular Biology and Genetics Unit, Jawaharlal Nehru Centre for Advanced Scientific Research, Bangalore, India under the supervision of Prof. Namita Surolia and that it has not been submitted elsewhere for the award of any degree or diploma.

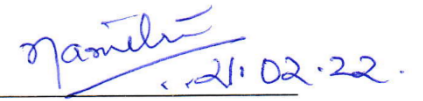
In keeping with the general practice in reporting scientific observations, due acknowledgement has been made whenever the work described is based on the findings of other investigators.



Ananya Ray

CERTIFICATE

I hereby declare that the matter embodied in the thesis entitled “**Deciphering the role of *P. falciparum* Autophagy in Mechanisms of ER Homeostasis and Artemisinin Resistance**” has been carried out by Ms. Ananya Ray at the Molecular Biology and Genetics Unit, Jawaharlal Nehru Centre for Advanced Scientific Research, Bangalore, India under my supervision and that it has not been submitted elsewhere for the award of any degree or diploma.



Prof. Namita Surolia
(Research Supervisor)

Acknowledgements

I would like to express my heartfelt gratitude to my supervisor Prof. Namita Surolia for giving me the opportunity to work in her laboratory and introducing me to the exciting field of molecular parasitology. While this has been a challenging project, she provided me with inspiration, encouragement, confidence, and unwavering support throughout the work and writing of this thesis. She has been incredibly supportive throughout the low points in my Ph.D., never allowing my spirits to sink. In addition, Prof. Surolia's enthusiasm for science motivates me and she has served as an excellent role model for me as a woman in science. I wish to express my heartfelt gratitude to her.

I would also like to acknowledge Prof. Avadhesha Surolia at IISc, under whom I worked for my master's dissertation and later as a project assistant. Those two years at IISc planted the seed for research in my mind and ultimately led me here. I will always be indebted to Avadhesha Sir for his encouraging, motivating, and captivating words about science.

I would like to thank Prof. Ranga Uday Kumar and Prof. James Chelliah, members of my GSAC committee, for their insightful suggestions and critical comments. My sincere thanks to former and present MBGU chairmen Prof. Anuranjan Anand, Prof. Ranga Uday Kumar and Prof. Maneesha Inamdar for providing excellent core departmental facilities. I would also like to acknowledge Prof. MRS Rao, Prof. Anand, Prof. Ranga, Prof. Inamdar, Prof. Tapas Kundu, Prof. Hemlatha Balaram, Prof. Kaustav Sanyal, Prof. Ravi Manjithaya, Prof. Chelliah, Dr. Kushagra Bansal and Dr. Sheeba Vasu for their course work and useful feedback during our annual work presentations. A special thanks to Prof. MRS Rao and Dr. Kushagra Bansal for reviewing our manuscript and providing their valuable comments. I owe my gratitude to Prof. Utpal Tatu (IISc) for his valuable suggestions during my comprehensive examination. I would also like to thank my collaborators, Dr. Krishanpal Karmodiy (IISER, Pune) and Dr. Ashalatha Mamidi (IISc) for extending their instant support and contribution to my work.

I am extremely grateful for the intra-mural financial assistance from JNCASR received towards my PhD. JNCASR's in-house facilities have been extremely beneficial to my work. I thank all the instrument in-charges and faculty in-charges for the smooth operation of the facility. I'd also like to thank Suma Ma'am and Kirthana for their assistance with confocal microscopy.

I have had the good fortune and pleasure of working alongside some extremely supportive colleagues. I sincerely acknowledge the help and support of my senior, Dr. Shiny, for her guidance and support during the initial years of my research. Dr. Palak, for being such an amazing person who has always been approachable and pleasant. A special thanks to Miti for her cooperation and help towards this research, as well as for being a compassionate friend. My warm thanks to Dr. Mayur, Ashvini, Akshaya, Satish, Thejaswita, Aniket, Shashwat, and Narmatha for helping me in my work and creating an amiable lab environment. A special thanks to Sudhakar bhaiya for excellent upkeep of the lab and ensuring that all reagents and equipment are available in time and within reach; without him our lab could not function.

A special thanks to my friends at JNCASR, Neha and Pallabi, for always being willing to talk about anything, supporting me in navigating this journey, and providing me with a plethora of good memories. I also would like to thank my friends outside JNCASR- Ekta, Deeksha, Heena, Meenakshi, Usha, Ria and Shreya for their unconditional love and support.

Words are inadequate to acknowledge my family for their enormous contribution and support towards my accomplishments. I am extremely grateful to Lakshay, for his unconditional support and encouragement throughout my Ph.D. He believed in me regardless of my self-doubts.

The biggest fortune of my life has to be my loving and wonderful parents. My mother, Manju Ray, has always been instrumental in instilling the concept of "nothing is impossible" in my young mind. She always kept giving, asking for nothing in return, like mothers do. My father, Gautam Ray, instilled in me a sense of the importance of righteousness and honesty in life. Despite our hardships, my parents ensured that I had a modest upbringing and my education was never compromised. My gratitude for these incredibly beautiful human beings will never be sufficient, but I want to express my heartiest thanks for the unconditional love and affection they have shown me throughout my life.

Synopsis

Malaria has been a scourge to the human civilization for centuries and remains a major health concern even today with 241 million new cases and 627,000 deaths documented in 2020 (WHO, 2021b). *Plasmodium falciparum* is the most virulent of all malaria causing parasites that infect humans. The asexual development of parasites within the red blood cells (RBCs) is associated with the manifestation of clinical symptoms and pathologies of malaria. Recovery from *P. falciparum* infection relies on the administration of effective anti-malarials, in particular, treatment with the frontline Artemisinin-based Combination Therapies (ACTs). ACT co-formulates the fast-acting artemisinin (ART)-based drugs with long-lasting anti-malarial partner drugs (sulfadoxine-pyrimethamine, mefloquine, lumefantrine, piperaquine, or amodiaquine) that effectively remove residual parasites (Aweeka and German, 2008; WHO, 2016; White et al., 2014). ART and its derivatives are highly potent and can rapidly induce a parasitocidal effect that eliminates all asexual parasite stages (Balint, 2001). Therefore, the ongoing malaria control programs and further eradication efforts depend heavily on the efficacy of ART.

ART is a sesquiterpene lactone that is naturally derived from the herb *Artemisia annua* (Sweet Wormwood). ART activation by heme derived from hemoglobin catabolism causes widespread damage to the parasite. Cleavage of the endoperoxide bond upon activation releases Reactive Oxygen Species (ROS), which further act promiscuously on protein targets, causing alkylation. This leads to the accumulation of misfolded proteins in the ER lumen, initiating ER stress (Bridgford *et al.*, 2018; Wang *et al.*, 2015; Xie *et al.*, 2020). In general, cells are equipped with multiple stress response pathways for processing misfolded proteins and regulating ER homeostasis. As the major site of protein synthesis and folding, ER plays an important role in maintaining cellular protein homeostasis. Accumulation of misfolded protein in the ER lumen stimulates the Unfolded Protein Response (UPR) signaling pathway (Schröder and Kaufman, 2005). UPR acts by increasing the ER's capacity to accommodate protein aggregates and facilitating their re-folding by initiating its transcriptional and translational stress sensors. Bioinformatic analyses indicate that *P. falciparum* lacks the transcriptional branch of UPR and therefore relies primarily upon the translational regulatory arm (Chaubey *et al.*, 2014; Gosline *et al.*, 2011). The latter acts by

reducing general protein translation and increasing the translation of proteins necessary for survival during stress. *P. falciparum* shows growth retardation and latency upon ART treatment, suggesting the participation of UPR translational arm in reducing protein synthesis. ART mediated ER stress, if remain unresolved, ultimately leads to parasite death (Bridgford *et al.*, 2018). Maintenance of the cellular proteome is thus essential for parasite viability.

Regardless of the efficacy of ART, emergence of ART resistant strains in the Greater Mekong Sub-region (GMS) of Southeast Asia has weakened the effectiveness of ACT (Ashley *et al.*, 2014; Noedl *et al.*, 2008). Reports of reduced susceptibility to the ACT regime are also appearing from Africa (Borrmann *et al.*, 2013). Interestingly, resistance to anti-malarials such as sulfadoxine, pyrimethamine, and chloroquine has also emerged from the Pailin Province of the GMS before spreading to malaria-endemic countries of Africa (Mita *et al.*, 2011; Roper *et al.*, 2004; Verdrager, 1986). Thus, ART resistance poses a serious concern for the emergence of multi-drug resistance in these regions and its spread to other malaria-endemic countries. Understanding the molecular mechanisms of ART resistance, therefore, is crucial for controlling the disease and for future development of novel anti-malarials.

Resistance manifests as decreased susceptibility to ART in *P. falciparum* carrying mutations in the β -propeller domain of the Kelch13 (*PfK13*) protein (Ariey *et al.*, 2014; Miotto *et al.*, 2015). The major *PfK13* variants identified in *P. falciparum* include C580Y, R539T, Y493H, I543T and N458Y; C580Y being prevalent in >50 % parasites across Southeast Asia (Anderson *et al.*, 2017; Ariey *et al.*, 2014; Imwong *et al.*, 2017; Siddiqui *et al.*, 2020). Further, background mutations in genes encoding coronin, atg18, ubp1, crt, mdr2, etc., are also reported to regulate the degree of ART resistance (Demas *et al.*, 2018; Henrici *et al.*, 2020; Miotto *et al.*, 2015; Wang *et al.*, 2016).

Recent studies investigating the role of *PfK13* C580Y mutation in ART resistance have proposed two mechanisms involving the ‘proteostasis pathways in the ER and cytoplasm’ (Bhattacharjee *et al.*, 2018; Suresh and Haldar, 2018) and the ‘reduced hemoglobin endocytosis’ (Birnbaum *et al.*, 2020). The first mechanism encompasses increased ER-phosphatidylinositol-3-phosphate (ER-PI3P) vesiculation, UPR, and the oxidative stress response pathway (Suresh and Haldar, 2018). As a predicted substrate adaptor for the E3 ligase, *PfK13* binds to and ubiquitinates phosphatidylinositol-3-kinase (*PfPI3K*),

facilitating its proteasomal degradation. The *PfK13* C580Y mutation prevents *PfPI3K* ubiquitination and degradation resulting in increased levels of *PfPI3K* and its product PI3P (Mbengue *et al.*, 2015). Elevation of PI3P increases ER-PI3P vesiculation and these vesicles are disseminated throughout the parasite and in the host RBC. Since the PI3P vesicles are enriched in proteins related to the UPR and oxidative stress response pathways, they are presumed to enhance the parasite's capacity to overcome damage from ART mediated protein alkylation and proteopathy (Bhattacharjee *et al.*, 2018). Thus, amplification of PI3P vesiculation is proposed to be a major determinant of ART resistance. Next, a link between the *PfK13* C580Y mutation and diminished hemoglobin endocytosis by the parasite proposes another mechanism for resistance (Birnbaum *et al.*, 2020). *PfK13* and its associated proteins participate in the parasite hemoglobin endocytosis pathway and thus can regulate hemoglobin uptake. The C580Y mutation reduces availability of heme derived from hemoglobin degradation at the ring stage, leading to dormancy and a consequent delay in progression to the trophozoite stage. Since ART is activated by iron derived from hemoglobin, the diminished availability of hemoglobin confers ART resistance (Birnbaum *et al.*, 2020).

Each of these pathways as well as PI3P vesiculation, can independently activate autophagy, a process involving degradation and recycling of part of the cytoplasm containing protein aggregates and damaged organelles (Mizushima, 2007). Cells utilize autophagy as a stress response pathway to restore cellular homeostasis (Ryter *et al.*, 2013). While various theories hypothesize the participation of parasite autophagy-like machinery in mechanisms of ART resistance (Haldar *et al.*, 2018; Suresh and Haldar, 2018), it has not yet been experimentally demonstrated. *P. falciparum* has a limited set of partially conserved autophagy-related (ATG) proteins encoded in its genome such as *PfATG1*, *PfATG18*, and the two ubiquitin-like conjugation systems *PfATG5-PfATG12* and *PfATG8-PE*. *PfATG8* and *PfATG18* are associated with apicoplast biogenesis and are also involved in the parasite autophagy-like pathway (Agrawal *et al.*, 2020; Bansal *et al.*, 2017; Joy *et al.*, 2018; Pang *et al.*, 2019; Tomlins *et al.*, 2013). As a member of the PROPPIN (β -propellers that bind polyphos-phoinositides) family, ATG18 binds to PI3P, which facilitates its localization to the autophagosomes (Dove *et al.*, 2004; Rieter *et al.*, 2013). Similar to its yeast counterpart, *PfATG18* also utilizes PI3P for its association with membranes for carrying out downstream functions (Bansal *et al.*, 2017). This is consistent with reports demonstrating that *PfATG18* participates in parasite autophagy-like pathway along with being trafficked

to the food vacuole (FV) through hemoglobin containing vesicles (HCv) in a PI3P dependent manner (Agrawal *et al.*, 2020). Also, a particular mutation in *Pf*ATG18, T38I, is strongly selected under ART resistance and confers fitness advantage to parasites by providing faster growth rates under nutrient limited conditions (Breglio *et al.*, 2018; Wang *et al.*, 2016). With this backdrop, the study presented in this thesis attempts to decipher the role of parasite autophagy in the two proposed mechanisms underlying ART resistance.

Chapter 1 provides a review of the literature relevant to the present thesis. Following a brief overview of malaria, the chapter introduces the pressing problem of ART resistance in *P. falciparum* that has threatened global malaria elimination. The mechanism of ART activation leading to increased ER stress response and proteotoxicity mediated parasite death are highlighted. Following this, a detailed description of the two proposed mechanisms of ART resistance involving the ‘proteostasis pathways in the ER and cytoplasm’ mitigating ART mediated proteopathy and the ‘reduced hemoglobin endocytosis pathway’ mediating decreased ART activation are presented. A link between *Pf*K13 C580Y mutation and increased PI3P vesicles, UPR and oxidative stress response pathways is elaborated with emphasis on the amplification of ER-PI3P vesiculation as the key mediator of resistance. As various theories have hypothesized the involvement of parasite autophagy in mediating ART resistance, an overview of the general autophagy process is presented. Several stages in the autophagy pathway in eukaryotes that require the coordinated activity of various ATG proteins are discussed. Finally, the partially conserved autophagy process in early-divergent eukaryotes, in particular, *Plasmodium* is summarized, highlighting the known roles of a few key parasite ATG proteins.

Chapter 2 describes the materials and methods used in the study. Materials such as chemical reagents, small molecule inhibitors, antibodies, strains, plasmids and primers are listed. Experimental methodologies for *in vitro* *P. falciparum* culturing of the wildtype 3D7, ART resistant K13^{C580Y} and isogenic K13^{WT} strains, growth-inhibition assays, cloning, transformation in *S. cerevisiae* and generation of transgenic parasite line are elaborated. This chapter also includes details of live cell imaging using various markers such as ER-Tracker, Mito-Tracker, and GFP as well as the analytical methods such as quantitative Real-time PCR, Immunofluorescence and Western blot.

Chapter 3 encompasses the results obtained in this study and is divided into two parts. The first part elucidates the crosstalk between ER stress, UPR and autophagy-like pathway in

P. falciparum. To determine activation of the UPR signaling pathway upon ER stress, parasites were treated with dihydroartemisinin (DHA), an active ART metabolite. DHA exposure was found to elicit expansion of the parasite ER as well as induction of the UPR translational stress sensors, consistent with previous reports showing DHA mediated ER stress responses (Bridgford *et al.*, 2018). To understand the involvement of autophagy-like pathway in *P. falciparum* during ER stress, quantification of the number of autophagosome-like structures as well as relative expression levels of two key parasite ATG proteins, *PfATG8* and *PfATG18*, were analysed. Compared to control parasites, the number of *PfATG8* (the autophagosome marker) labelled puncta denoting autophagosome-like structures and the expression levels of *PfATG8* and *PfATG18* protein increases in the parasites exposed to DHA. Additionally, the impairment of autophagy activation upon treatment with the mammalian PERK inhibitor GSK2606414, which specifically blocks UPR/PERK activation, confirms the observed increase in expression levels of autophagy proteins upon DHA exposure is directly mediated through UPR. Altogether, this study establishes parasite autophagy as an ER stress response pathway in *P. falciparum* triggered upon UPR activation (Ray *et al.*, 2022, mBio).

To further expand our understanding of how ER stress stimulates parasite autophagy, it is essential to explore protein complexes involved in initiating autophagy. The yeast/human protein ATG1/ULK1 is a kinase which initiates autophagy upon activation by recruiting other ATG proteins to the PAS (Mizushima, 2010). Thus, functional characterization of putative *PfATG1*, an ortholog of yeast ATG1, will provide mechanistic insights into processes that integrate ER stress response to autophagy in the malaria parasite. This work demonstrates that putative *PfATG1* expresses during all the blood stages of *P. falciparum* and is present as distinct cytoplasmic puncta which colocalize partially with *PfATG8*, the autophagy marker protein, and organelle such as ER, which serves as membrane source for autophagosome biogenesis (Shibutani and Yoshimori, 2014). A specific small molecule inhibitor of *HsULK1*, MRT68921 (Petherick *et al.*, 2015), inhibits parasite growth and decreases expression levels of autophagy proteins downstream of putative *PfATG1*. This study thus suggests the role of putative *PfATG1* as a canonical autophagy protein in *P. falciparum*.

The second part of Chapter 3 focuses on investigating the role of parasite autophagy in regulating the mechanisms of ART resistance. An ART resistant field isolate carrying the

C580Y mutation in *PfK13* ($K13^{C580Y}$) shows basal level increase in expression of *PfATG8* and *PfATG18*, both at the transcript and protein levels compared to its isogenic counterpart ($K13^{WT}$). Additionally, increase in the number of *PfATG18* labelled puncta colocalizing with *PfATG8* decorated autophagosome-like vesicles in the ART resistant parasites relative to its isogenic one indicates activation of the autophagy-like pathway in resistant parasites. The increased number of PI3P labelled puncta observed in the $K13^{C580Y}$ parasites relative to $K13^{WT}$ is consistent with previous reports showing induced ER-PI3P vesiculation upon resistance (Suresh and Haldar, 2018). Further, a decrease in the IC50 value of MRT68921 in the resistant parasites compared to its isogenic one emphasizes the importance of autophagy in the survival of ART resistant parasites. Also, $K13^{C580Y}$ parasites show an increase in *PfATG18* labelled puncta colocalizing with PI3P compared to $K13^{WT}$ at the basal levels as well as upon induction of autophagy by incubating parasites with starvation media. Since PI3P is known to induce autophagy in yeast and eukaryotes by providing a platform for recruitment of various ATG proteins (such as ATG18) to the autophagosomes (Dall'Armi *et al.*, 2013), these results demonstrate a functional autophagy pathway that responds to autophagy induction under starvation.

To determine if *PfK13* decorated vesicles are the same subcellular compartments on which *PfATG18* and PI3P colocalize, localization of *PfK13* with respect to *PfATG18* and PI3P were analysed. *PfK13*-PI3P and *PfK13*-*PfATG18* were found to partially colocalize on HCv which are discrete vesicles transporting host derived hemoglobin to the parasite FV. The data also shows increased colocalization of *PfK13* and *PfATG18* towards the parasite periphery at ring stage while they are localized close to the FV in trophozoites, which is speculated to be due to their enhanced co-trafficking to the FV in the trophozoite stage (Ray *et al.*, 2022, mBio).

Chapter 4 encompasses an overall summary, presents an outlook of the findings, followed by future directions for the work. The present study demonstrates that the stress induced parasite autophagy underpins various mechanisms of ART resistance and advances the understanding of the two recently proposed ART resistance mechanisms. DHA induced UPR results in increased autophagy in the parasite, which may render fitness advantage during resistance. Although DHA reduces global protein synthesis through phosphorylation of *PfeIF2 α* , increased expression levels of ATG proteins signify the importance of autophagy in alleviating the effect of protein misfolding as a result of DHA exposure. Given

the increased levels of *PfATG8* and *PfATG18* and their colocalization in resistant parasites, relative to its isogenic counterpart, the role of parasite autophagy in regulating various mechanisms of ART resistance is discussed. As *PfK13* mutant parasites display increased number of PI3P bound *PfATG18* vesicles at the basal level and upon autophagy induction by starvation, it establishes a conserved role of *PfATG18* in parasite autophagy and proposes the presence of *PfATG18* on the ER-PI3P vesicles. Activation of autophagy is significantly higher in the resistant isolate than in the sensitive one, indicating the reliance on autophagy for parasite fitness. Next, co-trafficking of *PfK13* with *PfATG18* and PI3P on parasite hemoglobin trafficking vesicles reveals an association between autophagy and hemoglobin endocytosis, a pathway proposed to be involved in ART resistance. As the putative *PfATG1* is found to be localized to autophagosome-like structures in nutrient-rich conditions in *P. falciparum*, the role *PfATG1* in basal autophagy is hypothesized. Additionally putative *PfATG1* responds to inhibition by a specific ULK1 inhibitor by inhibiting parasite growth and decreasing expression levels of autophagy proteins downstream of *PfATG1*, thus proposing a conserved role of *PfATG1* as a member of the parasite autophagy initiation complex.

As a future perspective, insights into the role of *PfATG18* in proteostasis mechanisms of ART resistance and the hemoglobin endocytosis pathway can be obtained by identifying interacting partners of *PfATG18*. Additionally, since modulation of autophagy by starvation or pharmacological inhibition by MRT68921 has a more profound effect on the resistant parasites than its isogenic counterpart, exploring the possibility of the parasite autophagy-like pathway as a novel target for developing anti-malarials is presented.

Table of Contents

DECLARATION	v
CERTIFICATE	vii
Acknowledgements.....	ix
Synopsis	xii
List of Figures	xxiv
List of Tables	xxvii
List of Abbreviations	xxviii
1. Introduction.....	1
1.1 Malaria	1
1.1.1 Global burden of Malaria.....	2
1.1.2 Malaria burden in India.....	3
1.1.3 Diagnosis, prevention and cure.....	4
1.2 Biology of the <i>Plasmodium</i> species	5
1.2.1 Taxonomic classification	5
1.2.2 Dynamic lifecycle of <i>Plasmodium</i> species infecting humans.....	5
1.2.3 The intraerythrocytic developmental cycle of <i>P. falciparum</i>	8
1.3 Stress pathways in <i>P. falciparum</i>	10
1.3.1 Endoplasmic reticulum stress	14
1.4 Antimalarial drug targets and resistance	16
1.5 Mechanisms of Artemisinin action	19
1.5.1 Activation of Artemisinin	21
1.5.2 Cellular targets of activated Artemisinin	22
1.5.3 Mechanisms for maintaining cellular homeostasis	23
1.6 Mechanism of Artemisinin resistance	24

1.6.1	ART resistance in the early ring stage <i>P. falciparum</i>	25
1.6.2	<i>PfK13</i> as the major molecular maker for ART resistance	26
1.6.3	<i>PfKelch13</i> structure and mechanism of action	27
1.6.4	Proteostasis mechanisms of ART resistance.....	29
1.6.5	<i>P. falciparum</i> hemoglobin endocytosis pathway mediated ART resistance	32
1.7	An overview of Autophagy	33
1.7.1	The discovery of Autophagy.....	35
1.7.2	Functional roles of Autophagy.....	36
1.7.3	Molecular mechanism of Autophagy.....	37
1.7.4	Modulation of the autophagic flux.....	41
1.7.5	Signaling pathways regulating Autophagy	41
1.7.6	Role of Phosphatidylinositol 3-phosphate in Autophagy	42
1.7.7	Selective Autophagy	43
1.8	Interplay between ER stress and Autophagy.....	44
1.8.1	ER-phagy	46
1.8.2	RecovER-phagy	46
1.9	The Autophagy machinery in <i>P. falciparum</i>	48
1.9.1	Role of Autophagy-related proteins in <i>P. falciparum</i>	51
1.9.2	Role of Autophagy in ART resistance	54
1.10	Thesis objectives.....	54
2	Materials and Methods.....	61
2.1	Materials used in the study.....	61
2.1.1	Chemical reagents.....	61
2.1.2	Antibodies	61
2.1.3	Strains and plasmids	62
2.2	Culturing of parasites	63

2.2.1	<i>P. falciparum</i> strains used.....	63
2.2.2	<i>In vitro</i> culturing of <i>P. falciparum</i>	64
2.2.3	Parasite growth assessment by Giemsa stain.....	64
2.2.4	Synchronization of the parasites.....	64
2.2.5	Freezing and thawing of cultures.....	64
2.2.6	Parasite treatment with small molecule inhibitors.....	65
2.3	Growth-inhibition assay.....	66
2.4	Molecular cloning.....	66
2.4.1	<i>P. falciparum</i> mRNA extraction and cDNA synthesis.....	66
2.4.2	Agarose gel electrophoresis.....	67
2.4.3	Generation of clones.....	67
2.4.4	Episomal transfection of <i>P. falciparum</i>	69
2.4.5	Transformation in yeast.....	70
2.5	Quantitative Real-Time PCR.....	70
2.6	Fluorescence microscopy.....	71
2.6.1	Immunofluorescence Assay.....	71
2.6.2	Zenon labelling.....	72
2.6.3	Labelling of Endoplasmic Reticulum with ER-tracker and Mitochondrion with Mito-tracker.....	73
2.6.4	Confocal microscopy and image processing.....	73
2.7	Protein analysis.....	74
2.7.1	Preparation of parasite lysate.....	74
2.7.2	Preparation of yeast lysate.....	74
2.7.3	Separation of protein by SDS-PAGE.....	74
2.7.4	Immunoblot analysis.....	74
2.8	Functional complementation of <i>PfATG1</i> in <i>S. cerevisiae</i>	75
2.8.1	Yeast strains and growth conditions.....	75
2.8.2	mCherry- <i>ScATG8</i> procession assay.....	76

2.9	Quantification and statistical analysis	76
3	Results.....	79
3.1	Understanding the cross-talk between ER stress, UPR and autophagy-like pathway in <i>P. falciparum</i>	79
3.1.1	<i>P. falciparum</i> remains viable upon treatment with clinically relevant dose of DHA	81
3.1.2	DHA induced ER stress activates the UPR pathway	83
3.1.3	DHA induced UPR pathway activates parasite autophagy.....	88
3.2	Deciphering the role of putative <i>PfATG1</i> (PF3D7_1450000) in the autophagy-like pathway in <i>P. falciparum</i>	91
3.2.1	Bioinformatic analysis of putative ATG1 homolog in <i>P. falciparum</i>	93
3.2.2	Putative <i>PfATG1</i> localizes on the autophagosome-like vesicles in <i>P. falciparum</i>	95
3.2.3	Specific ULK1/ATG1 inhibitor, MRT68921, modulates parasite autophagy and survival of <i>P. falciparum</i>	98
3.2.4	<i>PfATG1</i> -GFP is unable to complement autophagy or cytoplasm-to-vacuole functions in <i>S. cerevisiae</i>	102
3.3	Investigating the role of parasite autophagy-like pathway in regulating various mechanisms of artemisinin resistance in <i>P. falciparum</i>	109
3.3.1	Basal expression of autophagy proteins is higher in ART resistant isolate compared to the isogenic isolate	111
3.3.2	Starvation induces parasite autophagy in ART resistant as well as the isogenic isolate	119
3.3.3	Parasite Autophagy regulates the survival of ART resistant isolate.....	124
3.3.4	<i>PfK13</i> and <i>PfATG18</i> are trafficked to the food vacuole through hemoglobin containing vesicles (HCv) in the ART resistant isolate	126
4	Discussion.....	133

4.1	Artemisinin induced UPR pathway activates <i>P. falciparum</i> autophagy	133
4.2	Putative <i>Pf</i> ATG1 (PF3D7_1450000) participates in the autophagy-like pathway in <i>P. falciparum</i>	137
4.3	<i>P. falciparum</i> autophagy underpins various mechanisms of artemisinin resistance	139
4.4	Conclusion and key findings	143
Appendices.....		147
Appendix 1: Multiple sequence alignment between <i>Sc</i> ATG1, <i>Pf</i> ATG1 and <i>Hs</i> ULK1		147
Appendix 2: Codon optimized sequence of <i>Pf</i> ATG1 gene.....		149
References.....		151

List of Figures

Figure 1.1 Global distribution of malaria-endemic regions.....	3
Figure 1.2 The life cycle of <i>Plasmodium</i>	7
Figure 1.3 Three-dimensional organization of the intraerythrocytic stages of <i>P. falciparum</i>	10
Figure 1.4 Stress response pathways in protozoan parasites	11
Figure 1.5 Stress response integration through phosphorylation of eukaryotic initiation factor-2 α	13
Figure 1.6 Molecular mechanism involved in UPR signaling.....	16
Figure 1.7 Antimalarial drug targets in <i>P. falciparum</i>	19
Figure 1.8 (a) Structure of Artemisinin and its derivatives and (b) activation of dihydroartemisinin	20
Figure 1.9 Artemisinin induced stress responses in <i>P. falciparum</i>	24
Figure 1.10 Mechanism of action of Kelch-like proteins under normal and stressed conditions.....	28
Figure 1.11 Proteostasis mechanisms of ART resistance	31
Figure 1.12 Model depicting the mechanism of ART resistance associated with <i>PfK13</i> mutations in <i>P. falciparum</i>	33
Figure 1.13 Illustration showing the types of autophagy.....	34
Figure 1.14 Schematic showing the mechanism of autophagy and modulators of the pathway.....	40
Figure 1.15 Schematic representation of the mechanisms of ER stress mediated autophagy	45
Figure 1.16 Schematic representation of the role of SEC62 in protein translation and revoER-phagy process	47
Figure 1.17 Schematic representation of the conservation of the autophagy machinery in <i>P.</i> <i>falciparum</i>	51
Figure 2.1 Vector maps of the plasmids	63
Figure 2.2 Confirmation of clones	69
Figure 3.1 <i>P. falciparum</i> remains viable upon incubation with 700 nM DHA	82
Figure 3.2 Expression and localization of <i>PfSEC62</i> -GFP in the intraerythrocytic stages of <i>P. falciparum</i>	84

Figure 3.3 DHA induced ER stress leads to expansion of the parasite ER	86
Figure 3.4 DHA induced ER stress leads to phosphorylation of <i>PfeIF2α</i> and upregulation of <i>PfBiP</i>	88
Figure 3.5 DHA induced ER stress activates parasite autophagy.....	89
Figure 3.6 DHA mediated activation of parasite autophagy is triggered by the UPR pathway	91
Figure 3.7 Sequence and structure-based comparison of putative <i>PfATG1</i>	94
Figure 3.8 Putative <i>PfATG1</i> is present as punctate structure in the IE stages of <i>P. falciparum</i>	96
Figure 3.9 Putative <i>PfATG1</i> localizes on autophagosome-like vesicles and the ER in <i>P. falciparum</i>	98
Figure 3.10 Effect of MRT68921, a specific autophagy inhibitor, on the growth of <i>P. falciparum</i>	99
Figure 3.11 Parasite autophagy is inhibited through treatment with MRT68921.....	101
Figure 3.12 Overexpression of <i>PfATG1</i> -GFP in <i>S. cerevisiae</i> and <i>PfATG1</i> -GFP does not mediate formation of autophagic bodies in <i>atg1Δ</i> yeast strain during nitrogen starvation	104
Figure 3.13 <i>PfATG1</i> -GFP does not complement autophagy functions in <i>atg1Δ</i> yeast strain	106
Figure 3.14 <i>PfATG1</i> -GFP does not localize on the PAS in <i>atg1Δ</i> yeast strain.....	108
Figure 3.15 Ring-stage survival assay (RSA) for the K13 ^{WT} and K13 ^{C580Y} isolates.....	112
Figure 3.16 Parasites show increased basal transcript levels of <i>Pfatg8</i> and <i>Pfatg18</i> in K13 ^{C580Y} compared to K13 ^{WT} parasites	114
Figure 3.17 Parasites show increased basal protein expression levels of <i>PfATG8</i> and <i>PfATG18</i> in K13 ^{C580Y} compared to K13 ^{WT} parasites	115
Figure 3.18 <i>PfATG18</i> shows increased localization to autophagosome-like vesicles in K13 ^{C580Y} compared to K13 ^{WT} parasites	116
Figure 3.19 Increased number of PI3P, <i>PfATG8</i> and <i>PfATG18</i> labelled vesicles in K13 ^{C580Y} compared to K13 ^{WT} parasites	119
Figure 3.20 Starvation induces the expression levels of <i>PfATG8</i> and <i>PfATG18</i> in K13 ^{C580Y} as well as K13 ^{WT} parasites	120
Figure 3.21 Starvation increases the number of PI3P labelled vesicles in K13 ^{C580Y} as well as K13 ^{WT} parasites	121

Figure 3.22 Starvation increases the number of *Pf*ATG18 labelled vesicles colocalizing with PI3P in K13^{C580Y} as well as K13^{WT} parasites 123

Figure 3.23 K13^{C580Y} parasites are more sensitive to autophagy inhibition than K13^{WT} 125

Figure 3.24 *Pf*ATG18 is present on PI3P and *Pf*FP2 labelled vesicles in the K13^{C580Y} parasites..... 127

Figure 3.25 *Pf*K13 is present on PI3P and *Pf*FP2 labelled vesicles in the K13^{C580Y} parasites 128

Figure 3.26 *Pf*K13 and *Pf*ATG18 are trafficked to the FV through HCv in the K13^{C580Y} parasites..... 130

Figure 3.27 *Pf*K13 and *Pf*ATG18 localize near the parasite periphery in ring stage K13^{C580Y} parasites..... 131

Figure 4.1 Model representing role of autophagy in mechanisms of ART resistance..... 144

List of Tables

Table 1.1 Classification of the human malaria parasite.....	5
Table 1.2 Conserved Autophagy proteins in <i>P. falciparum</i>	49
Table 2.1 Details of primers used for cloning.....	68
Table 2.2 <i>P. falciparum</i> transfection mix	69
Table 2.3 Yeast transformation mix.....	70
Table 2.4 List of primers used for Real-time PCR	71
Table 2.5 List of antibodies and their dilutions used in Immunofluorescence analysis	72
Table 2.6 List of antibodies and their dilutions used in Western blot analysis	75
Table 2.7 Genotypes of various yeast strains utilized in this study	76

List of Abbreviations

3-MA	3-methyladenine
ACT	artemisinin-based combination therapy
AIM	ATG8 interacting motif
ALP	alkaline phosphatase
Ape1	aminopeptidase 1
ART	artemisinin
ATG	autophagy-related gene
ATG1	autophagy-related protein 1
ATG8	autophagy-related protein 8
ATG18	autophagy-related protein 18
CPY	carboxypeptidase Y
CRT	chloroquine resistance transporter
Cvt	cytoplasm-to-vacuole pathway
DHA	dihydroartemisinin
DIC	differential interference contrast
DV	digestive vacuole
EEF	exoerythrocytic form
ER	endoplasmic reticulum
FP2	falcipain-2
FRRG	Phe-Arg-Arg-Gly
FV	food vacuole
GFP	green fluorescent protein
GMS	greater Mekong Sub-region
GWAS	genome-wide association study
HCv	hemoglobin containing vesicles
IE	intraerythrocytic
LC3	Microtubule-associated protein 1A/1B-light chain 3
MDR1	multidrug resistant protein 1
MSP1	merozoite surface protein 1
PAS	pre-autophagosomal structure or phagophore assembly site
PE	phosphatidylethanolamine

PERK	protein kinase RNA-like endoplasmic reticulum kinase
PI	phosphatidylinositol
PI(3,5)P₂	phosphatidylinositol 3,5-bisphosphate
PI3K	phosphatidylinositol-3-kinase
PI3P	phosphatidylinositol-3-phosphate
PKA	protein kinase A
PM-II	plasmepsin II
PMSF	phenylmethanesulphonyl fluoride
PROPPINs	β -propellers that bind polyphosphoinositides
PV	parasitophorous vacuole
PVM	parasitophorous vacuolar membrane
RBC	red blood cell
ROS	reactive oxygen species
SDS	Sodium dodecyl sulfate
SEM	Standard error of the mean
TORC1	target of rapamycin complex 1
Ubl	ubiquitin-like
UPS	ubiquitin-proteasome system
UPR	unfolded protein response

Chapter 1

Introduction

1.1 Malaria

The earliest evidence of *Plasmodium*, the causative agent of malaria, was found in 30 million years old mosquitoes preserved in amber, predating human civilization (Poinar, 2005). The first written account of repeated paroxysmal fever with occurrences of enlarged spleen, symptoms typically associated with malaria, dates back to 2700 BC in the ancient Chinese medical text *Nei Ching*. Multiple other written records, such as the Mesopotamian clay tablets (2000 BC), the Egyptian *Eberus papyrus* (1570 BC) and Indian scriptures (600 BC), all mention similar malaria fever occurrences. In 400 BC, Hippocrates linked the disease with close proximity to foul air or “miasma” rising from swamps, which, if inhaled, caused malaria (Cox, 2010). The term “malaria” also derives its origin from the miasma theory, having been coined from the Italian words, “mal” and “aria”, which refer to “bad” and “air”, respectively (Hempelmann and Krafts, 2013).

The advent of microscopes in the 1600s enabled the identification of microorganisms as the main cause of various infectious diseases. Naturally, the hunt for a malaria-causing microbe began, but it took nearly 250 years to definitively identify the underlying cause. Scientific studies on the parasite intensified only after Alphonse Laveran, a military surgeon, observed pigmented parasites in the blood samples of patients suffering from malaria and identified them as unicellular protozoa. About 2 decades later in 1897, Sir Ronald Ross showed transmission of avian malaria by mosquitoes. Both these discoveries were awarded the Nobel prize in 1907 and 1902, respectively. Subsequently, scientists were able to conclusively demonstrate that human malaria is transmitted through the *Anopheles* mosquitoes. A more comprehensive account of the parasite life-cycle took another 70 years

to uncover. At present, the genomes of the malaria mosquito *Anopheles gambiae*, as well as the human infecting parasite *P. falciparum*, have been sequenced (2002) and our knowledge of both the vector and the parasite has greatly improved (Cox, 2010; Dagen, 2020; Gelband *et al.*, 2004).

As we now know, malaria is caused by a unicellular protozoan parasite of the genus *Plasmodium* and is transmitted to humans through the bite of a female *Anopheles* mosquito carrying the parasite. The five *Plasmodium* species that most commonly infect humans are *P. falciparum*, *P. vivax*, *P. malariae*, *P. ovale* and *P. knowlesi*. *P. falciparum* and *P. vivax* are the most prevalent ones, but *P. falciparum* is responsible for the vast majority of malaria-related deaths worldwide (WHO, 2021a). Clinical symptoms of malaria include periodic high fever, muscle aches, shaking chills, and vomiting. If left untreated, the disease can result in splenomegaly, or enlargement of the spleen. Infection with *P. falciparum* also causes fatal damage to multiple organs such as the liver, kidneys, and lungs, as well as severe anemia, altered consciousness, and coma in cases of cerebral malaria, which usually results in the patient's death (Phillips, Burrows and Manyando, 2017).

1.1.1 Global burden of Malaria

As of 2020 (WHO, 2021b), malaria is still an endemic in 85 countries, putting nearly half of the world's population at high risk of contracting the disease. The majority of these countries are located in tropical and sub-tropical regions of Central and Southern America, Africa, South-east Asia, Middle-east, the Indian subcontinent, and Oceania (Figure 1.1). Pregnant women, children, patients with HIV/AIDS, and people with low immunity levels dwelling in areas with high rates of malaria transmission are significantly more likely to contract the disease. In 2020 alone, an estimated 241 million malaria cases and 627,000 malaria-related deaths were reported, with the majority of deaths occurring in children under the age of five. The statistics indicate a significant increase in 2020 owing to service disruptions caused by the COVID-19 pandemic, with additional 14 million cases and 69,000 deaths reported (WHO, 2021b). According to these estimates, malaria is among the most lethal communicable diseases encountered by humans.

While approximately 1.7 billion cases and 10.6 million deaths have been averted over the last two decades owing to various successful malaria elimination programs, the disease is

far from being eradicated (WHO, 2021b). Even today, malaria remains a threat to public health as well as a burden to the socio-economic systems of endemic countries. Additionally, resistance to anti-malarial drugs used to combat this disease has evolved in lockstep with the increasing caseloads.

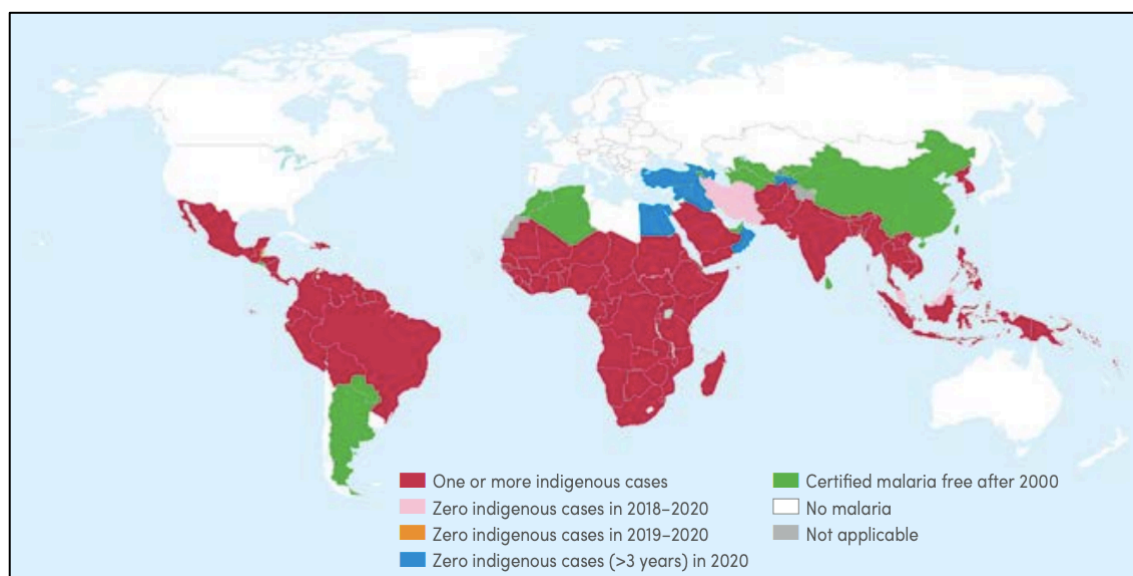


Figure 1.1 Global distribution of malaria-endemic regions

A map showing the trend of malaria incidence from 2000-2020 in different countries. (Data sourced from World Malaria Report, WHO, 2021).

1.1.2 Malaria burden in India

The public health care system of India, the second most populated country in the world, has faced various obstacles including the appropriate execution of surveillance programs aimed at containing the spread of malaria. The country recorded its worst malaria outbreak in the 1950s with 75 million cases and 0.8 million deaths. The situation improved significantly following the National Malaria Control Program (NMCP) in 1953, which resulted in a dramatic reduction in the number of cases, to less than 50,000 and reported zero mortality until 1961 (Das *et al.*, 2012). However, malaria resurfaced in the 1970s, and India now accounts for an astounding 83 % of all malaria cases and 82 % of all deaths from the region of South-East Asia as reported in 2020 (WHO, 2021b). *P. falciparum* and *P. vivax* are the two major *Plasmodium* species that infect humans in India and have contributed equally to the overall malaria burden in 2019 (“NCVBDC, 2021”, n.d.).

1.1.3 Diagnosis, prevention and cure

The WHO-recommended method of diagnosing malaria focuses on two important components of the disease, namely, detection of symptoms such as fever and presence of parasites in the patient's blood. Clinical diagnosis is made by monitoring the patient's symptoms (fever, perspiration, chills, headache, vomiting etc.) which are more often non-specific and overlap with those of other infectious diseases. Knowledge of the patient's risk of exposure, including travel history to malaria-endemic regions can aid in diagnosis. Microscopic diagnostics detect the presence of parasites by examining a thin blood smear under a light microscope. Prior to examination, the smear is stained with Giemsa stain to distinctively identify the parasites. Additionally, the 'Rapid Diagnostic Tests' (RDTs) are used to immunologically detect parasite antigens in the patient's blood. RDTs give rapid detection within 2-15 minutes of the test, enabling healthcare personnel to make timely decisions regarding the course of treatment (Phillips, Burrows, Manyando, *et al.*, 2017).

Over the last 2 decades, increased access to malaria prevention tools and effective tactics such as mosquito vector control and the use of preventive chemotherapies has had a substantial impact on reducing the global malaria burden. In malaria-endemic regions, WHO-recommended tools to prevent infection include the use of bed-nets, indoor insecticides and repellents, periodic preventive treatment for children and pregnant women, prompt diagnosis and testing, and a swift treatment of confirmed cases with antimalarials, primarily Artemisinin-based Combination Therapy (ACT). Additionally, the use of seasonal malaria chemoprevention, intermittent preventive treatment of infants (IPTi) and pregnant women (IPTp), chemoprophylaxis, and mass drug administration have complemented the ongoing malaria control campaign (Phillips, Burrows, Manyando, *et al.*, 2017). Since October 2021, broad use of the world's first malaria vaccine, RTS, S has been recommended. RTS, S targets the pre-erythrocytic stage of the parasite and is engineered with *P. falciparum* circumsporozoite protein (CSP), repeat region (R), T-cell epitope (T), and hepatitis B virus surface antigen (S). The recombinant vaccine has been shown to provide significant protection against *P. falciparum* malaria in young African children, providing much needed optimism towards malaria control (Heppner Jr et al., 2005; WHO, 2018).

1.2 Biology of the *Plasmodium* species

1.2.1 Taxonomic classification

Plasmodium is a member of the Apicomplexa, a large phylum of parasitic alveolates. Unicellular parasites from the phylum Apicomplexa are characterized by the presence of specialized complex of apical secretory organelles such as micronemes, rhoptries, and dense granules. These apical complexes are required during invasion of host cells (Cowman and Crabb, 2006). *Plasmodium* is classified as an Apicomplexan parasite in the order Haemosporida, which includes all parasites that live inside red blood cells (RBCs). Based on the method of asexual reproduction and the presence of a pigment called hemozoin, the order is further classified into four families, of which *Plasmodium* belongs to the Plasmodiidae. Over 200 species of *Plasmodium* have been discovered to date, each capable of infecting a wide variety of hosts, most notably, amphibians, reptiles, birds, and mammals. Only five of these 200 species, however, are capable of infecting humans (Table 1.1) (Perkins, 2014).

Domain	Eukaryota
Superphylum	Alveolata
Phylum	Apicomplexa
Class	Aconoidasida
Order	Haemosporida
Family	Plasmodiidae
Genus	<i>Plasmodium</i>
Species	<i>falciparum</i>
	<i>vivax</i>
	<i>malariae</i>
	<i>ovale</i>
	<i>knowlesi</i>

Table 1.1 Classification of the human malaria parasite

1.2.2 Dynamic lifecycle of *Plasmodium* species infecting humans

Characteristic features of the parasite lifecycle are largely conserved across *Plasmodium* species that infect humans. *Plasmodium* parasites alternate their lifecycle between a female *Anopheles* mosquito and a human host and require unique “zoite” forms to invade various cells at specific stages. Multiple rounds of asexual replication occur throughout the

lifecycle, spanning various stages and cell types. Asexual replication occurs in both human liver cells and RBCs, whereas sexual stages are initiated by the formation of gametocytes in the RBCs. Gametogenesis and meiosis require transmission to the mosquito host. Numerous parasites are formed during asexual replication in the circulating RBCs, though only a small fraction of these differentiate into sexual stages (Cowman *et al.*, 2016).

Once the infected mosquito takes a human blood meal, it injects sporozoites ('sporos' means 'seeds') into the skin. Due to their motile nature, sporozoites enter the bloodstream and travel to the liver, where they are able to escape the host immune cells. After crossing the liver sinusoids, sporozoites invade the hepatocytes where they establish a parasitophorous vacuole (PV) and differentiate. Sporozoites undergo multiple rounds of asexual replication, forming a multinucleated schizont/meront that encloses thousands of daughter merozoites ('meros' means 'piece'), establishing the 'Exo-erythrocytic schizogony'. This marks the asymptomatic stage of malaria infection (Figure 1.2). At this stage, parasite species such as *P. vivax* and *P. ovale* can enter a state of latency through the formation of a non-replicating 'hypnozoite' that allows their long-term survival (Vaughan and Kappe, 2017).

A second phase of asexual replication begins with the egress of merozoites from the hepatocyte that then enter the bloodstream (Cowman *et al.*, 2012). The erythrocytic schizogony phase begins with the invasion of RBCs by merozoites. This phase is divided into three developmental stages, namely, ring, trophozoite, and schizont. Intraerythrocytic schizogony results in asexual replication at the schizont stage with the formation of 8-32 merozoites over a course of 24–72 h period (number of merozoites and time of replication varies between species). Merozoites re-invade fresh RBCs to complete one 'Intraerythrocytic Developmental Cycle' (IDC). Parasites establish infection through repeated rounds of invasion and growth (Figure 1.2). The clinical symptoms of malaria are associated with the IDC stage, during which infected RBCs hemolyze, releasing parasite materials that trigger the host-immune response (Cowman *et al.*, 2012).

A few asexual parasites undergo differentiation to form gametocytes, initiating the sexual cycle. Mature gametocytes circulate in the peripheral blood for several days before being ingested by a new mosquito during a blood meal. Shortly after entering the mosquito midgut, the female gametocyte differentiates into a macrogamete while the male

gametocytes into 8 microgametes. A single microgamete fuses with the macrogamete to form a diploid zygote. The zygote develops into a motile ookinete that crosses the midgut epithelial wall, forming an oocyst. The third cycle of asexual replication begins with replication of the oocyst which results in the formation of thousands of haploid daughter sporozoites. These sporozoites mature inside the salivary glands of the mosquito and remain there until they are transmitted to a new human host (Figure 1.2), commencing a new cycle (Baton, 2005; Venugopal *et al.*, 2020).

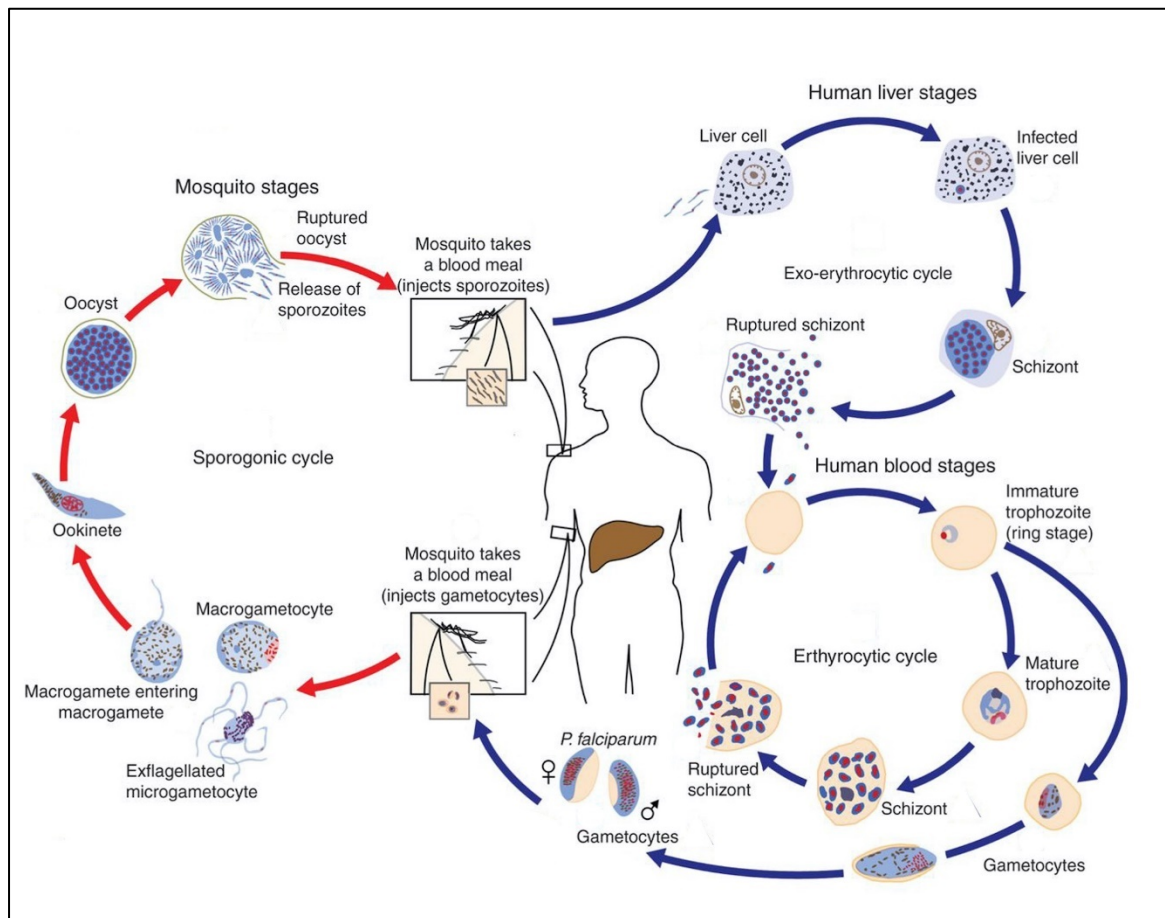


Figure 1.2 The life cycle of *Plasmodium*

The life cycle of *Plasmodium* involves an invertebrate vector i.e., female *Anopheles* mosquito and a vertebrate host i.e., human. Figure adapted from Centres for Disease Control and Prevention, 2020.

1.2.3 The intraerythrocytic developmental cycle of *P. falciparum*

The merozoite stage: Invasion of erythrocytes by parasites is a rapid process mediated by crucial molecular interactions between the merozoite and the RBC surface. Merozoites are oval-shaped structures measuring 1.6 μm in length and 1 μm in width with a protruding flat end. Regardless of their small size, merozoites are sufficiently equipped to egress from the RBC of its origin and invade a new RBC. Once on the RBC surface, the merozoites reorient themselves toward their apical pole, which aids in the formation of a tight junction between the parasite and the host, initiating its entry into the RBC, and later, the feeding process. The apex of the merozoites contain secretory vesicles such as rhoptry and micronemes that facilitate their attachment to the host RBC. Additionally, the merozoite harbors organelles necessary for survival within the RBC, including a basally placed nucleus, numerous ribosomes, a single mitochondria and plastid, and a minimal cytoskeleton system that assists in maintaining its shape (Figure 1.3a). Antigens present on the merozoite surface, such as the *P. falciparum* merozoite surface protein 1 (*PfMSP1*) and apical membrane antigen 1 (*PfAMA1*) mediate the initial attachment and apical reorientation, respectively. (Bannister *et al.*, 2000; Crabb *et al.*, 2004; Mitchell *et al.*, 2004)

The ring stage: Following invasion, the merozoite form develops into a ring-shaped structure that resembles a biconcave disc, thick at the ends and thin in the middle. The thick rim includes major organelles like the nucleus, apicoplast, ER, mitochondria, Golgi, and ribosomes. At this stage, the parasite begins feeding on the hemoglobin present in the RBC cytosol, which enters the parasite via small, dense ring-like vesicles on the parasite periphery called cytostomes (Figure 1.3b). Hemoglobin is degraded inside the parasite food vacuole (FV), generating amino acids and a by-product, ‘heme’. While amino acids are used for synthesizing new proteins, the heme is polymerized into inert, non-toxic crystals termed hemozoin which remain inside the FV throughout the intraerythrocytic cycle (Coronado *et al.*, 2014). As the ring grows, the parasitophorous vacuolar (PV) membrane extends into RBCs and alters the RBC membrane by enhancing its adhesion to blood vessels, including the placenta (Bannister *et al.*, 2000; Goldberg and Zimmerberg, 2020).

The trophozoite stage: The development of a ring into a young trophozoite is facilitated by expansion of its PVM which stretches to form narrow finger-like projections collectively known as the ‘tubovesicular network’ (TVN) that extends into the RBC. Along with its size

and shape, the ring alters the functioning of its key organelles, upon development into the trophozoite. This stage exports a large number of parasite proteins into the RBC surface and cytoplasm. Thus, the parasite ER as well as the number of ribosomes involved in synthesizing and folding nascent proteins are abundant in trophozoites and help in increasing their protein synthesis capacity. The mitochondria and apicoplast grow in size to facilitate increased metabolism. The increased surface area of the parasite aids in the extension of the TVN into the RBC cytosol. Maurer's clefts are parasite-induced vesicular structures in the RBCs that originate from the TVN. They serve as a platform for trafficking parasite proteins to the RBCs, promoting knob formation on the RBC surface (Figure 1.3c). Among the proteins that are exported, *PfEMP1* promotes the selective adhesion of infected RBCs to the blood endothelial membrane, resulting in sequestration of trophozoites and schizonts. Sequestration of parasitized RBC in brain and placenta blood capillaries leads to the development of cerebral and placental malaria, respectively (Bannister *et al.*, 2000; Elliott *et al.*, 2008).

The schizont stage: At this stage, the parasites are involved in repeated nuclear divisions. Endomitotic nuclear division takes place, with chromosomes and spindle apparatus remaining within the nuclear envelop. Following this, the mitotic spindle elongates and separates a set of attached chromosomes into two nuclei without disintegrating the nuclear envelop. This process is repeated until 8-32 daughter nuclei are formed. Nuclear division is accompanied by continuous uptake of host hemoglobin and export of parasite proteins into the RBC. Following nuclear division, the PVM and RBC membranes are ruptured, releasing merozoites that invade fresh RBCs (Figure 1.3d) and the intraerythrocytic cycle continues (Bannister *et al.*, 2000).

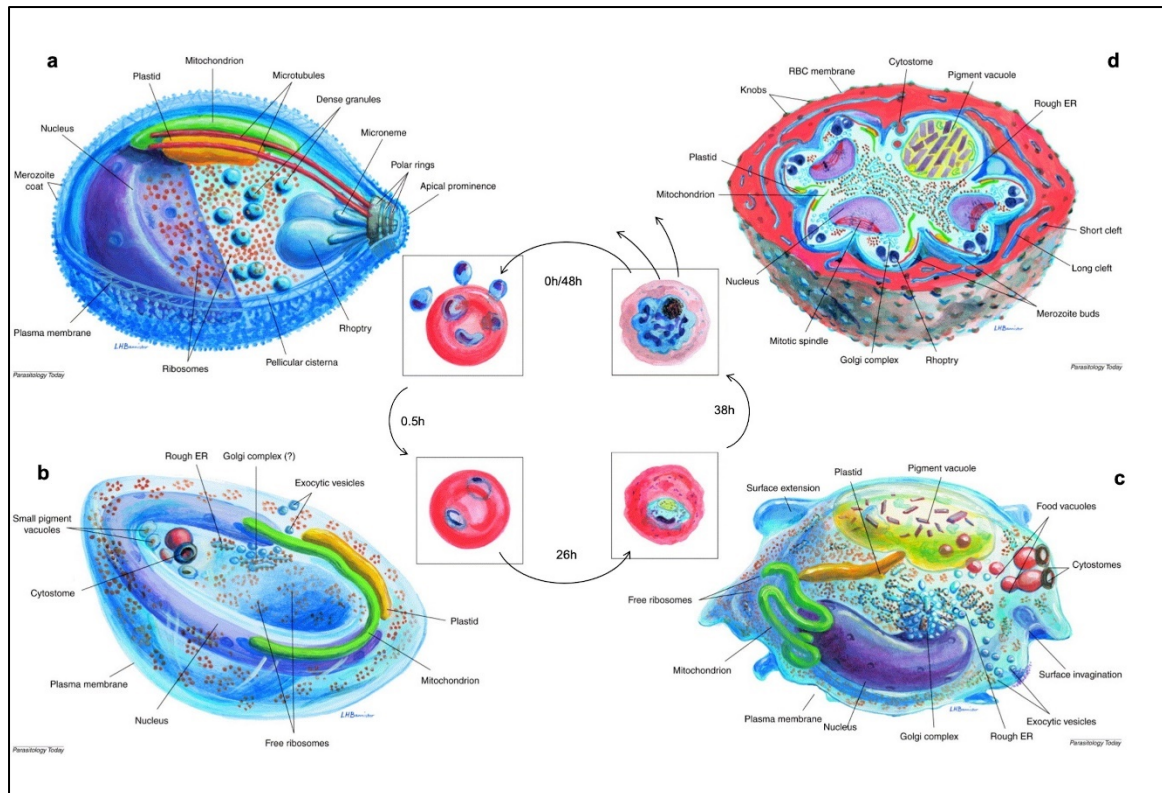


Figure 1.3 Three-dimensional organization of the intraerythrocytic stages of *P. falciparum*

Schematic representation of (a) Merozoite, (b) Ring, (c) Trophozoite, and (d) Schizont. Adapted from Bannister et al., 2000, with permission from 2000 Elsevier Science Ltd.

1.3 Stress pathways in *P. falciparum*

Protozoan parasites have complex life cycles, often alternating between multiple hosts or persisting in the environment as a cyst until the availability of a new host. The capacity of the parasites to adapt to environmental stimuli and stress, as well as to persist in sub-optimal circumstances, is critical to their viability and successful growth through their life cycle. Similar to higher eukaryotes, parasitic protozoa are known to employ various stress response pathways to cope with stressful environment. The activation of antioxidants, heat shock proteins, or acidocalcisomes assists in reducing various extra and intracellular stress stimuli by stabilizing misfolded proteins as well as regulating stress response pathways. Cellular damage may also activate several stress signaling cascades, such as those mediated by eIF2 kinases or MAPKs (Vonlaufen *et al.*, 2008), resulting in changes in gene expression related to stress alleviation (Figure 1.4).

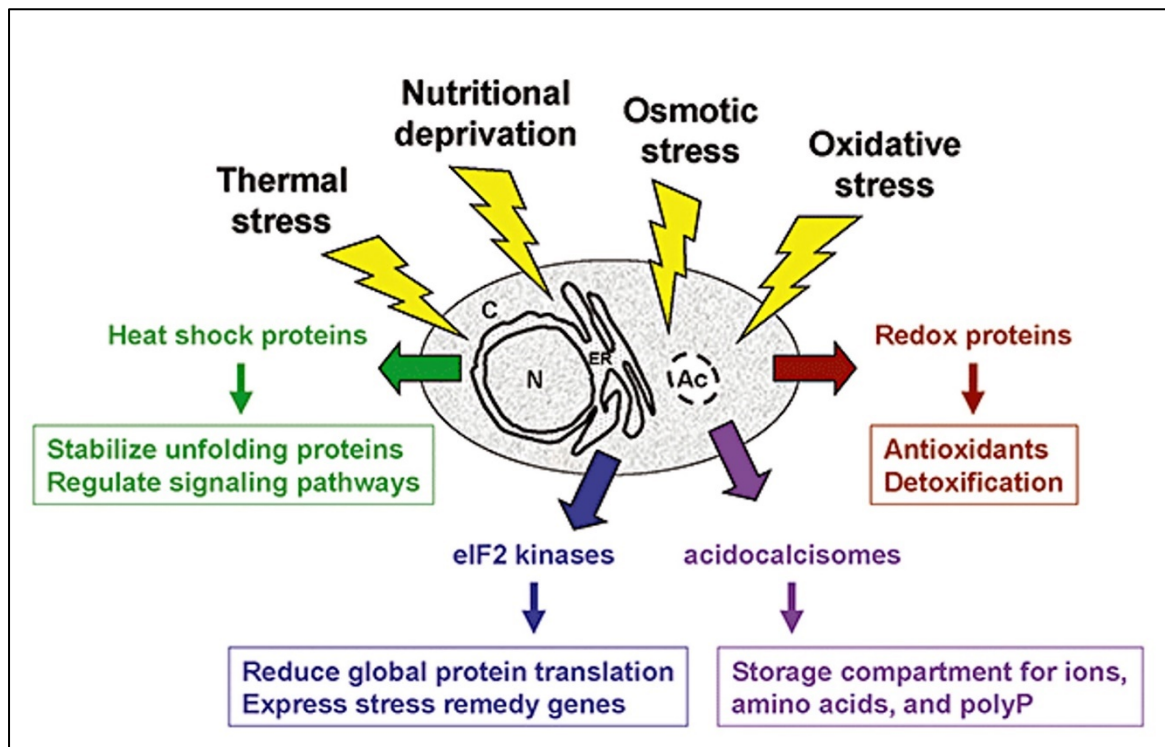


Figure 1.4 Stress response pathways in protozoan parasites

Overview of the protozoan stress responses. Antioxidants (red), heat shock proteins (green), acidocalcisomes (Ac, purple), nucleus (N), cytoplasm (C), and endoplasmic reticulum (ER) Reproduced from Vonlaufen et al., 2008, with permission from the 2008 Blackwell Publishing Ltd.

P. falciparum too is exposed to a variety of stressors during its life cycle, including host immune responses, nutrient deprivation, microaerophilic conditions, temperature variations, and drug exposure (Babbitt *et al.*, 2012; Chaubey *et al.*, 2014; Engelbrecht and Coetzer, 2013). Hemoglobin breakdown in the parasite releases toxic free heme, resulting in substantial oxidative stress and disruption of the cell's redox equilibrium (Becker *et al.*, 2004; Percário *et al.*, 2012). In addition, *P. falciparum* has a high replication rate and relies on its protein trafficking system to export numerous parasite proteins to the host RBC for membrane remodeling. Approximately 8 % of parasite proteome involved in structural and antigenic alteration of the RBC, as well as supplying enough machinery for host nutrient uptake and protein export, is folded and secreted from the parasite ER. (Hiller *et al.*, 2004; Marti *et al.*, 2004). All the proteins secreted by a cell are initially checked for quality-control by the ER resident chaperones and then transported to their final destination via the Golgi complex. Given the critical role of protein trafficking to the host in malaria

pathogenesis, *P. falciparum* is likely to experience ER stress throughout its intraerythrocytic life cycle.

Stress response is primarily mediated through the regulation of gene expression, which is achieved by modulating the transcription and translation processes. Most eukaryotic cells have stress activated kinases, such as c-Jun N-terminal Kinases (JNKs) and p38 Mitogen-Activated Protein Kinases (MAPs), that respond to a wide range of stress conditions (Engelberg, 2004). Although there are two MAPK homologs in the parasite kinome, none of them is involved in stress response. The *P. falciparum* kinome, on the other hand, has a phylogenetic cluster of three kinases with similarity to eukaryotic Initiation Factor 2 α (eIF2 α) kinases, which regulate translation in other organisms in response to stress (Ward *et al.*, 2004).

Phosphorylation of eIF2 α at Serine 51 in response to stress is a well-studied post-transcriptional regulatory mechanism that regulates translation initiation (Murtha-Riel *et al.*, 1993; Proud, 2005). In eukaryotes, the process of phosphorylation is mediated by four different eIF2 α kinases, namely, general control non-derepressible-2 (GCN2), RNA-dependent protein kinase (PKR), heme-regulated inhibitor kinase (HRI), and PKR-like endoplasmic reticulum kinase (PERK). These enzymes have a common catalytic domain, which enables them to phosphorylate the same substrate, but they possess distinct accessory domains that control kinase activity in response to diverse signals. The histidyl-tRNA synthetase (HisRS) like domain in GCN2 is the primary amino acid sensing motif that is stimulated upon starvation and triggers kinase activation (Wek *et al.*, 1995). The transmembrane domain of PERK enables its localization to the ER membrane. The N-terminal domain of PERK extends into the ER lumen to detect misfolded proteins, whereas the catalytic domain towards the cytoplasm binds to substrate and initiates its effector mechanisms. PKR has an RNA binding domain that is able to detect viral infection, while HRI harbors heme binding sites that regulate translation of the globin chain in response to heme availability. Thus, the eIF2 α kinases are able to integrate a variety of stress signals into a single pathway (Chen and London, 1995; Holcik and Sonenberg, 2005; Proud, 2005; Wek *et al.*, 2006).

Translation initiation is dependent on the assembly of the 80S ribosome on the mRNA, which is regulated by a set of proteins called the eukaryotic initiation factors (eIFs).

Assembly of the 43S pre-initiation complex is dependent on attachment of the ternary complex consisting of the heterotrimeric G-protein eIF2 (α , β and γ subunits), GTP, and the methionyl-initiator tRNA (met-tRNA_i) (Holcik and Sonenberg, 2005). The process of initiating translation and releasing the initiation factors requires the hydrolysis of GTP to GDP, which results in the formation of an inactive eIF2-GDP complex. Prior to initiating further rounds of translation, eIF2 should be reactivated by conversion of GDP for GTP. A phosphate group present on the α subunit of eIF2 restricts conversion of inactive eIF2-GDP to the active eIF2-GTP by decreasing the activity of the eIF2 β guanine nucleotide exchange factor (Sudhakar *et al.*, 2000). This results in global translation repression, which aids in energy and nutrient conservation and provides time for the cell to adjust to the stress conditions (Figure 1.5). Despite the widespread decrease in translation, some mRNAs are translated, and their products eventually modulate the stress response (Fennell *et al.*, 2009).

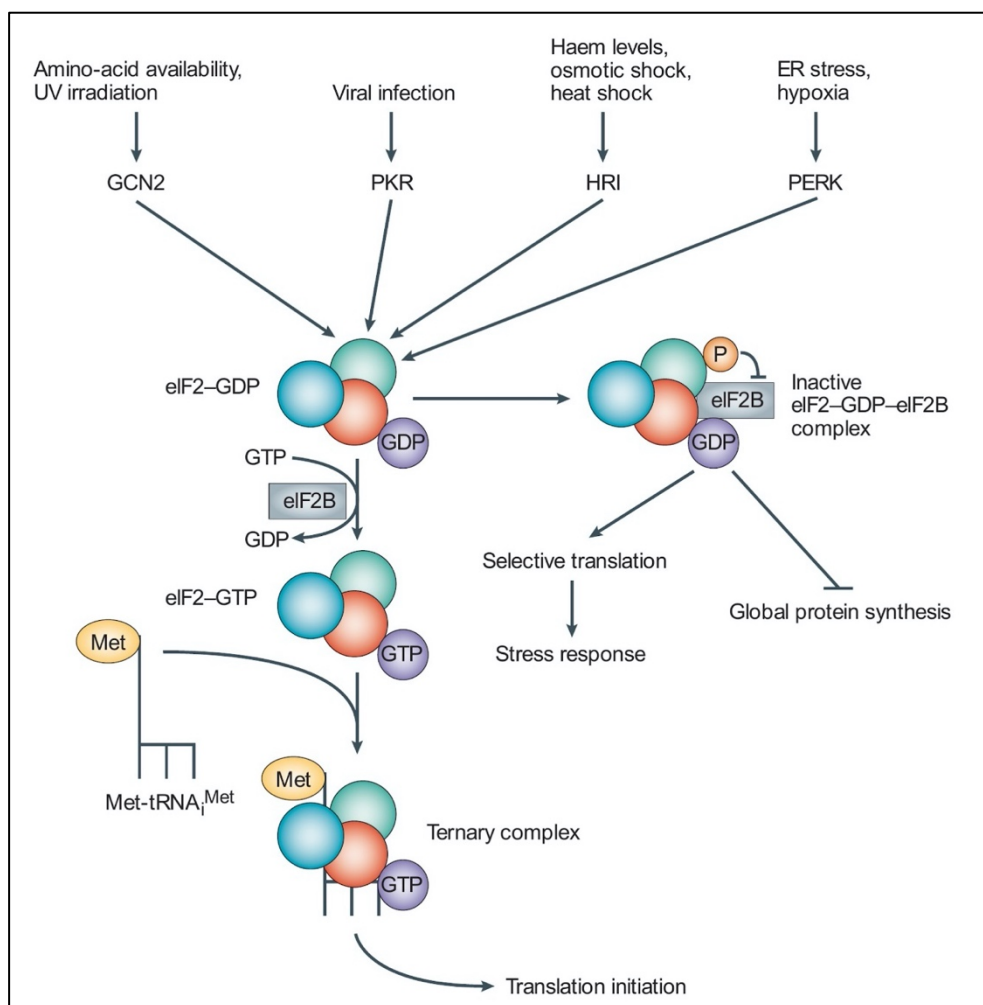


Figure 1.5 Stress response integration through phosphorylation of eukaryotic initiation factor-2 α

Four eIF2 α kinases, GCN2, PKR, HRI and PERK integrate various stress signals into a single pathway. Reproduced from Holcik and Sonenberg, 2005, with permission from 2005, Nature Publishing Group.

1.3.1 Endoplasmic reticulum stress

Several studies on cellular adaptative mechanisms to cope with ER stress have identified the Unfolded Protein Response (UPR) as a signaling pathway that is triggered upon accumulation of misfolded protein in the ER. UPR acts by maintaining a balance between the folding capacity of the ER and the amount of misfolded proteins. In yeast and other eukaryotes, the three ER integral membrane-sensing proteins that control activation of the UPR signaling pathway during ER stress include the inositol-requiring enzyme 1 α (IRE1 α), activating transcription factor-6 (ATF6), and protein kinase RNA (PKR)-like ER kinase (PERK) (Smith and Wilkinson, 2017).

Upon the accumulation of misfolded proteins, the ER resident BiP chaperone dissociates from the luminal domains of these sensors to bind misfolded proteins, thus converting the monomeric UPR sensors to active dimeric states. Splicing of X-box binding protein 1 (XBP1) transcripts by IRE1 α leads to the formation of a transcription factor XBP1-S that increases expression levels of genes such as ER chaperones and components of the ER-associated degradation (ERAD) machinery. While chaperones increase protein folding capacity of the ER, the ERAD aids in the degradation of misfolded proteins from the ER, thereby promoting ER homeostasis (Lee *et al.*, 2003; Vembar and Brodsky, 2008). Cleavage of ATF6 by cellular proteases produces a transcriptionally active polypeptide that migrates to the nucleus where it upregulates transcription of ER luminal chaperones, ERAD components and XBP1 (Wu *et al.*, 2007; Yamamoto *et al.*, 2007; Yoshida *et al.*, 2001). PERK is a serine threonine kinase that phosphorylates eIF2 α , protein involved in translation initiation, causing attenuation of global protein translation. This relieves the load on the ER to invest chaperones in the folding of freshly prepared protein. The cell does, however, allow translation of the transcription factor ATF4, which in turn increases transcription of several stress response genes such as the C/EBP homologous protein (CHOP), driving transcription of the pro-apoptotic gene, as well as several core autophagy genes (ATG3, ATG7, ATG5, ATG10, ATG12, ATG1611) involved in the degradation of misfolded protein aggregates (B'chir *et al.*, 2013; Marciniak *et al.*, 2004). Taken together, the

inhibition of protein translation combined with increased expression of ER chaperones and other stress response proteins decreases accumulation of misfolded proteins. In the event that UPR fails to maintain homeostasis and ER stress prolongs, apoptotic factors are activated, resulting in cell death (Figure 1.6).

Bioinformatic analysis revealed absence of a UPR transcriptional response (IRE1 α and ATF6) in *P. falciparum*, thus relying on the translational arm of the UPR due to the presence of a conserved PERK like eIF2 α kinase (Figure 1.6) (Chaubey *et al.*, 2014; Gosline *et al.*, 2011). *P. falciparum* encodes three eIF2 α kinases, namely, *PfeIK1*, *PfeIK2*, and *PfPK4*. Although, the *PfeIK1* responds to amino acid starvation during the intraerythrocytic stage, it is not essential for parasite development (Babbitt *et al.*, 2012; Fennell *et al.*, 2009). The *PfeIK2* regulates sporozoite latency during the sexual stage inside the mosquito salivary glands (Zhang *et al.*, 2010). *PfPK4* is essential for development of the parasite inside the RBCs and mediates antimalarial drug-induced latency, causing parasite recrudescence and treatment failure (Zhang *et al.*, 2012, 2017). Additionally, *P. falciparum* harbors a conserved BiP chaperone localized to the parasite ER, indicating a functional UPR machinery based on BiP-PERK signaling (Cortés *et al.*, 2020). Several proteins involved in the ERAD and autophagy degradation pathways are also conserved in the protozoan parasite (Hain and Bosch, 2013; Harbut *et al.*, 2012). Taken as a whole, the PERK-eIF2 α mediated UPR and its downstream effector pathways can work in concert to process misfolded proteins and restore ER homeostasis.

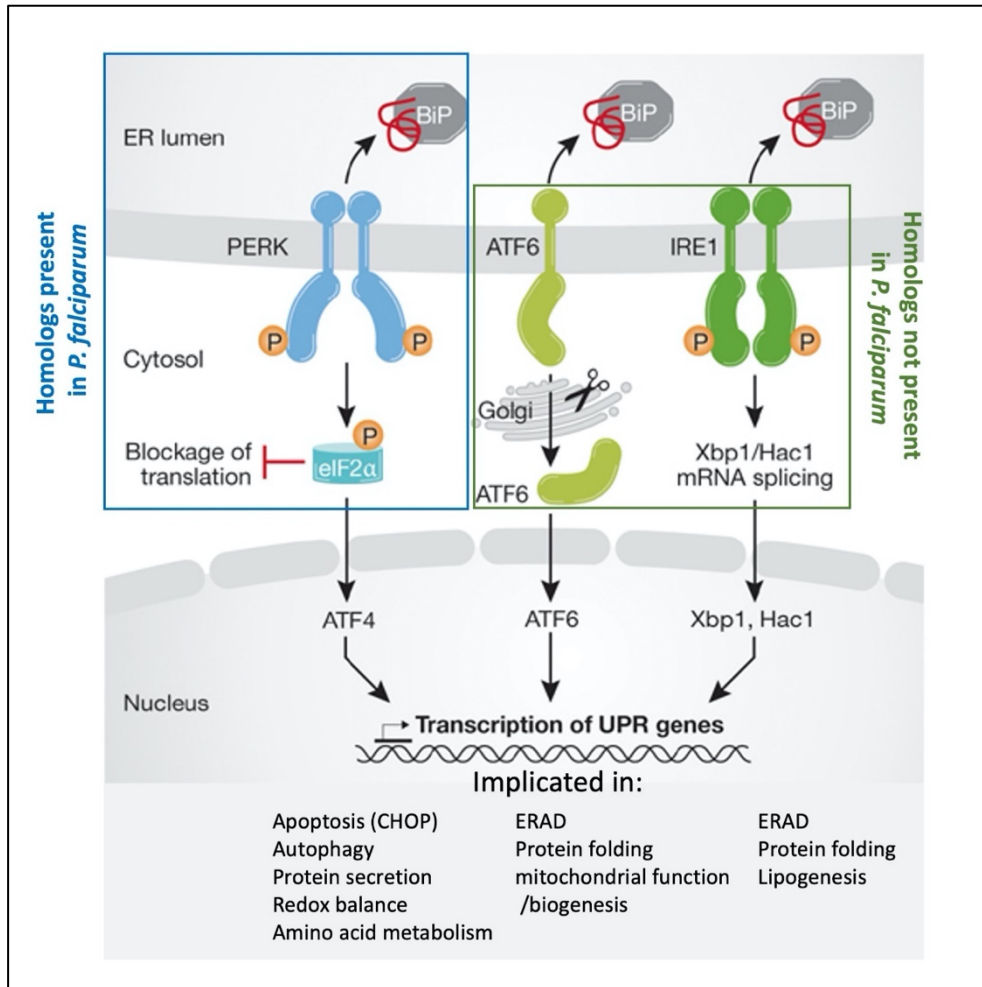


Figure 1.6 Molecular mechanism involved in UPR signaling

The three UPR sensors on the ER membrane: PERK, ATF6 and IRE1. Adapted from Cyr and Hebert, 2009, with permission from 2009 European Molecular Biology Organization.

1.4 Antimalarial drug targets and resistance

The antimalarial drugs currently in use can be broadly classified into three categories based on their chemical composition and mechanism of action. Quinine, quinidine, chloroquine, mefloquine, lumefantrine, halofantrine, amodiaquine, cycloquine, etc., are all examples of aryl amino alcohol compounds. Antifolate compounds include pyrimethamine, trimethoprim, proguanil, etc. The endoperoxide compounds include artemisinin, dihydroartemisinin, artemether, artesunate, etc. All currently available antimalarial classes are directed against the asexual trophozoite and schizont stages. Antifolates, primaquine, and atovaquone are also effective against parasites at the liver stage. Endoperoxides are active against all asexual blood-stage parasites (Figure 1.7). Drug resistance can arise as a

consequence of randomly occurring genetic mutations in a parasite population. Antimalarial resistance is mediated by one of four mechanisms: by processes that diminish drug toxicity, by a direct catalytic mechanism, by amplification of a gene encoding target enzymes, or by transporters that expel the drug out of the parasite. (Haldar *et al.*, 2018; Kumar *et al.*, 2018).

Chloroquine prevents the polymerization of free heme released during the digestion of host hemoglobin, thus disrupting hemozoin formation. The reactive free heme lyses membranes resulting in parasite death. Chloroquine resistance occurs as a result of reduced chloroquine accumulation in the parasite FV. Mutations in the *P. falciparum* chloroquine-resistance transporter (*PfCRT*) present at the FV lead to rapid chloroquine efflux from the digestive vacuole. Chloroquine was used for four decades until the emergence of chloroquine-resistance in Southeast Asia, followed by its spread to other malaria-endemic countries. Replacement of chloroquine with mefloquine also faced the wrath of resistance. Mutations in another efflux pump present on the FV membrane and encoded by the *P. falciparum* multidrug resistance protein (*PfMRD1*) confer resistance to mefloquine (Haldar *et al.*, 2018).

Antifolates such as pyrimethamine are used in combination with long-lasting sulfadoxine to treat *P. falciparum* malaria. While sulfadoxine targets the *P. falciparum* dihydropteroate synthase (*PfDhps*), pyrimethamine inhibits the activity of dihydrofolate reductase (*PfDhfr*), both enzymes involved in the folate pathway. Unfortunately, resistance to this combination has increased as a result of mutations in the catalytic sites of the enzymes or gene amplification. Sulfadoxine–pyrimethamine resistance in Africa has been conferred by multiple mutations in the *PfDhps* (A437G, K540E) and *PfDhfr* (N51I, C59R, S108N) genes. Additionally, mutations in the gene encoding *P. falciparum* mitochondrial electron donor cytochrome b (*PfCytB*) render resistance to atovaquone, a naphthoquinone class of drug. When combined with proguanil, atovaquone targets *PfCytB*, resulting in the dissipation of parasite mitochondrial membrane potential (Haldar *et al.*, 2018).

The artemisinin class of drugs (ARTs) has multiple targets inside the parasite and has been suggested to induce stress mediated parasite death (Tilley *et al.*, 2016). Due to their excellent safety profile and rapid parasitocidal effect, remission of fever is rendered faster than any other known antimalarial (Nosten *et al.*, 2007; White, 2008). Treatment with ARTs

results in a 10,000 fold decrease in parasite load every 48-hrs that corresponds to one intraerythrocytic lifecycle of the parasite (White, 2008, 2014). Clinical failures and spread of chloroquine resistance in the latter half of the 20th century replaced the existing treatment regime with Artemisinin-based Combination Therapy (ACT) as the frontline treatment for uncomplicated *P. falciparum* malaria. ACTs co-formulate ARTs with partner drugs viz sulfadoxine-pyrimethamine, mefloquine, lumefantrine, piperaquine, or amodiaquine (Aweeka and German, 2008; Chawira and Warhurst, 1987; Cui and Su, 2009). The underlying rationale is that ARTs rapidly clear parasites from a patient's bloodstream, while their short half-life (~1-3h) is compensated by the action of partner drugs that are effective in removing residual parasites (Tilley *et al.*, 2016).

A decreased susceptibility of *P. falciparum* towards ARTs and the partner drugs has emerged in Southeast Asia's Greater Mekong Sub-region (GMS), declining efficacy of the ACT regime (Dondorp *et al.*, 2009; Noedl *et al.*, 2008). Clinical evidence of ART resistance was first reported in western Cambodia in 2009, shown as reduced susceptibility of *P. falciparum* to artesunate monotherapy. The resistance manifested itself as an increased average clearance time of 84 hours following a seven-day course of artesunate, compared to 48 hours in patients from outside Cambodia (Dondorp *et al.*, 2009). Unfortunately, resistance to sulfadoxine-pyrimethamine and chloroquine also emerged from the Pailin Province of the GMS before spreading to malaria endemic countries of Africa (Mita *et al.*, 2011; Roper *et al.*, 2004; Verdrager, 1986; Vinayak *et al.*, 2010). Thus, ART resistance poses a serious concern for the emergence of multi-drug resistance in these regions and its spread to other malaria-endemic countries. Consequently, monitoring the sensitivity of the currently used ACT drugs has become critical for effective treatment of malaria. Novel antimalarial drugs are currently being developed but are not commercially available yet. In the future, decreased susceptibility to ART may develop into full-blown resistance, making it critical to decipher the molecular mechanism of ART resistance for disease elimination.

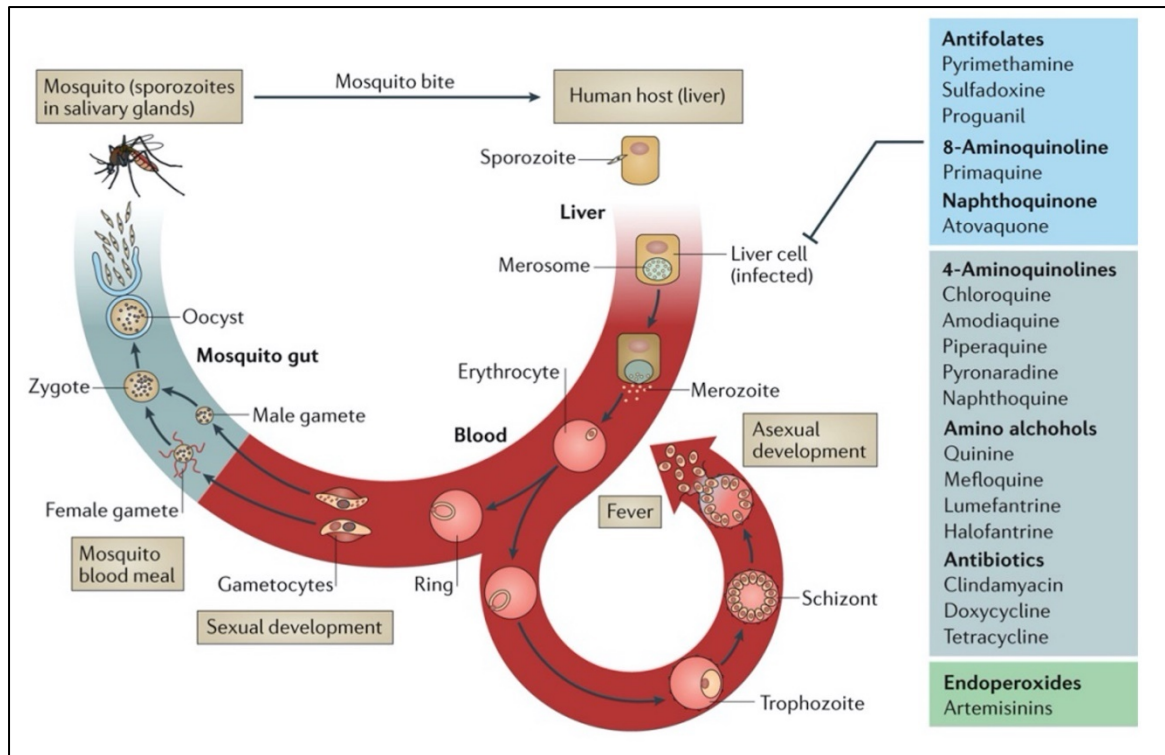


Figure 1.7 Antimalarial drug targets in *P. falciparum*

Stages of *P. falciparum* targeted by known antimalarials. Reproduced from Haldar et al., 2018, with permission from 2018, Nature Publishing Group.

1.5 Mechanisms of Artemisinin action

In 1967, a nationwide search by the Chinese government for novel antimalarial drugs led to the development of ART. The Chinese herb *Artemisia annua*, also known as Sweet Wormwood, exhibited significant inhibitory activity against malaria parasites. TU You-You's extraction of the active compound, ART, from the herb using ether at low temperatures earned her the 2015 Nobel Prize in Medicine. Numerous ART derivatives have been synthesized following initial purification, including the active *in vivo* metabolite of all ARTs, dihydroartemisinin (DHA), artesunate, and artemether (Figure 1.8a), which offer improved efficacy and bioavailability as compared to ART (Lu *et al.*, 2019).

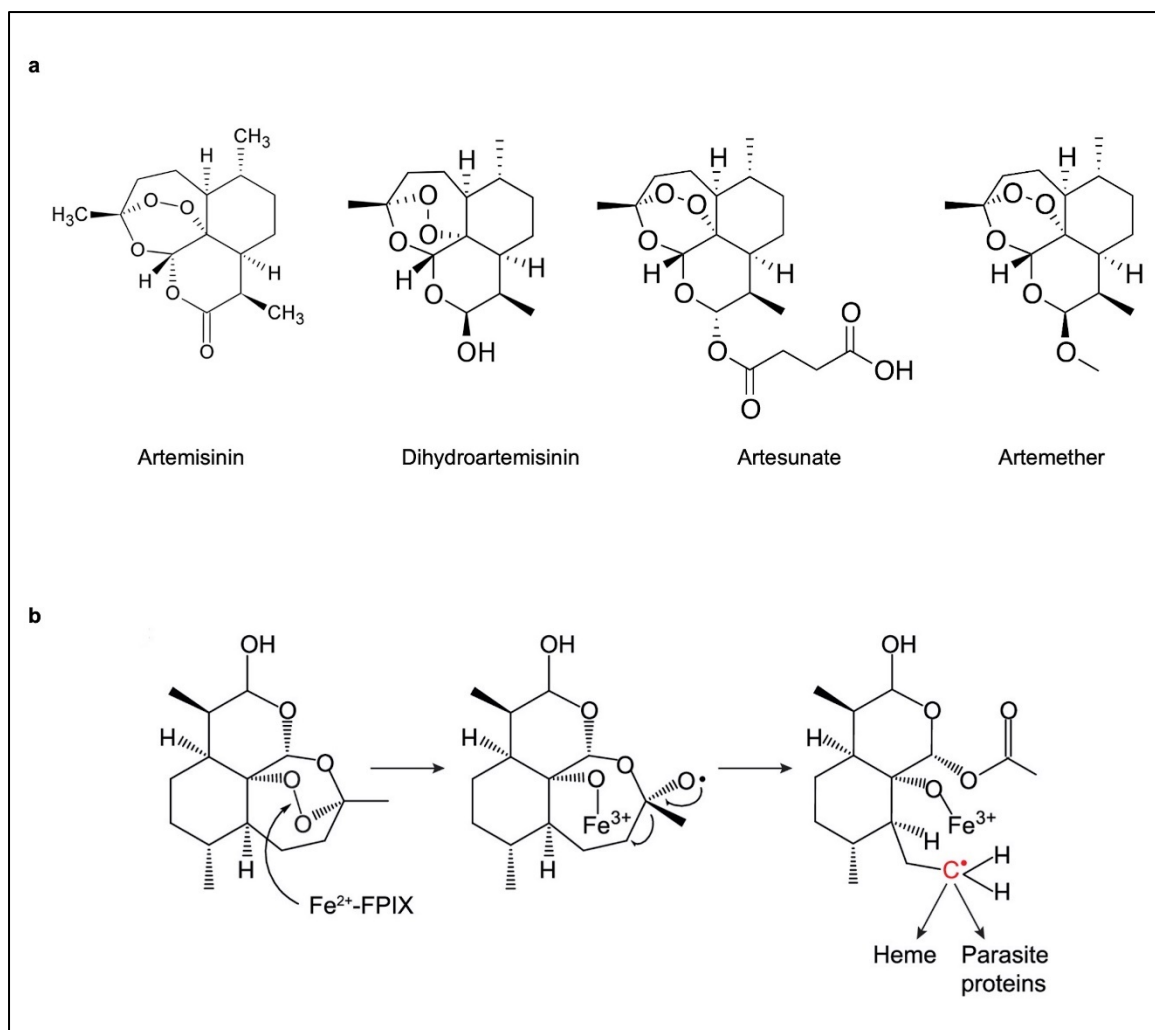


Figure 1.8 (a) Structure of Artemisinin and its derivatives and (b) activation of dihydroartemisinin

(a) The parent molecule, Artemisinin, is naturally derived from the herb *Artemisia annua*. DHA, Artesunate and Artemether are synthetic derivatives of artemisinin. Images licensed under CC-BY

(b) Activation of DHA. Heme (Fe^{2+} -FPIX) initiates the cleavage of the endoperoxide bond, generating a short-lived alkoxy radical. Thermodynamic rearrangement results in the formation of a primary carbon-centered free radical (red), which alkylates heme and parasite proteins. Reproduced from Rosenthal and Ng, 2020, with permission from 2020, American Chemical Society.

1.5.1 Activation of Artemisinin

ART and its derivatives are sesquiterpene lactones integrating a 1,2,4-trioxane moiety and an endoperoxide bridge (Wang *et al.*, 2019). ARTs are considered as prodrugs since several derivatives are rapidly converted *in vivo* to the active DHA form, and their mode of action depends on activation by cleavage of the endoperoxide bond (O'Neill *et al.*, 2010). Activation involves the iron-catalyzed reductive scission of the endoperoxide bond that generates a highly reactive carbon-centered free radical (Figure 1.8b). This reaction is essential for its antimalarial activity, as compounds such as deoxyartemisinin, which lack the endoperoxide bridge, remain inactive even in the presence of iron (Tilley *et al.*, 2016).

The primary source of iron in *Plasmodium* parasites is heme, which is generated from degradation of the host hemoglobin. A series of proteases, including falcipains and plasmepsins, are involved in degradation of hemoglobin inside the parasite FV. Cleavage of hemoglobin by these proteases generates small peptides which are further acted upon by amino peptidase to generate the final breakdown product: amino acids, which are subsequently released into the cytoplasm. Additionally, the degradation of hemoglobin produces toxic heme, which is detoxified by conversion to Fe³⁺ heme dimers, culminating in the formation of chemically inert hemozoin crystals. The majority of the proteolysis reaction occurs during the trophozoite stage of the IDC when parasites intake large quantities of hemoglobin from the host RBC and transport it to the FV. While parasites sequester the majority of heme into hemozoin, some heme remains in the reduced Fe²⁺ form and is able to activate ARTs (Tilley *et al.*, 2016).

As ART activation is mostly reliant on hemoglobin degradation, its activity is limited to parasitized RBCs (Wang *et al.*, 2015), which explains why ARTs are non-toxic to uninfected RBCs, mature gametocytes, and liver stages (Adjalley *et al.*, 2011; Meister *et al.*, 2011), which do not digest hemoglobin. This also explains why ART susceptibility varies with the parasite stage. Trophozoites degrade hemoglobin at a higher rate than other intraerythrocytic stages, making them especially sensitive to ARTs. Mid-ring stages digest less hemoglobin and are thus less susceptible to ARTs. Interestingly, ARTs are effective against early ring stages. This is assumed to be owing to the digestion of host hemoglobin obtained from the *de novo* heme biosynthesis pathway. However, because of the limited

quantity of heme generated by the biosynthetic pathways, activation in early rings is limited (Tilley *et al.*, 2016; Wang *et al.*, 2015).

1.5.2 Cellular targets of activated Artemisinin

Till date, the exact mechanism of ART action remains elusive. Free radicals generated during ART activation are believed to react rapidly with accessible nucleophiles on proteins, unsaturated membrane lipids, as well as heme present in the parasite, resulting in widespread alkylation and eventually parasite death (Tilley *et al.*, 2016).

Recent studies have identified protein targets of ART in the parasite using chemical proteomic approaches. The proteins identified are localized to various sub-cellular compartments and are involved in vital functions such as hemoglobin digestion, antioxidant defence, and glycolysis. ART activation also leads to disruption of multiple cellular processes crucial for parasite viability, such as hemoglobin degradation, glycolysis, ribonucleoside biosynthesis, and the regulation of protein translation. Given the wide range of parasite proteins targeted by ART, it was hypothesized that parasite killing occurs as a result of ART mediated promiscuous alkylation of parasite proteins, disrupting essential homeostasis pathways. Interestingly, *Pf*ATP6, the *P. falciparum* orthologue of mammalian Sarco-ER Ca-ATPases (SERCA) which was initially considered as a potential target of ART (Eckstein-Ludwig *et al.*, 2003), was also identified in these chemical proteomics studies as one of the many targets of ART (Ismail *et al.*, 2016; Tilley *et al.*, 2016; Wang *et al.*, 2015). In addition to this, studies have demonstrated DHA mediated inhibition of the parasite proteasome machinery, leading to the accumulation of polyubiquitinated proteins, indicating widespread protein damage that can lead to parasite death (Bridgford *et al.*, 2018).

Another direct target of ART that has not been identified in the chemical proteomic studies is the *P. falciparum* phosphatidylinositol-3-kinase (*Pf*PI3K), an ortholog of mammalian Vps34. DHA reversibly binds to, and inhibits the enzyme activity of *Pf*PI3K in ring stage parasites, hence inhibiting the phosphorylation of phosphatidylinositol (PI), which consequently prevents production of the lipid phosphatidylinositol 3-phosphate (PI3P). Treatment of parasites with wortmannin, a known *Pf*PI3K inhibitor, restricts delivery of host hemoglobin to the parasite FV, suggesting that the kinase plays a role in hemoglobin

endocytosis. Incubation of parasites with ART also yields a similar inhibitory effect on hemoglobin endocytosis, implying a role of *Pf*PI3K in ring stage infection. This study uncovered the possibility of many unidentified reversible targets of ART that play a crucial role in parasite survival (Mbengue *et al.*, 2015; Tilley *et al.*, 2016).

In addition to protein damage, toxicity of ARTs is also mediated through alkylation of reactive heme species, leading to formation of cytotoxic ART-heme adducts, as well as generation of reactive oxygen species (ROS). Accumulation of ROS in the parasite impairs its antioxidation capacity and damages organelles such as mitochondria and macromolecules like DNA (Siddiqui *et al.*, 2021).

Altogether, these reports suggest that ART mediated parasite death is a culmination of various stresses, such as ER stress due to widespread protein damage, oxidative stress caused by ROS generation, and proteasome stress because of the loss of proteasome function (Figure 1.9). With the wide range of sub-cellular targets, ART activation results in significant cellular damage (Siddiqui *et al.*, 2021).

1.5.3 Mechanisms for maintaining cellular homeostasis

The ART mediated promiscuous alkylation of cellular targets damages the parasite proteome, resulting in a buildup of misfolded proteins and activation of the stress responses. Accumulation of misfolded proteins upon parasite exposure to DHA was demonstrated through the binding of a thiol reactive and fluorogenic dye, tetraphenylethene maleimide (Chen *et al.*, 2017). Additional studies with parasites expressing a destabilized form of the fluorescently tagged GFP (GFP-DD) observed a decrease in fluorescence activity below its baseline signal upon exposure to DHA (Bridgford *et al.*, 2018), further indicating misfolding of proteins as a consequence of ART action. Reports have shown growth retardation in ring and early trophozoite stage parasites following exposure to sub-lethal doses of DHA, implying initiation of an ER stress response signaling through PERK-eIF2 α mediated translational attenuation (Dogovski *et al.*, 2015). The phosphorylation status of *PfeIF2 α* later revealed evidence of the activation of the ER stress response pathway in response to DHA exposure. Increased phosphorylation of *PfeIF2 α* in parasites exposed to very short pulse of DHA, and its decrease upon inhibiting the activity of PERK, demonstrates activation of the PERK-eIF2 α mediated ER stress response pathway

(Bridgford *et al.*, 2018). Interestingly, studies have shown that ART promotes dormancy in parasites through the phosphorylation of *PfeIF2 α* . Inhibiting the *Plasmodium* eIF2 kinase PK4 prevents parasites from entering latency and completely eliminates recrudescence after ART treatment. Thus, the malaria parasite appears to rely on the UPR signaling pathway for survival in the face of cellular damage caused by ART (Zhang *et al.*, 2017).

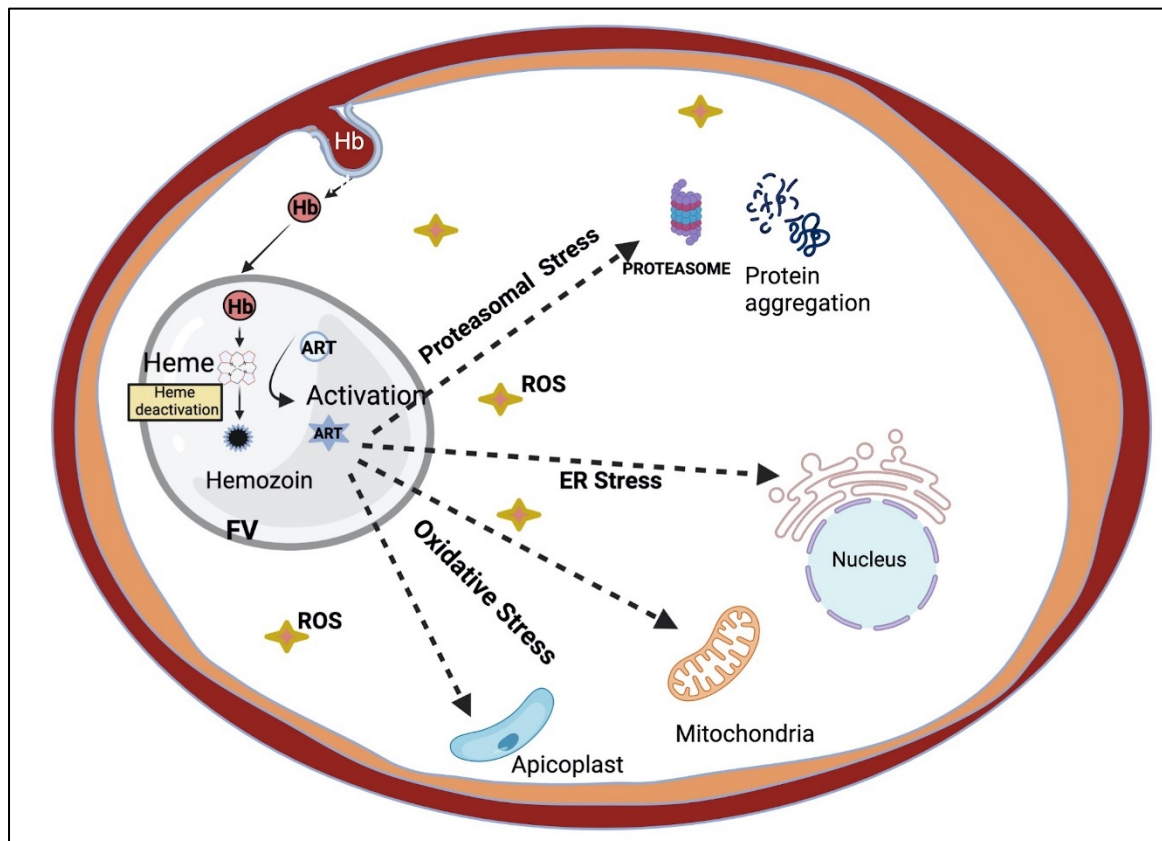


Figure 1.9 Artemisinin induced stress responses in *P. falciparum*

Artemisinin exposure results in ER, oxidative and proteasome stress.

1.6 Mechanism of Artemisinin resistance

ARTs are known to rapidly kill parasites and clear the load of parasite biomass from the bloodstream. Clinical resistance to ART, therefore, is attributed to the persistence of residual parasitemia in patients beyond three days of treatment with either ART monotherapy or ACTs. A more precise way of defining clinical ART resistance is to

quantify the parasite clearance half-life which exceeds 5.5h in resistant *P. falciparum* compared to ~2h in sensitive ones (Ashley *et al.*, 2014; Dondorp *et al.*, 2009; Noedl *et al.*, 2008; Van Der Pluijm *et al.*, 2019). Patients infected with ART resistant parasites, however, can still completely eliminate their remaining parasite load following prolonged therapy with ACTs. Thus, failure to respond to the standard three-day course of ACT can be overcome by increasing the duration of ART monotherapy to 7 days or by sequential treatment with ART monotherapy for 3 days followed by 3 days of ACT. (Ashley *et al.*, 2014; Sutherland *et al.*, 2021). Additionally, slow clearance of parasites under ACT treatment imposes an additional burden on the partner drugs which has led to the emergence of partner drug resistance (Phyo *et al.*, 2016). Increased occurrence of resistance to partner drug can result in complete failure of the ACT regime.

1.6.1 ART resistance in the early ring stage *P. falciparum*

Due to the short half-life of ARTs (~1h), standard *in-vitro* drug susceptibility studies involving 72 hours of drug exposure to the parasites have proved ineffective in distinguishing slow clearing ART resistant parasites from fast clearing susceptible parasites (Fairhurst and Dondorp, 2016; Klonis *et al.*, 2013). Modelling studies have indicated the slow clearance phenotype observed in ART resistant parasites is a result of reduced sensitivity of early rings to ART (Saralamba *et al.*, 2011). Experiments with pharmacologically relevant exposures of ART show the greatest variation in ART susceptibility between slow and rapid clearing isolates occurs at the early ring stages. Witkowski *et al.* developed a reliable assay for the definitive identification of ART resistant parasites, taking into consideration that the delayed parasite clearance phenotype is a consequence of decreased ART sensitivity at the ring stage (Witkowski *et al.*, 2013). The Ring Survival Assay (RSA) measures the viability of tightly synchronized early ring stage parasites (0-3h hpi) which are exposed to a pulse dose of 700 nM DHA for 4-6 h. The drug containing medium is then removed and parasites are restored to normal culturing conditions. The percentage of surviving parasites is estimated by microscopic analysis after 72 hpi (Witkowski *et al.*, 2013). The survivability of ART resistant parasites ranges between 2 % and 45 %, while sensitive parasites are most often completely eliminated (Sutherland *et al.*, 2021; Witkowski *et al.*, 2013).

1.6.2 *PfK13* as the major molecular maker for ART resistance

Genetic background has a profound effect on the acquisition and maintenance of ART resistance. The reduced *P. falciparum* clearance phenotype observed after ART treatment allowed for the determination of the genetic basis for decreased drug sensitivity. The seminal discovery that sparked the uncovering of the genetic architecture of ART resistance occurred in 2014, when a specific mutation, M476I, was found in the *P. falciparum* Kelch13 (*PfK13*) gene on chromosome 13. The mutation was identified in a parasite strain F32 from Tanzania after exposing the *in vitro* cultures to intermittent ART drug pressure for ~5 years. A whole genome sequencing analysis of parasite field isolates revealed numerous mutations in the carboxy terminus of the “ β -propeller” domain of the *PfK13* protein. These mutations exhibited strong correlations with both increased RSA values and a prolonged parasite clearance half-life, implying that *PfK13* is a major determinant of the reduced clearance phenotype (Ariey *et al.*, 2014).

Nearly 200 *PfK13* mutations have been reported from Southeast Asian countries and other malaria-endemic areas to date (Ménard *et al.*, 2016; Project, 2016). However, through gene-editing experiments, a small number of them have been linked to ART resistance. These *PfK13* mutations include C580Y, Y493H, R539T I543T, N458Y, M476I and R591H; C580Y being prevalent in >50 % of parasites across Southeast Asia (Ariey *et al.*, 2014; Siddiqui *et al.*, 2020; Straimer *et al.*, 2015). The increased incidence of C580Y is partly due to epistatic interactions from background genetic mutations that compensate for the fitness loss incurred by parasites during resistance. (Miotto *et al.*, 2015; Nair *et al.*, 2018; Straimer *et al.*, 2017).

The geographical distribution of the *PfK13* C580Y mutation in GMS reveals distinct patterns, with C580Y being more prevalent in the eastern GMS countries of Vietnam, Cambodia, Laos, and eastern Thailand, whereas F446I is more prevalent in the western GMS countries of Yunnan province of China, Myanmar, and western Thailand. The observed disparity is thought to be the result of different demographic histories, drug use, parasite strains, genetic background, and mosquito vectors in these regions. ART resistant strains in Cambodia, for example, include diverse background mutations in the gene encoding *P. falciparum* ferredoxin, multidrug resistance-2 (*PfMDR2*), chloroquine resistance transporter (*PfCRT*), and apicoplast ribosomal protein-S10 (*PfAPRS10*). It is

thought that as *PfK13* mutant alleles present the parasite with growth disadvantages, these background genetic mutations may compensate for the loss through activation of pathways/proteins that aid in parasite growth. Additionally, the parasite's genetic background influences resistance, as parasites with the identical C580Y mutation but a different genetic background proved to be either less fit or neutral in *in vitro* studies (Siddiqui *et al.*, 2021).

1.6.3 *PfK13* structure and mechanism of action

Following the elucidation of its importance in ART resistance, *PfK13* has become the focus of various studies. Sequence analysis has revealed that *PfK13* constitutes of 726 amino acids with an N-terminal sequence specific to *Plasmodium* spp., followed by a putative BTB/POZ (BR-C, ttk and bab/ Pox virus and Zinc finger) domain and six Kelch β -propeller domain at the C-terminus (Ariey *et al.*, 2014). The domain architecture of *PfK13* is similar to the other Kelch-like (KLHL) protein family found in humans, wherein the BTB/POZ domain is present at the N-terminus and 5-6 Kelch motifs at the C-terminus (Dhanoa *et al.*, 2013). The BTB/POZ domain helps in protein-interaction and is found in proteins with diverse functionality, including those involved in protein degradation as well as transcriptional and cytoskeletal regulation (Chaharbakhshi and Jemc, 2016). The BTB/POZ domain is known to bind with a member of the family of E3 ubiquitin ligases, cullin 3, and the downstream Kelch region acts as a substrate adaptor. Thus, Kelch-like proteins serve as substrate adaptors for the E3 ligase, leading to polyubiquitination of specific substrates by an E2 ubiquitin-conjugating enzyme (Figure 1.10), followed by their degradation within the ubiquitin proteasome machinery (Furukawa *et al.*, 2003; Stogios *et al.*, 2005).

The sequence of *PfK13* Kelch domain shares 25–30 % of its identity with the human Kelch-like proteins, namely KLHL8 (Kelch-like protein 8) and Keap1 (Kelch-like ECH associated protein 1). In other eukaryotes, Keap1 acts as a negative regulator of the transcription factor Nrf2 (nuclear erythroid 2-related factor 2), which regulates cellular pathways in response to oxidative stress. As a substrate for the cullin E3 ligase/Keap1 complex, Nrf2 is rapidly ubiquitinated and degraded inside the proteasome during normal conditions. Oxidative stress modifies a few cysteine residues in Keap1, reducing its ability to bind to and degrade Nrf2 by the proteasomal machinery. Accumulated Nrf2 traffics to the nucleus, where it binds to the promoter regions of antioxidant response genes, hence increasing their

expression levels. Reports suggest a Keap1-like function of *PfK13* in the malaria parasite. Mutations in the β -propeller region of *PfK13* that are associated with ART resistance, can impair its interactions with a transcription factor, resulting in increased levels of the transcription factor. *PfPI3K* is one of the known substrates of *PfK13*, although it is not a transcription factor (Cullinan *et al.*, 2003; Tilley *et al.*, 2016).

Although *PfK13* is considered indispensable for parasite survival (Bridgford *et al.*, 2018), very little is known about the protein's exact function in the parasite. Recent studies, however, have proposed two mechanisms of ART resistance that link the mutant *PfK13* with increased protein homeostasis (Suresh and Haldar, 2018) and a reduced hemoglobin endocytosis pathway (Birnbaum *et al.*, 2020) in the parasite.

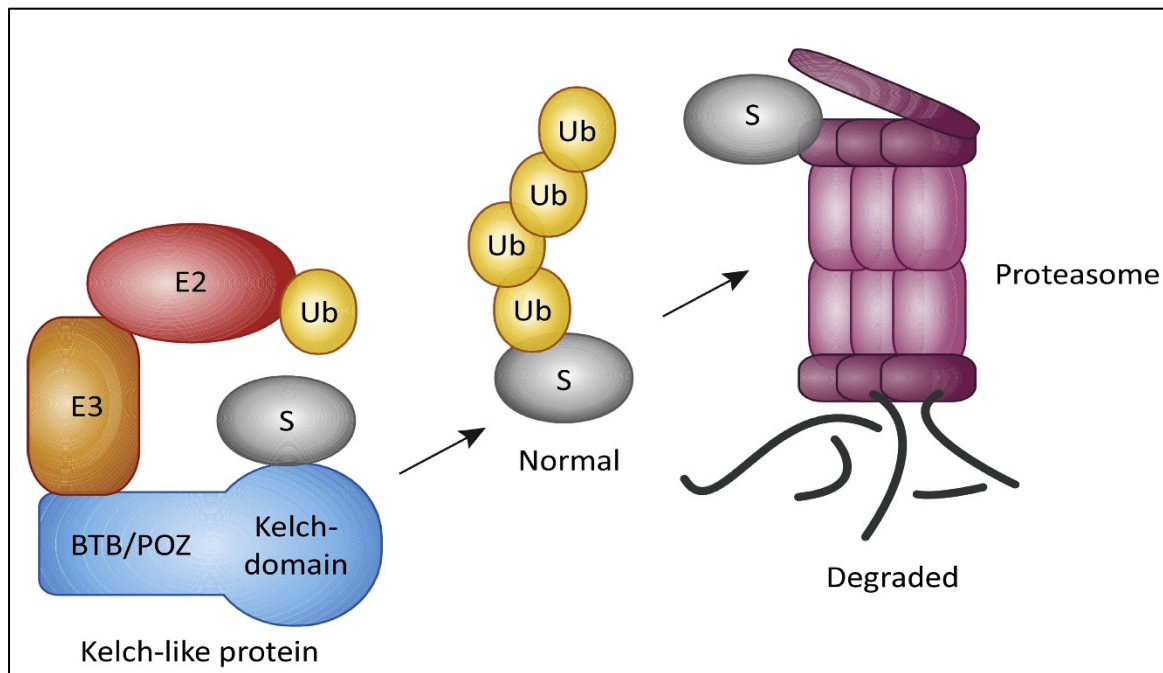


Figure 1.10 Mechanism of action of Kelch-like proteins under normal and stressed conditions

The BTB/POZ domain interacts with an E3 ubiquitin ligase complex, aiding the ubiquitylation of a specific substrate (S) bound via the Kelch propeller domain, resulting in the substrate's proteasome-mediated degradation. Under conditions of cell stress, the interaction of the Kelch-like protein with the substrate is disrupted, allowing the substrate to function. Reproduced from Tilley *et al.*, 2016, with permission from 2016 Elsevier Ltd.

1.6.4 Proteostasis mechanisms of ART resistance

Activation of ART generates free radicals through the cleavage of the endoperoxide bond causing promiscuous alkylation of parasite proteins and, eventually, parasite death. The killing mechanism could be mediated by proteopathy, which is defined as death caused by widespread protein-toxicity. To mitigate ART induced proteopathy, parasites require multiple cellular functions for the removal of misfolded proteins and their replacement by enhancing the protein folding capacity, increasing protein translation, and vesicular expansion mediated dissipation of stress-responsive factors attributed to proteostasis. The proposed mechanisms for ART resistance in *P. falciparum* unify the ER and cytoplasmic proteostasis pathways, involving the phosphatidylinositol-3-phosphate (PI3P) vesicle expansion and upregulation of parasite stress response pathways mediated through the UPR (Haldar *et al.*, 2018; Suresh and Haldar, 2018).

Global transcriptional profiling of ART resistant clinical isolates demonstrated an increase in the transcription of two major parasite chaperone complexes, namely, the reactive oxidative stress complex (ROSC), which is linked to the UPR signaling pathway, and the T-complex protein 1 (TCP1) ring complex (TRiC) of small cytoplasmic chaperonins. The study proposes that increased chaperone complexes have a role in alleviating levels of harmful protein aggregates that accumulate in the ER and cytoplasm following ART activation, which may contribute to the parasite's ART resistance mechanisms (Mok *et al.*, 2015).

PfK13, a predicted substrate adapter of cullin E3 ligase, regulates the expression levels of the protein *PfPI3K*. Wildtype *PfK13* binds to and ubiquitinates *PfPI3K*, facilitating its proteasomal degradation. On the other hand, mutant *PfK13* C580Y undergoes conformational changes that prevent *PfPI3K* ubiquitination and degradation, thereby causing increased levels of *PfPI3K* and its product PI3P. Elevation of PI3P during ART resistance or transgenic expression of HsVPS34, the human homolog of *PfPI3K*, in parasites lacking the *PfK13* mutation results in increased ART resistance, as shown by higher RSA values (Mbengue *et al.*, 2015). Increased PI3P levels lead to amplification of ER-PI3P vesicles, which are dispersed throughout the parasite and are also transported to the host RBC (Figure 1.11a). To unveil the constituents of the PI3P vesicle, biochemical and proteomic analysis of the vesicles were performed (Bhattacharjee *et al.*, 2018). Firstly,

ART resistant parasites with increased ER-PI3P vesiculation displayed *PfK13* on these vesicles. These *PfK13* decorated PI3P vesicles are enriched in proteins involved in folding, quality control, and export. The vesicle proteome shows high overlap with various UPR and oxidative stress responses that are associated with ART resistant field isolates. Additionally, these PI3P vesicles contain *PfBiP* that can enhance the protein folding capacity of the parasite ER and activate the UPR stress sensor PERK. This could lead to the observed phosphorylation of the *PfeIF2 α* in ART resistant parasites, which is followed by translational repression and lowering of general protein synthesis. Additionally, the presence of *PfTRiC* in these PI3P decorated vesicles can enable proper folding of misfolded proteins accumulated in the parasite cytoplasm (Suresh and Haldar, 2018). The parasite degradation system consisting of the ERAD-proteasome and the autophagy pathways, can remove the remaining misfolded proteins from the ER and cytoplasm.

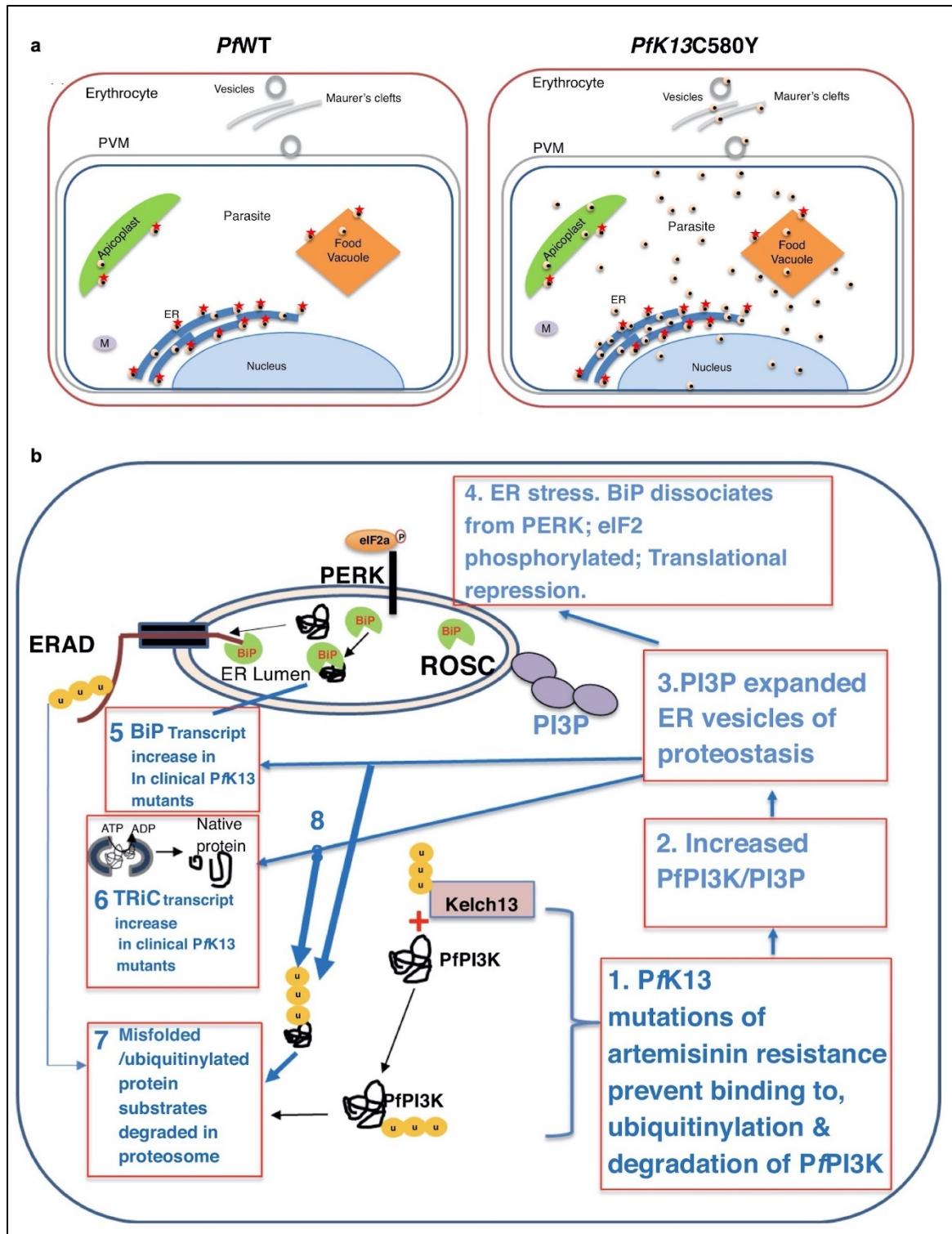


Figure 1.11 Proteostasis mechanisms of ART resistance

(a) Model depicting expansion of PI3P vesicles in sensitive ($K13^{WT}$) and ART resistant ($K13^{C580Y}$) *P. falciparum*. (b) A unifying model depicting proteostasis in the ER and cytoplasm of $K13^{C580Y}$ parasites. Adapted from Suresh and Haldar, 2018, licensed under CC-BY.

Altogether, amplification of PI3P vesicles is proposed to be a major determinant of ART resistance. The model proposed by Suresh *et al.*, (Figure 1.11b) unifies the aforementioned mechanisms to overcome damage caused by protein alkylation and proteopathy, leading to parasite death by proposing expanded ER-vesiculation, the major reason for proteostasis (Suresh and Haldar, 2018).

1.6.5 *P. falciparum* hemoglobin endocytosis pathway mediated ART resistance

The interactome of *PfK13* suggests involvement of a variety of cellular processes. *PfK13* is known to localize adjacent to the parasite cytostomes and interact closely with proteins involved in the endocytosis pathway. The study identified *P. falciparum* Epidermal Growth Factor receptor substrate-15 (*PfEps15*) as an interactor of *PfK13*. In other eukaryotes, the homolog of *Eps15* functions as an ubiquitin receptor that interacts with the Adaptor Protein-2 (AP-2) complex to mediate both clathrin-dependent and independent endocytosis. *PfK13* also interacts with the *P. falciparum* Ubiquitin Binding Protein-1 (*PfUBP1*), a homolog of which is implicated in promoting endocytic recycling in yeasts (Birnbaum *et al.*, 2020). Furthermore, immunoprecipitation and immunofluorescence analyses revealed that proteins from the Rab family GTPase involved in endocytosis and secretion, as well as transport vesicle related proteins, interact with *PfK13* (Gnädig *et al.*, 2020). This indicates a strong association of *PfK13* with proteins of the endocytosis and vesicle transport pathway. The pulldown study results were supplemented with fluorescent microscopic analysis, which established *PfK13* as a part of the parasite endocytosis machinery involved in host hemoglobin uptake (Xie *et al.*, 2020).

A recent study established a link between *PfK13* C580Y mutation and diminished hemoglobin endocytosis by the parasite, proposing another mechanism for ART resistance (Birnbaum *et al.*, 2020). *PfK13* and its associated proteins participate in the parasite hemoglobin endocytosis pathway and thus can regulate the amount of host hemoglobin taken up by the parasite. The study suggests destabilization of *PfK13* that harbors the C580Y mutation, resulting in decreased *PfK13* abundance and reduced availability of heme derived from hemoglobin degradation at the ring stage. Since ART is activated by iron derived from hemoglobin, the diminished availability of hemoglobin results in decreased ART induced proteotoxic stress and parasite killing, thus conferring ART resistance. Additionally, inactivating *PfK13*, particularly at the ring stage, decreased endocytosis and

brought resistant parasites to levels comparable to those with the *PfK13* C580Y mutation (Birnbaum *et al.*, 2020).

The study demonstrates *PfK13* and its associated proteins as regulators of host hemoglobin endocytosis in the parasite, which in turn controls the availability of hemoglobin for degradation and consequently the concentration of activated ART, as depicted in the model (Figure 1.12).

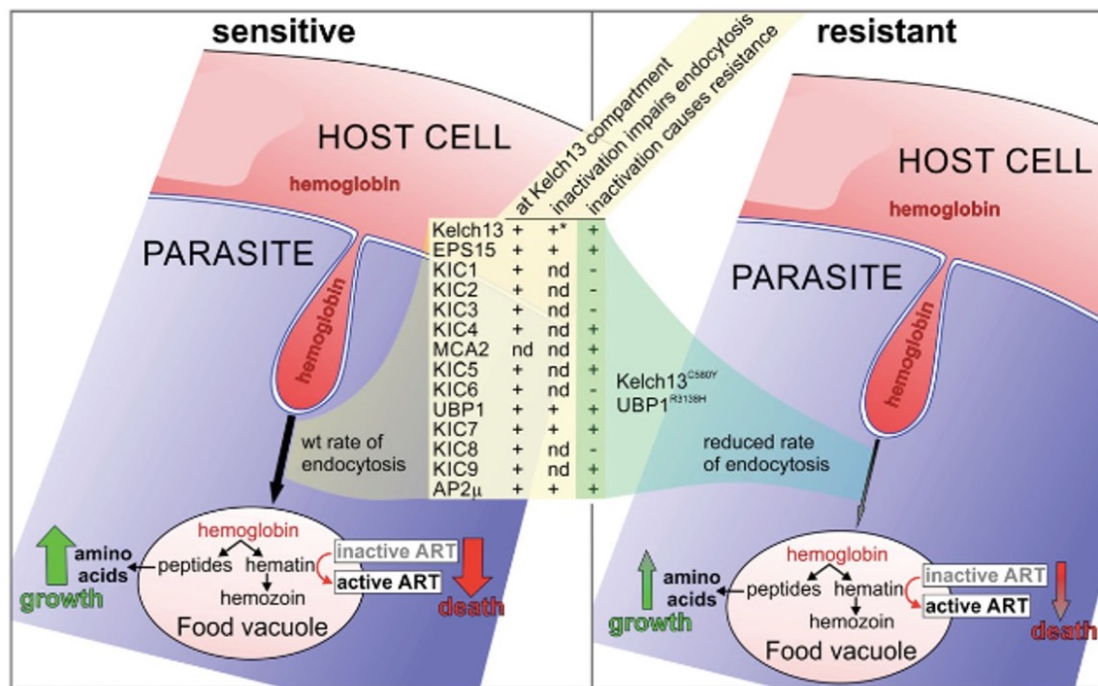


Figure 1.12 Model depicting the mechanism of ART resistance associated with *PfK13* mutations in *P. falciparum*

Mutations in *PfK13* and its associated proteins mediates ART resistance by decreasing endocytosis of host hemoglobin. Reproduced from Birnbaum *et al.*, 2020, with permission from American Association for the Advancement of Science.

1.7 An overview of Autophagy

Organisms rely on continuous synthesis and degradation of cellular components to maintain a proper balance between the organelles, proteins, and metabolites within the cell (Ohsumi, 2014). The process of autophagy is an intracellular degradation pathway that eliminates damaged or unwanted cellular components through the lysosome-mediated

degradation system (Mizushima, 2007). Based on the mechanistic and morphological features, autophagy is classified into macroautophagy, microautophagy, and chaperone-mediated autophagy (CMA). Macroautophagy, subsequently referred to as ‘autophagy’, is the most predominant form of autophagy. It entails the sequestration and transport of damaged organelles and toxic proteins to the lysosomes via double-membrane vesicles (Feng *et al.*, 2014; Yorimitsu and Klionsky, 2005). Microautophagy derives its name from the ‘micro’ sized cytoplasmic segment that is directly engulfed by the lysosome. The cytoplasmic cargo is enwrapped by lysosome membrane invaginations and taken up for degradation (Mijaljica *et al.*, 2011). CMA refers to the chaperone mediated selective degradation of a specific pool of cytosolic proteins. The chaperone Hsp70 recognizes substrate proteins with a particular KFERQ-like sequence (Massey *et al.*, 2004), and the proteins are directly shuttled across the lysosomal membrane (Figure 1.13).

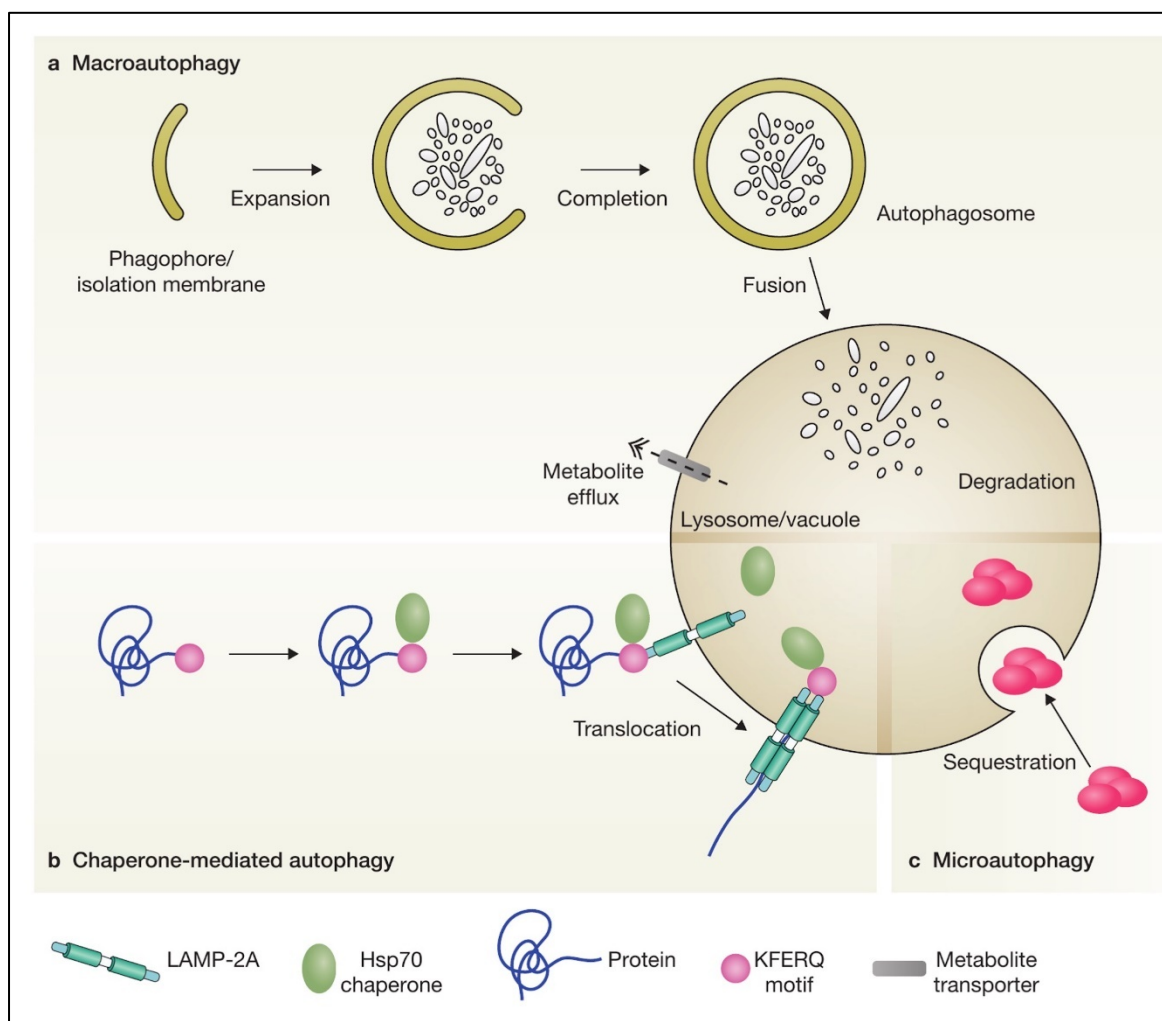


Figure 1.13 Illustration showing the types of autophagy

Different types of autophagy: (a) Macroautophagy, (b) Chaperone-mediated autophagy and (c) Microautophagy. Reproduced from Boya et al., 2013, with permission from 2013, Nature Publishing Group.

1.7.1 The discovery of Autophagy

The term “autophagy” has been in use since the 1860s to refer to the concept of the human body feeding off itself as a means of self-nourishment during times of nutrient deprivation. Almost a century later, the discovery of lysosomes in rat liver cells by Christian de Duve in 1955 allowed the identification of autophagy as a mechanism for delivering intracellular materials to the lysosome for degradation (De Duve *et al.*, 1955, 1963). The process of degradation of intracellular components was initially provided by S Clark, who observed, in addition to lysosomes, amorphous substances and mitochondria within irregularly shaped vacuoles in mouse kidney cells (Clark, 1957; Novikoff, 1959). These substances were subsequently identified as lysosomal enzymes. Shortly after that, Arstila and Trump demonstrated the existence of double membrane-bound structures encapsulating cytoplasmic components and organelles but lacking hydrolytic enzymes. These structures form first and then fuse with lysosomes (Arstila and Trump, 1968). Based on these discoveries, in 1963, Christian de Duve coined “autophagy”, a term derived from the Greek word for “self-eating”, as the process of delivering intracellular components to lysosomes for their degradation (De Duve *et al.*, 1963), in contrast to endocytosis, which encompasses the route taken by particles from outside to the lysosomes.

An understanding of the molecular mechanisms of autophagy facilitated the detection and genetic manipulation of the pathway, culminating in a rapid unravelling of the field. In the late 1990s, genetic screens identified 15 yeast mutants showing defects in protein turnover. This resulted in the identification of the first set of autophagy-related genes (Tsukada and Ohsumi, 1993). Yoshinori Ohsumi and his colleagues made the breakthrough, earning him the 2016 Nobel Prize for elucidating mechanisms underlying the process of autophagy. Following his work, independent genetic screens identified other autophagy-related mutant genes affecting the cytoplasm-to-vacuole targeting (CVTs) pathway, autophagic degradation of peroxisomes, and glucose-induced selective autophagy (GSAs) to mention a few (Harding *et al.*, 1995; Sakai *et al.*, 1998; Yuan *et al.*, 1997). The first autophagy-related (ATG) gene to be identified was ATG1. At present, about 42 ATG genes have been

identified in yeast, the majority of which have homologs in other eukaryotes. 18 of these are classified as ‘core’ autophagy genes, whereas the remainder are involved in certain specific types of autophagy. Deciphering the role of autophagy in human health and disorders such as ageing and longevity, cancer, neurodegenerative diseases, and the innate and adaptive response to pathogens has resulted in significant advancements in autophagy research.

1.7.2 Functional roles of Autophagy

Autophagy is involved in a variety of physiological and pathological roles, including cell survival, intracellular quality control, maintenance of homeostasis, protein transport, anti-aging, cell differentiation and development, innate and adaptive immunity, tumor suppression, and cell death. The diverse roles of autophagy can be attributed to either “induced” or “basal” autophagy. The former acts as an adaptive catabolic process that is initiated in response to various metabolic stresses, whereas the latter performs the routine housekeeping function that eliminates defective proteins and organelles. The broad functions of autophagy have been discussed subsequently (Levine and Kroemer, 2008; Yin *et al.*, 2016).

1.7.2.1 Physiological roles of Autophagy

Quality control and homeostasis: The cell disposes damaged proteins and worn-out organelles via autophagy. Basal autophagy functions at a low level for quality-control mechanism, and is vital for maintaining homeostasis, especially during cell division. As a result, autophagy-deficient mutants in numerous types of cells have a higher amount of abnormal proteins and damaged organelles. The process is also useful for eliminating undesirable organelles, such as peroxisomes and mitochondria, in order to maintain steady-state quantities of these organelles. (Mizushima, 2007).

Development: The ability of autophagy to rapidly respond to external cues, and to alter the intracellular architecture, is crucial for cellular remodelling during organism development. Thus, the inability of autophagy-defective mutants in various model organisms to survive beyond a certain stage demonstrates the significance of this system during development. (Yin *et al.*, 2016).

Cell death: In terms of cell fate determination, there is a substantial interplay between autophagy and apoptosis. Both processes occur downstream of common signals involving the tumor suppressor p53 and BH3-only proteins, which send both internal and external death signals. They also share regulatory components and mutually regulate each other. The process of autophagy precedes apoptosis as the primary response to cellular damage. In case where autophagy is unsuccessful in eliminating the damage, apoptosis is induced by blocking the autophagy pathway (Yin *et al.*, 2016).

1.7.2.2 Pathological roles of Autophagy

Diseases: In addition to maintaining a normal cellular physiology, autophagy plays fundamental role in cellular health. Dysfunction of autophagy has been linked to a variety of pathophysiological conditions, including cancer and neurodegenerative diseases. Among the essential functions of autophagy is the removal of damaged proteins and organelles. Therefore, defects in the process result in accumulation of protein aggregates in neuronal cells, causing diseases such as Parkinson, Alzheimer, and Huntington. Autophagy is also implicated in cancer. In the early stages, autophagy acts as a tumor suppressor by disposing damaged proteins and organelles. However, in the later stages, it functions as a tumor protector by supplying the cancer cells with abundance of nutrients that promote cell survival (Klionsky and Codogno, 2013; Mizushima, 2007).

Ageing and longevity: Cells' ability to perform autophagy reduces significantly with age. Studies in human cells, rodents, and *C. elegans*, have indicated an age-related reduction in lysosomal function, which inhibits autophagic flux. Short lived *S. cerevisiae* mutants, when screened for age related factors, identified several ATG null mutants including ATG1, ATG18, ATG7 and Beclin1. ATG knockouts mice are not viable upon arrival in the postnatal period. Ageing in drosophila is also associated with decreased expression of various ATG genes (Aman *et al.*, 2021; Rubinsztein *et al.*, 2011).

1.7.3 Molecular mechanism of Autophagy

The most important phase in the autophagic process is the sequestration of a portion of the cytoplasm by a new double-membrane compartment called the "autophagosome". A series of dynamic events leads to the formation of an autophagosome, which includes the development of a membrane sac (phagophore) that extends on both sides, culminating in a

cup-shaped structure that seals, forming a double membrane autophagosome enveloping a part of the cytoplasm. The fusion of the autophagosome with the lysosome results in the formation of a single-membrane vesicle called the “autolysosome”, which is degraded by lysosomal hydrolases. The degradation products, such as amino acids, are exported to the cytoplasm and repurposed as a source of energy or in the synthesis of macromolecules (Ohsumi, 2014).

The field of autophagy has witnessed extensive research efforts, which have resulted in a detailed understanding of the functions of the core ATG proteins. In yeast cells, their functions are categorized into six distinct complexes: the ATG1 kinase complex, the ATG14-containing class III phosphoinositide 3-kinase (PI3K) complex I, the PI3P-binding ATG2-ATG18 complex, the ATG5-ATG12 conjugation system, the ATG8 conjugation system, and the integral membrane protein ATG9 (Figure 1.14). The process of autophagy involving the participation of these core ATG proteins can be divided into several sequential steps: induction and nucleation, expansion, maturation, fusion, degradation and efflux (Kirkin, 2020; Mizushima, 2018; Yin *et al.*, 2016). Following sections discuss the various autophagy events and the machinery involved.

Induction and nucleation:

Physiological stress stimuli such as nutrient deprivation or treatment with pharmacological molecules trigger an intracellular signaling cascade that results in the onset of autophagy. The target of rapamycin complex 1 (TORC1) detects the decrease in nutrient availability and inhibits the activity of TOR, a negative autophagy regulator. In yeast, the core ATG proteins assemble at the phagophore assembly site (PAS) thereby commencing phagophore nucleation. The ATG1 kinase, regulatory protein ATG13 and the scaffolding ternary subcomplex consisting of ATG17, ATG31, and ATG29 comprise the initiation complex recruited to the PAS (Figure 1.14). While the exact membrane source for PAS is uncertain, several intracellular compartments have been identified as its probable source. These include the ER, Golgi, ER-Golgi intermediate compartment, mitochondria, plasma membrane, and recycling endosomes (Delorme-Axford *et al.*, 2015). Further, the recruitment of ATG proteins to the PAS is crucial for phagophore expansion. The class III PI3K complex I consisting of the lipid kinase Vps34, Vps15, ATG6, ATG14, and ATG38 is recruited to the PAS after autophagy induction. At the PAS, Vps34 generates PI3P from

PI which is essential for accurate localization of the ATG18-ATG2 complex (Figure 1.14). This complex then recruits ATG8, ATG9, and ATG12 to the PAS (Yin *et al.*, 2016).

Expansion:

The ATG12 and ATG8 ubiquitin-like (Ubl) conjugation systems are involved in the expansion of the phagophore membrane. Both ATG12 and ATG8 are structurally similar to ubiquitin but are not homologs. ATG12 forms a Ubl conjugation with ATG5 which is mediated by ATG7, an E1-like enzyme, and ATG10, an E2-like enzyme. This conjugation recruits a small coiled-coil protein ATG16 forming the multimeric ATG12–ATG5–ATG16 complex. In yeast and high eukaryotes, ATG12-ATG5 conjugation occurs constitutively and permanently. A different type of conjugation attaches another Ubl protein, ATG8 to the lipid phosphatidylethanolamine (PE). The formation of ATG8–PE involves the protease ATG4, which exposes the C-terminal glycine of ATG8. The E1 and E2-like enzymes ATG7 and ATG3, respectively and the ATG12–ATG5–ATG16 complex which functions as an E3-like enzyme (Figure 1.14), accelerate ATG8 conjugation (Geng and Klionsky, 2008; Yin *et al.*, 2016).

Additionally, the transmembrane protein ATG9 is involved in elongation of the phagophore. ATG9 recycles between the PAS and peripheral sites which serve as membrane sources for the PAS. ATG9 multimerizes with other ATG proteins including ATG11, ATG23, and ATG27 which aid in the anterograde transport of ATG9 from the membrane sources to the PAS (Figure 1.14). The retrograde transport from PAS to the peripheral sites is mediated by the ATG1 initiation complex. The ability of ATG9 to traffic and multimerize contributes towards recruiting membrane for phagophore expansion and is thus crucial for autophagosome formation (Parzych and Klionsky, 2014).

Maturation and fusion:

The expanding phagophore matures and closes to form the double membrane autophagosome. It subsequently tethers/docks and fuses with the vacuole (in yeast and plant cells) or lysosome (in metazoans), forming the autolysosome. Autophagosomes can also fuse with endosomes forming “amphisomes” which are then fused with vacuoles/lysosomes. The docking and fusion involve SNARE proteins such as VAM7, VAM9, and syntaxin 17. The outer membrane of the autophagosome fuses with the

vacuole, while the inner membrane along with the cytoplasmic materials is released into the vacuolar/lysosome lumen (Parzych and Klionsky, 2014; Yin *et al.*, 2016).

Degradation and recycling:

Upon delivery of the cargo inside the vacuole/lysosome, the autophagosome membrane is degraded by ATG15, a putative lipase, leading to degradation of the cytoplasmic materials by the resident hydrolases. Macromolecules generated during cargo degradation are released into the cytosol by the help of various permeases including ATG22 (Yin *et al.*, 2016).

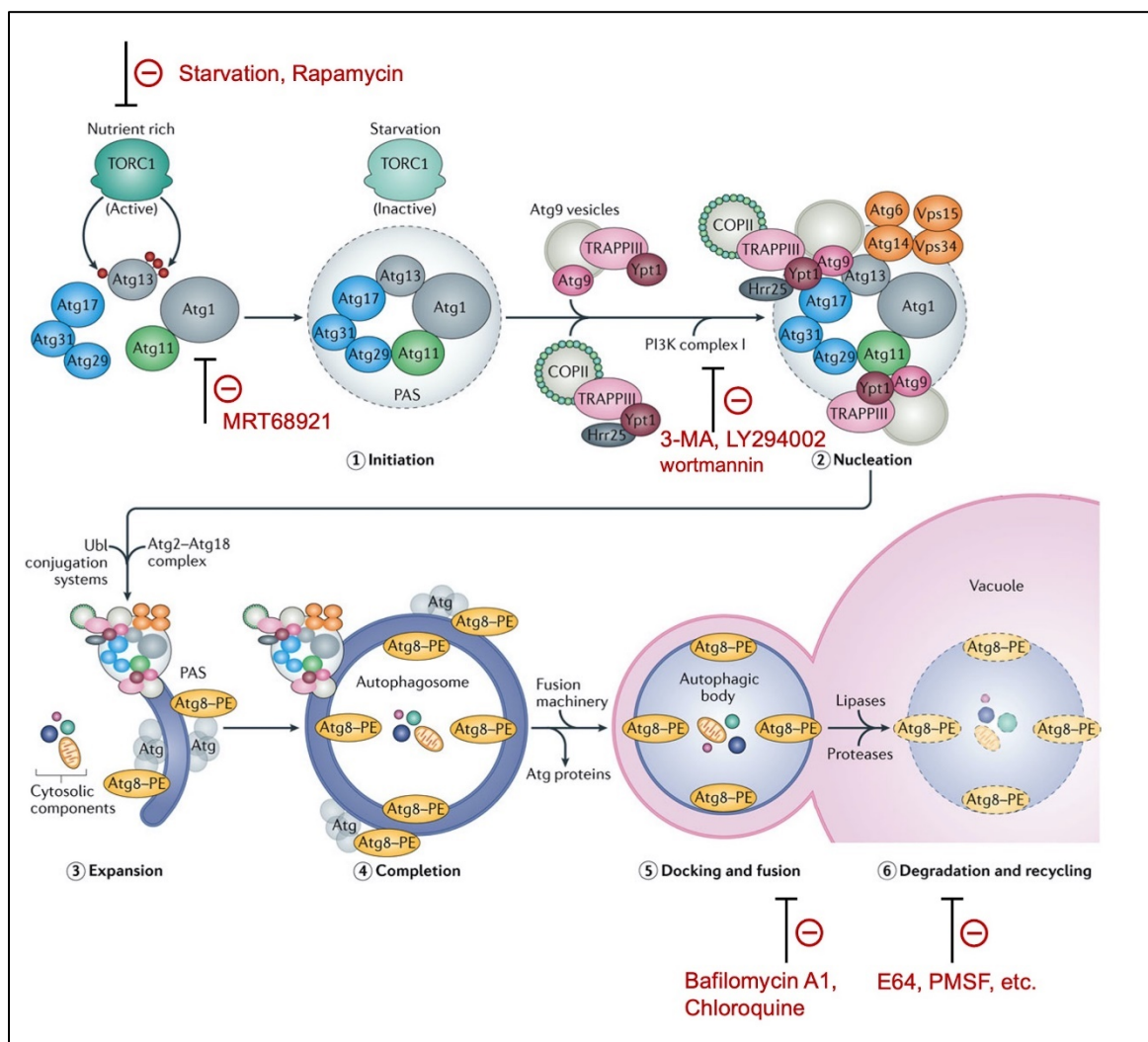


Figure 1.14 Schematic showing the mechanism of autophagy and modulators of the pathway

The mechanical properties of autophagy and the protein machinery. The autophagy activators and inhibitors, as well as the autophagy steps influenced by these modulators, are listed. Adapted from Farré and Subramani, 2016, with permission from 2016, Nature Publishing Group.

1.7.4 Modulation of the autophagic flux

Autophagosomes are formed as an intermediary structure in the autophagy process. An equilibrium between the rate of autophagosome generation and degradation inside the vacuole is referred to as the autophagic flux. Induction of the autophagic flux is mediated through amino acid starvation, mTOR inhibitor rapamycin, and ER stress inducers such as Thapsigargin, Brefeldin A, and Tunicamycin. It is reduced when autophagy is inhibited upstream of autophagosome formation using ATG1 inhibitor MRT68921 and PI3K inhibitors such as 3-methyladenine (3-MA), wortmannin, and LY294002. The vacuolar-type H⁺-ATPase inhibitor Bafilomycin A1 inhibits autophagy following autophagosome formation, resulting in a decrease in autophagic flux but an accumulation of autophagosomes in the cytosol and an increase in autophagosome number. Chloroquine and hydroxychloroquine, lysosomal lumen alkalizers, limit lysosomal function, resulting in a decrease in autophagic flux but an increase in autophagosome number, similar to Bafilomycin A1 therapy. Acid protease inhibitors like Leupeptin, E64d, and Pepstatin A stop autophagosome components from degrading (Figure 1.14) (Mizushima *et al.*, 2010; Yang *et al.*, 2013; Yin *et al.*, 2016).

1.7.5 Signaling pathways regulating Autophagy

Autophagy plays an important role in maintaining cellular homeostasis as well as survival under a wide range of stress conditions such as nutrient deprivation, absence of growth factors, hypoxia, oxidative and ER stress. Thus, the process of autophagy requires regulation at various stages to avoid either excessive or inadequate activity. Numerous studies have focused on how autophagy is maintained at low levels during normal conditions and its induction/downregulation upon exposure to various stimuli. A well-defined regulatory network has been found to modulate the activity of the autophagy pathway in response to both extracellular and intracellular stresses (Yin *et al.*, 2016).

The TOR kinase and the cAMP-dependent protein kinase A (PKA) are involved in sensing nutrient starvation. TOR is a negative regulator of autophagy that senses and integrates

several environmental signals to prevent catabolism and coordinate cell growth. During nutrient-rich conditions, the TOR kinase phosphorylates ATG1 and ATG13, preventing the formation of the ATG1-ATG13-ATG17-ATG31-ATG29 complex and thus suppressing activation of autophagy. Upon amino acid starvation or treatment with rapamycin, a TOR inhibitor, ATG13 is rapidly dephosphorylated which increases its binding with and activation of ATG1 and subsequent induction of the autophagy process. Given its role in energy/glucose dependent regulation, PKA is activated in the presence of glucose. Activated PKA phosphorylates ATG1 and ATG13, thus preventing autophagy activation. Additionally, PKA can suppress autophagy by indirectly activating the TOR kinase via inhibition of the AMP-activated protein kinase (AMPK). AMPK is another energy-sensing kinase that responds to intracellular levels of AMP and ATP to regulate autophagy. Decreased energy levels activate AMPK, which is a negative regulator of TOR and acts by inhibiting activity of the TOR kinase, hence inducing the autophagy pathway (Parzych and Klionsky, 2014; Yin *et al.*, 2016).

ER stress can also trigger the process of autophagy by activating the three regulators of the UPR signaling pathway (IRE1, ATG6 and PERK), in addition to releasing ER resident Ca^{2+} into the cytoplasm, which, in turn, activates AMPK that inhibits TOR. Additional signals that induce autophagy include hypoxia and the unavailability of growth factors, both of which partially regulate autophagy via TOR. Thus, involvement of TOR in the regulatory mechanism of autophagy marks its importance in the study of this pathway (Høyer-Hansen and Jäättelä, 2007; Parzych and Klionsky, 2014; Yin *et al.*, 2016).

1.7.6 Role of Phosphatidylinositol 3-phosphate in Autophagy

Phosphatidylinositol 3-phosphate (PI3P) is a phospholipid found in cell membranes that aids in the recruitment of a variety of proteins to the membranes, the majority of which are involved in protein trafficking (Gillooly *et al.*, 2001). PI3P and its effectors participate in several aspects of autophagy, including the biogenesis, maturation, and intracellular trafficking of autophagosomes. Studies have proposed local PI3P synthesis on the isolation membrane, promotes its negative curvature and regulates autophagosome size. In mammalian cells, PI3P production has also been observed on the elongating isolation membrane tips, and it has been postulated that this process facilitates the expansion and sealing of the edges of the membrane. The majority of hypotheses, however, explain PI3P's

actions through effector proteins having PI3P-binding motifs, such as the FYVE, PX, or WD40 domains. Additionally, localized PI3P synthesis has been proposed as a means of establishing a membrane platform for concentrating and spatially coordinating particular effectors required for downstream signal transduction and autophagy progression (Dall'Armi *et al.*, 2013).

Numerous PI3P effectors have been shown to be involved in the initiation of autophagy. In mammalian cells, PI3P effector proteins include the PROPPIN family of WD-repeat proteins that interact with phosphoinositides. The PROPPIN family is characterized by its WD40 repetitions, which contain a seven-bladed β -propeller fold and feature two pseudo-equivalent PI3P binding sites as well as a FRRG motif essential for the PROPPIN family to perform autophagic functions. The WIPI-1, and 2 PROPPINs are implicated in the induction of autophagy in mammals. WIPI-1 and WIPI-2 are recruited to membrane sources during autophagy initiation and are involved in the development and maturation of the isolation membrane, respectively. These two proteins are phylogenetically related to yeast ATG18, which has also been implicated in the initiation stage, albeit more indirectly through the shuttling of ATG9 and ATG2 in both the Cvt and autophagy pathways. Additional PI3P effectors involved in the initiation stage have been identified, in yeast, including ATG21 and YGR223c (Dall'Armi *et al.*, 2013).

1.7.7 Selective Autophagy

Activation of autophagy during conditions of nutrient and energy deprivation or metabolic perturbations is essentially non-specific, and can be mediated by recycling components of the cytoplasm via the bulk degradative pathway. Autophagy can also be highly selective to facilitate cellular homeostasis by removing damaged or excess components before they become toxic to the cells. Selective autophagy involves the presence of degradation cues, and involvement of selective autophagy receptors that enable ATG proteins to recognize their cargo. The yeast Cvt pathway is the best characterized selective autophagy-like mechanism, utilizing the core ATG machinery to deliver a precursor form of the hydrolase, aminopeptidase I, to the vacuole (Yin *et al.*, 2016).

Several types of selective autophagy have been studied so far, including specific autophagic cargoes such as mitochondria, peroxisomes, ER, bacterial pathogens, and ubiquitinated

proteins. Degradation of peroxisomes through autophagy, termed pexophagy, is initiated under normal growth conditions to maintain the organelle turnover in the cells. As peroxisomes are involved in a number of metabolic functions in the cell, dysfunction of the organelle negatively affects human health. Thus, the role of pexophagy is important in maintaining adequate cellular physiology. Another form of selective autophagy with mitochondria as the cargo is termed mitophagy. It involves selective degradation of the mitochondria in order to sustain steady-state turnover of the organelle, the development and remodelling of certain cell types as well as clearance of worn-out mitochondria. Damaged ER or accumulation of excess ER chaperones and membrane is degraded through the process of ER-phagy. Cells also utilize autophagy to precisely target ubiquitin-tagged proteins. Xenophagy refers to a process by which intracellular bacteria are targeted by ubiquitin-binding proteins for degradation in the autolysosomes. Aggregates of ubiquitinated proteins are also cleared through the process of aggrephagy. Overall, cells utilize the processes of selective autophagy for maintaining cellular homeostasis, and consequently, the organismal health (Parzych and Klionsky, 2014).

1.8 Interplay between ER stress and Autophagy

Under ER stress, signals from the ER stimulate autophagy to either help cells cope with ER stress or participate in the mechanism of non-apoptotic cell death. Intracellular Ca^{2+} released from the ER lumen in response to stress, activates the calmodulin-dependent kinase beta ($\text{CaMKK}\beta$)/AMPK dependent pathway. Thus, TOR inhibition on the ATG1 complex is relieved leading to autophagy initiation. Additionally, ER stress mediated activation of the UPR signaling transducers regulates autophagy at various stages in the process, in particular, induction, nucleation, and elongation. Accumulation of misfolded proteins in the ER lumen stimulates oligomerization and autophosphorylation of IRE1. Activated IRE1 promotes autophagy by releasing free Beclin-1, the mammalian homolog of yeast ATG6, from the Beclin-1/Bcl-2 complex, to form a complex with Vps34 and initiate nucleation of the autophagy isolation membrane. In addition, splicing of the X-box binding protein-1 (XBP-1) transcription factor by IRE1 triggers transcription of Beclin-1 thus inducing autophagy. The activation of PERK reduces global protein translation through $\text{eIF2}\alpha$ phosphorylation along with enabling translation of ATF4. ATF4 increases transcription of ATG12 and activates the C/EBP-homologous protein (CHOP) which promotes the transcription of ATG5. ATG5 and ATG12, form a complex with ATG16

which positively regulates the autophagy elongation process. ER stress also activates the third arm of the UPR, the ATF6 transcription factor, to indirectly activate CHOP and induce autophagy (Figure 1.15) (Carreras-Sureda *et al.*, 2018; Song *et al.*, 2018).

Electron microscopy studies from the 1980s first revealed the presence of dilated ER in autophagic vacuoles within cells (Clarke, 1990). Later, a direct link between ER stress and induced autophagy was provided by treating yeast cells with known ER stressors, such as, dithiothreitol (DTT) which inhibits the formation of disulfide bonds or tunicamycin that inhibits N-glycosylation. Both DTT and tunicamycin activated the UPR pathway and increased the kinase activity of ATG1 along with formation of PAS thus inducing the ATG-dependent autophagy process (Yorimitsu *et al.*, 2006). Autophagy mediated selective turnover of the ER plays a critical role in the maintenance of ER homeostasis. Following are details of the types of selective autophagy that are induced upon ER stress.

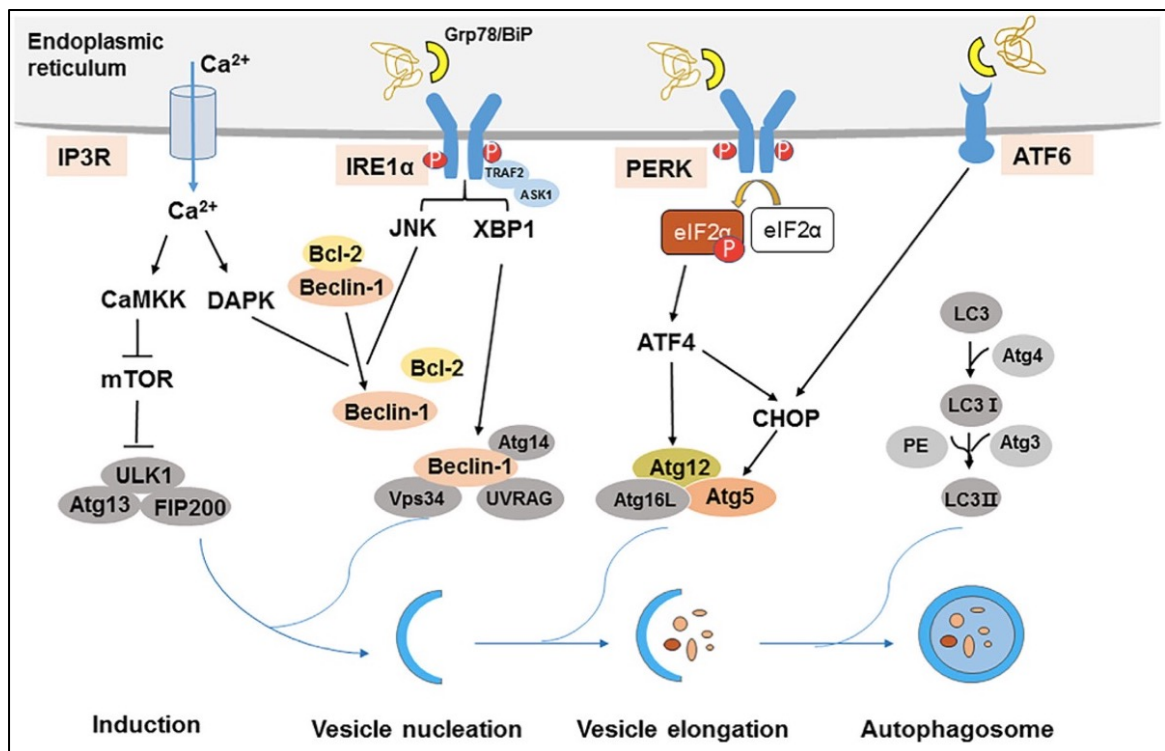


Figure 1.15 Schematic representation of the mechanisms of ER stress mediated autophagy

Autophagy can be induced by ER stress through IRE1 α , PERK, ATF6, and Ca²⁺ signaling pathways. Reproduced from Song *et al.*, 2018, with permission from 2017 Wiley Periodicals, Inc.

1.8.1 ER-phagy

During ER stress, the ER is selectively delivered to and degraded inside the lysosome via a process known as ER-phagy. ER homeostasis relies on specific ER-resident protein receptors, that directly bind to ATG8/LC3 via an LC3-interacting region (LIR)/ATG8-interacting motif (AIM), leading to selective elimination of the ER.

ER-phagy is induced in budding yeast *S. cerevisiae* by overexpression of integral membrane proteins, suppression of TOR in response to nitrogen deficiency, or incubation with rapamycin. Receptors controlling the transport of ER portions harboring excess membrane proteins to the digestive vacuole in yeast have not been identified. By contrast, ER-phagy receptors have been identified and characterized for rapamycin and starvation induced ER-phagy. The ATG8-binding proteins ATG39 and ATG40 label the ER and nuclear envelope membrane that are to be delivered to the yeast vacuole for clearance. The reticulon-homology domain (RHD) in ATG40 is crucial for membrane shaping and facilitating ER fragmentation. Both ATG39 and ATG40 contain an AIM, which facilitates their interaction with the membrane-bound ATG8 (Grumati *et al.*, 2018).

FAM134B (family with sequence similarity 134) is a member of the FAM134 reticulon protein family in higher eukaryotes such as mammals. It has a RHD motif that promotes ER membrane curvature, as well as a LIR motif that aids in binding to the LC3 present on the phagophore membrane. This suggests that FAM134B functions as an ER-phagy receptor. FAM134B mediated ER degradation increases in cells under nutrient starvation. RTN3 is another ER-phagy receptor that becomes more active upon starvation. It is a member of the RHD-containing proteins (RTN1–4), that are involved in membrane curvature in the tubular ER. The N-terminal cytosolic region of the protein includes six LIRs that interact with LC3. Cell-cycle progression gene 1 (CCPG1) acts as an ER-phagy receptor upon induction of ER stress. Endogenous CCPG1 is activated in response to ER stress that brings about autophagic degradation of the peripheral ER (Grumati *et al.*, 2018).

1.8.2 RecovER-phagy

The process involves selective delivery of ER components to the autolysosomes for clearance upon resolution of ER stress. During ER stress, the signaling sensors direct the UPR to increase production of ER-resident chaperones to reduce the load of misfolded

proteins in the ER lumen. Inability of UPR to restore normal ER functions can lead to activation of cell death responses (Walter and Ron, 2011). Thus, upon resolution of ER stress, a recovery phase is required to restore ER homeostasis. The recovery phase, known as recoverER-phagy, entails reestablishing the pre-stress levels ER chaperones (Fumagalli *et al.*, 2016). The ER transmembrane protein SEC62 (Secretory Protein 62), is part of the ER translocation complex and is involved in the import of newly synthesized proteins into the ER lumen. SEC62 has been shown to participate in the process of recoverER-phagy. It harbors a LIR motif in its C-terminal cytosolic domain, that facilitates its association with LC3 present on the autophagosomes (Figure 1.16). SEC62 is believed to exit the ER translocon complex prior to its participation in recoverER-phagy, which is functionally distinct from protein translocation (Fumagalli *et al.*, 2016; Grumati *et al.*, 2018).

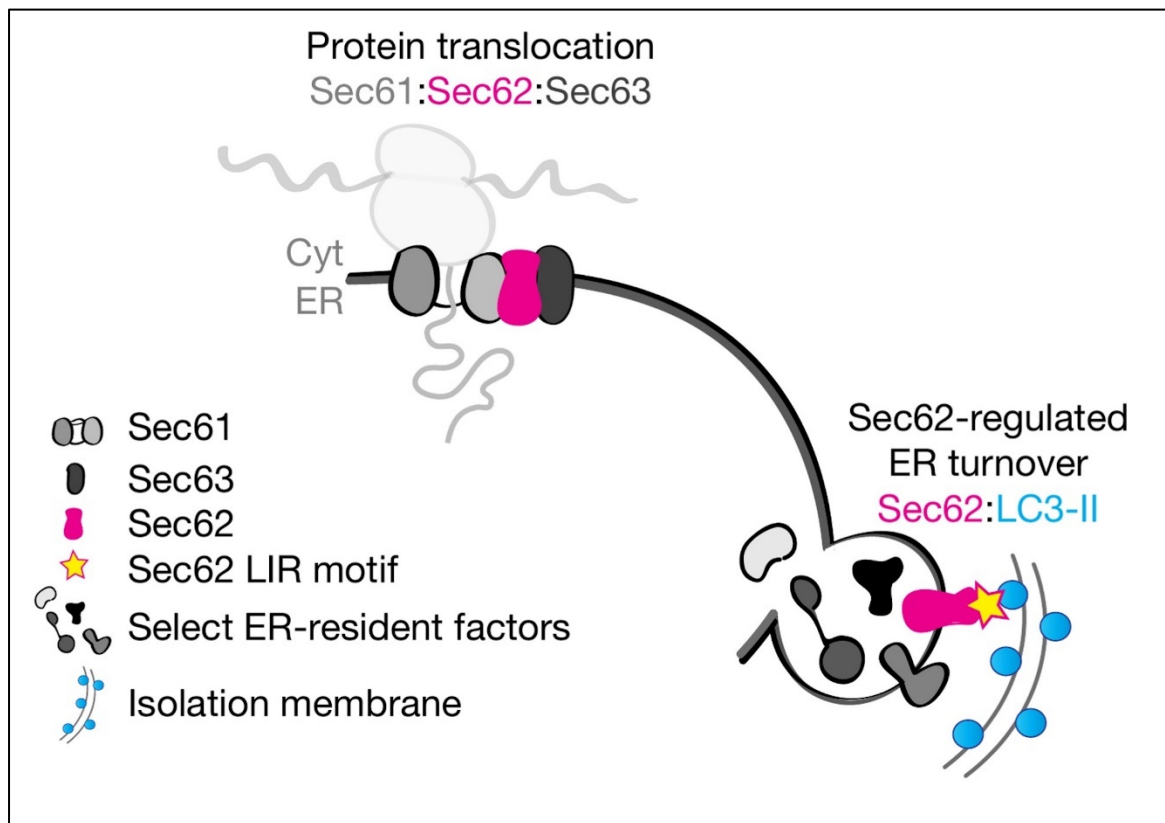


Figure 1.16 Schematic representation of the role of SEC62 in protein translation and recoverER-phagy process

Translocon component SEC62 as a component of the protein translocon machinery and as an autophagy receptor present on the ER membrane. Reproduced from Fumagalli *et al.*, 2016, with permission from 2016, Nature Publishing Group.

1.9 The Autophagy machinery in *P. falciparum*

Each year, millions of individuals worldwide are infected with the protozoan parasite *P. falciparum*, resulting in thousands of fatalities (WHO, 2020). Throughout its intraerythrocytic life cycle, the parasite experiences heat, nutritional, ER, oxidative, and other stressors (Babbitt *et al.*, 2012; Chaubey *et al.*, 2014; Engelbrecht and Coetzer, 2013) and undergoes differentiation, which involves degradation of stage-specific organelles and proteins (Cervantes *et al.*, 2014). In yeast, over 42 autophagy-related proteins have been identified till date, but only a small number of ATG proteins are conserved in *P. falciparum* (Table 1.2). Dissecting the autophagy-like pathway and its function in stress responses would give vital insights into mechanisms that contribute to survival and homeostasis, which would aid in the development of novel antimalarial therapies.

Stage of autophagy	<i>S. cerevisiae</i> homolog	<i>P. falciparum</i> homolog	Identity with <i>S. cerevisiae</i> homolog
Induction	ATG1	PF3D7_1450000	2.40e-22
	ATG13		
	ATG17	PF3D7_1120000	1.4e-10
	ATG29		
	ATG21		
Nucleation	Vps34	PF3D7_0515300	8.50e-75
	Vps15	PF3D7_0823000	2.2e-14
	Vps30/ATG6		
	ATG14		
IM Assembly/ATG9 cycling	ATG2	PF3D7_1320000	0.0034
	ATG18	PF3D7_1012900	5.1e-31
	ATG9		
Vesicle expansion and completion	ATG4	PF3D7_1417300	4.5e-09
	ATG8	PF3D7_1019900	3.10e-24
	ATG3	PF3D7_0905700.1	3.30e-40
	ATG7	PF3D7_1126100	4.0e-09

	ATG10		
	ATG12	PF3D7_1470000	3.4e-09
	ATG16		
	ATG5	PF3D7_1430400	3.3e-05

Table 1.2 Conserved Autophagy proteins in *P. falciparum*
Adapted from Navale et al., 2014, licensed under CC-BY.

Bioinformatic analyses have identified a few autophagy-related genes in *P. falciparum*. Although multiple hits for the autophagy master regulator TOR have been found, these findings are more closely related to Phosphatidylinositol 4-Kinases (PI4K). In yeast, ATG1 and ATG17, in conjunction with ATG13, constitute the autophagy initiation complex. Bioinformatically, homologs of yeast ATG1 and ATG17 have been identified in the malaria parasite, however ATG13 seems to be absent. The putative *Pf*ATG1 has a conserved kinase domain but lacks the ATG13 binding motif, probably due to the absence of ATG13 in the parasite. In yeast and humans, *Pf*ATG1 includes many putative ATG8-interacting motifs that facilitate ATG1 binding to ATG8 in an ATG13-independent manner. Further, functional investigations are required to determine whether the identified ATG1 homolog in *P. falciparum* functions in a similar manner to that of yeast or human ATG1/ULK1. The components of yeast PI3K complex, VPS34, VPS15, ATG6, and ATG14, appear to be present in the parasite. While *Pf*Vps34 is a well-characterized protein found in *P. falciparum*, Vps15 and ATG14 have been identified but remain uncharacterized. However, the parasite does not have any ortholog of ATG6. ATG9, a transmembrane protein needed for membrane recycling, is not conserved in *P. falciparum*. ATG18 has a homolog in the malaria parasite which is predicted to have a WD repeat motif that folds into a conserved seven-bladed β -propeller structure. *Pf*ATG18 also has a conserved PI3P-binding motif (FRRG), due to which it has been identified as a PI3P effector in parasites (Bansal *et al.*, 2017; Hain and Bosch, 2013; Navale *et al.*, 2014). A possible homologue of ATG18's binding partner, ATG2, was also identified in *P. falciparum* (Figure 1.17), but is currently annotated as a putative rhoptry protein (Hallée *et al.*, 2018).

Proteins such as, ATG8, ATG3, ATG4, and ATG7, essential for the ATG8 conjugation system, are conserved in the malaria parasite. *PfATG8* has a glycine residue at the C-terminus, much like other apicomplexan parasites including *Toxoplasma* and *Trypanosoma* (Hain and Bosch, 2013). As a result, the putative ATG4 orthologue is probably critical for recycling misconjugated ATG8. *PfATG7* is a parasite-specific E1-like enzyme that interacts with *PfATG8* (Cervantes *et al.*, 2014). ATG3, a protein similar to E2, is found in the genome of *P. falciparum* and contains an LIR motif. The structure of the ATG8-ATG3 complex in this parasite has been determined, revealing that *PfATG3* has an extra loop that is not found in human ATG3 (Figure 1.17). Thus, *PfATG3* has been recommended as a therapeutic target against *P. falciparum* (Hain *et al.*, 2012, 2014, 2016).

P. falciparum genome contains homologs of ATG5, ATG12, and ATG16, however ATG16 is not present. Due to the fact that *PfATG5* is larger than its yeast and mammalian counterparts, BLAST analysis reveals a lack of identity (Brennand *et al.*, 2011; Duszenko *et al.*, 2011; Hain and Bosch, 2013; Rigden *et al.*, 2009). Recently studies have shown that during the evolution of apicomplexans like *Toxoplasma* and *Plasmodium*, as well as certain yeast species like *Komagataella phaffii* (*Pichia pastoris*), the interaction between ATG5 and ATG12 shifted from covalent to non-covalent. The C-terminal glycine residue in both ATG12 and E2-like enzyme ATG16 is required for covalent binding, but is missing in these species. This non-covalent ATG12-ATG5 complex may enable ATG8-PE conjugation, thus suggesting the evolution of the ubiquitin-like covalent conjugation into a more straightforward non-covalent interaction (Pang *et al.*, 2019). *P. falciparum* also expresses Rab7 and SNAREs which are necessary for autophagosome-lysosome fusion. ATG15, the lipase responsible for degrading the autophagosome membrane, and Prb1, the vacuolar proteinase, are absent in *P. falciparum*. The parasite's FV, on the other hand, contains multiple falcipain enzymes involved in hemoglobin degradation. Additionally, ATG22, the amino acid efflux pump on eukaryotic lysosomes, is identified (Figure 1.17) (Hain and Bosch, 2013).

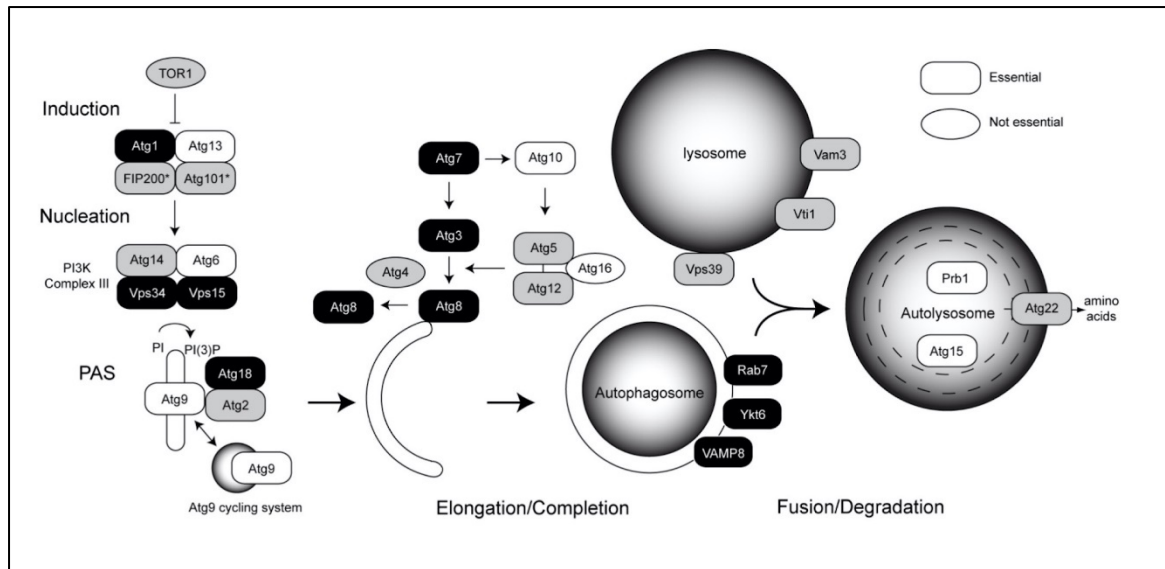


Figure 1.17 Schematic representation of the conservation of the autophagy machinery in *P. falciparum*

Black box indicates strong evidence for homology; grey box indicates less clear homology and white box indicates no ortholog identified in *P. falciparum* by BLAST analysis. Reproduced from Hain and Bosch, 2013, licensed under CC-BY.

1.9.1 Role of Autophagy-related proteins in *P. falciparum*

Malaria parasites undergo several morphological and functional changes during their life cycle, encompassing 15 functionally distinct stages. Autophagy has been implicated in critical stages of parasite development, including the removal of micronemes during the differentiation of sporozoites to merozoites in liver stage parasites (Jayabalasingham *et al.*, 2010). Since ATG8 is associated with both premature and mature autophagosomes and the amount of lipidated ATG8 correlates with the number of autophagosomes, it is frequently used as an autophagosome marker (Kitamura *et al.*, 2012). Concomitantly, ATG8 present in *P. berghei* (*PbATG8*), the species of *Plasmodium* that infects rodents, has been shown to colocalize with the apical microneme before its expulsion from the RBC, thus assisting in parasite remodelling and mediating differentiation. A slight increase in expression levels of *PbATG8* results in the formation of immature merozoites incapable of causing blood stage infection (Voss *et al.*, 2016). Similarly, autophagy may play a role in the differentiation of blood stage parasites to gametocytes, as shown by a decrease in the amount of *PfATG8*-labelled structures in the gametocyte stage (Cervantes *et al.*, 2014). Additionally, when the baseline level of autophagy is blocked by MRT68921 or 3-MA, the

parasite's viability and capability to invade fresh RBC diminish, suggesting that basal autophagy is required for *P. falciparum* growth (Joy *et al.*, 2018).

PfATG8, *PfATG18* and *PfATG5* have also been implicated in the canonical autophagy-like pathway in the parasite. Expression levels of *PfATG8* and *PfATG18* increase in response to autophagy induction by brief starvation and decrease to baseline levels upon incubation with the autophagy inhibitor 3-MA. Additionally, it has been demonstrated that *PfATG8*, *PfATG18*, and *PfATG5* are present on autophagosome-like structures during normal growth conditions and their levels increase with autophagy induction (Agrawal *et al.*, 2020; Joy *et al.*, 2018).

1.9.1.1 Involvement in parasite apicoplast biogenesis

The apicoplast is a relict, non-photosynthetic plastid present in the majority of apicomplexans. The apicoplast includes enzymes that are involved in the production of type II fatty acids, which are essential for isoprenoid biosynthesis, as well as in the heme biosynthetic pathway (Surolia and Surolia, 2001; Wilson, 2005). Tetracyclines have been demonstrated to impede apicoplast protein translation, resulting in the loss of apicoplast and death of the parasite during the second replication cycle, a phenomenon termed as “delayed death” (Dahl *et al.*, 2006).

Numerous reports suggest *PfATG8* plays a non-canonical role in apicoplast biogenesis. Under normal growth conditions, partial localization of ATG8 with the apicoplast has been observed in *P. berghei* and *P. falciparum*. The protein is also required for apicoplast branching and segregation throughout the asexual developmental stages (Cervantes *et al.*, 2014; Jayabalasingham *et al.*, 2010; Kitamura *et al.*, 2012; Tomlins *et al.*, 2013). As a consequence, knockdown of *PfATG8* inhibits parasite growth during the second replication cycle, which is associated with the delayed death phenomena, owing to loss of apicoplast (Walczak *et al.*, 2018). Additionally, it has been shown that an OTU-like cysteine protease is essential for apicoplast maintenance and controls the deconjugation of *PfATG8* from the apicoplast membrane (Datta *et al.*, 2017).

PfATG18 is also involved in apicoplast biogenesis, and its depletion leads to the loss of apicoplast, which is reflected in growth attenuation in the second replication cycle of the

parasite. *PfATG18* is also suggested to influence the association of *PfATG8* with the apicoplast membrane (Bansal *et al.*, 2017). Further, involvement of *PfATG18* in the parasite autophagy-like pathway is not influenced by its role in apicoplast biogenesis, as localization of *PfATG18* on autophagosome-like structures is unaffected by the absence of apicoplast. Given that *PfATG8* knockdown had no effect on *PfATG18* localization, *PfATG18* may operate upstream of *PfATG8* (Agrawal *et al.*, 2020).

1.9.1.2 Role in maintenance of parasite vacuolar homeostasis trafficking pathway

Vacuoles are involved in a wide range of biological processes, including degradation of cellular components, maintaining cellular homeostasis, storing ions and metabolites, transporting nutrients and regulating growth through the cell cycle (Li and Kane, 2009). Yeast frequently experiences nutrient deprivation and osmotic stress. The cell maintains homeostasis by rapidly altering the vacuolar morphology through vacuole fission or fusion in response to changes in the intracellular ion and water concentrations (Mijaljica *et al.*, 2007). ATG18 is involved in maintenance of vacuolar homeostasis. Yeast strains devoid of ATG18 have an abnormally large vacuole. Binding of ATG18 with PI3P and phosphatidylinositol 3,5-bisphosphate (PI(3,5)P₂) assists its localization to the yeast vacuole, where it participates in vacuole fission activity (Dove *et al.*, 2004).

Previous findings from our group demonstrated that *P. falciparum* FV undergoes fission and fusion, resulting in multilobed FV as well as the participation of *PfATG18* in the FV dynamics. Additionally, the expression of *PfATG18* in yeast cells lacking *ScAtg18* restores vacuolar morphology and is involved in vacuolar fission. Although binding of ATG18 with Phosphatidylinositol 3,5-bisphosphate [PI(3,5)P₂] facilitates ATG18's vacuole localization (Dove *et al.*, 2004), absence of PI(3,5)P₂ in *P. falciparum* (Tawk *et al.*, 2010), causes *PfATG18* to bind to PI3P for its association with the parasite FV and carry out fission processes. Treatment of parasites with proteasome inhibitor MG132 results in increased FV fragmentation along with enrichment of *PfATG18* at the multilobed vacuolar interface, which reaffirms the role of *PfATG18* in vacuole fission (Agrawal *et al.*, 2020).

Furthermore, *PfATG18* has been shown to traffic to the parasite FV via hemoglobin containing vesicles (HCv) (Agrawal *et al.*, 2020), which are vesicles for transporting host hemoglobin to the parasite FV (Elliott *et al.*, 2008). The ability of *PfATG18* to bind to PI3P

mediates its association with HCv (Agrawal *et al.*, 2020), which has been demonstrated to be essential for hemoglobin trafficking to the FV (Jonscher *et al.*, 2019; Vaid *et al.*, 2010).

1.9.2 Role of Autophagy in ART resistance

Various theories proposing the molecular mechanism underlying ART resistance have hypothesized the involvement of parasite autophagy-like pathway in resistance to frontline antimalarials (Suresh and Halder, 2018). Increased ER-PI3P vesiculation, UPR, and oxidative stress response pathways are the proteostasis mechanisms suggested to contribute to ART resistance. While it is well established that UPR and PI3P promote autophagy in higher organisms to clear misfolded proteins, the role of parasite autophagy in these mechanisms of resistance has yet to be proven experimentally. A recent report analyzing the targets of ART in the malaria parasite identified *PfATG18* as one of the targets, indicating their association in the parasite (Wang *et al.*, 2015). A Genome-Wide Association Study (GWAS) from the GMS region identifying gene polymorphism in resistant field isolates has associated a non-synonymous mutation in *PfATG18* with ART resistance. Substituting a single amino acid, threonine, at the 38th position with isoleucine (T38I) or asparagine (T38N) results in a decreased rate of parasite clearance in patients treated with an ART derivative (Miotto *et al.*, 2015; Wang *et al.*, 2016).

Recently, a study looked at the role of the T38I polymorphism in imparting ART resistance in *P. falciparum*. CRISPR/Cas9 editing of the *PfATG18* gene was used to introduce a T38I mutation into a K13-edited Dd2 parasite. *PfATG18* T38I mutant parasites demonstrated increased resistance to ART, as compared to wide-type. Even in the absence of K13 R539T mutation, *PfATG18* T38I was shown to provide resistance. Interestingly, this mutation also improves parasite survival under conditions of glucose deprivation. At a 50 % reduction in nutritional content, the *PfATG18* T38I parasite strain was more viable than wild type parasites or parasites with the K13 mutation R539T. For these reasons, autophagy-like pathway is believed to provide a fitness advantage to ART resistant parasites (Breglio *et al.*, 2018).

1.10 Thesis objectives

Throughout its life cycle, *P. falciparum* is exposed to a multitude of challenges, posed by the host immune system as well as environmental and intracellular perturbations. Since the

parasite relies primarily on secretory processes for pathogenesis, it has a high replication rate in order to synthesize and fold numerous proteins for export to the host RBC, allowing for host cell remodelling and infection establishment. The parasite also experiences nutrient deprivation, febrile cycles of high and low temperatures and pharmacological inhibitions as a result of treatment with front-line antimalarials like ART (Babbitt *et al.*, 2012; Engelbrecht and Coetzer, 2013). The activation of ART by heme-derived iron, generated during hemoglobin catabolism in the parasite, leads to the formation of free oxygen radicals. These free radicals alkylate proteins promiscuously, resulting in the buildup of misfolded proteins in the parasite (Tilley *et al.*, 2016). These factors can exert a significant stress on the protein folding machinery of the ER, causing ER stress and, amid prolonged stress, parasite death.

The malaria parasite has acquired intricate mechanisms to evade death and cope with the detrimental consequences of antimalarial drug treatment. At present, *P. falciparum* has developed resistance to majority of the antimalarial drugs, including chloroquine, sulfadoxine-pyrimethamine, and mefloquine (Halder *et al.*, 2018). The situation has deteriorated further with the emergence of resistance to ART, the principal component of the first-line ACT regimen. The emergence and development of ART resistance associated with mutations in *PfK13* (Ariey *et al.*, 2014), a protein predicted to function as a substrate adaptor for ubiquitin E3 ligase, has sparked interest in understanding the molecular processes underlying resistance. The C580Y mutation in *PfK13* is identified as the key determinant for ART resistance in the background of other mutations in genes encoding coronin, atg18, ubp1, crt, mdr2, etc. (Demas *et al.*, 2018; Henrici *et al.*, 2020; Miotto *et al.*, 2015; Wang *et al.*, 2016). It is suggested that while *PfK13* mutant alleles present the parasite with growth disadvantages, these background genetic mutations may compensate for the loss by activating pathways or proteins that facilitate parasite development (Siddiqui *et al.*, 2021). Furthermore, studies attempting to elucidate the molecular basis of ART resistance have proposed two mechanisms linking the C580Y mutation in *PfK13* to enhanced proteostasis, which involves maintenance of protein homeostasis coupled to vesicular remodelling (Bhattacharjee *et al.*, 2018; Suresh and Halder, 2018), and the reduced hemoglobin endocytosis mediating decreased ART activation in the parasite (Birnbbaum *et al.*, 2020).

Given that *P. falciparum* has been able to maintain a complex lifecycle for thousands of years and develop resistance to several antimalaria drugs, it must have evolved a reliable ER stress response mechanism capable of restoring ER homeostasis. The malaria parasite proteome contains proteins involved in response to ER stress, such as the canonical UPR pathway, comprising of the ER-resident chaperone *PfBiP* and the *PfPERK-PfeIF2 α* that drive global translational attenuation in the parasite (Gosline *et al.*, 2011). *P. falciparum*'s genome also encodes a small number of partially conserved autophagy-related proteins that have been implicated in autophagy-like processes in the parasite (Hain and Bosch, 2013). In yeast and other eukaryotes, autophagy acts as an effector pathway downstream of UPR (Smith and Wilkinson, 2017). It is a cell survival mechanism in which a portion of the cytoplasm containing protein aggregates as well as damaged organelles is degraded and recycled (Mizushima, 2007). Thus, cells utilize autophagy as an ER stress response pathway to restore homeostasis. The majority of autophagy related studies in *P. falciparum* have focused on the autophagy proteins *PfATG8* and *PfATG18*, which have been implicated in many roles in the malaria parasite, including the canonical autophagy process and apicoplast biogenesis (Agrawal *et al.*, 2020; Bansal *et al.*, 2017; Joy *et al.*, 2018; Tomlins *et al.*, 2013). Additionally, the parasite also harbors a putative *PfATG1* protein (Hain and Bosch, 2013), whose mammalian ortholog is involved in autophagy initiation and can stimulate autophagy upon ER stress induction. Although *P. falciparum* is equipped with multiple autophagy-like proteins, there is no experimental evidence of the involvement of parasite autophagy as an ER stress response pathway in restoring ER homeostasis.

Furthermore, ART resistant parasites show increased expression of major parasite chaperones involved in the UPR and oxidative stress pathways. Studies have demonstrated that increased PI3P vesicles, generated as a consequence of mutant *PfK13*'s inability to ubiquitinate and degrade *PfPI3K* in the proteasome, are enriched in proteins involved in the UPR and oxidative stress response pathways (Bhattacharjee *et al.*, 2018). Since, the PI3P vesicles are disseminated throughout the parasite and in the host RBC, they are presumed to enhance parasite's ability to overcome damage from ART mediated protein alkylation and proteopathy (Suresh and Haldar, 2018). Increase in PI3P levels, even by transgenic methods, are capable of conferring ART resistance in parasites without the *PfK13* C580Y mutation (Mbengue *et al.*, 2015). Thus, it is imperative to understand the downstream PI3P effector proteins and pathways crucial for resistance. PI3P is known to

trigger autophagy in yeast and other eukaryotes, by providing a platform for the recruitment of various ATG proteins, such as ATG18, to the pre-autophagosomal membrane, and therefore modulating membrane curvature for autophagosome assembly and maturation (Dall'Armi *et al.*, 2013). Interestingly, a particular mutation in *PfATG18* is strongly selected under ART resistance and confers fitness advantage to parasites by providing faster growth rates under nutrient limited conditions (Breglio *et al.*, 2018; Wang *et al.*, 2016). Hence, mutations in *PfATG18* could be selected during resistance to compensate for the parasite fitness loss associated with resistance. While various theories hypothesize the involvement of parasite autophagy-like pathway in proteostasis mechanisms of ART resistance, this has not yet been experimentally demonstrated.

PfK13 regulates hemoglobin endocytosis, hence controlling the amount of host hemoglobin taken up by the peripherally localized parasite vesicles called cytosomes. The C580Y mutation in *PfK13* decreases hemoglobin uptake capacity, decreasing the amount of heme available for ART activation and thereby establishing ART resistance (Birnbaum *et al.*, 2020). *PfK13* localizes to endocytic and secretory vesicles, including those labelled with PI3P, which are significantly increased in the C580Y mutant parasites (Bhattacharjee *et al.*, 2018; Gnädig *et al.*, 2020; Siddiqui *et al.*, 2020; Yang *et al.*, 2019). However, there is no experimental evidence suggesting presence of *PfK13* on HCv which are endocytic vesicles transporting hemoglobin to the parasite FV. Additionally, studies have demonstrated that *PfATG18* is transported to FV through the HCv (Agrawal *et al.*, 2020), which might be mediated by *PfATG18*'s ability to bind to PI3P (Bansal *et al.*, 2017). Thus, it is crucial to determine the whether *PfK13* co-traffics with *PfATG18* to the parasite FV.

The work presented in this thesis aims to study in detail the involvement of parasite autophagy-like pathway in mechanisms of ER homeostasis and ART resistance. The following objectives were defined to achieve the aim of the study:

1. Understanding the cross-talk between ER stress, UPR, and autophagy-like pathway in *P. falciparum*.
2. Deciphering the role of putative *PfATG1* in the autophagy-like pathway in *P. falciparum*.

3. Investigating the role of parasite autophagy-like pathway in regulating proteostasis mechanisms of ART resistance.
4. Elucidating participation of the autophagy-like protein *PfATG18* in *PfK13* associated hemoglobin endocytosis pathway.

Chapter 2

Materials and Methods

2.1 Materials used in the study

2.1.1 Chemical reagents

RPMI 1640, HEPES, Sodium bicarbonate (NaHCO₃), Hypozanthine, D-sorbitol, Saponin, MRT68921, GSK2606414, 2,3-Butanedione monoxime, Hoechst 33258, Phenylmethylsulfonyl fluoride (PMSF), dimethyl sulfoxide (DMSO), Trizol reagent, DNase I, Diethyl pyrocarbonate (DEPC), oligonucleotides were purchased from Sigma-Aldrich, USA; RPMI 1640 without amino acid from HyClone Laboratories Inc., USA; AlbuMAX II from Gibco; Dihydroartemisinin from AK Scientific; Dynasore hydrate and PVDF membranes from Millipore Sigma, USA; WR99210 from Jacobus Pharmaceutical Co., USA; Paraformaldehyde and Glutaraldehyde from ProSciTech, EM-grade, Australia; VECTASHIELD from Vector Laboratories; Protein inhibitor cocktail from Roche; Clarity western ECL substrate and iTaq UniverSYBR Green from Bio-Rad; Zenon Alexa Fluor 488 Rabbit IgG Labeling Kit from ThermoFisher Scientific; Restriction enzymes, T4 DNA Ligase, M-MuLV Reverse Transcriptase and Oligo-dT primers from New England BioLabs, USA, Mito-Tracker Red CMXRos and ER-Tracker (BODIPY TR Glibenclamide) from Invitrogen.

2.1.2 Antibodies

2.1.2.1 Generation of polyclonal antibodies

For custom generation of anti-*Pf*ATG1 polyclonal antibodies in rabbit (Bioklone Biotech Private Limited, India), a 33 amino acid peptide sequence LKANIPPELLSKEKSLNIQPG LKNLLENILVHDP corresponding to the region of 262–294 amino acid in *Pf*ATG1 was selected due to its predicted high antigenicity. Anti-*PfeIF2 α* polyclonal antibodies were

custom synthesized in rabbit (Bioklone Biotech Private Limited, India) against the peptide sequence MEGMILMSELSKRRFRSVNKLIRVGRHEVVLRVDSQKGYI. The two antibodies were affinity purified and specificity of each antibody was verified using western blotting on the parasite lysate.

2.1.2.2 Other antibodies

Following commercially available antibodies were obtained from: mouse anti-PI3P antibody from Echelon Biosciences; rabbit anti-phospho-eIF2 α from Cell Signaling; rabbit anti-Actin antibody and mouse anti-GFP antibody from Sigma-Aldrich; mouse anti-KDEL antibody from Abcam; anti-rabbit and anti-mouse Alexa Fluor 488 as well as Alexa Fluor 568 from Invitrogen, anti-rabbit-HRP from Bio-Rad. *Plasmodium falciparum* specific antibodies previously generated in the lab were rabbit anti-PfATG18 from GenScript, USA and, rabbit anti-PfATG8 and anti-PfPTEX-150 from Genemed, Biotechnologies Inc. Rabbit anti-BiP antibody was obtained from MR4, Bei Resources; rabbit anti-PfK13 and anti-falcipain-2 antibodies were kindly gifted by Dr. Souvik Bhattacharya, JNU, New Delhi and Dr. Asif Mohammed, ICGEB, New Delhi respectively; rabbit anti-ApeI was kindly gifted by Prof. Klionsky, University of Michigan, Ann Arbor.

2.1.3 Strains and plasmids

For episomal expression in *P. falciparum*, genes were cloned in pARL-1a vector. The vector contains human dihydrofolate reductase (hDHFR) gene as the selectable marker which is constitutively expressed under the calmodulin (CAM) promoter. The gene of interest fused with a C-terminal fluorescent GFP tag was expressed under the chloroquine resistance transporter (CRT) promoter (Figure 2.1A) (Crabb et al., 2004). p415-ADH is a yeast expression shuttle vector which was used for the heterologous expression of *P. falciparum* proteins in the budding yeast *S. cerevisiae*. p415-ADH (size: 7747 bp) is a CEN/ARS low copy number plasmid consisting of an alcohol dehydrogenase (ADH) promoter, multiple cloning array, selectable leucine marker, and the CYC1 terminator sequences (Figure 2.1B). The pRS316 yeast expression vector with a selectable uracil marker contains the 2xmCherry-ScATG8 sequence (Figure 2.1C). This construct was kindly gifted by Prof. Yoshinori Ohsumi, Tokyo Institute of Technology, Tokyo and we received it from Prof. Ravi Manjithaya, JNCASR, Bangalore. *Escherichia coli* DH5 α competent cells were used for cloning.

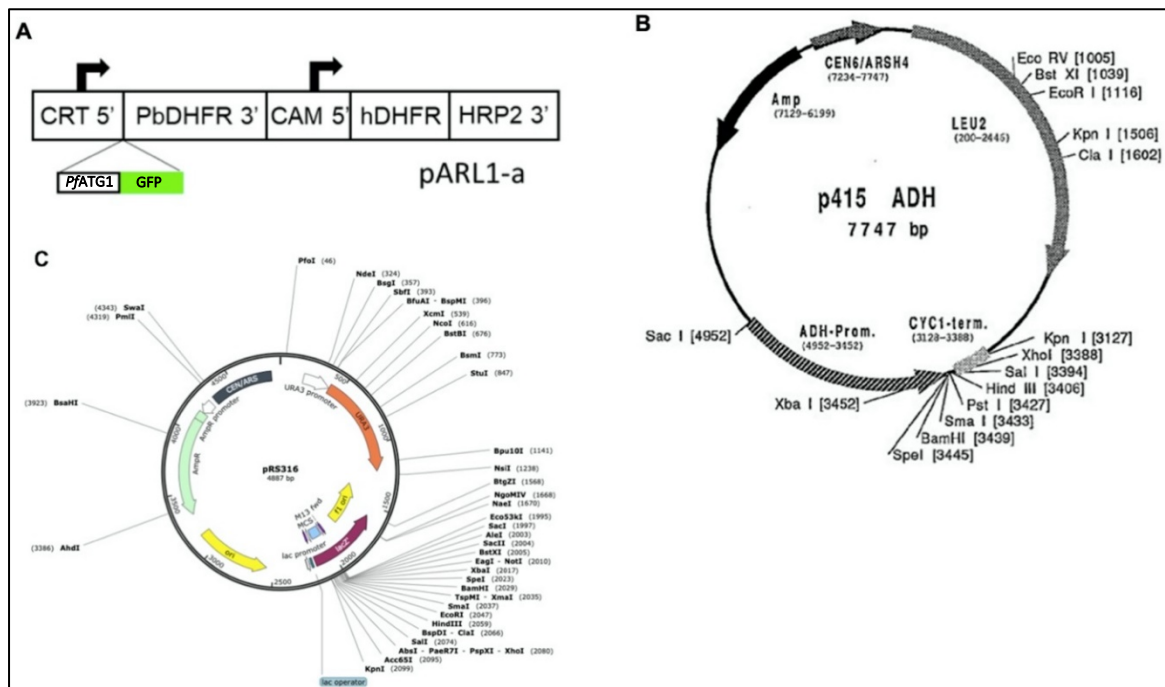


Figure 2.1 Vector maps of the plasmids

Vector maps of plasmids used for the construction of various expression cassettes used in this study.

2.2 Culturing of parasites

2.2.1 *P. falciparum* strains used

P. falciparum 3D7 strain was used in this study. The origin of 3D7 parasites is believed to have occurred in Africa (Preston *et al.*, 2014). Sequencing of its genome has led to increase in the overall characterization of the strain (Gardner *et al.*, 2002).

The *P. falciparum* strain IPC 3445, referred in the study as K13^{C580Y} (a field isolate from Pailin carrying the C580Y mutation in the b-propeller domain of *PfK13* protein) and the isogenic strain IPC Cam2_rev, referred in the study as K13^{WT} (having the mutation reversed to the wildtype) have been obtained through BEI Resources (<http://www.mr4.org>), NIAID, NIH. The *P. falciparum* strain, IPC 3445 (MRA-1236) is contributed by Didier Menard, Institut Pasteur, Paris, France and *P. falciparum* strain, IPC Cam2_rev (MRA-1253), was contributed by David A. Fidock, Columbia University, New York, USA (Straimer *et al.*, 2015).

2.2.2 *In vitro* culturing of *P. falciparum*

Parasite cultures were maintained by a standard candle jar method (Trager and Jensen, 1976) and cultured in O⁺ human RBCs using complete RPMI 1640 supplemented with 25 mM HEPES, 0.2 % NaHCO₃, 0.5 mM hypoxanthine, 0.5 % (w/v) AlbuMAX II and 5 % (v/v) heat-inactivated O⁺ human serum. For starvation experiments, cultures were maintained in RPMI 1640 without amino acids and serum for ninety minutes. Sub-culturing was done every two days to maintain the parasitemia at around 5 %. For isolation of parasites, RBCs were lysed using 0.03 % (w/v) saponin incubated for 10 min on ice, followed by centrifugation. The pellet obtained was washed using cold phosphate-buffered saline pH 7.4 (1X PBS).

2.2.3 Parasite growth assessment by Giemsa stain

For regular culturing as well as morphology and growth assays, the parasite stage, parasitemia and morphology was monitored by making a thin smear on the glass slide. Fixation was done in 100 % methanol and followed with staining in 10 % (v/v) Giemsa stain. Dried up slides were viewed at 100x magnification in a compound microscope under oil immersion.

2.2.4 Synchronization of the parasites

Cultures were synchronized by treatment with 5 % D-sorbitol (Lambros and Vanderberg, 1979). Ring stage parasite (0-18 hpi) infected-RBC cultures were pelleted by centrifugation (1300 rpm) for 7 minutes and resuspended in 5 x volume of 5 % D-sorbitol (w/v) for 5 minutes. After centrifugation, the pellet was washed twice with 10 x volume of incomplete RPMI. The supernatant was discarded and pellet re-suspended in pre-warmed RPMI-1640 media complete with 5 % NaHCO₃.

2.2.5 Freezing and thawing of cultures

For freezing, RBCs containing synchronized ring-stage parasites with ~5 % parasitemia were subjected to centrifugation (1300 rpm) for 3 minutes. After discarding the supernatant, the infected RBCs were re-suspended in 1.5 x pellet volume of fetal bovine serum (FBS) and 2.5 x pellet volume of the Freezing solution (28 % glycerol, 3 % sorbitol, 0.65 % NaCl,

H₂O), the latter added dropwise with agitation. The parasite containing RBCs were transferred to a sterile cryovial aliquoted to 1 mL and stored in the liquid nitrogen tank.

For thawing of the parasite cultures, frozen aliquots were briefly warmed at room temperature and contents of the vial transferred to a 50 mL glass tube with a sterile pipette. 0.1 x pellet volume of 12 % NaCl was added dropwise with agitation. After 5 minutes of incubation at room temperature, 10 x pellet volume of 1.6 % NaCl was added to the infected RBCs. The solution was transferred to a 15 mL glass tube and centrifuged (1300 rpm) for 5 minutes. The supernatant was discarded and pellet washed with incomplete media. The parasite containing RBCs were incubated with 100 µL fresh RBCs and 5 mL culture media and were maintained under standard culture conditions.

2.2.6 Parasite treatment with small molecule inhibitors

Young trophozoite-stage parasites were treated with the following small molecule inhibitors: 700 nM DHA for indicated time points, 2.5 µM MRT68921 for 1.5h, 30 µM GSK2606414 for 2.5h, 200 µM Dynasore hydrate for 4h and 25 mM 2,3-Butanedione monoxime (BME) for 1h. The treated parasites were subjected to isolation with saponin for protein expression analysis or fixed with paraformaldehyde for Immunofluorescence analysis.

For the viability assay, parasites were incubated with a small molecule inhibitor for the indicated time period and then washed twice with incomplete RPMI media. Parasites were incubated into complete RPMI media for 30h and Giemsa stained blood smears were made. Parasitemia was calculated by counting the number of rings per 10,000 RBCs, which represents viable parasites. Live parasites were also determined by labelling parasite nucleus with Hoechst33258 and mitochondrion with 100 nM Mito-tracker Red CMXRos (Jogdand et al., 2012).

2.3 Ring-stage Survival Assay (RSA)

Prior to the assay, K13^{WT} and K13^{C580Y} parasites were synchronized with 5 % sorbitol. Synchronous schizonts with 10–12 nuclei were purified using a Percoll discontinuous gradient (35 %/75 %), washed in complete media, and cultured for 3 h with fresh RBCs. To eliminate remaining schizonts, cultures were treated with 5 % sorbitol, adjusted to a hematocrit of 2 % and a parasitemia of 1 % by adding uninfected RBCs and then divided into two parallel cultures. The RSA was performed immediately following the invasion, using 0–3 h post-invasion rings. The cultures were either exposed to 0.1 % DMSO (control) or 700 nM DHA (treated) for 6 h, washed with incomplete media to remove the drug and resuspended in complete media. Giemsa stained thin blood smears were prepared. Survival rates were determined microscopically by counting the number of viable parasites developing into healthy rings or trophozoites at 66 h post drug removal. Roughly 10,000 RBCs were assessed for each sample. Survival rates were expressed as ratios of viable parasitemia in DHA exposed and DMSO exposed samples (Witkowski *et al.*, 2013).

2.4 Growth-inhibition assay

To assess the effect of the small molecule inhibitor MRT68921 on *P. falciparum* growth, parasites were tightly synchronized by sorbitol treatment. Ring stage parasites (3D7, K13^{WT} and K13^{C580Y} strains) with 1 % parasitemia and 3 % hematocrit were incubated with various concentrations of MRT68921 (5000nM, 2500nM, 1000nM, 800 nM, 650 nM, 400 nM, 250 nM, 100 nM and 50 nM in triplicate) in a 96-well cell culture plate. Thin blood smears were made from each well at ~72 hpi and stained with Giemsa for analysis in the microscope. The percentage of parasites in the next life-cycle was calculated for each concentration of MRT68921 and were plotted as a function of MRT68921 concentration using GraphPad and the half-maximal inhibitory concentration (IC₅₀) was estimated using the dose-response function of GraphPad.

2.5 Molecular cloning

2.5.1 *P. falciparum* mRNA extraction and cDNA synthesis

The open reading frame (ORF) of *P. falciparum* genes mentioned in this study contains multiple intronic sequences. Thus, RNA isolated from the *in vitro* 3D7 culture was used cloning. The parasite pellets were obtained by above mentioned saponin treatment and total

RNA was extracted using Trizol reagent following the manufacturer's protocol. The RNA was reconstituted in MiliQ water and treated with RNase-free DNase I to remove any genomic DNA contamination. 1 µg of the extracted RNA was then used for the cDNA synthesis using the M-MuLV Reverse Transcriptase and Oligo-dT primers in a 20 µl reaction. Another set of cDNA synthesis reaction was set without the reverse transcriptase enzyme which served as the negative control.

2.5.2 Agarose gel electrophoresis

The cDNA fragments were analysed by resolving on an agarose gel containing ethidium bromide. The gel was prepared using 1 % (w/v) agarose dissolved in 1x TAE buffer (40 mM Tris base, 20 mM acetic acid, 1 mM Na₂EDTA, pH 8). cDNA samples were mixed with bromophenol blue dye and loaded on the agarose gel followed by electrophoresis at 100 V for 30-40 minutes in TAE buffer. As a reference, the first lane was loaded with 0.5 µL of 1 kb DNA ladder for determining the size of the cDNA bands. The bands were visualized using GelDoc XR under long wavelength UV.

2.5.3 Generation of clones

The cDNA obtained after total RNA isolation was used for amplifying the respective genes using gene-specific primers (Table 2.1). Amplicons were purified by agarose gel extraction. Both the purified DNA (1 µg), termed as insert, and the vector (1 µg) were subjected to digestion at 37°C for 12 h with their respective restriction enzymes in the recommended digestion buffers.

Primer Name	Plasmid	Restriction Site	Primer	5'-3' primer sequence	Tm
SEC62-FP	pARL-1a	KpnI	FP	GGCCGGTACCATGAGTAACAG AATGGAGGA ATTAG	57
SEC62-RP	pARL-1a	AvrII	RP	GCGCCCTAGGATTGTCTGATT TATCAAACA TGCTTC	57
SEC62-iFP	pARL-1a	-	FP	GGATTTACAAGTGCAGCAGCA GCAGTTAG AAAATGTTTCTTAAAG	57

SEC62-iRP	pARL-1a	-	RP	CTTTAAGAAACATTTTCTAACT GCTGCTGCTGCACTTGTAAT CC	57
ATG1c-o-FP	p415-ADH	XbaI	FP	GGCCTCTAGAATGGGTTCCAC AATCTCCAAAAG	57
ATG1c-o-RP	p415-ADH	BamHI	RP	GCGCGGATCCATTGGTAATCT TCTTTAAGAAAAATGTGTATC TCTTC	57
ScATG1-FP	p415-ADH	XbaI	FP	GGCCTCTAGAATGGGAGA CATTAAAAATAAAGATCA CAC	57
ScATG1-RP	p415-ADH	BamHI	RP	GCGCGGATCCATTTTGGT GGTTCATCTTCTGCCTC	57

Table 2.1 Details of primers used for cloning

The table contains name of the primers, cloning plasmid vector, restriction enzymes, the nucleotide sequence of the primer with the restriction site highlighted in green and T_m of the primers.

The digested products were purified by gel extraction. Ligation reactions were carried out at 1:5 molar ratio of vector to insert using T4 DNA ligase at 16°C overnight. The ligation reactions were transformed into *E. coli* (DH5α) competent cells by electroporation, and plated onto LB agar containing appropriate antibiotic (ampicillin or kanamycin) which depends on the selectable marker gene in the vector. Random colonies were inoculated in LB broth containing the selectable antibiotic. Upon isolation of the plasmid, colonies positive for the clone were screened for the presence of cloned insert by double restriction digestion. Positive clones were also verified by gene amplification using gene-specific primers and sequencing (Figures 2.2A, 2.2B and 2.2C).

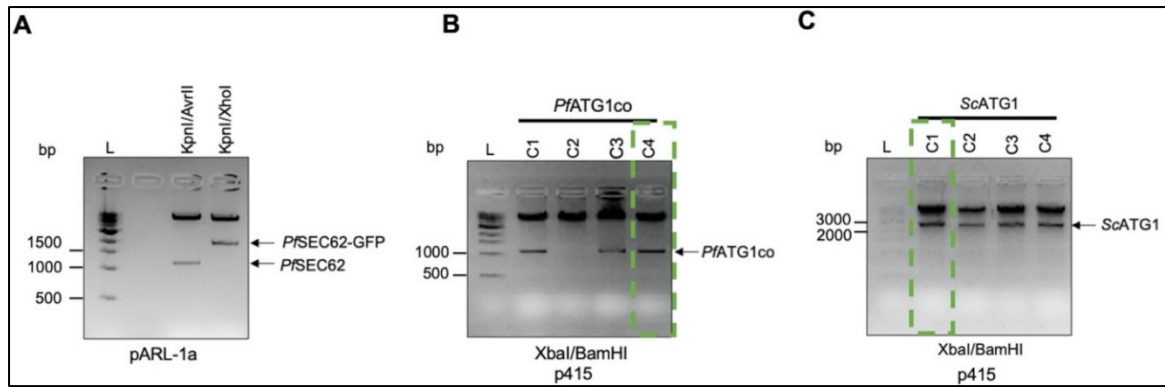


Figure 2.2 Confirmation of clones

Confirmation of clones with various constructs is shown by restriction digestion of the clones for the release of insert fragment of the expected size. For each construct, the restriction enzymes and the vector used for cloning are indicated below their respective agarose gel images. L-DNA ladder, C1-4-clones screened. (A) *PfSEC62* in pARL-1a vector, (B) *PfATG1* in p415 vector, and (C) *ScATG1* in p415 vector. Dotted green lines on a particular clone represent the chosen clone (by sequencing) used in the study.

2.5.4 Episomal transfection of *P. falciparum*

Transfection in *P. falciparum* 3D7 parasites was done as previously described (Fidock and Wellems, 1997). Briefly, synchronized ring stage parasites with 5 % parasitemia were mixed with CytoMix (Table 2.2) containing 100 µg of plasmid (pARL-1a-*PfSEC62*-GFP). This was electroporated using GenePulser II (0.31 kV, 960 µF) and resuspended immediately in complete media containing fresh RBC. Subsequently, the culture was maintained in 2.5 nM WR99210.

CytoMix components	Concentration (mM)
CaCl ₂	0.15
KCl	120
EGTA	2
K ₂ HPO ₄ /KH ₂ PO ₄	10
MgCl ₂	5
HEPES, pH 7.6	25

Table 2.2 *P. falciparum* transfection mix

The list of components required for preparation of the CytoMix to carry out episomal transfection in *P. falciparum*.

2.5.5 Transformation in yeast

Lithium acetate/single-stranded carrier DNA/PEG method was used for transformation in yeast. A single colony of the yeast strain from a YPD agar plate was inoculated into 5 ml liquid medium (YPD broth) and incubated at 30°C overnight, 200 rpm. The titer of the primary culture was diluted to OD600 = 0.2 (2×10^6 cells ml⁻¹) and allowed to grow for 3-4 h until OD600 reaches to 1 (1×10^7 cells ml⁻¹). The cells were harvested by centrifugation at 3,000×g, followed by washing the cell pellet twice with sterile water. The pellet was then resuspended in 1 ml of sterile water and 100 µl of the cell suspension was used for each transformation. Yeast cells were then resuspended in 360 µl of transformation mix containing 5 µg plasmid DNA (Table 2.3) and incubated at 42°C for 40 min. Positive transformants were selected by enabling the transformed cells to grow on synthetic defined medium lacking leucine and uracil (0.17 % yeast nitrogen base, 0.5 % ammonium sulfate, 2 % agar, 2 % dextrose, 0.002 % histidine, 0.002 % methionine).

Transformation Mix components	Vol (µL)
PEG 3350 (50 % (w/v))	240
LiAc 1.0 M	36
Single stranded DNA carrier (2 mg ml ⁻¹)	50
Plasmid DNA plus sterile water	34
Total volume	360

Table 2.3 Yeast transformation mix

The list of components required for preparation of the transformation mix to carry out transformation in yeast. Adapted from Gietz and Schiestl, 2007, with permission from 2007, Nature Publishing Group.

2.6 Quantitative Real-Time PCR

Parasite pellets isolated by saponin lysis were resuspended in Trizol reagent for 10 minutes at room temperature followed by the addition of chloroform. The phase separation provided

by Trizol-chloroform was used to separate the RNA from DNA and cellular proteins. in the cell. The isolated RNA was treated with RNase-free DNase I to remove any genomic DNA contamination. 1µg of the extracted RNA was then used for the cDNA synthesis using M-MuLV Reverse Transcriptase and Oligo-dT primers in a 20 µl reaction. Another set of cDNA synthesis reaction was set without the reverse transcriptase enzyme as a negative control. Quantitative real-time PCR reaction with 10 ng of cDNA was used to amplify the gene of interest, *PfATG8* and *PfATG18*. Primer sequences used to amplify regions in the genes are mentioned below (Table 2.4). SYBR Green-based fluorescent tag was used for DNA labelling in CFX96 Touch™ real-time PCR Detection System (Bio-Rad, USA) and abundance of each transcript was determined using the threshold cycle (CT). The housekeeping gene β -Actin was used to normalize the gene expression and fold differences in the expression of these genes were calculated using the $2^{-\Delta\Delta CT}$ method (Livak and Schmittgen, 2001).

Target	Amplicon size	Primer	5'-3'sequence	Tm
<i>PfATG8</i>	116	FP	CATCAACATATTAATCAAAGTGCATATGG	55
		RP	AAATCTTGCATTAACAATCCTGTTTTAGG	55
<i>PfATG18</i>	127	FP	ATATGTAAAGGAAAAAATGTATCCCC	55
		RP	GCAAACTCCATTCAC TATT TAAATAC	55
		RP	GTA ATC TGC AAA CTA AAT CAA CAA CTG	55
<i>PfACTIN</i>	131	FP	CCATGAAAATTAAAGTTGTTGCACCAC	55
		RP	TTGGTCCTGATTCATCGTATTCCTC	55

Table 2.4 List of primers used for Real-time PCR

2.7 Fluorescence microscopy

2.7.1 Immunofluorescence Assay

The assay was performed as described previously (Tonkin *et al.*, 2004). Parasite infected RBCs were washed thrice with 1X PBS and fixed at room temperature for 30 min using 4 % paraformaldehyde and 0.0075 % glutaraldehyde in PBS. After fixation, cells were washed thrice followed by permeabilization at room temperature for 10 min using 0.1 % Triton X-100/PBS. Blocking was done at 4°C for 1h using 3 % BSA/PBS followed by incubation with the primary antibody (Table 2.5) in 3 % BSA/PBS at room temperature for

1h. This was followed with three washes and incubation with secondary antibodies using 3 % BSA/PBS at room temperature for 1 h. After staining the nucleus with Hoechst 33258, cells were mixed with VECTASHIELD and then mounted over glass slides and observed under a confocal microscope.

Primary/Secondary	Antigen	Dilution	Animal raised in
Primary	<i>Pf</i> ATG8	1:600	Rabbit
Primary	<i>Pf</i> ATG18	1:400	Rabbit
Primary	<i>Pf</i> ATG1	1:200	Rabbit
Primary	<i>Pf</i> K13	1:400	Rabbit
Primary	<i>Pf</i> Falcpain-2	1:400	Rabbit
Primary	<i>Pf</i> PTEX-150	1:300	Rabbit
Primary	KDEL	1:200	Rabbit
Primary	PI3P	1:500	Mouse
Primary	GFP	1:200	Mouse
Secondary	Alexa Fluor 488	1:200	Rabbit
Secondary	Alexa Fluor 488	1:200	Mouse
Secondary	Alexa Fluor 568	1:200	Rabbit
Secondary	Alexa Fluor 568	1:200	Mouse

Table 2.5 List of antibodies and their dilutions used in Immunofluorescence analysis

2.7.2 Zenon labelling

For co-immunolocalization of antibodies belonging to the same species, Zenon labelling was used. The first primary antibody was labelled using the Immunofluorescence assay protocol mentioned above. The second primary antibody was conjugated with Zenon rabbit IgG 488 in a 6:1 molar ratio (supplier recommendation). Samples were incubated with this

complex for 40 minutes followed by imaging within 1 h to avoid dissociation of the complex.

2.7.3 Labelling of Endoplasmic Reticulum with ER-tracker and Mitochondrion with Mito-tracker

For endoplasmic reticulum (ER) labelling, 1 mL of parasite infected RBCs was incubated with pre-warmed 1000 nM ER-Tracker Red (BODIPY TR Glibenclamide) for 1 h at 37°C with intermittent tapping. Cells were then washed thrice with pre-warmed PBS and was observed directly under a confocal microscope. Similarly, 1 mL of parasite infected RBCs were incubated with pre-warmed 100 nM Mito-Tracker Red CMXRos for 30 minutes at 37°C to stain mitochondrion. Cells were then washed thrice with pre-warmed PBS and was either fixed to perform Immunofluorescence or observed directly under a confocal microscope.

2.7.4 Confocal microscopy and image processing

GFP-expressing *P. falciparum* transfectants were mounted over a glass slide and images immediately. Yeast cells were centrifuged at 20000×g for 2min and spotted on a 2 % (w/v) agarose pads and covered with a glass-slip for microscopy. Transgenic parasites expressing *PfSEC62-GFP* and yeast transformants expressing *PfATG1-GFP* were observed under ZEISS LSM 700 confocal microscope (Carl Zeiss, Germany) using a 488 nm laser and 63×1.4 NA oil objective in case of parasite infected RBCs and 100×1.4 NA oil objective for yeast cells. Immunofluorescence signals from fixed samples were observed under ZEISS LSM 700 and Airyscan confocal microscope. ER-Tracker Red (BODIPY TR Glibenclamide) and Mito-Tracker Red CMXRos labelled parasites were imaged using the 555 nm laser. Nucleus was labelled using Hoechst 33342 and observed under ZEISS LSM 700 using a 405 nm laser. Image processing was performed with Imaris (Bitplane, Zurich, Switzerland) and Zen (blue edition). The distance was quantified using the line profile in Zen software and the degree of colocalization was measured by the Pearson's coefficient (R).

2.8 Protein analysis

2.8.1 Preparation of parasite lysate

Parasite pellet is isolated by saponin lysis were resuspended in 1 % Triton X-100 lysis buffer (1 % Triton X-100 in 1X PBS, 1x Complete EDTA-free Protease Inhibitor Cocktail, 1mM PMSF) or 2x SDS Laemmli sample buffer (50 mM Tris-Cl pH6.8, 100 mM DTT or 1 % β -ME, 2 % SDS, 10 % Glycerol, and protease inhibitor cocktail). The resuspended parasites were lysed by passing through the syringe 5 times with intermittent cooling. Protein extracts were obtained in the supernatant by high-speed centrifugation. The standard Bradford method was then used to estimate protein concentration (Kruger, 2009).

2.8.2 Preparation of yeast lysate

Yeast extracts were prepared by trichloroacetic acid (12.5 % TCA w/v) precipitation of the exponentially growing yeast cell cultures, followed by washing the pellets with ice-cold (80 %) acetone (thrice) and air-drying. The pellets were resuspended in 1 % SDS-0.1 N NaOH solution (Mishra *et al.*, 2017). Protein extracts were obtained in the supernatant by high-speed centrifugation.

2.8.3 Separation of protein by SDS-PAGE

The parasite and yeast samples were mixed with 5 \times Laemmli sample buffer and boiled at 95°C for 10 minutes followed by loading onto a SDS-PAGE gel. Varying percentages of SDS-PAGE gels were used, depending on the molecular weights of proteins to be analysed. *PfSEC62*, *PfATG1*, *PfATG18*, *PfATG8*, phosphorylated *PfeIF2 α* , total *PfeIF2 α* and *PfBiP* were separated using either 12 % or 15 % resolving gels and stacking gel was composed of 5 % acrylamide. The samples were electrophoresed in 1x running buffer (Tris-glycine-SDS). Gels were proceeded for western blotting.

2.8.4 Western analysis

The proteins were transferred from SDS-PAGE gels to Immobilon PVDF membranes using the wet transfer apparatus from BioRad at 100V for 1h. Following transfer, membranes were incubated with 5 % skim milk in 1x PBS for 1h at room temperature with gentle shaking. Membranes were then probed with primary antibodies (Table 2.6) diluted in 5 % (w/v) skim milk in PBS at 4°C, overnight. After washing the membranes thrice with high

salt (NaCl- 58.5 gm, Triton X-100- 0.5 mL, EDTA- 2 gm, 1 M Phosphate buffer, pH = 7.0- 50 mL, 949.5 mL distilled water) and low salt (NaCl- 3 gm, Triton X-100- 0.5 mL, EDTA- 2 gm, 1 M Phosphate buffer, pH = 7.0- 50 mL, 949.5 mL distilled water) buffers, membranes were incubated with horseradish peroxidase-conjugated secondary antibodies (Table 2.6) diluted in 1 % (w/v) skim milk in 1x PBS for 1h at room temperature. The membranes were washed again with high and low salt buffers. Western blot signals were developed by Clarity western ECL substrate and imaged using ChemiDoc™ Imaging System from Bio-Rad.

Primary/Secondary	Antigen	Dilution	Animal raised in
Primary	<i>PfATG8</i>	1:4000	Rabbit
Primary	<i>PfATG18</i>	1:4000	Rabbit
Primary	<i>PfATG1</i>	1:1000	Rabbit
Primary	<i>PfBiP</i>	1:2500	Rabbit
Primary	phospho-eIF2 α	1:500	Rabbit
Primary	total-eIF2 α	1:500	Rabbit
Primary	β -Actin	1:4000	Rabbit
Primary	GFP	1:1000	Mouse
Secondary	anti-rabbit	1:3000	Goat
Secondary	anti-mouse	1:3000	Goat

Table 2.6 List of antibodies and their dilutions used in Western blot analysis

2.9 Functional complementation of *PfATG1* in *S. cerevisiae*

2.9.1 Yeast strains and growth conditions

The wild type and knockout mutant (*atg1 Δ*) yeast strains were derived from BY4741. Genotype of various strains used in the study are listed in Table 2.7. Yeast cells were cultured in YPD media (1 % Yeast extract, 2 % Peptone, 2 % Dextrose) grown at 30°C, 180 rpm. For autophagy induction, cells were cultured in synthetic defined medium devoid

of nitrogen source (SD-N; 0.17 % yeast nitrogen base lacking ammonium sulfate and amino acids and containing 2 % dextrose) for 3-6 h. For western blot analysis and microscopic studies, yeast cells were collected at different time points as mentioned in the experiments. Cells were also incubated with 1 mM PMSF for 4 h in order to inhibit degradation of autophagic bodies inside the yeast vacuole.

Strain	Genotype	Source
BY4741	MATa his3 Δ leu2 Δ ura3 Δ met15 Δ	Brachmann <i>et al.</i> , 1998
sAR1	BY4741 GFP::LEU2 2xmCherry-ScATG8::URA3	This study
sAR2	BY4741 GFP::LEU2 2xmCherry-ScATG8::URA3 atg1 Δ ::KanMX4	This study
sAR3	BY4741 PfATG1-GFP::LEU2 2xmCherry-ScATG8::URA3 atg1 Δ ::KanMX4	This study
sAR4	BY4741 ScATG1-GFP::LEU2 2xmCherry-ScATG8::URA3 atg1 Δ ::KanMX4	This study

Table 2.7 Genotypes of various yeast strains utilized in this study

2.9.2 mCherry-ScATG8 procession assay

S. cerevisiae strains containing a 2xmCherry-ScATG8 (pRS316 vector) plasmid were grown in the synthetic defined medium lacking leucine and uracil at 30°C, 180 rpm. The titer of the primary culture was diluted to OD₆₀₀ = 0.2 and allowed to grow until the OD₆₀₀ reached ~0.7. Yeast cultures were transferred to a nitrogen deprived medium (SD-N) and samples were collected after the indicated time point. The collected cells were then used to visualize the mCherry signal by fluorescence microscopy.

2.10 Quantification and statistical analysis

All the statistical tests were performed using GraphPad Prism-9 software. The data points are expressed as mean \pm SEM. Statistical significance was quantified using unpaired Student's t-test, **** = P < 0.0001, *** = P < 0.0005, ** = P < 0.005, * = P < 0.05 and ns represents non-significant. Densitometry analysis of specific bands in western blotting was

performed using ImageJ software. The IC₅₀ estimation curve for the autophagy inhibitor MRT68921 was plotted using dose-dependent function of GraphPad Prism.

Chapter 3

Results

3.1 Understanding the cross-talk between ER stress, UPR and autophagy-like pathway in *P. falciparum*

Throughout its life cycle, *P. falciparum* is subjected to a wide range of stresses, including host immunological responses, nutrient deprivation, microaerophilic environments, temperature fluctuations, and exposure to anti-malarial drugs (Babbitt *et al.*, 2012; Chaubey *et al.*, 2014; Engelbrecht and Coetzer, 2013). Due to the large amount of proteins that are to be exported to the host RBC for remodelling, the metabolically active trophozoite and schizont stages have a high replication rate. All proteins secreted by a cell are first quality-controlled in the ER and then delivered to their ultimate destination through the Golgi complex. Given the crucial role of protein trafficking in malaria pathogenesis, *P. falciparum* is likely to be subjected to ER stress throughout its intraerythrocytic life cycle. In yeast and other eukaryotes, the three ER integral membrane-sensing proteins that control activation of the UPR signaling pathway during ER stress include the IRE1 α , ATF-6, and PERK (Smith and Wilkinson, 2017). Bioinformatic studies have shown that *P. falciparum* lacks a transcriptional response to the UPR (IRE1 α and ATF6), depending instead on the translational arm of the UPR owing to the existence of three conserved PERK like eIf2 α kinases and a downstream translation initiation factor, *PfeIF2 α* (Chaubey *et al.*, 2014; Gosline *et al.*, 2011).

The WHO recommends ACTs as the first-line therapy for uncomplicated *P. falciparum* malaria (WHO, 2021b). ART is activated by iron-catalysed reductive scission of the endoperoxide bond, which helps in rapidly inducing a parasitocidal effect that eliminates all intraerythrocytic stages of the parasite (Tilley *et al.*, 2016). Recent reports demonstrate

that ART mediated promiscuous alkylation of cellular targets damage the parasite proteome, resulting in a build-up of misfolded protein and activation of the ER stress response, which is characterised by *PfeIF2 α* phosphorylation and reduced global translational (Bridgford *et al.*, 2018). Additionally, ART induces dormancy in parasites by phosphorylation of *PfeIF2 α* (Zhang *et al.*, 2017). Thus, the malaria parasite appears to rely on the UPR signaling pathway for survival in the face of cellular damage caused by ART. ART resistant parasites are characterized by enhanced stress response pathways. Transcriptomic and proteomic analyses of clinical field isolates and laboratory engineered ART resistant parasites reveal upregulated chaperones and proteins involved in the ROSC and UPR pathways (Mok *et al.*, 2015; Stokes *et al.*, 2021). This indicates that ER quality control mechanisms may be involved in re-establishing ER homeostasis, which may contribute to resistance development.

Despite the involvement of a reliable ER stress response pathway in the mechanisms of ER homeostasis, effector pathways acting downstream remain to be elucidated. Autophagy functions as an effector pathway downstream of the UPR in yeast and other eukaryotes (Smith and Wilkinson, 2017). In yeast, higher ER volume is associated with an increase in autophagosome numbers under ER stress (Bernales *et al.*, 2006). The translational UPR arm controlled by PERK-eIF2 α allows the transcription factor ATF4 to be translated, increasing the production of numerous ATG proteins (Song *et al.*, 2018). The *P. falciparum* genome encodes a limited number of partially conserved autophagy-related proteins that are involved in autophagy-like processes in the parasite (Hain and Bosch, 2013). An important question in the field is whether parasites employ the autophagy-like mechanism to restore ER homeostasis after ART induced ER stress, and if so, whether this is mediated through the UPR.

To address this, we first assessed the effect of DHA (active ART metabolite) mediated ER stress on the UPR pathway by analysing parasite ER expansion and activation of the UPR translational arm, both of which are beneficial for maintaining ER homeostasis. To visualize the expansion and morphology of the parasite ER, we fluorescently tagged *PfSEC62* with GFP. We demonstrate that DHA exposure elicits expansion of the parasite ER as well as increased phosphorylation of translation factor *PfeIF2 α* and expression levels of the ER resident chaperone *PfBiP*. Quantification of the number of autophagosome-like

structures as well as relative expression levels of two major parasite ATG proteins, *PfATG8* and *PfATG18*, were analysed to better understand the role of autophagy-like pathway in *P. falciparum* under ER stress. The number of *PfATG8* (the autophagosome marker) labelled puncta indicating autophagosome-like structures, as well as the expression levels of *PfATG8* and *PfATG18* protein, increases in DHA treated parasites compared to control parasites. The reduced expression of the ATG proteins in parasites treated with the mammalian PERK inhibitor GSK2606414, which specifically inhibits UPR/PERK activation, demonstrates that the observed increase in the expression levels of ATG protein in response to DHA is mediated through UPR. Taken together, our findings establish parasite autophagy as a DHA induced ER stress response pathway in *P. falciparum* that is triggered by UPR activation.

This work has been accepted for publication in the journal mBio. The complete reference is as follows:

Ray, A., Mathur, M., Choubey, D., Karmodiya, K., & Surolia, N. (2022) “Autophagy Underlies the Proteostasis Mechanisms of Artemisinin Resistance in *P. falciparum* Malaria”, mBio, doi: 10.1128/mbio.00630-22.

3.1.1 *P. falciparum* remains viable upon treatment with clinically relevant dose of DHA

Autophagy is a stress-induced cellular breakdown process that works to restore metabolic balance by catabolizing aggregated proteins, misfolded proteins, or damaged subcellular organelles (Song *et al.*, 2018). To study the autophagy pathway in response to DHA mediated ER stress in *P. falciparum*, we first assessed the effect of DHA on parasite viability. Synchronized young trophozoites were incubated with the clinically relevant dose of 700nM DHA for a brief period of one hour and thirty minutes (1.5 h) to mimic the short half-life of DHA in patient blood stream (Balint, 2001; Tarning *et al.*, 2012a). The treated parasites show no developmental abnormality or signs of delayed growth, as assessed with Giemsa stained thin blood smears (Figure 3.1A). The viability of parasites after DHA treatment was determined by staining *P. falciparum*-infected erythrocytes with Mito-Tracker Red CMXRos dye, which exclusively marks living cells with viable mitochondria (Jogdand *et al.*, 2012). *P. falciparum* cultures were separately incubated with no drug containing medium (control) or medium containing DHA for 1.5 h. The fluorescence of the

CMXRos dye, which represents viable parasite populations, was seen in both control and DHA treated parasites (Figure 3.1B), showing that parasites could tolerate DHA treatment for 1.5 h.

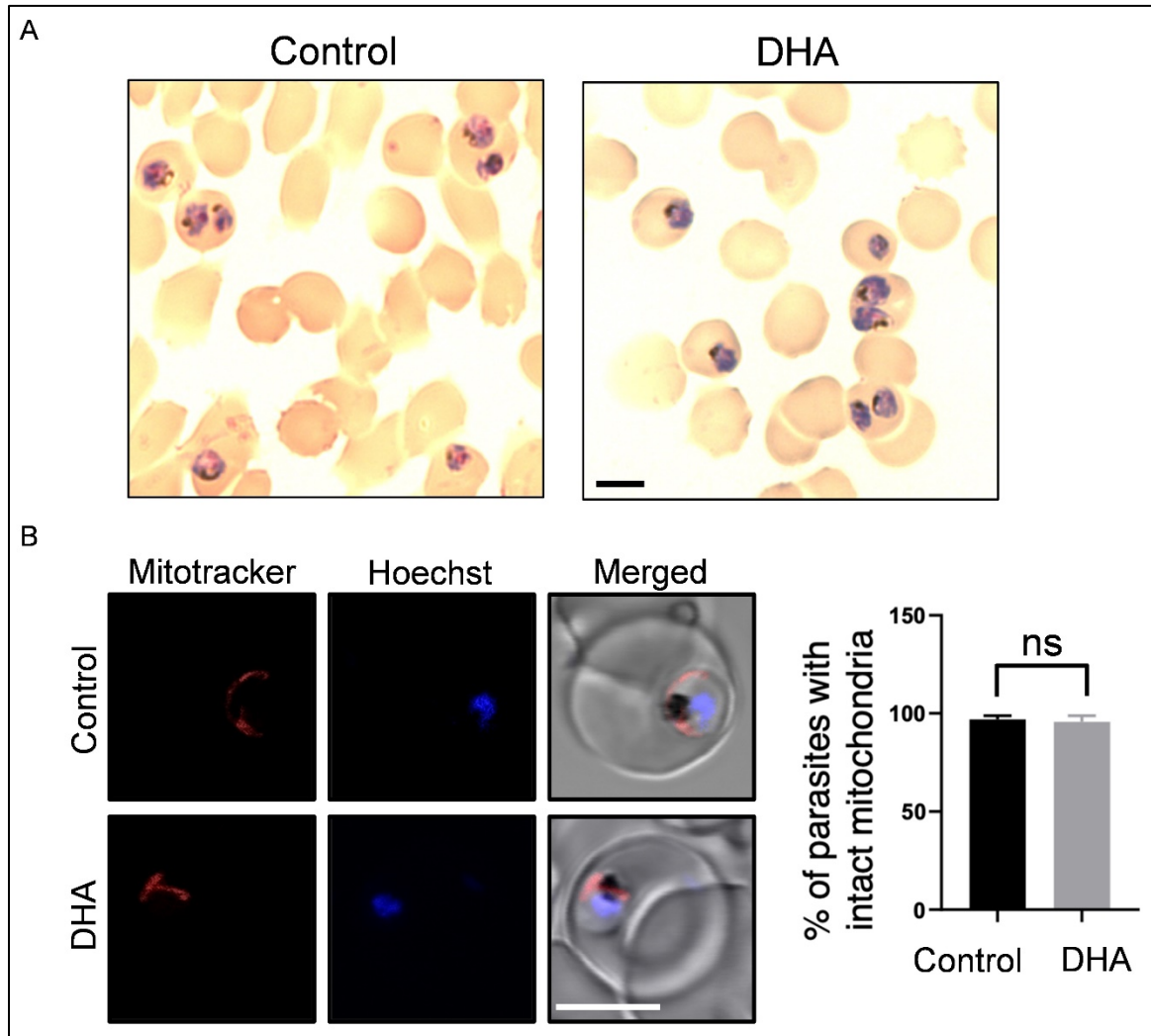


Figure 3.1 *P. falciparum* remains viable upon incubation with 700 nM DHA

(A) Representative images of Giemsa stained thin blood smears prepared from control and parasites treated with 700 nM DHA for 1.5h. $n = 3$ independent experiments, Scale bar: 5 μm . (B) Control and DHA treated parasites were labelled with Mito-Tracker Red CMXRos to detect live cell. Samples were analysed using confocal microscopy, Scale bar: 5 μm . Graph represents the percentage of parasites with intact mitochondria upon incubation with DHA. $N = 50$ parasites, $n = 3$ independent experiments. The data points are expressed as mean \pm standard error of the means (SEM). Statistical significance is quantified using unpaired Student's t-test, ns = non-significant.

3.1.2 DHA induced ER stress activates the UPR pathway

The UPR signaling pathway is activated upon ER stress in yeast, eukaryotes, as well as in *P. falciparum* (Bridgford *et al.*, 2018; Wu *et al.*, 2014; Zhang *et al.*, 2017). UPR acts by initiating its transcriptional and translational stress sensors and adjusting the ER's capacity, by expanding its volume, to accommodate protein aggregates and facilitate their re-folding (Bernales *et al.*, 2006; Calfon *et al.*, 2002; Harding *et al.*, 1999).

In order to analyse ER expansion, we visualized the parasite ER by fluorescently tagging *PfSEC62*, a translocon complex component present on the ER membrane, with GFP. *PfSEC62*-GFP was cloned into the pARL1-a transient expression vector for *P. falciparum* (Crabb *et al.*, 2004) and transfected into 3D7 parasites (Figure 3.2A). The localization of *PfSEC62*-GFP was followed in the IE stages of transfected parasites by live cell confocal microscopy (Figure 3.2B). In early stage parasites, fluorescent signals from *PfSEC62*-GFP appear to have a perinuclear distribution with 'horn-like' extensions protruding into the cytoplasm. In the later stages, the signals reveal a mesh-like network around each nucleus throughout the cytoplasm (Figure 3.2B). The observation corroborates with the extensive branching of the ER at the late trophozoite and schizont stages. The pattern of *PfSEC62*-GFP fluorescence throughout the IE stages indicates characteristic parasite ER morphology (van Dooren *et al.*, 2005; Lee *et al.*, 2008). Additionally, to determine whether *PfSEC62*-GFP localises correctly to the ER, immunofluorescence analysis was used to determine colocalization of *PfSEC62*-GFP with KDEL, a peptide sequence found at the C-terminus of eukaryotic proteins that are destined to relocate to the ER (Denecke *et al.*, 1992) and hence serves as an effective ER marker. Parasites stained with anti-GFP and anti-KDEL antibodies show localization of *PfSEC62*-GFP to largely overlap with KDEL, demonstrating that *PfSEC62*-GFP is retained in the ER and that the protein faithfully depicts the ER structure (Figure 3.2C).

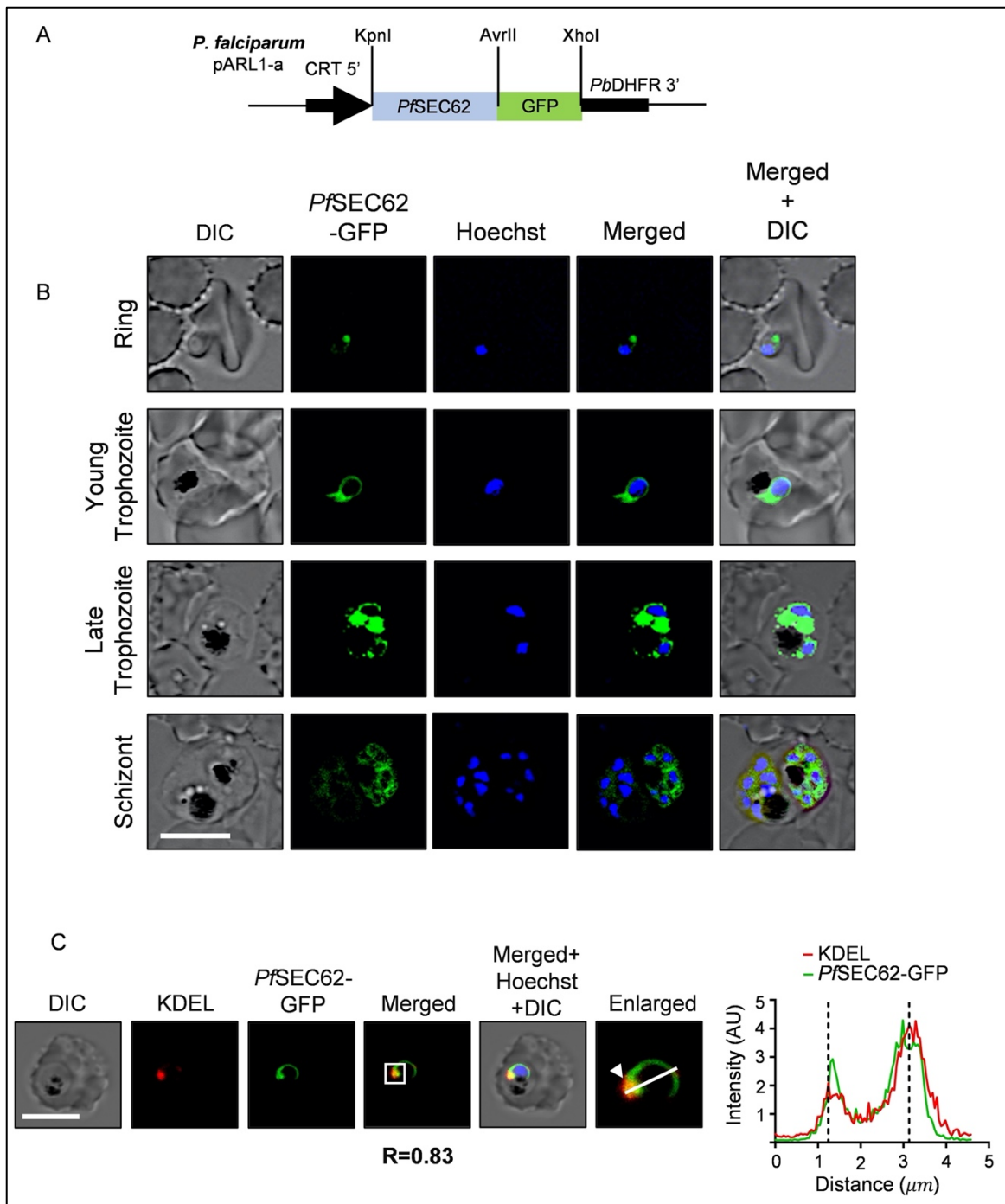


Figure 3.2 Expression and localization of *PfSEC62*-GFP in the intraerythrocytic stages of *P. falciparum*

(A) Schematic representation of recombinant vector constructs for episomal expression of *PfSEC62*-GFP in *P. falciparum* using expression vector pARL1-a. The complete coding sequence of *PfSEC62* without stop codon (blue) was cloned in frame with GFP (green) using unique restriction sites as indicated. The fusion protein is expressed under constitutively active promoter CRT. (B) Ring, early trophozoite, late trophozoite and schizont stages of *P. falciparum* were probed for the localization of *PfSEC62*-GFP by immunofluorescence analysis using anti-GFP antibodies

(1:200). Nucleus was stained with Hoechst. *Pf*SEC62 signal is present throughout the parasite perinuclear region in all blood-stages; N = 25 parasites, n = 3 experiments, Scale bar: 5 μ m. (C) Recombinant *P. falciparum* parasites were assessed for localization of *Pf*SEC62-GFP on ER using 1:200 diluted anti-GFP and anti-KDEL antibodies by immunofluorescence staining. Nucleus was stained with Hoechst. N = 25 parasites, n = 3 experiments, Scale bar: 5 μ m. Regions within the dashed white lines are enlarged and placed next to the merged panel to better represent colocalization. Extent of colocalization is represented using the Pearson's coefficient value (R) evaluated from the KDEL (red) and GFP (green) fluorescent signals within the white square region in the enlarged panel.

To determine UPR activation upon ER stress, we examined the ER expansion as a consequence of ART exposure to the parasites. Synchronized young trophozoites from *Pf*SEC62-GFP overexpressing 3D7 cultures were incubated with 700 nM DHA for 1.5h. The extent of expansion was estimated by measuring the distance of the *Pf*SEC62-GFP signals obtained from the line scan graphs of GFP fluorescence intensities (Figure 3.3A, enlarged panel) and the volume obtained from the 3D reconstructed confocal image (Figure 3.3B). The 'horn-like' extensions were observed to extend around the food vacuole in parasites incubated with DHA as compared to untreated parasites. As measured by the distance of the *Pf*SEC62-GFP signals, ER expansion was significantly higher in parasites incubated with DHA than in untreated ones (Figure 3.3C). As a control, the number of nuclei was calculated (Hoechst signal), and these were noted to remain constant, reflecting a uniform stage in the treated as well as the untreated parasites. Increased ER capacity may result in a reduction in the concentration of misfolded proteins in the ER lumen, thereby preventing protein aggregation and improving the parasite's ability to survive under ER stress.

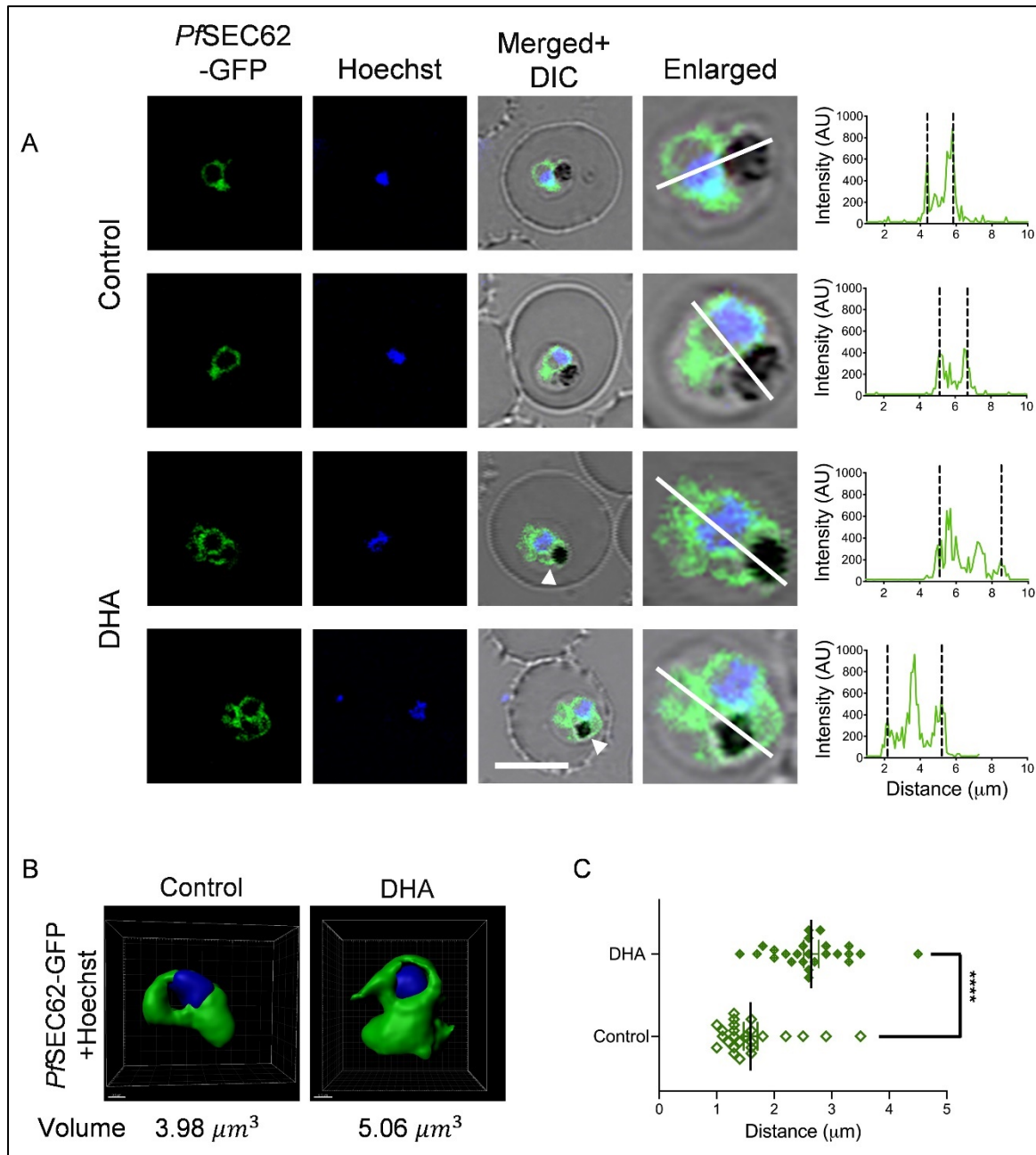


Figure 3.3 DHA induced ER stress leads to expansion of the parasite ER

To visualize the expansion and morphology of the parasite ER, we fluorescently tagged *PfSEC62*, a translocon complex component present on the ER membrane with GFP. (A) Live cell confocal microscopy images of *P. falciparum* 3D7 parasites overexpressing *PfSEC62*-GFP. ER expansion was observed after 1.5 h of incubation with DHA. *PfSEC62*-GFP signal extends into the parasite cytoplasm whereas it localizes to the nuclear periphery in control (untreated) parasites. ER expansion was analysed using GFP fluorescence intensities measured along the white line in the enlarged panel, and were plotted as the line scan graphs. Nucleus was stained using Hoechst. Scale bar: 5 μm . (B) 3D reconstruction with Z-stacks obtained from confocal images of control and of

parasites incubated with DHA overexpressing *PfSEC62-GFP*. Volume of ER was measured through the surface function in Imaris 3.0. (C) Scatter plot represents the extent of ER expansion as measured by the distance of *PfSEC62-GFP* signal (obtained from line scan graphs of GFP fluorescence intensities) in control and parasites incubated with DHA. N = 25 parasites, n = 3 independent experiments. The data points are expressed as mean \pm SEM. Statistical significance is quantified using unpaired Student's t-test, **** = P < 0.0001.

The phosphorylation status of *PfeIF2 α* was determined to assess if the UPR translational arm is activated during incubation of parasites with 700nM DHA. A significant increase in *PfeIF2 α* phosphorylation levels was observed after DHA treatment (~10 fold) as compared to the levels of total *PfeIF2 α* and the loading control β -Actin, which increased in a time-dependent manner (Figure 3.4A). One of the distinctive features of UPR in yeast and other eukaryotes is its ability to facilitate the production of ER chaperones, which enhances the ER's folding capability (Ellgaard *et al.*, 1999; Malhotra and Kaufman, 2007; Ron and Walter, 2007; Travers *et al.*, 2000). *PfBiP* is an ER resident chaperone whose protein expression levels are upregulated in response to ER stress in the closely related parasite species *Trypanosoma brucei* (Goldshmidt *et al.*, 2010). To examine if *PfBiP* is increased upon DHA induced ER stress, its levels were analysed by incubating parasites with 700 nM DHA for 1.5h. A ~2 fold upregulation of the expression levels of *PfBiP* upon DHA treatment (Figure 3.4B) was observed. Therefore, DHA induced ER stress activates *PfeIF2 α* and increases expression levels of *PfBiP*, the two major markers of UPR activation. Altogether, these results show DHA exposure elicits expansion of the parasite ER space and stress response machinery, beneficial for regulating protein homeostasis.

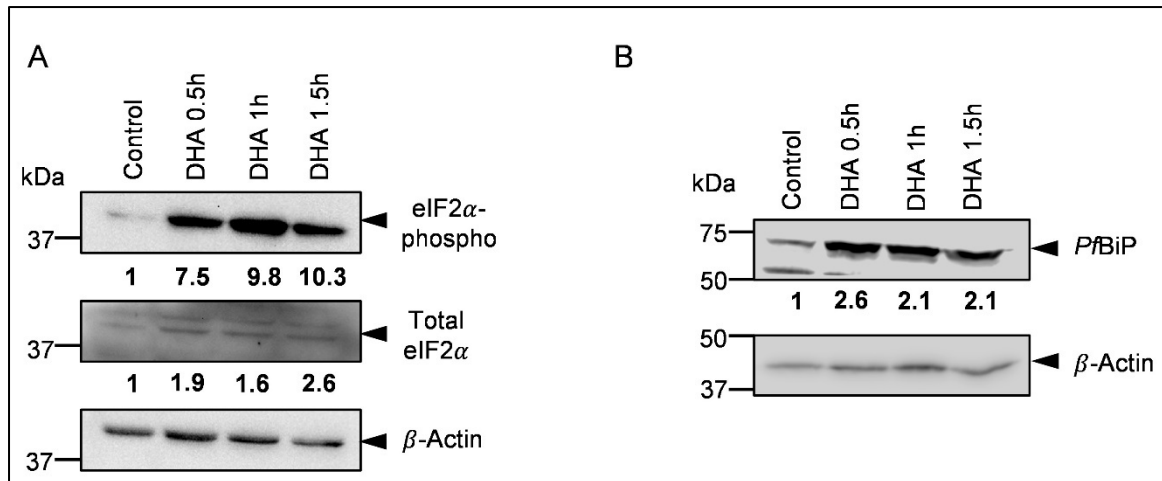


Figure 3.4 DHA induced ER stress leads to phosphorylation of *PfcIF2 α* and upregulation of *PfBiP*

Control and parasites incubated with DHA were harvested. Parasite lysates were subjected to western blot analysis and blots were probed with (A) phosphorylated-*PfcIF2 α* and total *PfcIF2 α* , and (B) *PfBiP* antibodies. β -Actin was used as the loading control. Fold difference, normalized with respect to control is shown below each blot.

3.1.3 DHA induced UPR pathway activates parasite autophagy

Autophagy is known to counterbalance UPR mediated ER stress in yeast and higher organisms through sequestration and subsequent degradation of excess ER containing toxic protein aggregates (Bridgford *et al.*, 2018; Ogata *et al.*, 2006; Yorimitsu *et al.*, 2006). Our recent study demonstrated *PfSEC62* as an ER resident autophagy receptor (Mamidi *et al.*, 2019), implicating recover-phagy to re-establish ER homeostasis upon resolution of ER stress in the parasite. Since there has been no experimental proof showing involvement of parasite autophagy upon induction of ER stress, we investigated the same by incubating young trophozoites with DHA (700 nM, 1.5 h) and analysed for the presence of autophagosome-like structures. Immunofluorescence analysis for quantifying the number of *PfATG8* (the autophagosome marker) labelled puncta, revealed the number to be significantly higher upon DHA treatment as compared to the control (Figures 3.5A and 3.5B). Our finding is in line with previous studies demonstrating an increase in the number of GFP-ATG8 punctate structures in yeast cells upon ER stress induction (Yorimitsu *et al.*, 2006).

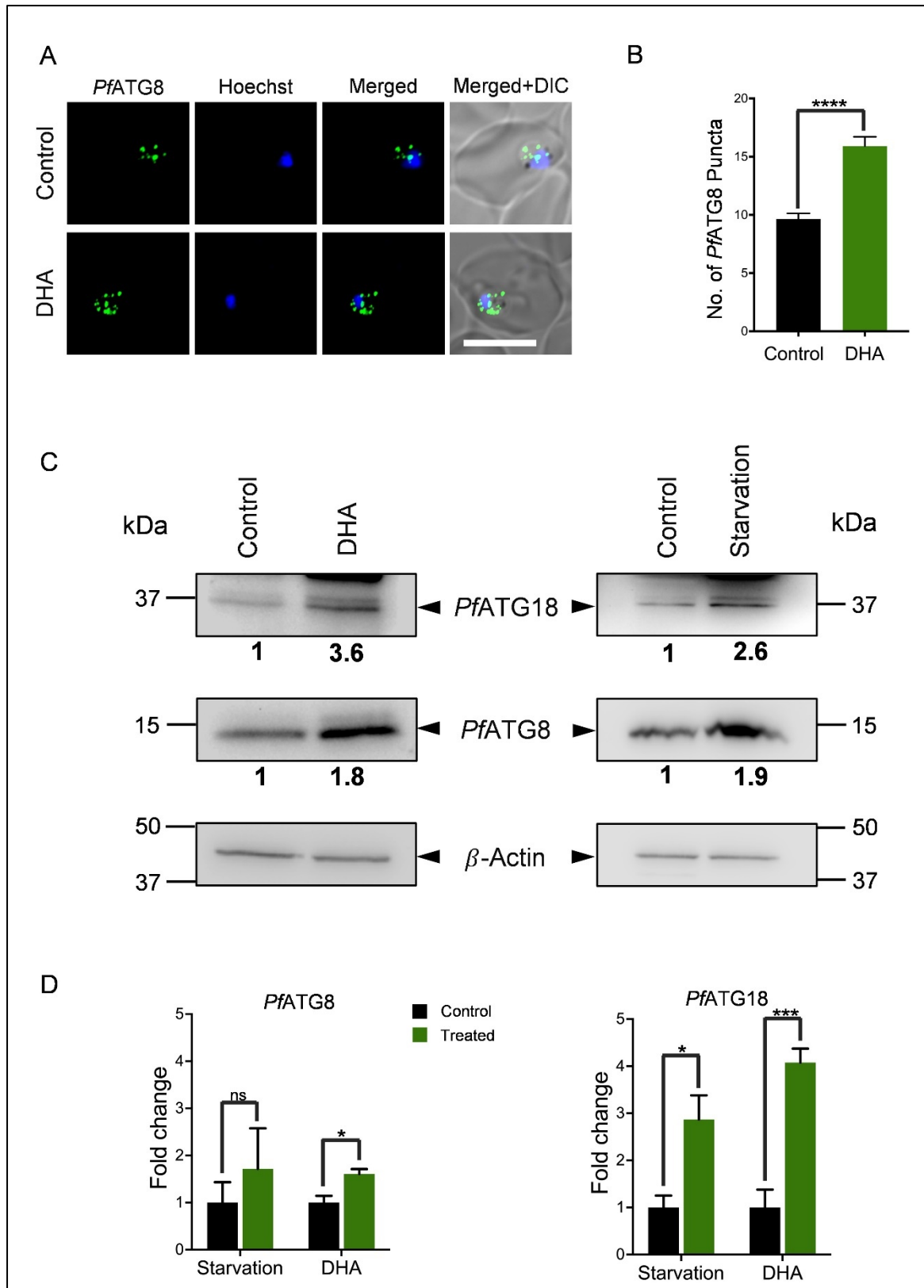


Figure 3.5 DHA induced ER stress activates parasite autophagy

(A) Immunofluorescence analysis of *P. falciparum* 3D7 parasites stained with anti-PfATG8 antibodies showing autophagosome-like structures in control and parasites incubated with 700 nM

DHA for 1.5 h. Nucleus was stained using Hoechst. Scale bar: 5 μ m. (B) Graph denotes the number of *Pf*ATG8 labelled puncta in control and parasites incubated with DHA. $N > 15$ parasites, $n = 3$ independent experiments. (C) *P. falciparum* 3D7 parasites were incubated with either 700 nM DHA or starvation media for 1.5 h and harvested. Parasite lysates were subjected to western blot analysis and blots were probed with *Pf*ATG8 and *Pf*ATG18 antibodies. β -Actin was used as the loading control. (D) Graphs showing the fold change of *Pf*ATG8 (left) and *Pf*ATG18 (right) protein expression levels upon incubation with DHA and starvation media. $n = 3$ independent experiments. The data points are expressed as mean \pm SEM. Statistical significance is quantified using unpaired Student's t-test, **** = $P < 0.0001$, *** = $P < 0.0005$, * = $P < 0.05$, ns = non-significant.

To investigate whether the enhanced number of autophagosome-like structures correlates with increased levels of autophagy proteins, expression levels of *Pf*ATG8 and *Pf*ATG18 were analysed. As our earlier studies (Agrawal *et al.*, 2020; Joy *et al.*, 2018) demonstrated increased levels of parasite autophagy proteins upon starvation, parasites were also incubated with starvation media as a control. Parasites incubated with DHA displayed upregulation in the expression levels of *Pf*ATG8 by ~ 1.8 fold and *Pf*ATG18 by ~ 3.5 fold (Figures 3.5C, left panel and 3.5D) with respect to control (untreated), as determined by western blot analysis. A similar trend in autophagy modulation was observed under starvation (Figures 3.5C, right panel and 3.5D), indicating stress mediated autophagy induction. The increased number of *Pf*ATG8 labelled vesicles together with upregulation in the expression levels of *Pf*ATG8 and *Pf*ATG18 indicates activation of the parasite autophagy upon DHA induced ER stress.

To confirm that the observed increase in expression levels of autophagy proteins upon DHA exposure is directly mediated through UPR, young trophozoites were treated with the mammalian PERK inhibitor GSK2606414, which specifically blocks UPR/PERK activation (Axten *et al.*, 2012). Incubation of young trophozoites with 30mM GSK2606414 for 2.5 h inhibited *PfeIF2 α* phosphorylation in response to a 1.5 h DHA pulse (Figure 3.6A), demonstrating that the *PfeIF2 α* phosphorylation elicited by DHA is a result of UPR activation upon ER stress and not due to any other cellular stress. Expression levels of autophagy proteins were monitored in parasites treated with GSK2606414 with and without DHA. The PERK inhibitor significantly reduced the basal and DHA induced expression levels of *Pf*ATG8 and *Pf*ATG18 (Figures 3.6A and 3.6B). As autophagy activation is considerably impaired upon disruption of the parasite UPR machinery, it signifies a role in

regulating ER-stress induced UPR. These results thus further establish parasite autophagy as an ER-stress response pathway in *P. falciparum* triggered upon UPR activation.

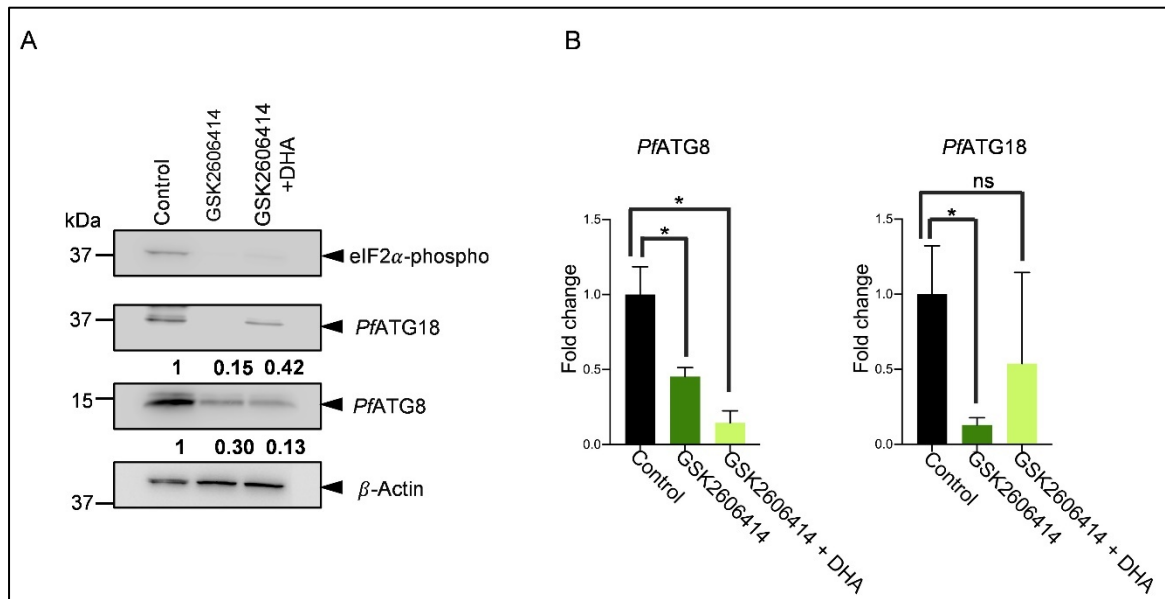


Figure 3.6 DHA mediated activation of parasite autophagy is triggered by the UPR pathway

(A) *P. falciparum* 3D7 parasites pre-incubated with 30 μ M GSK2606414 for 1 h were treated with 700nM DHA for 1.5h and then harvested. Parasite lysates were subjected to western blot analysis and blots were probed with PfATG8, PfATG18 and phosphorylated-eIF2 α antibodies. β – Actin was used as the loading control. n = 3 independent experiments. Fold difference, normalized with respect to control is shown below each blot. (B) Graphs showing the fold change of PfATG8 (left) and PfATG18 (right) protein expression levels upon incubation with GSK2606414 and GSK2606414+DHA. n = 3 independent experiments. The data points are expressed as mean \pm SEM. Statistical significance is quantified using unpaired Student’s t-test, * = P < 0.05, ns = non-significant.

3.2 Deciphering the role of putative PfATG1 (PF3D7_1450000) in the autophagy-like pathway in *P. falciparum*

To advance our understanding of how ER stress induces parasite autophagy, it is essential to investigate the protein complexes involved in autophagy initiation. In yeast and other eukaryotes, the core ATG proteins assemble at the PAS to initiate autophagosome nucleation. The ATG1 kinase, regulatory protein ATG13 and the scaffolding ternary subcomplex consisting of ATG17, ATG31 and ATG29 comprise the initiation complex

recruited to the PAS in yeast (Yin *et al.*, 2016). ATG1 is a serine/threonine kinase, with a conserved kinase domain at its N-terminus. The interaction of ATG1 with ATG13 and ATG17 stimulates ATG1 kinase activity, and the formation of this complex is essential for ATG1's function in autophagy initiation (Kabeya *et al.*, 2005). During nutrient-rich conditions, the TOR kinase phosphorylates ATG1 and ATG13, preventing the formation of the ATG1-ATG13-ATG17-ATG31-ATG29 complex, thus suppressing activation of autophagy. Upon amino acid starvation or treatment with rapamycin, a TOR inhibitor, ATG13 is rapidly dephosphorylated which increases its binding with and activation of ATG1 and subsequent induction of the autophagy process (Yin *et al.*, 2016).

ER stress is also known to activate autophagy. In yeast, ER stress induced by dithiothreitol (DTT) or tunicamycin (TM) increases ATG1 kinase activity. ER stress also induces the assembly of PAS and stimulates the formation and transport of autophagosomes to the vacuole (Yorimitsu *et al.*, 2006). Studies have also shown that the glycogen synthase kinase-3 β (GSK3 β)-Tat-interactive protein, 60 kDa (TIP60)-ULK1 signaling axis induces autophagy during ER stress. ER stress activates GSK3 β which in turn phosphorylates TIP60, triggering a TIP60-mediated acetylation of ULK1 and activation of autophagy (Nie *et al.*, 2016). Given that ATG1 lies at the crossroad of regulatory pathways and autophagy initiation, it is essential to characterize the protein in *P. falciparum* in order to elucidate its function and to gain a better understanding of how DHA induced ER stress drives parasite autophagy. Bioinformatic analyses identified homologs of yeast ATG1 and ATG17 in the malaria parasite, however ATG13, ATG31, and ATG29 seem to be absent. The putative *Pf*ATG1 kinase domain is conserved but lacks the ATG13 binding motif, most likely owing to the parasite lacking ATG13 (Hain and Bosch, 2013). Therefore, functional investigations are required to determine whether the identified ATG1 homolog in *P. falciparum* functions in a similar manner to that of yeast or human ATG1/ULK1.

The putative *Pf*ATG1 was characterised and its involvement in the autophagy-like pathway in *P. falciparum* is unravelled in this work. We show that putative *Pf*ATG1 is expressed throughout the parasite's blood stages and exists as discrete cytoplasmic puncta that colocalize with the autophagosome marker protein *Pf*ATG8, as well as the parasite ER, which is known to provide membranes for autophagosome biogenesis. MRT68921, a small molecule inhibitor of *Hs*ULK1, suppresses parasite growth and decreases the expression levels of other ATG proteins, thus corroborating with the reported autophagy inhibition in

MRT68921 treated mammalian cells. This demonstrates the putative ATG1's involvement as a canonical autophagy protein in *P. falciparum*. Although putative *PfATG1* exhibits a number of features consistent with an autophagy-like function in the parasite, when produced in the *atg1Δ S. cerevisiae* strain, *PfATG1*-GFP failed to localise to the PAS upon starvation and was unable to restore autophagy in ATG1 defective yeast cells.

3.2.1 Bioinformatic analysis of putative ATG1 homolog in *P. falciparum*

A homolog of ATG1 is identified in *P. falciparum* genome (PF3D7_1450000), which shares 31 % identity with 63 % query coverage with *HsULK1*, while sharing 28 % identity with 73 % query coverage with *ScATG1* (Figure 3.7A and Appendix 1). Although the identity is low, the putative *PfATG1* contains a conserved kinase domain (Navale *et al.*, 2014) (Figure 3.7A, kinase domain highlighted by a continuous grey line), which has been essential for autophagosome formation in other eukaryotes (Cheong and Klionsky, 2008a; Kamada *et al.*, 2000; Yeh *et al.*, 2011). The threonine at position 226 on *ScATG1*, which is required for proper autophagy induction (Yeh *et al.*, 2010), is replaced with another phosphorylatable serine residue (Figure 3.7A, highlighted by a green line), retaining the phosphorylation site in the activation loop of putative *PfATG1*.

The PlasmoDB database shows that the putative ATG1 gene is located on chromosome 14 of *P. falciparum*. It contains nine exons, with a transcript length of 1131 bp and translates into 376 amino acids long protein, while yeast and human ATG1/ULK1 comprise 897 and 1050 amino acid residues, respectively. The difference in the amino acid lengths of putative *PfATG1* with *HsULK1* or *ScATG1* is because putative *PfATG1* lacks the ATG13 binding microtubule interacting and transport (MIT) domains that are conserved in yeast and other eukaryotes (Navale *et al.*, 2014). The kinase domain, which is found at the N-terminus of *ScATG1* and *HsULK1*, spans nearly the whole length of the putative *PfATG1* (Figure 3.7A). The calculated molecular weight of the putative *PfATG1* protein is 43.7 kDa, and its isoelectric point is 9.58 due to the presence of multiple positively charged amino acids. The protein lacks a transmembrane domain and a signal peptide sequence and is thus predicted to be present in the parasite cytosol.

HsULK1 has a conserved three-dimensional structure that consists of the typical kinase fold with a large loop connecting the N- and C-terminal lobes (Lazarus *et al.*, 2015). The

three-dimensional structure of putative *PfATG1* was predicted using the bioinformatics tool Phyre2 (Protein Homology/analogy Recognition Engine V 2.0) and visualized by UCSF Chimera (Figure 3.7B). The structure-based comparison of *PfATG1* and *HsULK1* (PDB: 4TQ0) was performed by UCSF Chimera, which shows significant overlap (Figure 3.7B) between the two structures, indicating that putative *PfATG1* might have conserved the domain architecture of ATG1/ULK1.

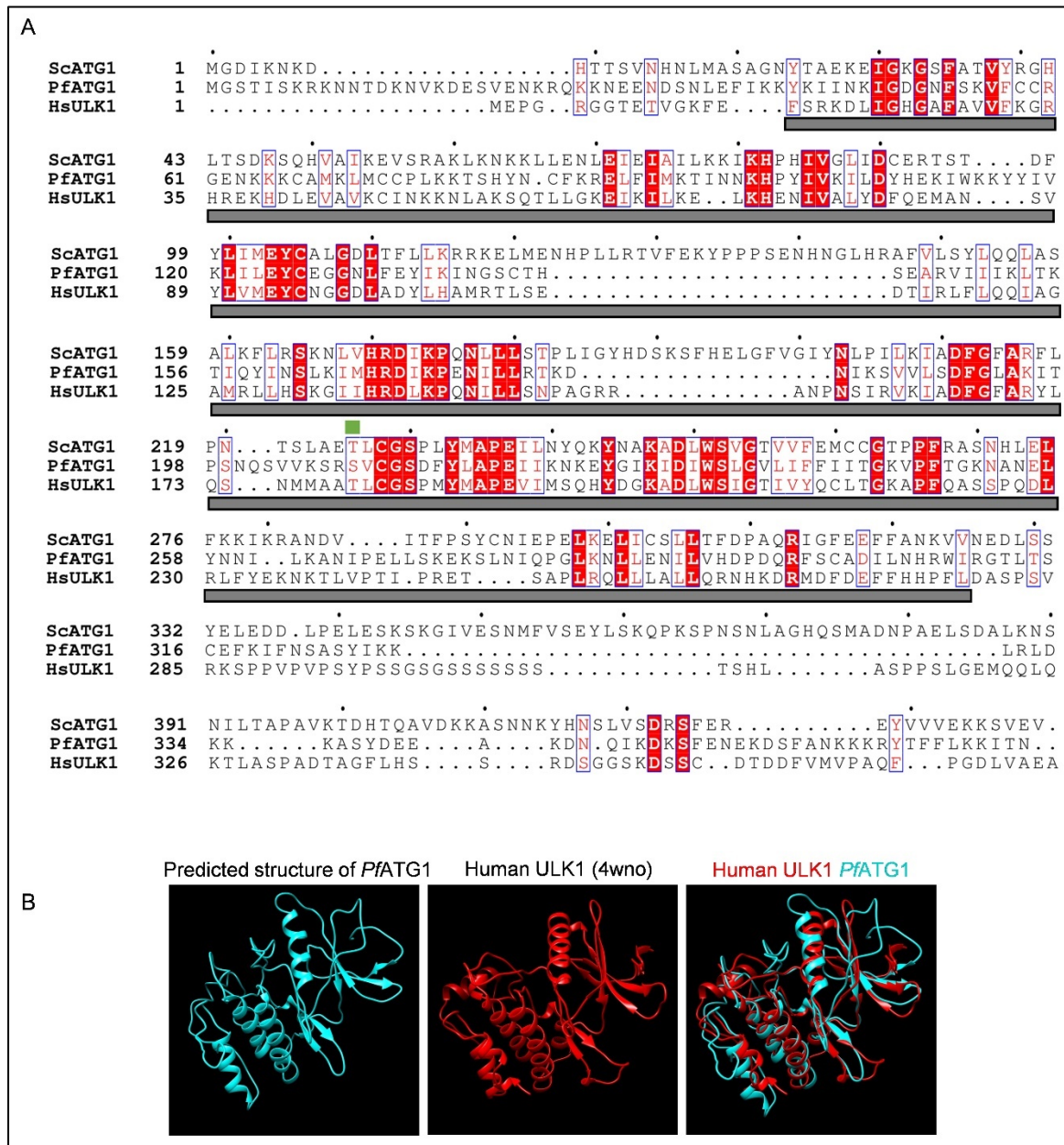


Figure 3.7 Sequence and structure-based comparison of putative *PfATG1*

(A) Sequence comparison of putative *PfATG1*, *ScATG1*, and *HsULK1* was performed by Clustal Omega and visualized by ESPrpt 3.0. The conserved residues are in the red box, kinase domain is 94 | Results

indicated by the grey bar. The green bar indicates conserved aspartic acid residue; T226 in *ScATG1*, T180 in *HsULK1*, and corresponding S208 in putative *PfATG1*. (B) Structure of putative *PfATG1* is predicted by Phyre2 and visualized by UCSF Chimera. Structure of putative *PfULK1* is obtained from PDB (4wno) and visualized by UCSF Chimera. Ribbon diagram of the predicted structure showing *PfATG1* in cyan and *PfULK1* in red.

3.2.2 Putative *PfATG1* localizes on the autophagosome-like vesicles in *P. falciparum*

To investigate the role of putative *PfATG1* in *P. falciparum* autophagy, anti-*PfATG1* antibodies were custom generated against the *PfATG1* peptide, LKANIPPELLSKEKSLNIQPGLKNLLENILVHDP (262-294), by Bioklone Biotech Private Ltd., India. Antibodies were validated for specificity against uninfected RBC and mixed culture blood-stage *P. falciparum* lysates. Anti-*PfATG1* antibodies detected a single band at the expected size (~45 kDa) corresponding to putative *PfATG1* in the parasite lysate by western blot analysis, but did not react with the uninfected RBC lysate (Figure 3.8A), indicating that the antibodies are specific for putative *PfATG1*.

To determine the intracellular localization of putative *PfATG1*, immunofluorescence assay of IE stages of *P. falciparum* was carried out. Parasites were fixed at ring (10 hpi), young trophozoite (22 hpi), late trophozoite (32 hpi), and schizont (40 hpi) stages. Using anti-*PfATG1* antibodies, putative *PfATG1* signals were observed during all asexual blood stages inside the parasite cytosol (Figure 3.8B). Additionally, putative *PfATG1* was associated with punctate structures of approximately 200-350 nm diameter (Figure 3.8B), which is similar to that of reported *PfATG8* vesicle size (Cervantes *et al.*, 2014; Navale *et al.*, 2014). The number of putative *PfATG1* labelled vesicles in rings, early trophozoites, late trophozoites, and schizonts was quantified and found to be approximately 3, 7, 12 and 13, respectively (Figure 3.8C), indicating that expression of putative *PfATG1* increases with the development of the asexual IE stages.

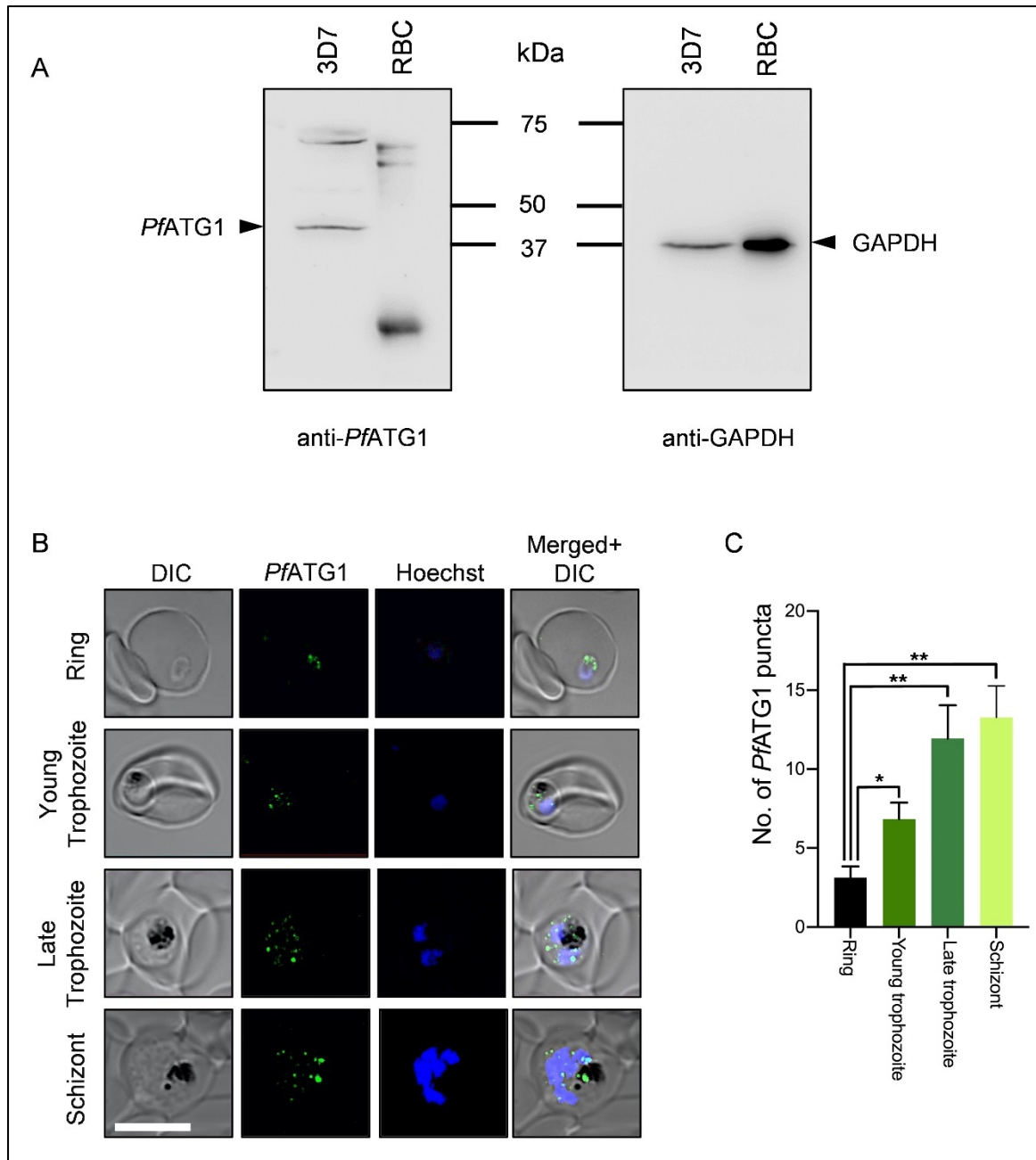


Figure 3.8 Putative *PfATG1* is present as punctate structure in the IE stages of *P. falciparum*

(A) Western blot analysis of *P. falciparum* 3D7 and RBC lysates. The endogenous *PfATG1* protein was detected by anti-*PfATG1* antibodies at the expected molecular size (~45 kDa). GAPDH was used as the loading control; n = 3 independent experiments. (B) Ring, early trophozoite, late trophozoite and schizont stages of *P. falciparum* were probed for the localization of putative *PfATG1* by immunofluorescence analysis using anti-*PfATG1* antibodies (1:200). Nucleus was stained using Hoechst. Putative *PfATG1* signal is present throughout the parasite in all blood-stages and appears to be associated with vesicular structures; N = 20 parasites, n = 3 independent experiments, Scale bar: 5 μ m. (C) Graph represents the number of putative *PfATG1* labelled puncta

vesicles in indicated parasite stages; N = 20 parasites, n = 3 independent experiments. The data points are expressed as mean \pm SEM. Statistical significance is quantified using unpaired Student's t-test, ** represents $P < 0.005$, * represents $P < 0.05$, analysed by unpaired Student's t test.

Autophagosomes are dynamic structures found in eukaryotes. ATG1 is one of the first proteins to be recruited to the isolation membrane during the early stages of autophagosome formation and remains there until the autophagosome is fully formed, whereas ATG8 is recruited to the autophagosome later in its biogenesis and remains associated with it until it fuses with the vacuole (Suzuki *et al.*, 2007). Given that putative *PfATG1* labelled vesicles appeared to be similar to *PfATG8* labelled vesicles, resembling autophagosomes, we validated the localization of putative *PfATG1* on autophagosomes by examining their colocalization with the autophagosome marker *PfATG8* (Tomlins *et al.*, 2013) at various IE stages of the parasite. Throughout the various IE stages, putative *PfATG1* positive puncta partially colocalized with *PfATG8* labelled vesicles (Figure 3.9A), suggesting the presence of putative *PfATG1* on autophagosome-like structures.

As autophagosome biogenesis occurs adjacent to the ER in higher eukaryotes (Shibutani and Yoshimori, 2014), we investigated the colocalization of putative *PfATG1* with *PfSEC62*, a parasite ER marker. *PfSEC62*, which localizes to the ER membrane, was used to label the parasite ER. In trophozoite stage parasites, putative *PfATG1* labelled vesicles colocalize partially with *PfSEC62* (Figure 3.9B), showing the presence of putative *PfATG1* on the organelle, which may play a key role in autophagosome formation.

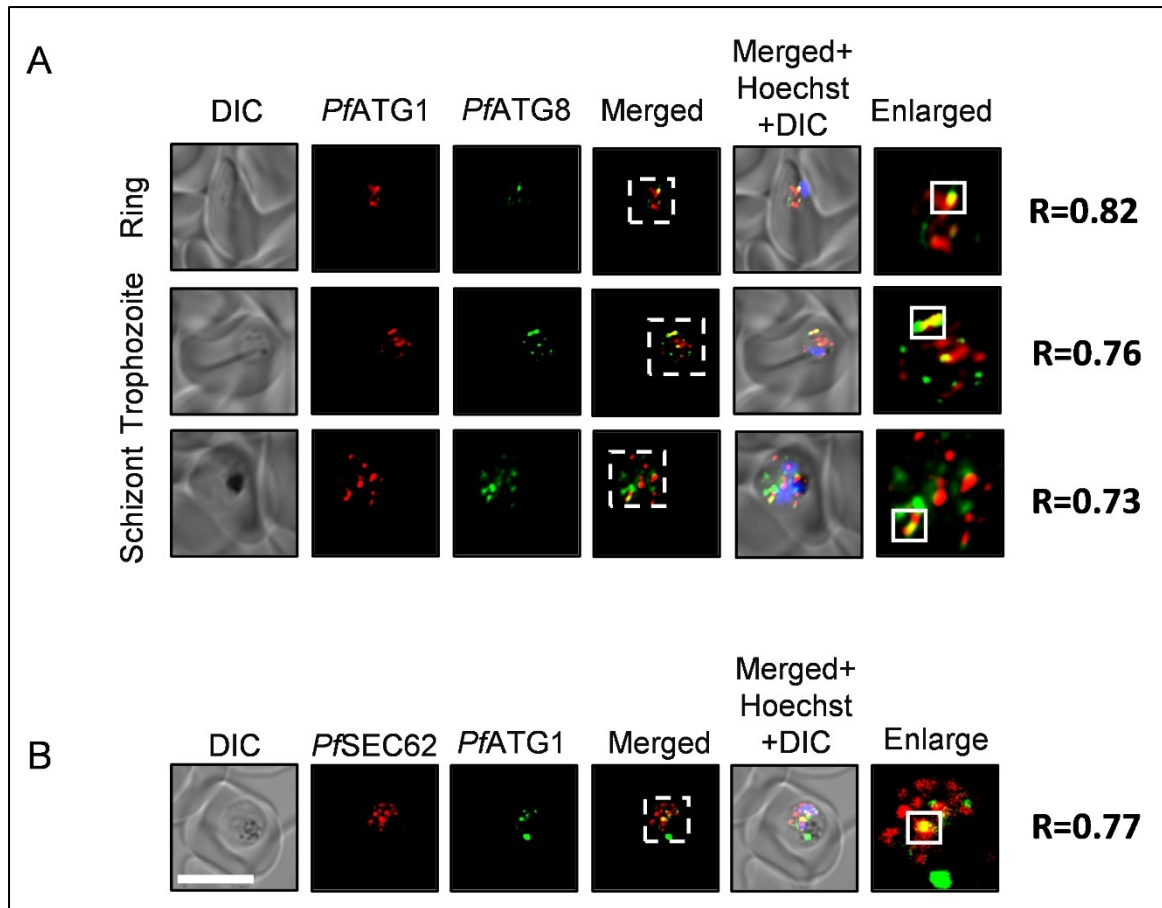


Figure 3.9 Putative *PfATG1* localizes on autophagosome-like vesicles and the ER in *P. falciparum*

(A) Intraerythrocytic stages of *P. falciparum* were evaluated for the localization of putative *PfATG1* on autophagosome-like vesicles immunolabelled with anti-*PfATG1* (1:200) and anti-*PfATG8* (1:600) antibodies were labelled using the Zenon antibody labelling system; N = 20 parasites, n = 3 independent experiments, Scale bar: 5 μm . (B) Young trophozoite stage parasites were evaluated for the localization of putative *PfATG1* on ER immunolabelled with anti-*PfATG1* (1:200) and anti-*PfSEC62* (1:400) antibodies were labelled using the Zenon antibody labelling system; N = 20 parasites, n = 3 independent experiments, Scale bar: 5 μm .

3.2.3 Specific ULK1/ATG1 inhibitor, MRT68921, modulates parasite autophagy and survival of *P. falciparum*

MRT68921 was identified in an *in vitro* screen of known kinase inhibitors against ULK1 and ULK2, homologs of *ScATG1* in humans (Petherick *et al.*, 2015). The compound reduces the conversion of LC3-I to LC3-II during autophagy induction upon starvation, indicating inhibition of the autophagic flux (Tanida *et al.*, 2008). *In vitro* profiling revealed

off-target effects of MRT68921 on TBK1 and AMPK-related kinases. However, the effect of MRT68921 on autophagic flux decrease was unaffected in cells lacking either TBK1 or liver kinase B1 (LKB1), a regulator of AMPK, indicating that neither TBK1 nor AMPK is necessary for compound-dependent autophagy inhibition. MRT68921 was likewise incapable of inhibiting autophagic flux in a drug-resistant mutant form of ULK1, implying that MRT68921 inhibits the autophagy pathway via ULK1 (Petherick *et al.*, 2015). These studies demonstrated the specificity of MRT68921 towards autophagy inhibition.

Here, we utilized MRT68921 to elucidate the role of parasite autophagy in *P. falciparum* growth and survival. Tightly synchronized early ring stage parasites (1 % parasitemia, 5 % hematocrit) were incubated with various concentrations of MRT68921 (50 nM, 100nM, 250 nM, 400 nM, 650 nM, 800 nM, 1000 nM, 2500 nM and 5000 nM) for 72 h. The cultures were replenished with media containing MRT68921 for the next 72 h. Giemsa stained smears from parasite cultures at the end of the assay were used to monitor the parasite morphology and invasion in the next cycle (Figure 3.10A). A dose-response curve was plotted to determine the relative parasite load with respect to increasing MRT68921 concentration. The IC₅₀ of MRT68921 obtained from the dose-response curve was 761.1 nM (Figure 3.10B), indicating MRT68921 has a dose-dependent inhibitory effect on parasite growth. The majority of parasites displayed developmental defects, and were unable to grow beyond healthy trophozoites in concentrations of MRT68921 beyond its IC₅₀.

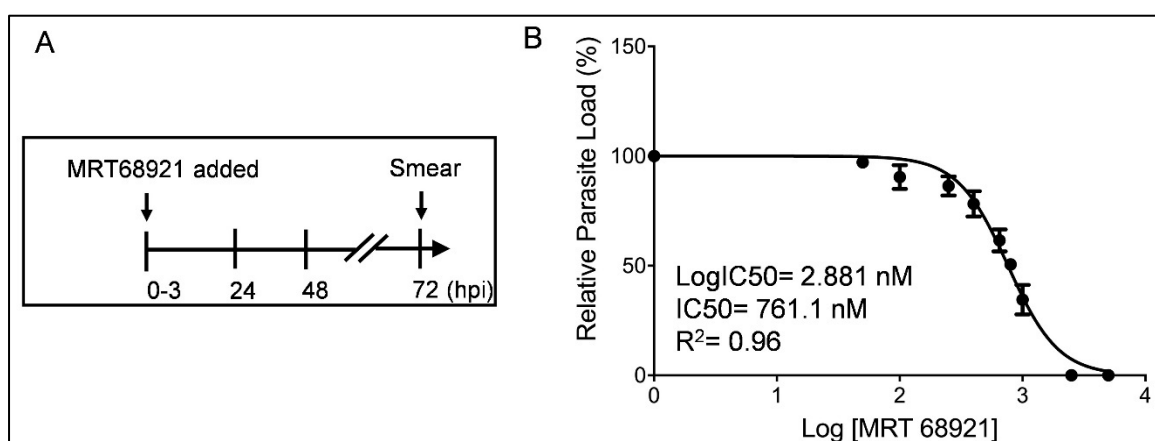


Figure 3.10 Effect of MRT68921, a specific autophagy inhibitor, on the growth of *P. falciparum*

(A) Schematic showing incubation of 0-3 hpi ring stage parasites with MRT68921, followed with change in culture media containing the inhibitor at 24 hpi and 48 hpi. The kink represents parasite reinvasion. Giemsa stained smears were prepared after 72 hpi. (B) The dose response curve showing percentage of relative parasite load at 72 hpi in *P. falciparum* 3D7 cultures. n = 3 independent experiments. The data points are expressed as mean \pm SEM.

To determine whether putative *PfATG1* is upstream of parasite autophagy-like proteins such as *PfATG8* and *PfATG18*, young trophozoites were treated with MRT68921. Parasites treated with 2.5 μ M MRT68921 for 1.5h with and without nutrient limiting conditions (to induce autophagy) showed no morphological abnormality or signs of delayed growth, as examined with Giemsa stained thin blood smears (Figure 3.11A). To assess the viability of treated parasites, cultures were supplemented with complete media devoid of the inhibitor and allowed to grow for an additional 30h. Upon recovery, parasitemia was determined by counting the iRBCs in a Giemsa stained blood smear (Figure 3.11B). Almost the whole parasite population (MRT68921: 96.79 ± 0.72 %; MRT68921 + starvation: 88.90 ± 0.49 %) was able to recover after supplementation by complete media (Figure 3.11B), indicating that the treated parasites were viable. Expression levels of autophagy proteins were monitored in parasites treated with MRT68921 in the presence and absence of starvation medium, which activates the parasite autophagy-like pathway. The specific autophagy inhibitor reduces the basal and starvation-induced expression levels of *PfATG8* and *PfATG18* (Figures 3.11C and 3.11D). Since inhibition of putative *PfATG1* activity significantly impairs autophagy activation, this suggests a role for putative *PfATG1* in regulating the parasite autophagy-like pathway.

antibodies. β -Actin was used as loading control. $n = 3$ independent experiments. Fold difference, normalized with respect to control is shown below each blot. (D) Graphs showing the fold change of *PfATG8* (left) and *PfATG18* (right) protein expression levels upon incubation with MRT68921 and MRT68921 + starvation. $n = 3$ independent experiments. The data points are expressed as mean \pm SEM. Statistical significance is quantified using unpaired Student's t-test, ** = $P < 0.005$, * = $P < 0.05$, ns = non-significant.

3.2.4 *PfATG1*-GFP is unable to complement autophagy or cytoplasm-to-vacuole functions in *S. cerevisiae*

To further validate the role of putative *PfATG1* in autophagy, functional complementation in *S. cerevisiae* was carried out. Accumulation of autophagic bodies in the yeast vacuole in response to nitrogen starvation, induced by treatment with the protease inhibitor phenylmethylsulphonyl fluoride (PMSF), is an indication of functional autophagy pathway (Tsukada and Ohsumi, 1993). Therefore, we studied the accumulation of autophagic bodies in *atg1 Δ* yeast cells expressing either *ScATG1*-GFP, *PfATG1*-GFP or GFP following nitrogen starvation and PMSF treatment. *S. cerevisiae atg1 Δ* strain transiently expressing *ScATG1*-GFP, *PfATG1*-GFP or GFP was generated. GFP was tagged either at the C-terminus of *ScATG1* or the codon-optimized *PfATG1* (sequence in Appendix 2), cloned into the yeast expression vector p415-ADH (Figure 3.12A) and transformed in yeast *atg1 Δ* cells. The expression of *ScATG1*-GFP, *PfATG1*-GFP and GFP was confirmed by western blot analysis with anti-GFP antibodies. Bands of the expected molecular weights, ~130 kDa ~70 kDa and ~26 kDa corresponding to *ScATG1*-GFP, *PfATG1*-GFP and GFP fusion protein, respectively, were observed in yeast lysate (Figure 3.12B). In the presence of PMSF, autophagic bodies were observed within the vacuole in *atg1 Δ* yeast cells expressing *ScATG1*-GFP (Figure 3.12C) as expected. These autophagic bodies were not detected within the vacuole of *atg1 Δ* yeast cells expressing either *PfATG1*-GFP or GFP (Figure 3.12C), indicating that *PfATG1*-GFP could not restore autophagy in autophagy-defective *atg1 Δ* yeast cells.

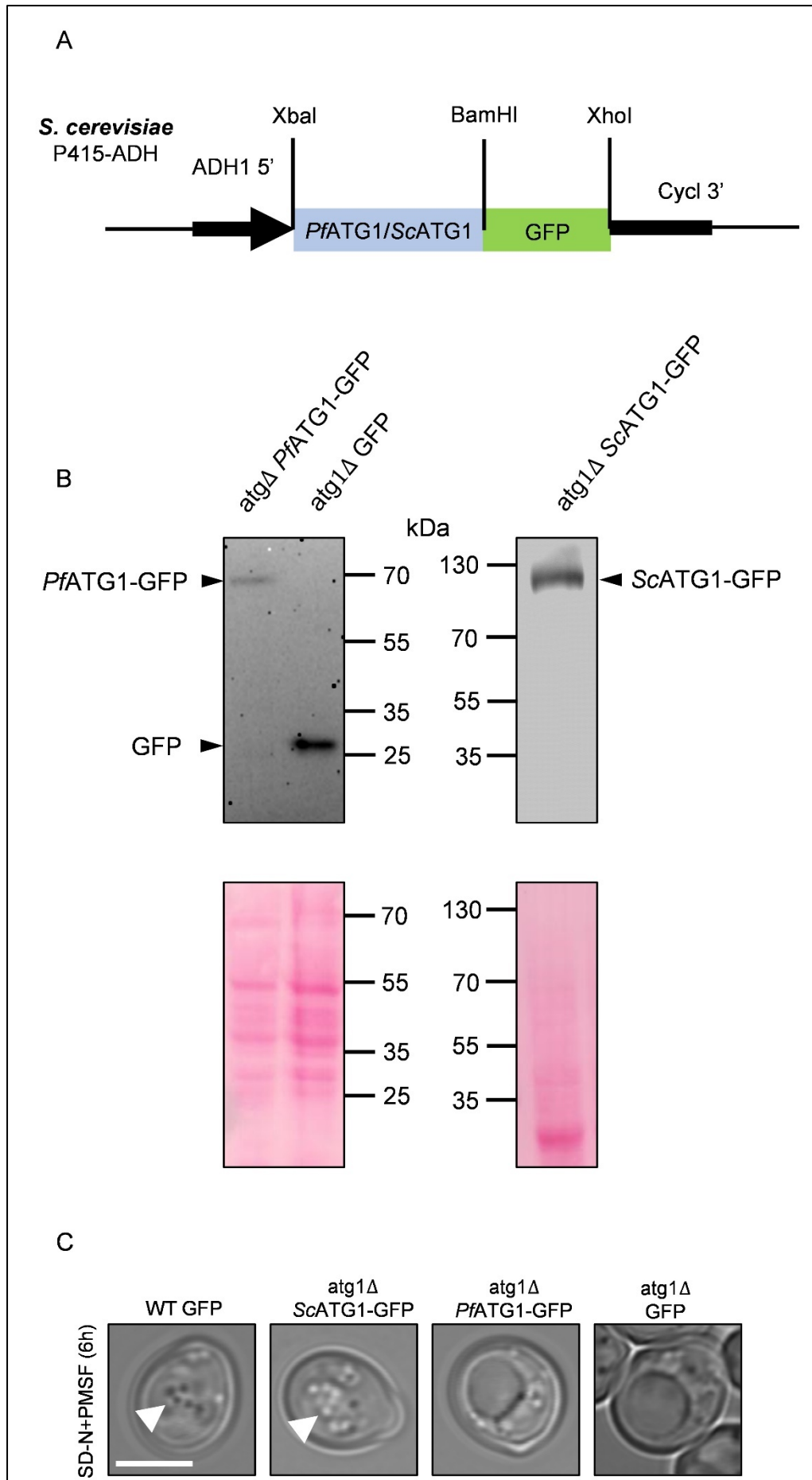


Figure 3.12 Overexpression of *PfATG1*-GFP in *S. cerevisiae* and *PfATG1*-GFP does not mediate formation of autophagic bodies in *atg1Δ* yeast strain during nitrogen starvation

(A) Schematic representation of recombinant vector constructs for episomal expression of *ScATG1*-GFP, *PfATG1*-GFP or GFP in *S. cerevisiae* using expression vector p415-ADH. The codon-optimized complete coding sequence of putative *PfATG1* without stop codon (blue) was cloned in frame with GFP (green) using unique restriction sites as indicated. (B) Western blot for yeast lysates overexpressing either *ScATG1*-GFP, *PfATG1*-GFP or GFP using anti-GFP antibodies detected *ScATG1*-GFP, *PfATG1*-GFP and GFP bands respectively. n = 3 independent experiments. (C) *PfATG1*-GFP could not participate in the formation of autophagic bodies in *atg1Δ* yeast cells. *atg1Δ* yeast cells expressing *ScATG1*-GFP, *PfATG1*-GFP, or GFP were incubated in SD(-N) medium containing 1mM PMSF at 30°C. Cells were observed under light microscopy after a 6 h incubation with PMSF (DIC images). Arrows indicate autophagic bodies in the yeast vacuole; N = 40 cells, n = 3 independent experiments, Scale bar: 5 μm.

Additionally, the mCherry-*ScATG8* processing assay was used to evaluate autophagic flux (Torggler *et al.*, 2017). In yeast, the deletion of the *ATG1* gene does not affect recruitment of *ATG8* to the perivacuolar region or the PAS, although autophagosome assembly is impaired in this mutant (Cheong *et al.*, 2008; Suzuki *et al.*, 2007). To evaluate autophagosome biogenesis in *atg1Δ* cells expressing *PfATG1*-GFP, we used fluorescence microscopy to monitor the autophagy flux using the mCherry-*ATG8* processing assay (Torggler *et al.*, 2017). As previously reported (Cheong *et al.*, 2008), the autophagy pathway was functional in wild type and *atg1Δ* cells expressing *ScATG1*-GFP, and the mCherry signal was seen in the vacuole upon nitrogen starvation (Figure 3.13A, upper two panels). However, in *atg1Δ* yeast cells expressing *PfATG1*-GFP or GFP, the mCherry signal accumulated at the perivacuolar region (Figure 3.13A, lower two panels), indicating that *PfATG1*-GFP could not restore the formation of autophagosome in *atg1Δ* yeast cells, corroborating our previous results. Upon quantifying the number of cells with mCherry-*ScATG8*-positive punctate structure in the perivacuolar region (Figure 3.13B) upon starvation, no significant differences were observed between the wild type yeast cells and *atg1Δ* cells expressing *ScATG1*-GFP. On the other hand, *PfATG1*-GFP or only GFP expressing *atg1Δ* cells, showed a significant increase in the number of cells with mCherry-*ScATG8*-positive punctate structure at the perivacuolar area as compared to *ScATG1* or wild type cells under autophagy conditions (Figure 3.13B). These results thus indicate that

*Pf*ATG1-GFP is unable to complement the biogenesis of autophagosomes in the *atg1Δ* yeast strain.

The Ape1 maturation assay is used to assess the activity of the Cytoplasm-to-Vacuole (Cvt) pathway (Lynch-Day and Klionsky, 2010; Torggler *et al.*, 2017). In wild type cells, precursor Ape1 (prApe1) is carried to the vacuole via the Cvt pathway, where it is proteolytically digested and transformed to the mature form (mApe1) (Torggler *et al.*, 2017). As expected, in wild type and *atg1Δ* cells expressing *Sc*ATG1-GFP, the mApe1 band was observed (Figure 3.13C), indicating a functional Cvt pathway (Torggler *et al.*, 2017). On the other hand, the mApe1 band was absent in *atg1Δ* cells expressing *Pf*ATG1-GFP or only GFP (Figure 3.13C), indicating that *Pf*ATG1-GFP was unable to complement the Cvt function in yeast. Together, these results demonstrate that *Pf*ATG1-GFP is unable to complement either autophagy or Cvt functions in yeast.

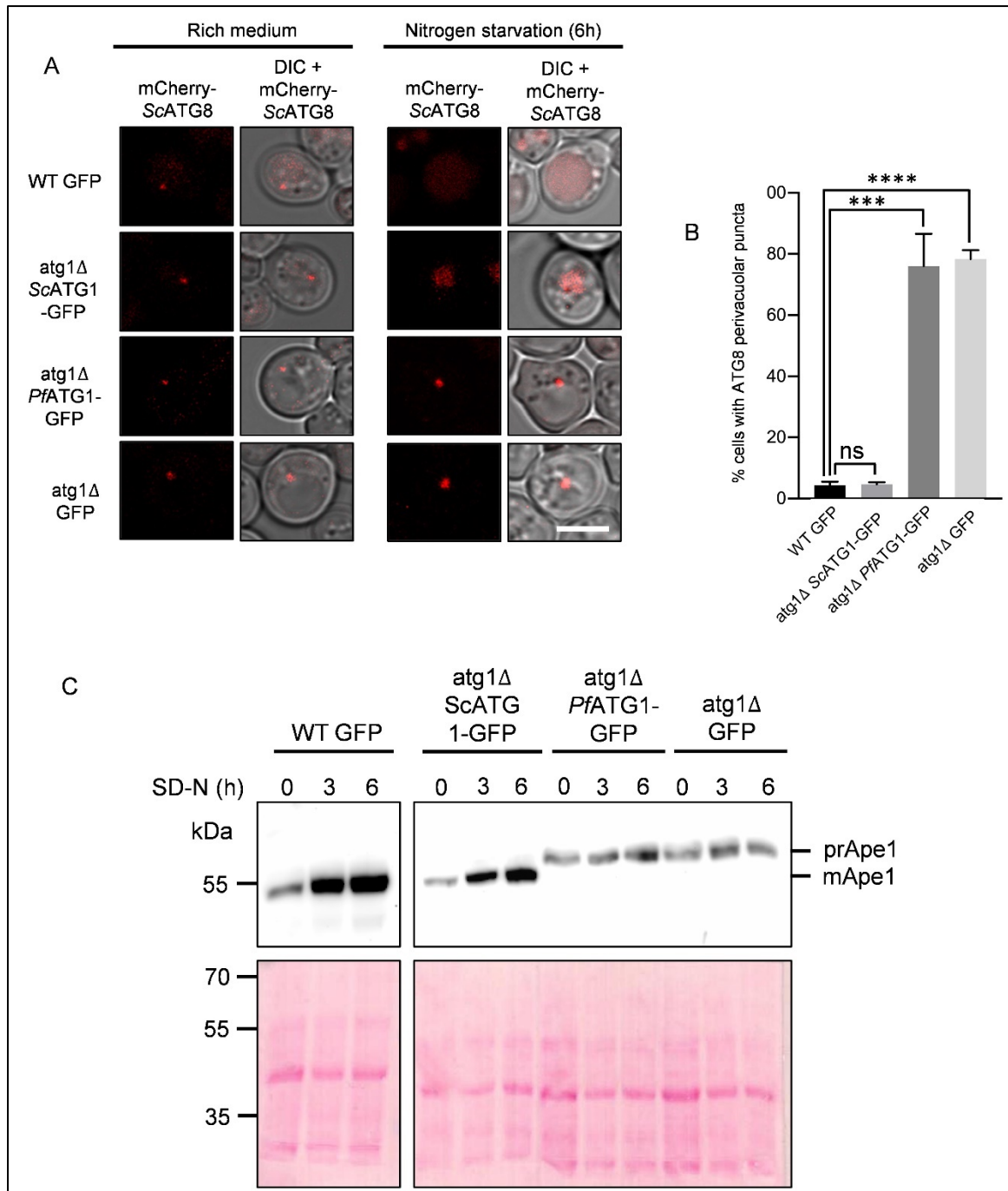


Figure 3.13 *PfATG1-GFP* does not complement autophagy functions in *atg1Δ* yeast strain

(A) mCherry-ScATG8 (ATG8 tagged with mCherry) was transformed in various yeast strains. Yeast strains were cultured in rich medium or a nitrogen-deprived medium for 6 h. Fluorescence microscopy was used to capture mCherry-ScATG8 signal; N = 100 cells, n = 3 independent experiments, Scale bar: 5 μ m. (B) The graph showing the percentage of cells with mCherry-ScATG8 puncta localized at the perivacuolar region upon 6 h of nitrogen starvation in the indicated yeast strains; N = 100 cells, n = 3 independent experiments. The data points are expressed as mean

± SEM. Statistical significance is quantified using unpaired Student's t-test, **** represents $P < 0.0001$, *** represents $P < 0.0005$, ns = non-significant. (C) Proteolytic maturation of ApeI was analysed by western blot using anti-ApeI antibodies (1:5000). A transfer blot stained with Ponceau demonstrates that the same amount of proteins from each fraction was resolved using SDS-PAGE. Samples were taken before and after nitrogen starvation of 3 and 6 h; n = 3 independent experiments.

Recruitment of ATG1 to the PAS is necessary for its autophagic function. Given that *Pf*ATG1-GFP was unable to restore autophagy in *atg1Δ* cells, we examined whether *Pf*ATG1-GFP labelled with mCherry-*Sc*Atg8 could localize to PAS. *Pf*ATG1-GFP was localized to the yeast periphery and did not colocalize with mCherry-*Sc*Atg8 under either nutrient-rich or deprived conditions (Figure 3.14A). *Sc*ATG1-GFP, on the other hand, was detected as punctate structures in the perivacuolar region, colocalizing with mCherry-*Sc*ATG8 in both nutrient-rich and deprived circumstances (Figure 3.14B). These findings indicate that *Pf*ATG1-GFP is incapable of associating with the PAS even upon nitrogen starvation.

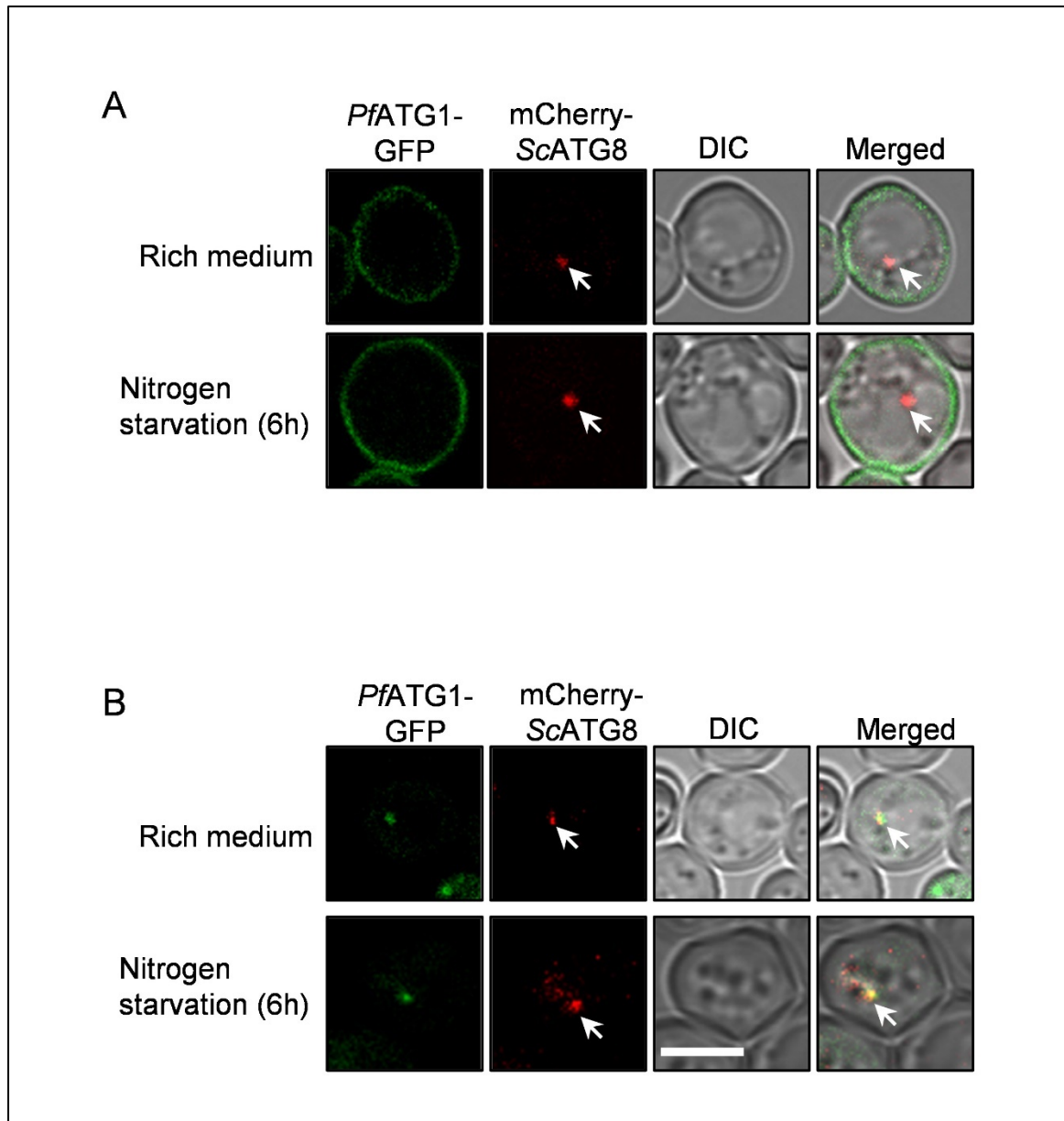


Figure 3.14 *PfATG1*-GFP does not localize on the PAS in *atg1Δ* yeast strain

(A) *atg1Δ* strain carrying *PfATG1*-GFP and mCherry-*ScATG8* was cultured in a nitrogen-deprived medium for 6 h, and the fluorescence signal was detected by live cell confocal microscopy. Arrows indicate mCherry-*ScATG8* signal at the PAS; N = 100 cells, n = 3 independent experiments, Scale bar: 5 μ m. (B) *atg1Δ* strain expressing *ScATG1*-GFP and mCherry-*ScATG8* was cultured in a nitrogen-deprived medium for 6 h, and the fluorescence signal was detected by live cell confocal microscopy. Arrows indicate mCherry-*ScATG8* signal at the PAS; N = 100 cells, n = 3 independent experiments, Scale bar: 5 μ m.

3.3 Investigating the role of parasite autophagy-like pathway in regulating various mechanisms of artemisinin resistance in *P. falciparum*

Genome-Wide Association Studies and whole genome sequencing of clinical and laboratory adapted ART resistant isolates have identified point mutations in the β -propeller domain of Kelch13 (*PfK13*) protein associated with ART resistance (Ariey *et al.*, 2014; Miotto *et al.*, 2015). The major *PfK13* variants identified in *P. falciparum* include C580Y, R539T, Y493H, I543T and N458Y; C580Y being prevalent in >50 % parasites across Southeast Asia (Anderson *et al.*, 2017; Ariey *et al.*, 2014; Imwong *et al.*, 2017; Siddiqui *et al.*, 2020). Further, background mutations in genes encoding coronin, atg18, ubp1, crt, mdr2, etc., are also reported to regulate the degree of ART resistance (Demas *et al.*, 2018; Henrici *et al.*, 2020; Miotto *et al.*, 2015; Wang *et al.*, 2016). Currently, there is very limited knowledge of the mechanism through which parasites eventually develop resistance to ART. Recent studies exploring the significance of the *PfK13* C580Y mutation in ART resistance have proposed the ‘ER and cytoplasmic proteostasis pathways’ (Suresh and Haldar, 2018) and ‘reduced hemoglobin endocytosis’ (Birnbaum *et al.*, 2020) as potential mechanisms of ART resistance. The first mechanism unifies the proteostasis pathways in the ER and cytoplasm, which involves phosphatidylinositol-3-phosphate (PI3P) vesicle expansion, UPR and oxidative stress response pathways (Bhattacharjee *et al.*, 2018; Mok *et al.*, 2015; Suresh and Haldar, 2018). The amplification of PI3P vesiculation disseminating proteins involved in the UPR, folding, quality control, and export is proposed to be a major determinant of resistance (Bhattacharjee *et al.*, 2018; Suresh and Haldar, 2018). The second proposed mechanism of ART resistance proposes that destabilization of *PfK13* harbouring the C580Y mutation results in decreased abundance of *PfK13* in the parasite and reduced availability of heme derived from hemoglobin degradation essentially at the ring stage. As ART is activated by heme derived from host hemoglobin, decreased hemoglobin availability results in reduced ART induced proteotoxic stress and parasite killing, conferring ART resistance (Birnbaum *et al.*, 2020).

While it is well established that UPR and PI3P stimulate the process of autophagy in higher organisms to remove misfolded proteins, the role of the parasite autophagy machinery in these mechanisms of resistance has yet to be proven experimentally. In yeast and metazoan,

autophagy serves as an important pathway for mitigating extensive cellular damage and thus may also be involved in regulating mechanisms of ART resistance. The autophagy protein, *PfATG18* is shown to have strong selection of mutation under ART resistance and a host of other compounds in standard drug sensitivity assays. Mutants for *PfATG18* are also reported to have altered susceptibility to a host of other compounds in standard drug sensitivity assays. Interestingly, presence of *PfATG18* T38I mutation confers fitness advantage to the parasites by enabling faster growth rates under nutrient limited environments and under ART treatment (Breglio *et al.*, 2018; Wang *et al.*, 2016). *PfATG18* binds to and utilizes PI3P for its association with membranes and performing downstream functions (Bansal *et al.*, 2017). Thus, the T38I mutations in *PfATG18* may provide critical insights into how autophagy and PI3P lipid metabolism may interact to alter ART sensitivity. Additionally, drug interaction studies have shown that ART directly targets and binds to *PfATG18* (Wang *et al.*, 2015). As a result, it would be interesting to explore the functions of parasite autophagy in the development and maintenance of ART resistance.

Interactions of *PfATG18* with PI3P and the reported *PfATG18* T38I mutation motivated us to carry out studies to understand the role of autophagy in the two proposed proteostasis mechanisms underlying ART resistance. The activation of parasite autophagy during ART resistance is demonstrated by the higher expression of *PfATG8* and *PfATG18*, both at the transcript and protein levels in the K13^{C580Y} isolate during the early ring and young trophozoite stages as compared to the K13^{WT}. The colocalization between *PfATG18* and the autophagosome marker protein *PfATG8* is also found to be increased in the ART resistant parasite relative to its isogenic counterpart. The increased number of PI3P labelled puncta observed in the K13^{C580Y} parasites relative to K13^{WT} is consistent with previous reports showing induced ER-PI3P vesiculation upon resistance (Bhattacharjee *et al.*, 2018). Both *PfATG8* and *PfATG18* also exhibit a similar increase in their puncta numbers in the K13^{C580Y} isolate relative to K13^{WT}. Autophagy induction through amino acid starvation further activates the pathway in both K13^{WT} and K13^{C580Y} isolates, while the colocalization of *PfATG18* and PI3P-labelled vesicles is increased in ART resistant parasites compared to isogenic parasites. Our study demonstrates a decrease in the IC₅₀ of the specific autophagy inhibitor MRT68921 in the K13^{C580Y} isolate as compared to the K13^{WT} one. We find that *PfATG18* is co-transported along with the resistant marker protein *PfK13* to the FV via the hemoglobin trafficking pathway. *PfK13* is present on hemoglobin containing

vesicles (HCv) to which *Pf*ATG18 and PI3P also colocalize. Overall, this work indicates the role of parasite autophagy in various ART resistance mechanisms.

This work has been accepted for publication in the journal mBio. The complete reference is as follows:

Ray, A., Mathur, M., Choubey, D., Karmodiya, K., & Surolia, N. (2022) “Autophagy Underlies the Proteostasis Mechanisms of Artemisinin Resistance in *P. falciparum* Malaria”, mBio, doi: 10.1128/mbio.00630-22.

3.3.1 Basal expression of autophagy proteins is higher in ART resistant isolate compared to the isogenic isolate

ART resistant field isolates are known to exhibit increased mRNA levels of UPR genes even at the basal level (Mok *et al.*, 2015). As demonstrated earlier, induced UPR activates parasite autophagy. We sought to determine whether a similar increase in the mRNA levels of parasite autophagy genes occurs in ART resistant isolates. Basal transcription profiles of *Pf*ATG8 and *Pf*ATG18 were compared between two parasite isolates, which are matched isogenically but differ only at the *Pf*K13 locus. The ART resistant strain Cam2^{C580Y} was originally isolated from a patient in Pailin infected with an ART resistant strain of *P. falciparum* and carrying the *Pf*K13 C580Y allele (K13^{C580Y}). This strain was subsequently genetically engineered to revert the C580Y allele to wildtype using zinc finger nucleases, yielding the Cam2 rev strain (K13^{WT}), restoring the ART sensitivity (Straimer *et al.*, 2015).

To calculate the degree of ART resistance of the K13^{C580Y} and K13^{WT} isolates, RSA_(0-3h) was performed. Parasite viability was determined microscopically through the examination of Giemsa stained blood smears by counting parasites which developed into rings or trophozoites with normal morphology after parasite invasion in the next life cycle. Percent survival was obtained by dividing parasitemia in the DHA treated culture by parasitemia in the untreated culture × 100 (Figure 3.15A). The survival rate of the K13^{WT} isolate was found to be ~0.6 %, while that of the K13^{C580Y} isolate was ~6.5 %, demonstrating that K13^{C580Y} is ART resistant (Figure 3.15B). Our RSA_(0-3 h) results corroborate with previous reports showing 2.4 % and 13 % survival in Cam2^{rev} and Cam2^{C580Y}, respectively (Straimer *et al.*, 2015).

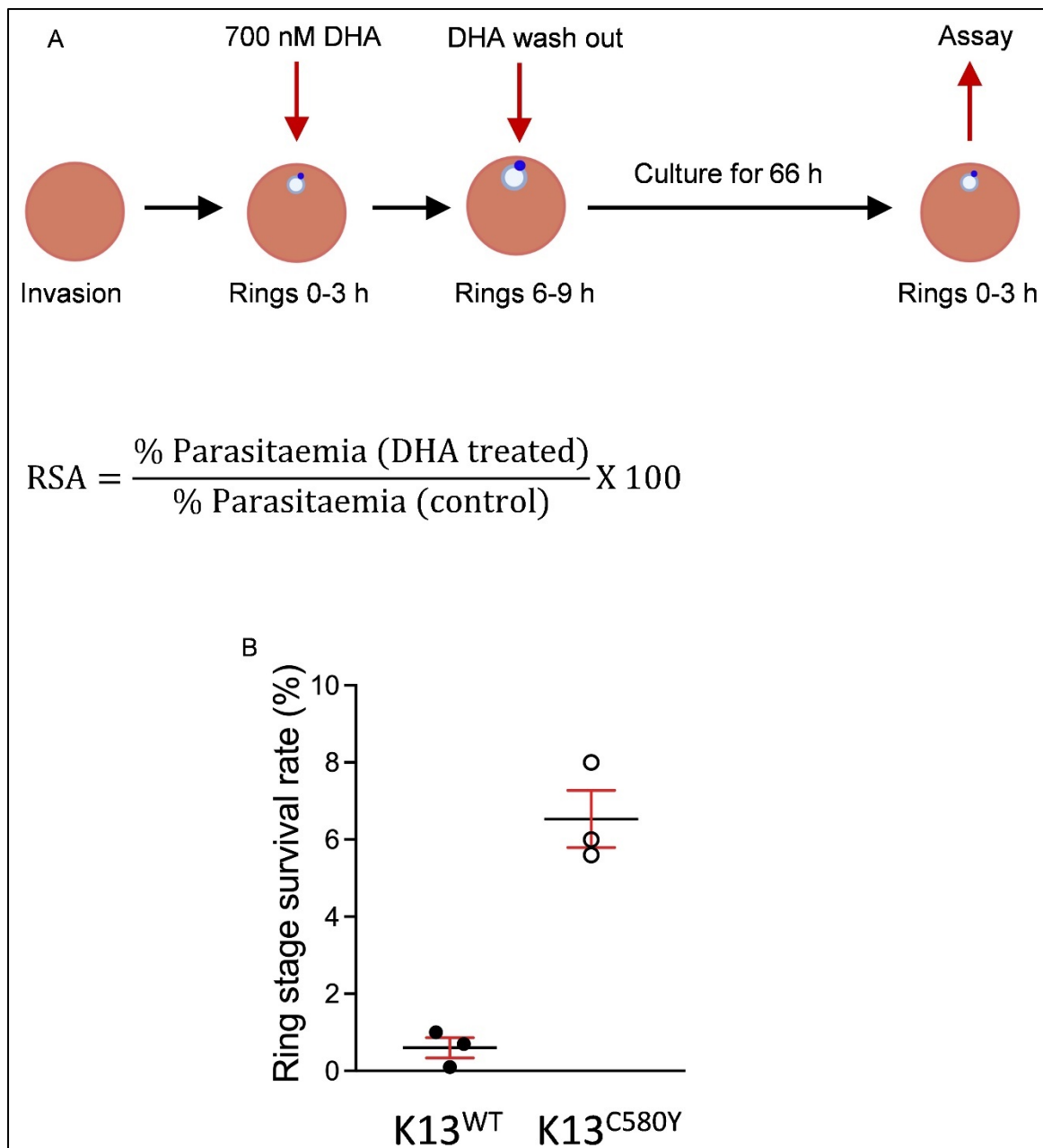


Figure 3.15 Ring-stage survival assay (RSA) for the K13^{WT} and K13^{C580Y} isolates

(A) Ring-stage Survival Assay (RSA) schematic showing exposure of 0-3 hpi rings to short pulses of 700 nM DHA for 6 h. After DHA washout, parasites are maintained in culture media for another 66 h and then assessed for survival. The survival rate is calculated as the percentage parasitemia in the 700 nM DHA treated cultures compared to the parasitemia in the untreated (control) cultures at the end of 72 h of RSA. (B) Graph showing the % survival rate in the RSA for the K13^{WT} and K13^{C580Y} isolates. n = 3 independent experiments.

Several ATG proteins, including mammalian orthologs of *PfATG8*, the LC3, and of *PfATG18*, the WIPI1, increase their transcript levels in response to external stress stimuli, indicating autophagy activation (Proikas-Cezanne *et al.*, 2007; Tsuyuki *et al.*, 2014). To determine the basal levels of *PfATG8* and *PfATG18* mRNA in synchronised early ring (0-3 hpi) and young trophozoite (~22-24 hpi) cultures of the K13^{WT} and K13^{C580Y} isolates, parasites were harvested and RNA isolated followed by cDNA synthesis. Quantitative real-time PCR was performed using *PfATG8*, *PfATG18*, and β -Actin gene-specific primers and the amplification product was observed on an agarose gel (Figure 3.16A). In the K13^{C580Y} parasites, relative gene expression of *PfATG8* was found to be upregulated by ~1.5 and ~3 fold in early rings and young trophozoites, respectively, compared to the K13^{WT} parasites (Figures 3.16B and 3.16C). The relative gene expression of *PfATG18* was found to be upregulated by ~6.5 and ~5 fold in early rings and young trophozoites, respectively, in the K13^{C580Y} parasites relative to K13^{WT} (Figures 3.16B and 3.16C). Concomitantly, western blot analysis showed an increase in the expression levels of *PfATG8* and *PfATG18* by ~2 fold in both early rings and young trophozoites of the ART resistant isolate compared to its isogenic counterpart (Figures 3.17A, 3.17B, 3.17C and 3.17D). The increase in protein levels of *PfATG8* and *PfATG18* upon starvation (Agrawal *et al.*, 2020; Joy *et al.*, 2018) and treatment with DHA (Figures 3.5C and 3.5D) signifies activation of the parasite autophagy-like pathway. Thus, the upregulation of *PfATG8* and *PfATG18*, both at the transcript and protein levels, indicates that the autophagy-like pathway in ART resistant K13^{C580Y} is activated.

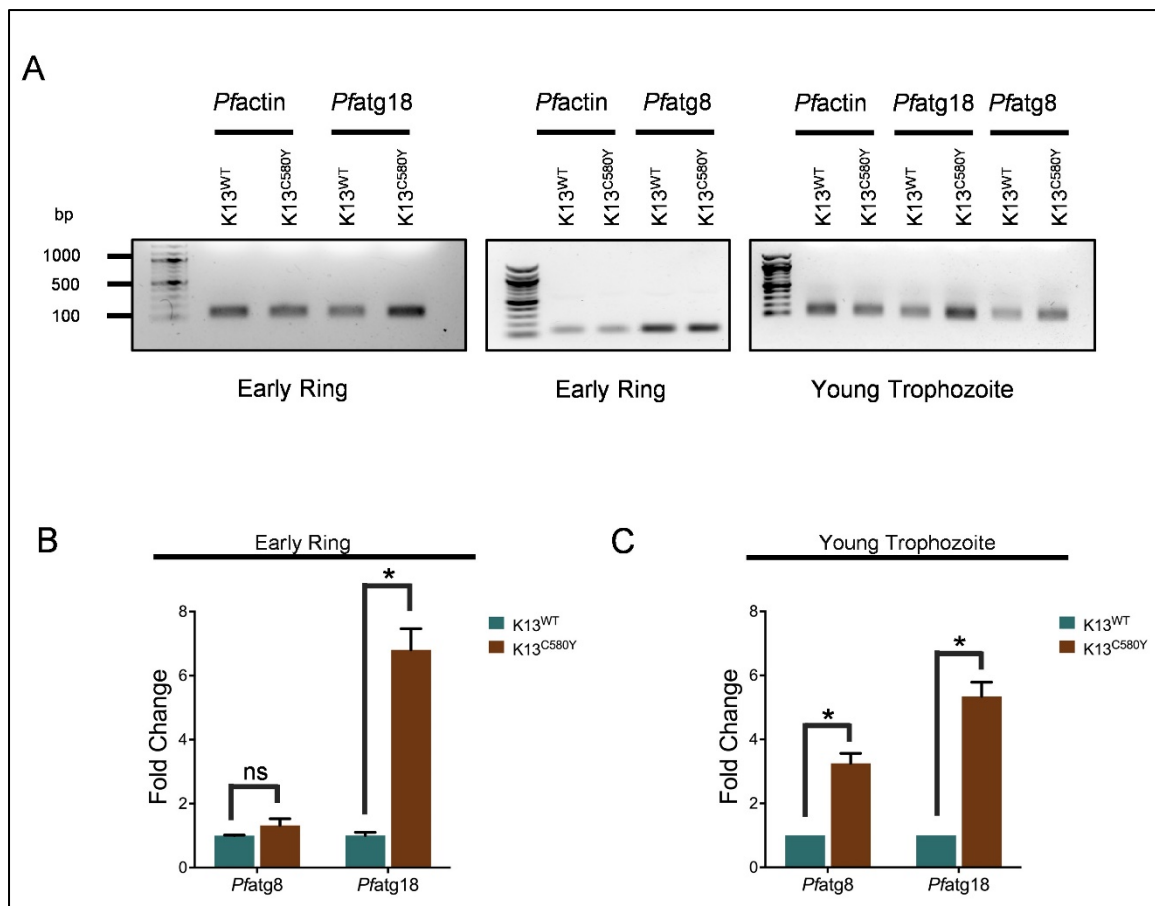


Figure 3.16 Parasites show increased basal transcript levels of *Pfatg8* and *Pfatg18* in K13^{C580Y} compared to K13^{WT} parasites

(A) Synchronized early rings and young trophozoites were isolated from K13^{C580Y} and K13^{WT} parasites. The basal expression levels of *Pfatg8* and *Pfatg18* were determined in the K13^{C580Y} and K13^{WT} parasites by RT-PCR. Agarose gel electrophoresis images showing Amplicons obtained from quantitative RT-PCR; n = 2 independent experiments. Graph showing fold change of *Pfatg8* and *Pfatg18* gene expression levels in ART resistant K13^{C580Y} early ring (B) and young trophozoite (C) stage parasites compared to isogenic isolate K13^{WT}, determined using quantitative RT-PCR. β -actin was used as the reference gene. Relative gene expression was determined using the $2^{-\Delta\Delta Ct}$ method. n = 2 independent experiments. The data points are expressed as mean \pm SEM. Statistical significance is quantified using unpaired Student's t-test, * = P < 0.05, ns = non-significant.

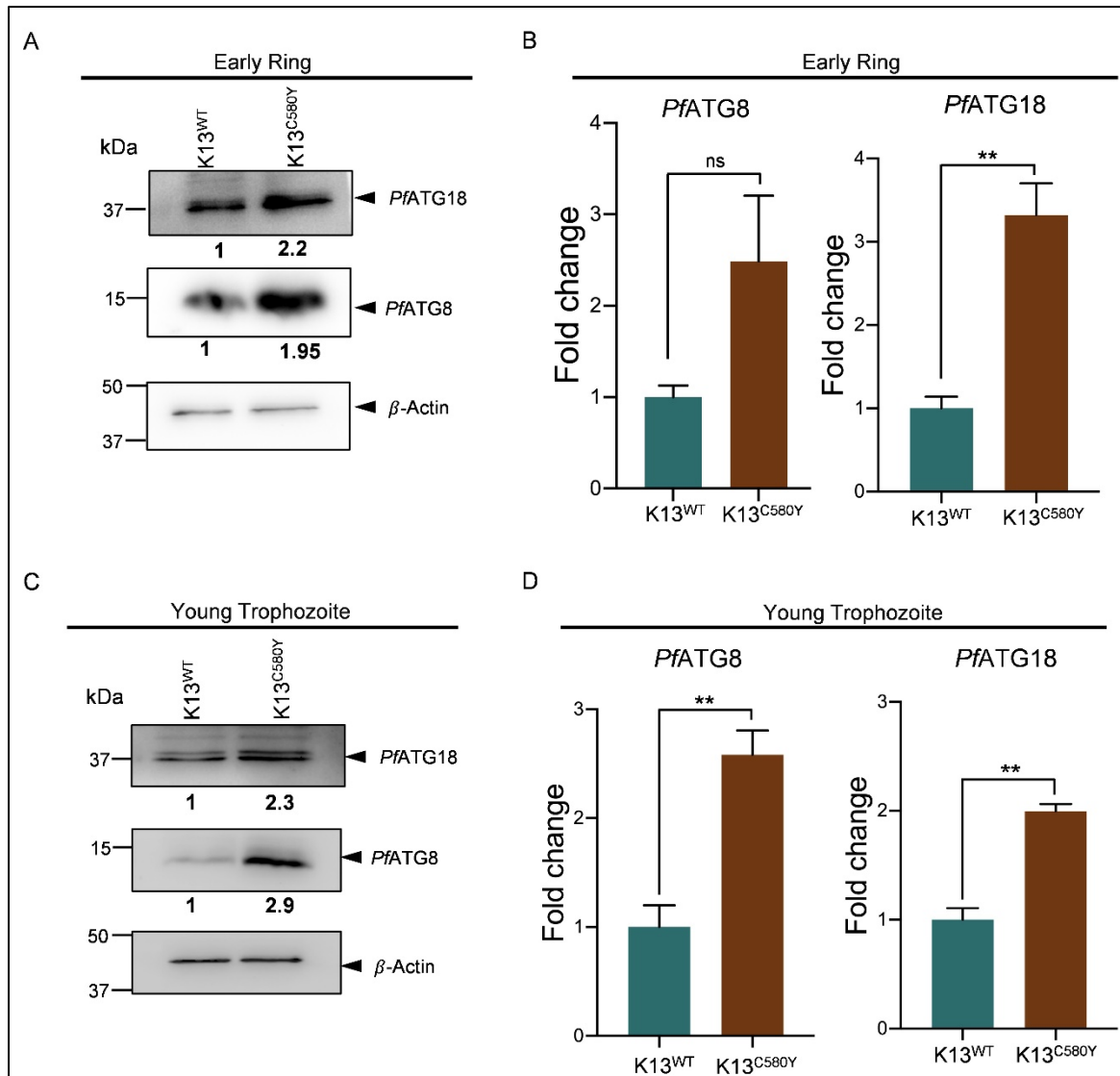


Figure 3.17 Parasites show increased basal protein expression levels of *PfATG8* and *PfATG18* in K13^{C580Y} compared to K13^{WT} parasites

Expression levels of proteins (*PfATG8* and *PfATG18*) in K13^{WT} and K13^{C580Y} early ring (A) and young trophozoite (C) stage parasites. Parasite lysates were subjected to western blot analysis and blots were probed with *PfATG8* and *PfATG18* antibodies. β -Actin was used as loading control. n = 3 independent experiments. Fold difference, normalized with respect to control is shown below each blot. Graphs showing fold change of *PfATG8* (left) and *PfATG18* (right) protein expression levels in K13^{C580Y} early ring (B) and young trophozoite (D) stage parasites relative to K13^{WT}. n = 3 independent experiments. The data points are expressed as mean \pm SEM. Statistical significance is quantified using unpaired Student's t-test, ** = P < 0.005, ns = non-significant.

As increased mRNA levels and puncta numbers of human WIPI1 are indicative of increased autophagosome numbers (Tsuyuki *et al.*, 2014), the number of *Pf*ATG18 decorated vesicles colocalizing with the autophagosome marker protein *Pf*ATG8 was determined using immunofluorescence analysis in K13^{WT} and K13^{C580Y} early ring and young trophozoite stage parasites (Figures 3.18A, and 3.18C). K13^{C580Y} parasites, in both early rings and young trophozoites, displayed ~2 fold increase in the number of *Pf*ATG18 labelled puncta colocalizing with *Pf*ATG8 as compared to K13^{WT} parasites (Figures 3.18B, and 3.18D). We also observed *Pf*ATG18 decorated puncta that do not colocalize with *Pf*ATG8 (Figures 3.18A and 3.18C). As *Pf*ATG18 is also present on numerous endocytic vesicles, including the HCv that traffics hemoglobin to the FV (Agrawal *et al.*, 2020), we speculate that the partial colocalization is due to *Pf*ATG18's localization to these endocytic vesicles. The increased colocalization of *Pf*ATG8 and *Pf*ATG18 decorated vesicles in K13^{C580Y} parasites over K13^{WT} parasites signifies the enhanced localization of *Pf*ATG18 to autophagosomes. This indicates that autophagy is activated in resistant parasites, regulating various mechanisms of ART resistance, and is thus not simply a reflection of autophagosome-like vesicles accumulating in the parasite cytoplasm.

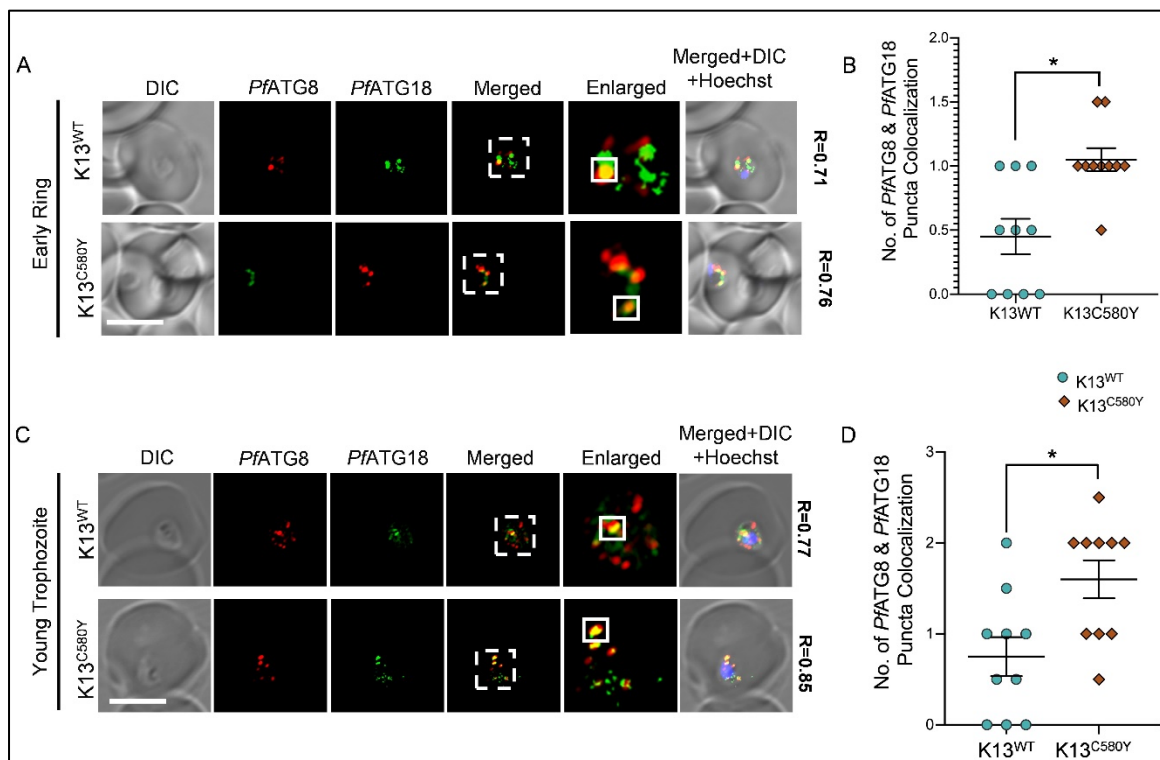


Figure 3.18 *Pf*ATG18 shows increased localization to autophagosome-like vesicles in K13^{C580Y} compared to K13^{WT} parasites

Immunofluorescence analysis of early ring (A) and young trophozoite (C) stage K13^{WT} and K13^{C580Y} parasites stained with *PfATG8* and *PfATG18* antibodies were labelled using the Zenon antibody labelling system. Regions within the dashed white lines are enlarged and placed next to the merged panel to better represent colocalization. Extent of colocalization between *PfATG8* (representing autophagosome-like vesicles) and *PfATG18* labelled puncta is represented by the Pearson's coefficient value (R) and evaluated from the *PfATG8* (red) and *PfATG18* (green) fluorescent signals within the white square region in the enlarged panel. Scatter plot representing the number of *PfATG8* and *PfATG18* colocalizing puncta in early ring (B) and young trophozoite (D) stage K13^{WT} and K13^{C580Y} parasites. N = 10 parasites, n = 3 experiments, Scale bar: 5 μ m. The data points are expressed as mean \pm SEM. Statistical significance is quantified using unpaired Student's t-test, * = P < 0.05.

Increased PI3P levels, even by transgenic methods, confer ART resistance and elevated PI3P promotes ER-PI3P vesiculation. As the levels of PI3P in ring stage parasites directly correlate with the degree of ART resistance (Mbengue *et al.*, 2015), we sought to determine PI3P levels in the *in vitro* K13^{WT} and K13^{C580Y} ring stage parasites. PI3P is indistinguishable from PI4P by mass spectrometry due to their identical mass and charge, and the lipid is undetectable with conventional western blot techniques. Thus, immunofluorescence analysis was performed to quantify the amount of PI3P present in both the parasite isolates. As expected, the number of PI3P labelled puncta increased significantly in K13^{C580Y} compared to K13^{WT} parasites (Figures 3.19A and 3.19B).

PI3P is known to induce autophagy in yeast and other eukaryotes by acting as a scaffold for the recruitment of multiple autophagy proteins to the pre-autophagosomal membrane, consequently modulating the membrane curvature required for autophagosome assembly and maturation (Dall'Armi *et al.*, 2013; Devereaux *et al.*, 2013). Therefore, we carried out studies to check whether higher levels of PI3P during resistance reflect an increase in parasite autophagy at the ring stage. Immunofluorescence analysis was used to quantify the number of *PfATG8* and *PfATG18* decorated puncta in K13^{WT} and K13^{C580Y} parasites. Similar to PI3P, we observe increased numbers of both *PfATG8* and *PfATG18* decorated puncta in K13^{C580Y} compared to K13^{WT} parasites (Figures 3.19A and 3.19B). Taken together, the increased expression levels of autophagy proteins during ART resistance demonstrates parasite autophagy as a survival mechanism.

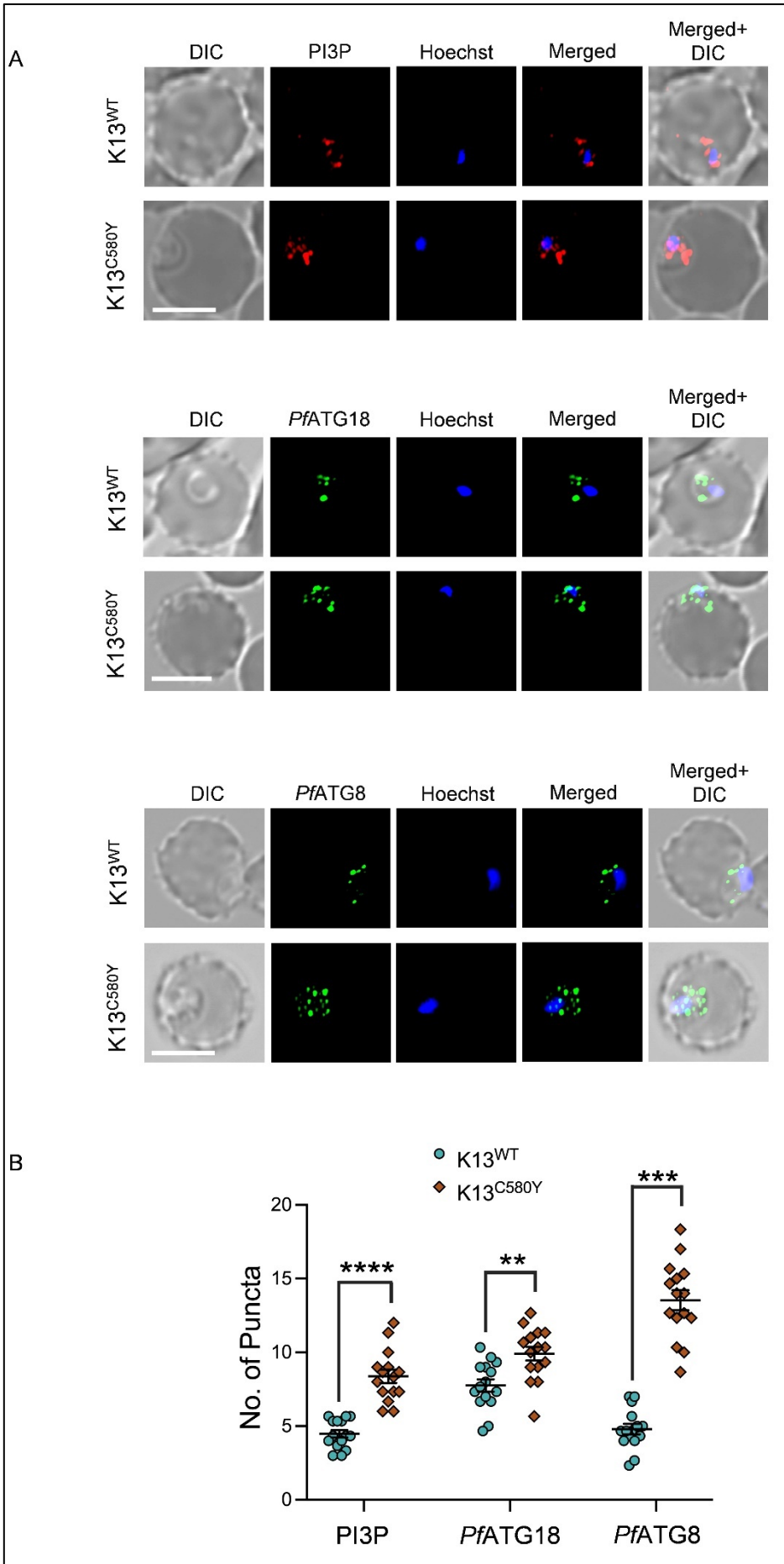


Figure 3.19 Increased number of PI3P, *Pf*ATG8 and *Pf*ATG18 labelled vesicles in *K13*^{C580Y} compared to *K13*^{WT} parasites

(A) Immunofluorescence analysis of *K13*^{WT} and *K13*^{C580Y} ring stage parasites stained with anti-PI3P, anti-*Pf*ATG18 and anti-*Pf*ATG8 antibodies showing number of PI3P, *Pf*ATG18 and *Pf*ATG8 labelled puncta. Nucleus was stained using Hoechst. N = 15 parasites, n = 3 independent experiments, Scale bar: 5 μ m. (B) Scatter plot showing number of PI3P, *Pf*ATG18 and *Pf*ATG8 labelled puncta in *K13*^{WT} and *K13*^{C580Y} parasites. N = 15 parasites, n = 3 independent experiments. The data points are expressed as mean \pm SEM. Statistical significance is quantified using unpaired Student's t-test, **** = P < 0.0001, *** = P < 0.0005, and ** = P < 0.005.

3.3.2 Starvation induces parasite autophagy in ART resistant as well as the isogenic isolate

As starvation increases the expression levels of parasite autophagy proteins in the wildtype 3D7 strain (Agrawal *et al.*, 2020; Joy *et al.*, 2018), we investigated whether a similar effect exists in the ART resistant and isogenic isolates. Western blot analysis was used to evaluate protein levels of *Pf*ATG8 and *Pf*ATG18 in synchronised young trophozoites after 1.5 h incubation with starvation media. The expression levels of *Pf*ATG8 increased by ~2 fold and *Pf*ATG18 by ~2.5 fold in both *K13*^{WT} and *K13*^{C580Y} parasites upon starvation (Figures 3.20A and 3.20B). The increase in *Pf*ATG8 and *Pf*ATG18 expression levels is comparable to that observed when 3D7 is incubated in starvation medium, indicating that both isogenic and resistant parasites have a functional autophagy pathway that responds to autophagy induction during starvation.

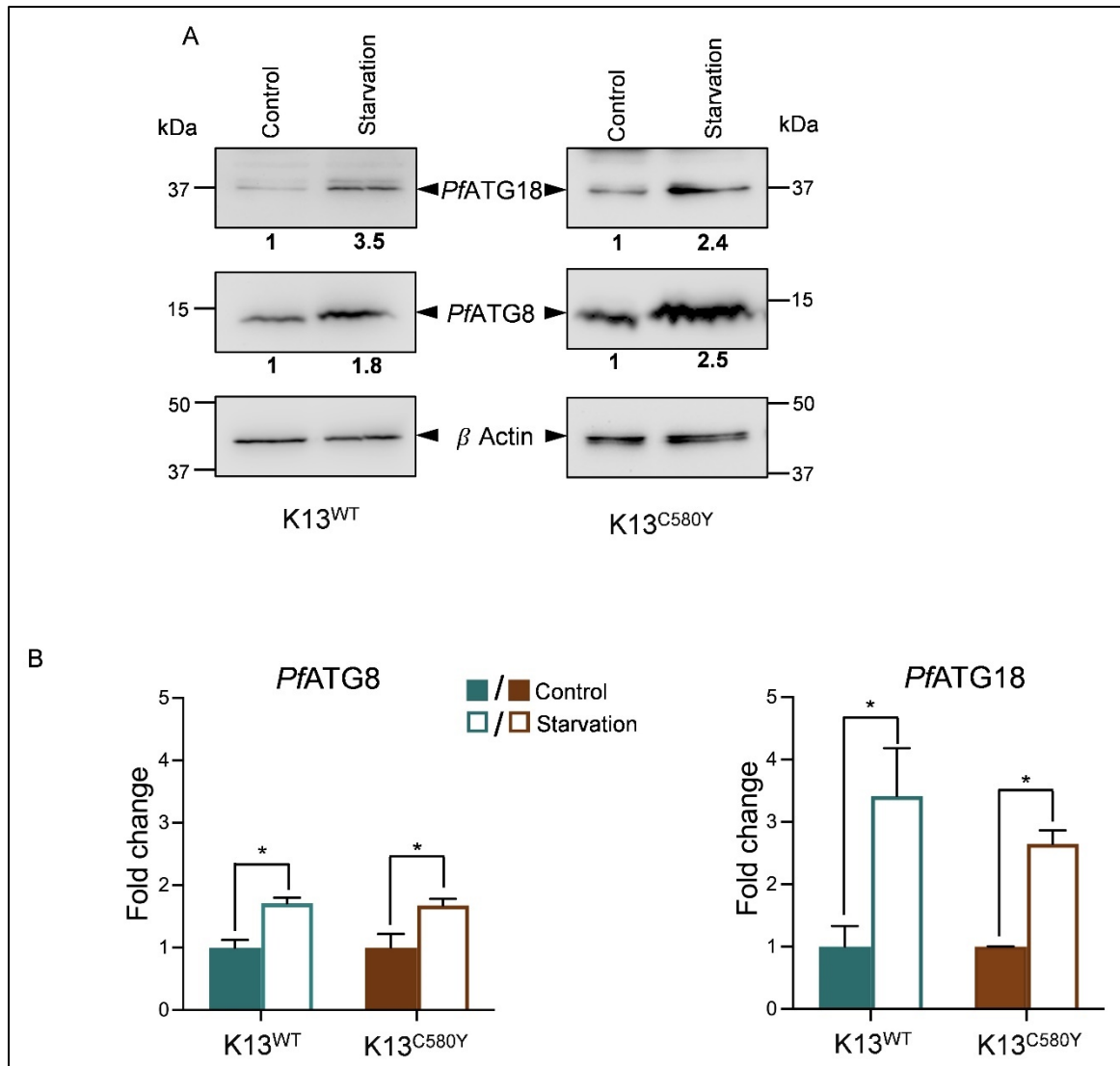


Figure 3.20 Starvation induces the expression levels of *PfATG8* and *PfATG18* in *K13^{C580Y}* as well as *K13^{WT}* parasites

K13^{WT} and *K13^{C580Y}* parasites were incubated with starvation media for 1.5 h. (A) Effect of starvation on *PfATG8* and *PfATG18* protein expression levels. *K13^{WT}* and *K13^{C580Y}* parasite lysates were subjected to western blot analysis and blots were probed with *PfATG8* and *PfATG18* antibodies. β -Actin was used as the loading control. n = 3 independent experiments. Fold difference, normalized with respect to control is shown below each blot. (B) Graphs representing fold change of *PfATG8* (left panel) and *PfATG18* (right panel) protein expression levels upon starvation. n = 3 independent experiments. The data points are expressed as mean \pm SEM. Statistical significance is quantified using unpaired Student's t-test, * = P < 0.05.

As the basal number of PI3P labelled vesicles is higher in the K13^{C580Y} than in the K13^{WT} ring stage parasites, we investigated the effect of starvation on the number of these PI3P labelled vesicles in both the parasite isolates. We observe an increase in the number of PI3P labelled puncta in both the K13^{WT} and K13^{C580Y} parasites upon starvation (Figures 3.21A and 3.21B), indicating enhanced PI3P vesiculation upon starvation.

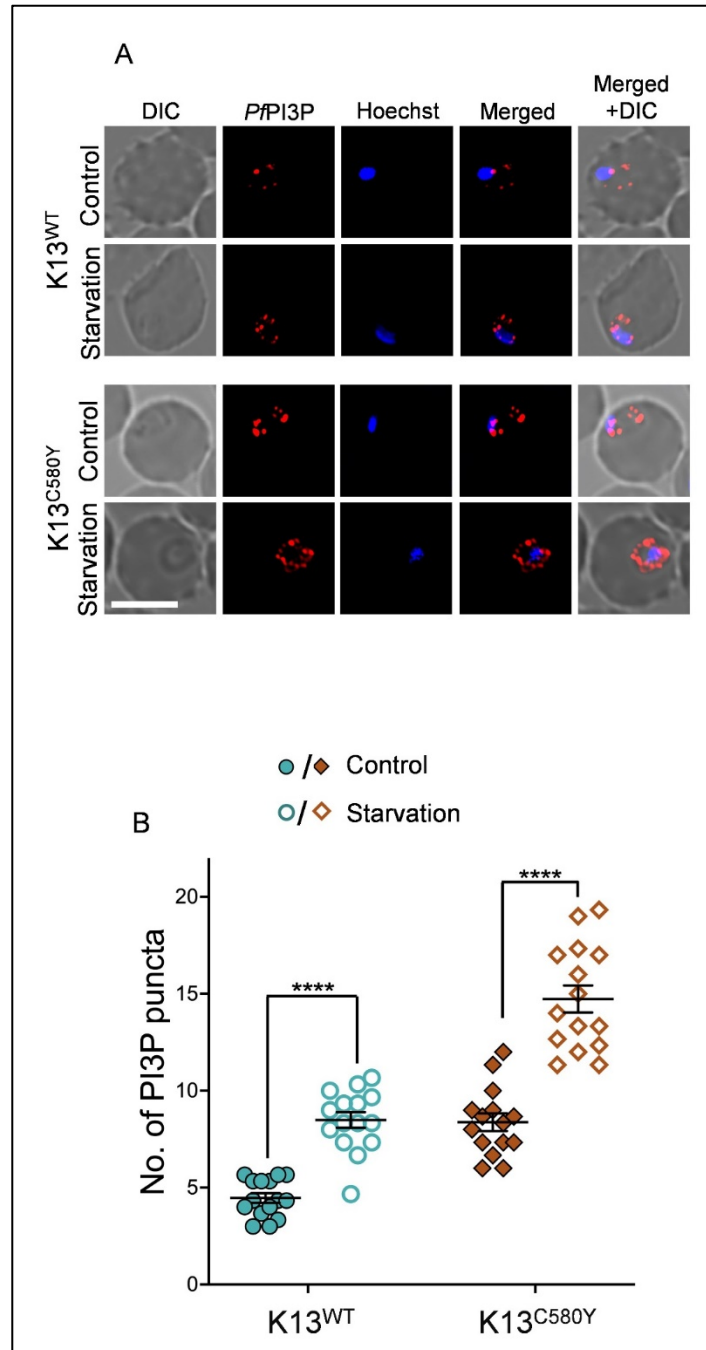


Figure 3.21 Starvation increases the number of PI3P labelled vesicles in K13^{C580Y} as well as K13^{WT} parasites

(A) Immunofluorescence analysis of K13^{WT} (top two panels) and K13^{C580Y} (bottom two panels) parasites stained with anti-PI3P antibody showing PI3P labelled puncta upon starvation. Nucleus was stained using Hoechst. N = 15 parasites, n = 3 independent experiments, Scale bar: 5 μ m. (B) Scatter plots representing the number of PI3P labelled puncta in K13^{WT} and K13^{C580Y} in control and starvation conditions. The data points are expressed as mean \pm SEM. Statistical significance is quantified using unpaired Student's t-test, **** = P < 0.0001, *** = P < 0.0005; ** = P < 0.005.

Increase in the number of autophagosomes reflect upregulation of autophagy. Since both *Pf*ATG18 and PI3P are present on cytoplasmic vesicles of 200 nm in diameter (Agrawal *et al.*, 2020), we investigated the number of these autophagosome-like structures in the ART resistant and isogenic parasites upon starvation by studying the colocalization of *Pf*ATG18 with PI3P-labelled puncta. Immunofluorescence analysis of synchronized rings incubated with starvation media for 1.5 h revealed an increase in the number of *Pf*ATG18 labelled puncta colocalizing with PI3P upon starvation in both K13^{WT} and K13^{C580Y} parasites (Figures 3.22A and 3.22B), the increase in colocalization being more significant in K13^{C580Y} (Figure 3.22B). Additionally, K13^{C580Y} parasites showed an increase in *Pf*ATG18 labelled puncta colocalizing with PI3P at the basal levels as compared to K13^{WT} (Figure 3.22B). This supports our findings that autophagy is activated in resistant parasites even in the absence of an external stress (such as starvation). The results obtained from colocalization studies corroborate our western blot analyses, demonstrating a functional autophagy pathway in both isogenic and resistant parasites that responds to autophagy induction under starvation. Moreover, activation of autophagy is significantly higher in resistant isolates than in the sensitive one (Figure 3.22B) which indicates the reliance on autophagy for parasite fitness. Collectively, our results suggest parasite autophagy as one of the key pathways involved in the maintenance of protein homeostasis during resistance.

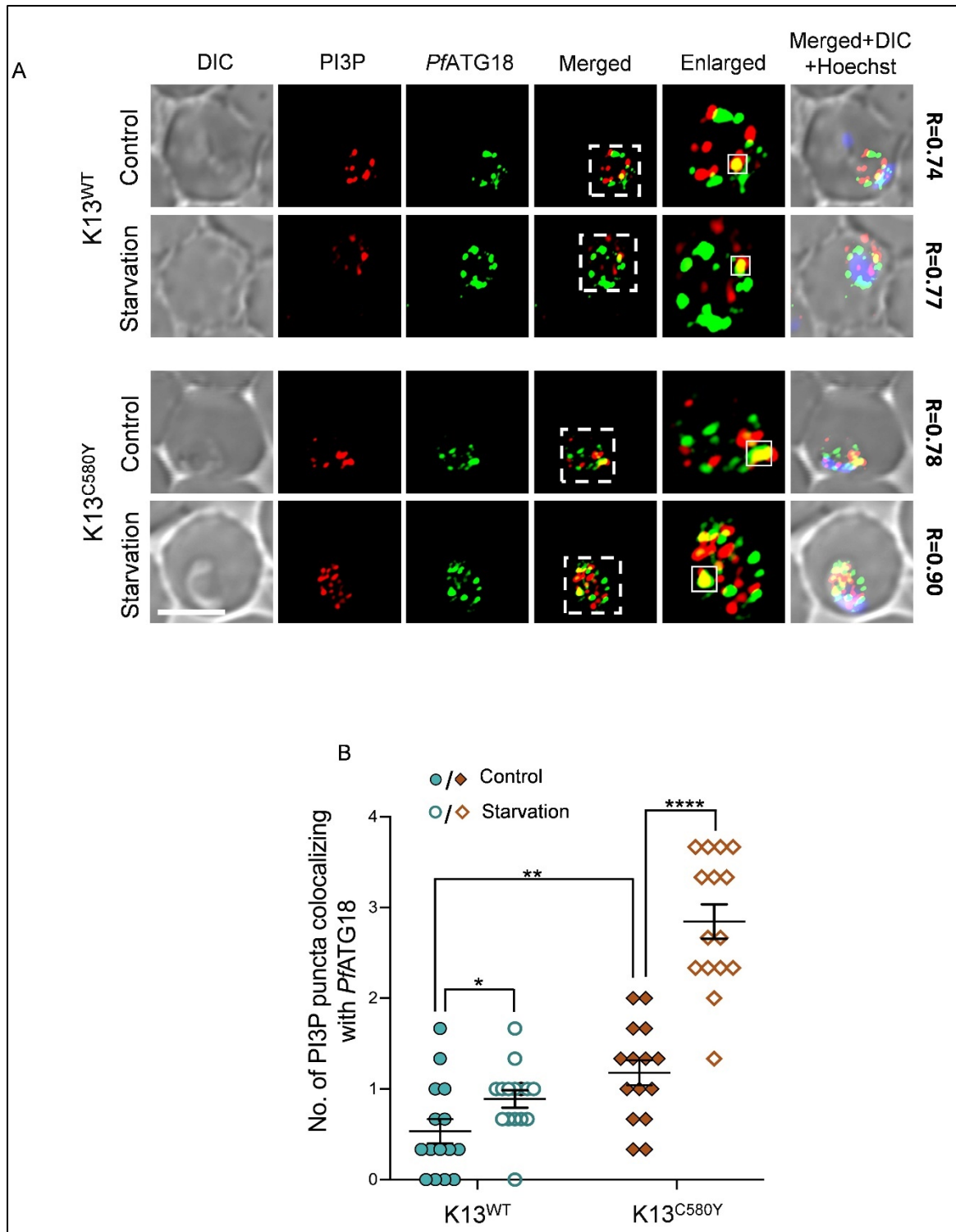


Figure 3.22 Starvation increases the number of *Pf*ATG18 labelled vesicles colocalizing with PI3P in K13^{C580Y} as well as K13^{WT} parasites

(A) Immunofluorescence analysis of K13^{WT} (top two panels) and K13^{C580Y} (bottom two panels) parasites stained with anti-PI3P and anti-*Pf*ATG18 antibodies showing colocalization of PI3P with *Pf*ATG18 labelled puncta upon starvation. Regions within the dashed white lines are enlarged and placed next to the merged panel to better represent colocalization. Extent of colocalization between

PI3P and *Pf*ATG18 is represented by the Pearson's coefficient value (R) evaluated from PI3P (red) and *Pf*ATG18 (green) fluorescent signals within the white square region in the enlarged panel. Nucleus was stained using Hoechst. (B) Scatter plot representing the number of colocalizing PI3P and *Pf*ATG18 labelled puncta in K13^{WT} and K13^{C580Y} parasites under control and starved conditions. N = 15 parasites, n = 3 independent experiments, Scale bar: 5 μ m. The data points are expressed as mean \pm SEM. Statistical significance is quantified using unpaired Student's t-test, **** = P < 0.0001, ** = P < 0.005, * = P < 0.05.

3.3.3 Parasite Autophagy regulates the survival of ART resistant isolate

To determine the effect of autophagy inhibition on the K13^{WT} and K13^{C580Y} parasites, we compared the IC₅₀ of MRT68921 between the two isolates by assessing the parasites' ability to invade fresh RBCs as an indication of development and survival in the presence of increasing concentrations of the autophagy inhibitor. Tightly synchronized early ring stage parasites from both the isolates (1 % parasitemia, 5 % hematocrit) were incubated with various concentrations of MRT68921 for 72h (Figure 3.23A). Giemsa stained smears from parasite cultures at the end of the assay were used to monitor the parasite morphology and invasion in the next cycle. Dose-response curve was plotted to determine the relative parasite load with respect to increasing MRT68921 concentration. The IC₅₀ of MRT68921 obtained from the dose-response curve for K13^{WT} parasites (726.7 nM) (Figure 3.23B) is comparable to the IC₅₀ of MRT68921 in 3D7 (761.1 nM) (Figure 3.10), indicating a similar dose-response relationship between the two strains. Meanwhile, a ~2 fold decrease in the IC₅₀ was observed in K13^{C580Y} parasites (380.6 nM) when incubated with MRT68921 compared to K13^{WT} (Figure 3.23B). The decreased IC₅₀ of MRT68921 further emphasizes the importance of autophagy in the survival of ART resistant parasites.

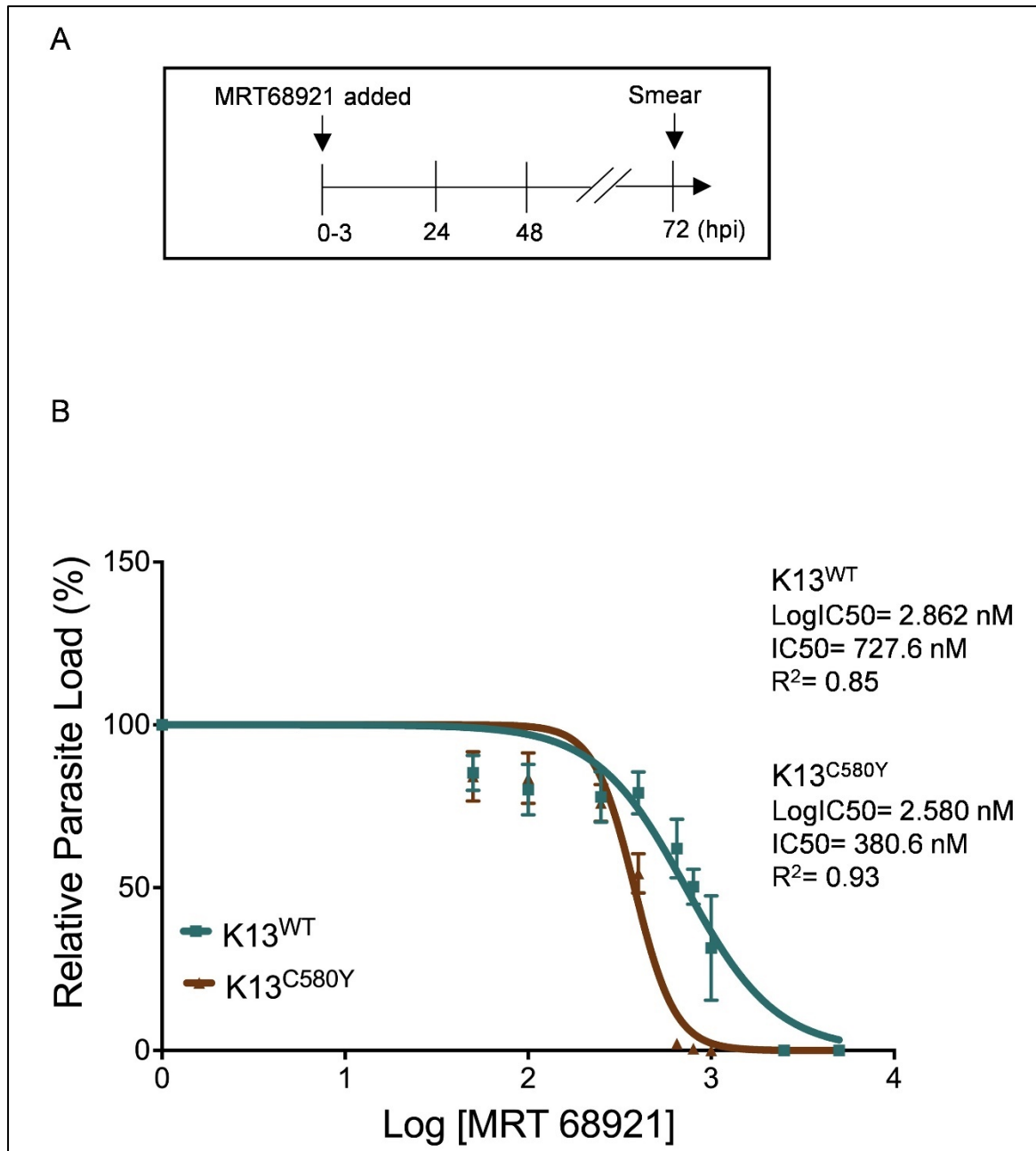


Figure 3.23 K13^{C580Y} parasites are more sensitive to autophagy inhibition than K13^{WT}

(A) Schematic showing various concentrations of MRT68921 treatment at 0-3 hpi, followed with change in culture media at 24 hpi and 48 hpi. The kink represents parasite reinvasion. Parasite growth assay was carried out after 72 hpi. (B) The dose response curve showing percentage of relative parasite load at 72 hpi in K13^{WT} (blue) and K13^{C580Y} (brown). n = 3 independent experiments. The data points are expressed as mean ± SEM.

3.3.4 *PfK13* and *PfATG18* are trafficked to the food vacuole through hemoglobin containing vesicles (HCv) in the ART resistant isolate

The endocytosis pathway in *P. falciparum* plays a crucial role in the host cell cytosol uptake (HCCU) involving the ingestion of host hemoglobin by the parasite (Spielmann *et al.*, 2020). Recent reports highlight the importance of *PfK13* in regulating endocytosis and it thus controls the amount of hemoglobin uptake by the peripherally localized parasite vesicles ‘cystosomes’ (Birnbaum *et al.*, 2020; Gnädig *et al.*, 2020; Yang *et al.*, 2019). These vesicles are formed due to the parasite plasma membrane invaginations that deliver host hemoglobin to the parasite food vacuole (Bakar *et al.*, 2010; Slomianny, 1990). *PfK13* localizes to various sub-cellular compartments in the parasite, including ER-PI3P vesicles, apicoplast, food vacuole (FV), and collar region of cystosomes (Bhattacharjee *et al.*, 2018; Birnbaum *et al.*, 2020; Suresh and Haldar, 2018; Yang *et al.*, 2019). However, there is no experimental evidence suggesting the presence of *PfK13* on HCv, which are discrete vesicles transporting host derived hemoglobin to the parasite FV (Elliott *et al.*, 2008).

Our previous report indicates the trafficking of *PfATG18* to the FV is via HCv and is mediated by the interaction of *PfATG18* with PI3P (Agrawal *et al.*, 2020). To investigate whether *PfK13* co-traffics with *PfATG18* to the FV, immunofluorescence analysis was carried out in the ART resistant K13^{C580Y} parasites. The cysteine protease falcipain-2 (*PfFP2*) is trafficked to the FV via HCv (Dasaradhi *et al.*, 2007) and was thus used to label the vesicles. *PfATG18* partially colocalized with both PI3P and *PfFP2* (Figures 3.24A and 3.24B) in the resistant K13^{C580Y} parasites similar to that observed in wildtype 3D7 parasites (Agrawal *et al.*, 2020). Also, partial colocalization of *PfK13* with PI3P and *PfFP2* (Figures 3.25A and 3.25B) was observed near the parasite periphery as well as in the cytoplasm, indicating the presence of both *PfK13* and *PfATG18* on HCv.

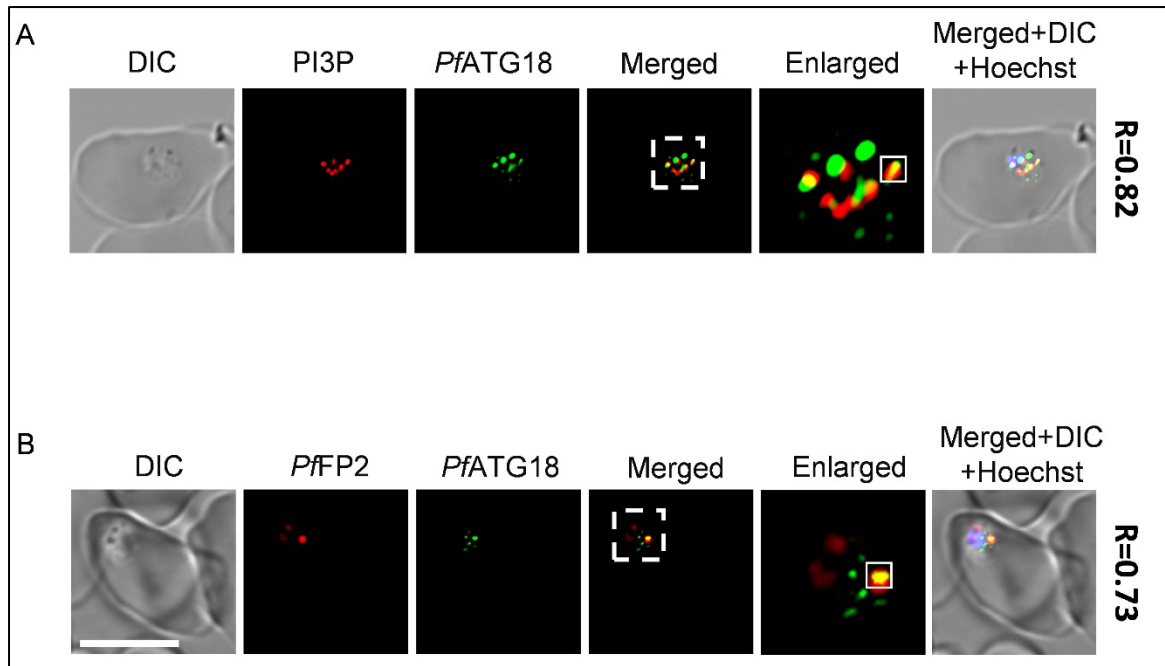


Figure 3.24 *PfATG18* is present on PI3P and *PfFP2* labelled vesicles in the K13^{C580Y} parasites

(A) Immunofluorescence analysis of K13^{C580Y} parasites stained with anti-PI3P and anti-*PfATG18* antibodies showing colocalization of PI3P with *PfATG18* labelled puncta. (B) Immunofluorescence analysis of K13^{C580Y} parasites stained with anti-*PfFP2* and anti-*PfATG18* antibodies were labelled using the Zenon antibody labelling system. Representative images showing colocalization of *PfATG18* with PI3P (A) and *PfFP2* (B) labelled puncta. N = 15 parasites, n = 3 independent experiments, Scale bar: 5 μ m. Regions within the dashed white lines are enlarged and placed next to the merged panel to better represent colocalization. Extent of colocalization is represented using the Pearson's coefficient value (R) evaluated from the PI3P and *PfFP2* (red) and *PfATG18* (green) fluorescent signals within the white square region in the enlarged panel. Nucleus was stained using Hoechst.

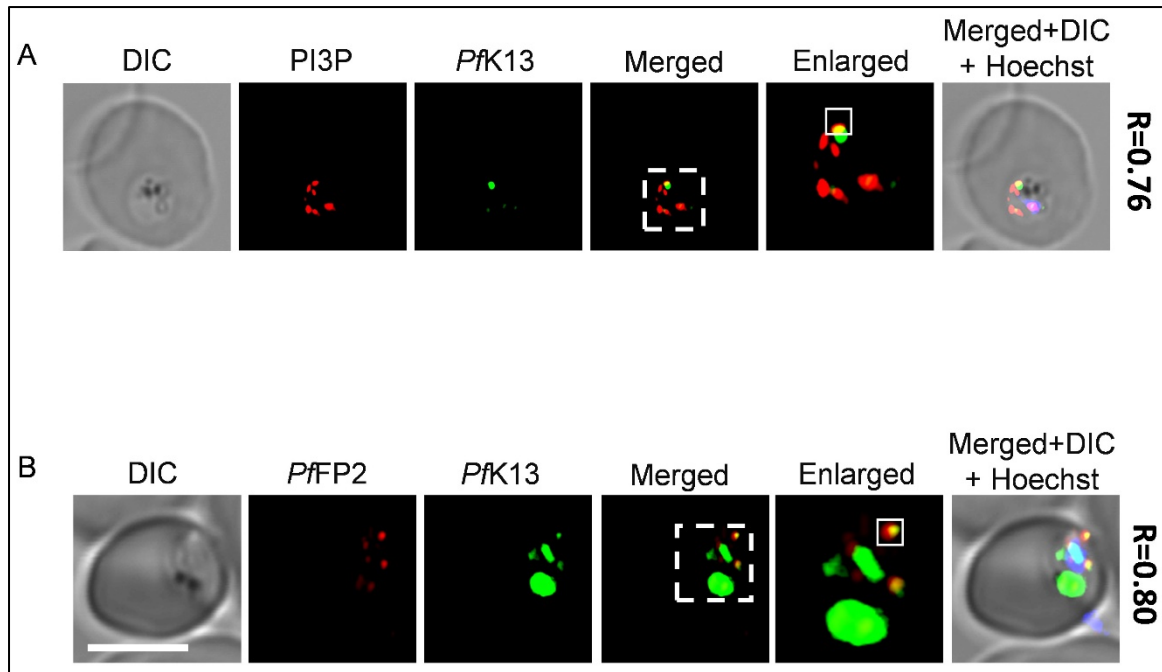


Figure 3.25 *PfK13* is present on PI3P and *PfFP2* labelled vesicles in the $K13^{C580Y}$ parasites

(A) Immunofluorescence analysis of $K13^{C580Y}$ parasites stained with anti-PI3P and anti-*PfK13* antibodies showing colocalization of PI3P with *PfK13* labelled puncta. (B) Immunofluorescence analysis of $K13^{C580Y}$ parasites stained with anti-*PfFP2* and anti-*PfK13* antibodies were labelled using the Zenon antibody labelling system. Representative images showing colocalization of *PfK13* with PI3P (A) and *PfFP2* (B) labelled puncta. N = 15 parasites, n = 3 independent experiments, Scale bar: 5 μ m. Regions within the dashed white lines are enlarged and placed next to the merged panel to better represent colocalization. Extent of colocalization is represented using the Pearson's coefficient value (R) evaluated from the PI3P and *PfFP2* (red) and *PfK13* (green) fluorescent signals within the white square region in the enlarged panel. Nucleus was stained using Hoechst.

To confirm the presence of *PfK13* and *PfATG18* on HCv, immunofluorescence analysis with *PfATG18* and *PfK13* antibodies was carried out at ring and young trophozoite stages of the $K13^{C580Y}$ parasites. Our results show colocalization of *PfK13* with *PfATG18* labelled puncta near the parasite periphery in rings suggesting their co-presence on cytosome-like structures (Figure 3.26A, upper panel). Presence of *PfATG18* and *PfK13* labelled puncta near the ring periphery was confirmed by labelling the Parasite Vacuolar Membrane (PVM) with a marker protein (Ho *et al.*, 2018), *PfPTEX-150* (Figures 3.27A and 3.27B). Parallely, *PfK13* colocalized with *PfATG18* labelled puncta near the FV in trophozoites (Figure 3.26A, lower panel) as implied by their localization near the parasite hemozoin. The

colocalization of *PfK13* with *PfATG18* labelled puncta near the parasite periphery in rings and near the FV in trophozoites indicates an increase in the co-trafficking of these two proteins to the FV via HCv in mature parasite stages.

Trafficking of HCv to the FV is assisted by the parasite actin-myosin motor system (Milani *et al.*, 2015). To further support that *PfATG18* and *PfK13* proteins are transported to the FV via the HCv, young trophozoites were treated with hemoglobin trafficking inhibitors (2,3-butanedione monoxime [BDM] and Dynasore) which block HCv transport to the FV. Parasites were incubated with myosin ATPase inhibitor BDM and Dynasore which inhibit the GTPase activity of dynamin, both causing accumulation of HCv to the parasite periphery (Milani *et al.*, 2015). Colocalization of *PfK13* with *PfATG18* labelled puncta was observed more towards the parasite boundary upon incubating parasites with these inhibitors as compared to the near FV localization seen in control (Figure 3.26B). These results further strengthen our proposition of a cross-talk between *PfK13* and *PfATG18* and is the key report of the parasite autophagy protein's association with the resistant marker *PfK13* in the background of ART resistance.

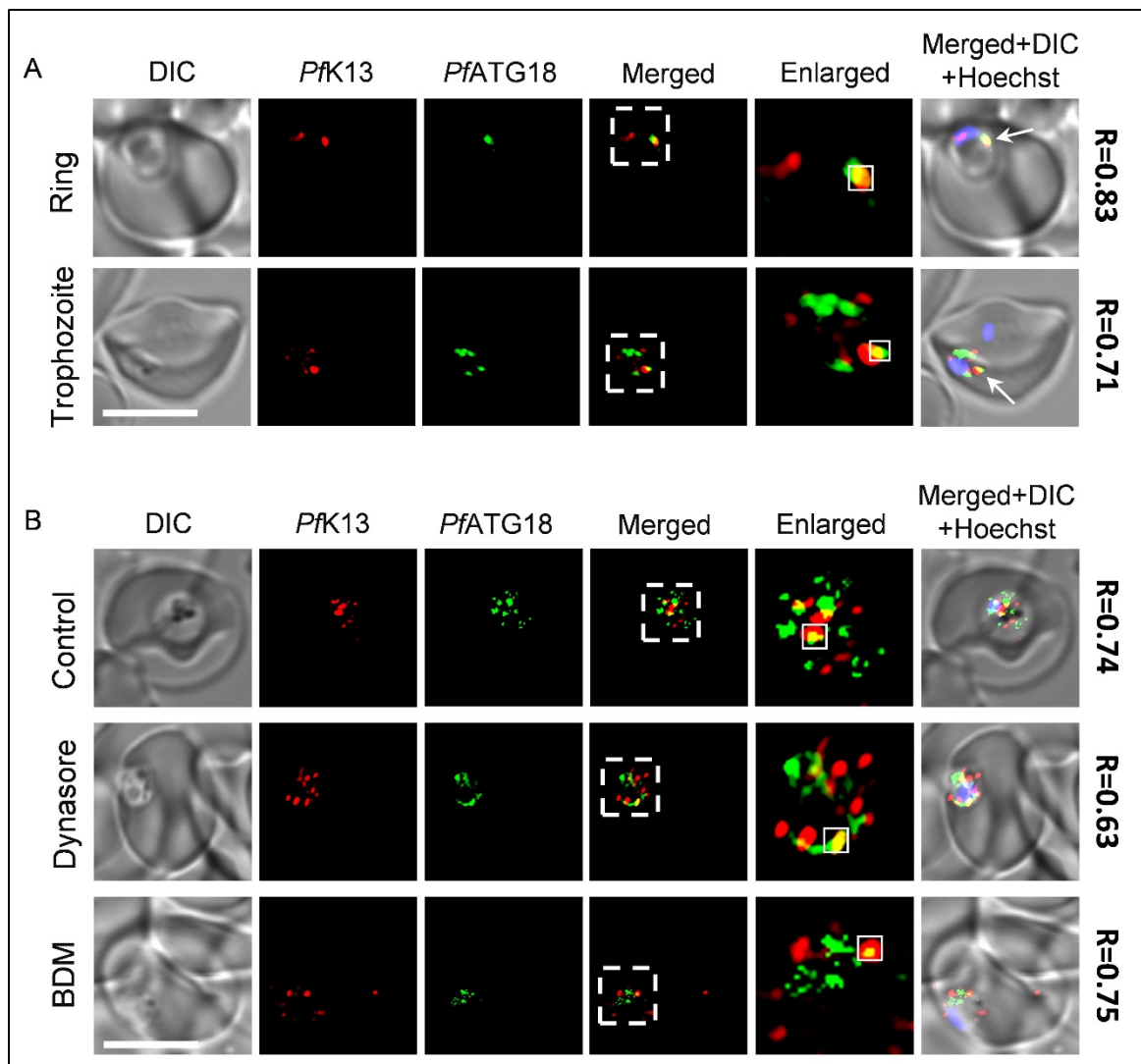


Figure 3.26 *PfK13* and *PfATG18* are trafficked to the FV through HCv in the $K13^{C580Y}$ parasites

(A) Immunofluorescence analysis of $K13^{C580Y}$ parasites stained with anti-*PfATG18* and anti-*PfK13* antibodies were labelled using the Zenon antibody labelling system, and showing colocalization of *PfK13* with *PfATG18* labelled puncta in rings (top panel) and young trophozoites (bottom panel). Rings show colocalization more towards the parasite boundary (white arrow) while trophozoites show more near the parasite FV (white arrow). N = 15 parasites, n = 3 independent experiments, Scale bar: 5 μ m. (B) *PfATG18* and *PfK13* are transported to parasite FV through the hemoglobin trafficking pathway. Localisation of *PfATG18* and *PfK13* labelled puncta upon incubation of parasites with hemoglobin trafficking inhibitors, 200 μ M Dynasore and 25 mM 2,3-Butanedione monoxime (BDM) were assessed using immunofluorescence analysis. $K13^{C580Y}$ parasites were stained with anti-*PfATG18* and anti-*PfK13* antibodies and labelled using the Zenon antibody labelling system. Incubation of parasites with inhibitors lead to colocalization of *PfATG18* and *PfK13* near the parasite periphery. N = 10 parasites, n = 3 independent experiments, Scale bar: 5 μ m.

Regions within the dashed white lines are enlarged and placed next to the merged panel to better represent colocalization. Extent of colocalization is represented using the Pearson's coefficient value (R) evaluated from the *PfK13* (red) and *PfATG18* (green) fluorescent signals within the white square region in the enlarged panel. Nucleus was stained using Hoechst.

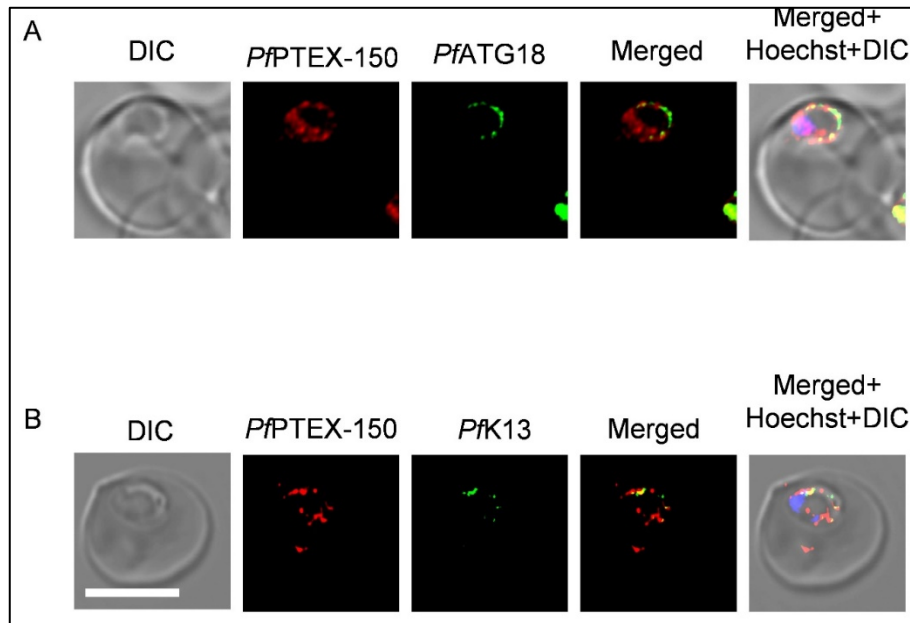


Figure 3.27 *PfK13* and *PfATG18* localize near the parasite periphery in ring stage $K13^{C580Y}$ parasites

(A) Immunofluorescence analysis of $K13^{C580Y}$ parasites stained with anti-*PfPTEX-150* and anti-*PfATG18* antibodies were labelled using the Zenon antibody labelling system. (B) Immunofluorescence analysis of $K13^{C580Y}$ parasites stained with anti-*PfPTEX-150* and anti-*PfK13* antibodies were labelled using the Zenon antibody labelling system. N = 15 parasites, n = 3 independent experiments, Scale bar: 5 μ m. Nucleus was stained using Hoechst.

Chapter 4

Discussion

4.1 Artemisinin induced UPR pathway activates *P. falciparum* autophagy

In this study, we find that DHA induced ER stress stimulates the UPR signaling pathway, which in turn triggers parasite autophagy. Our results showing increased phosphorylation of *PfeIF2 α* and upregulation of the ER-resident chaperone *PfBiP* together with expansion of the parasite ER upon incubation with DHA are consistent with previous reports showing ART induced ER stress responses. Additionally, DHA mediated ER stress increases the number of *PfATG8* labelled autophagosome-like vesicles as well as the expression levels of, *PfATG8* and *PfATG18*, indicating activation of the parasite autophagy pathway. Further, inhibition of the PERK-*PfeIF2 α* mediated UPR pathway leads to decreased expression of the autophagy proteins. The study provides experimental evidence for parasite autophagy as an ER stress response pathway triggered by the translational arm of the UPR.

As an early branching eukaryote, *P. falciparum* exhibits conserved as well as distinct features associated with the UPR. While the malaria parasite seems to lack homologs of ATF6 and IRE1, it possesses a cluster of three eIF2 kinases, PERK, and the downstream translation initiation factor *PfeIF2 α* (Gosline *et al.*, 2011). In the absence of IRE1 and ATF6, *Plasmodium* parasites are likely to be particularly susceptible to perturbations in the mechanisms of ER homeostasis. Conservation of the PERK-eIF2 α pathway in protozoan parasites indicates that the pathway evolved very early in eukaryotes and is crucial for protection from ER stress. ART exposure has been shown to cause promiscuous protein alkylation, resulting in the accumulation of misfolded proteins, activating the ER stress response, which is characterized by eIF2 α phosphorylation and reduction of global protein

translation (Bridgford *et al.*, 2018). ART induced phosphorylation of eIF2 α in *P. falciparum* acts as an ER stress sensor and promotes parasite dormancy, which helps in increasing the parasites' capacity to regulate damage mediated by ART (Zhang *et al.*, 2017). We also observe increased phosphorylation of *Pf*eIF2 α upon incubating parasites with the clinically relevant dose of 700nM DHA for a brief period (1.5h). The rationale for a brief DHA exposure was to reflect the short *in vivo* half-life of the drug (Balint, 2001; Tarning *et al.*, 2012b). Interestingly, we find increased expression of *Pf*BiP upon DHA treatment, which has not been previously demonstrated. In yeast and other eukaryotes, BiP is considered the master regulator for maintaining homeostasis during ER stress due to its ability to refold misfolded proteins accumulated in the ER, and modulate the activation of UPR signaling sensors (Lee, 2005). The observed increase in the chaperone level in response to DHA induced damage suggests a role of *Pf*BiP in maintaining ER homeostasis in the malaria parasite similar to that observed in other organisms.

In this study, parasites transiently expressing *Pf*SEC62GFP were used to show that DHA induces expansion of the parasite ER. The observed expansion is likely a result of the build-up of misfolded proteins in the ER lumen, as well as an increase in the amount of ER resident chaperones, such as *Pf*BiP, that are biosynthesized to fold excess misfolded proteins. Our findings are consistent with reports which show that the ER, in yeast and other eukaryotes, expands massively and localizes to the cellular periphery following activation of the UPR. It has been suggested that this expansion may help to accommodate newly synthesized proteins and limit misfolded protein aggregation by lowering their concentration in the ER lumen (Bernales *et al.*, 2006; Bommasamy *et al.*, 2009). In *P. falciparum*, DHA treatment increases the volume of the ER, which then extends to other portions of the parasite, in contrast to the organelle's perinuclear localization in control. In another protozoan parasite, *Trypanosoma brucei*, ER stress similarly results in dilatation of the ER lumen containing dense materials, demonstrating that the phenomenon of ER expansion in response to ER stress is conserved in early diverging eukaryotes (Goldshmidt *et al.*, 2010). Overall, our findings provide additional methods to monitor ER stress in the parasite and contribute to the body of evidence suggesting that ART induces an enhanced ER stress response.

An ongoing question is how PERK-*Pf*eIF2 α based UPR regulates DHA mediated protein misfolding and damage. Activation of the translational UPR arm may aid in the recovery

or protection of cells from damage caused due to DHA exposure, hence increasing cell survival. Inhibition of the kinase activity of PERK increases the sensitivity of other eukaryotes to ER stress, but this enhanced susceptibility is only partly restored by chemical suppression of protein synthesis, showing that PERK-mediated signaling is required for ER stress mitigation (Bertolotti *et al.*, 2000; Harding *et al.*, 2003). Given the absence of conventional transcription factors, in particular the bZIP family of transcriptional regulators to which the components of the UPR transcriptional regulatory arm, ATF6 and XBP1, belong (Coulson *et al.*, 2004), it is possible that *P. falciparum* needs to employ novel mechanisms to manage excess protein misfolding under ER stress. The transcription machinery in protozoan parasites is distinct from other eukaryotes due to the presence of a unique class of APetela-2 domains containing AP2 transcription factors. Parasites incubated with DTT, a known inducer of ER stress, show upregulation of multiple AP2 transcription factors as well as their cellular targets (Chaubey *et al.*, 2014). None of the AP2 transcription factors, however, include the transmembrane domain (Joyce *et al.*, 2013) required for them to function similarly to IRE1 or ATF6.

PERK mediated phosphorylation of eIF2 α decreases global protein translation, but also increases selective translation of particular mRNAs, such as the master regulator transcription factors GCN4 (Mueller and Hinnebusch, 1986) and ATF4 (Vattem and Wek, 2004) in yeast and higher eukaryotes, respectively. In this way, the PERK-eIF2 α based UPR contributes to alleviating ER stress by reprogramming gene expression. Although homologs of GCN4 and ATF4 have not been identified in *Plasmodium*, it is plausible that phosphorylation of *PfeIF2 α* facilitates the translation of other mRNAs in a similar manner. The PERK/eIF2 α pathway also initiates the transcription of genes related to autophagy in response to amino acid deprivation or ER stress, and the AFT4 transcription factor is essential for the upregulation of these genes (B'chir *et al.*, 2013). Although the *P. falciparum* genome contains a limited number of ATG genes (Cervantes *et al.*, 2014; Hain and Bosch, 2013; Navale *et al.*, 2014), some of them have been identified to be involved in both canonical and non-canonical autophagy related functions (Agrawal *et al.*, 2020; Bansal *et al.*, 2017; Joy *et al.*, 2018; Tomlins *et al.*, 2013). *Plasmodium* parasites likely engage autophagy-like proteins to reduce ER stress caused as a result of DHA mediated widespread damage.

Our results reveal that incubating *P. falciparum* with DHA activates an autophagy-like pathway. In addition to the increased number of *PfATG8* labelled vesicles, DHA exposure leads to heightened expression levels of both *PfATG8* and *PfATG18*. During autophagy induction, several ATG proteins localize to the PAS to initiate the process of autophagy. ATG8 is, however, the key autophagosome marker in yeast and other eukaryotes since it is the only ATG protein that is associated with both premature and mature autophagosomes and the lipidated form of ATG8 correlates with the number of autophagosomes, generated (Cheong and Klionsky, 2008b; Mizushima *et al.*, 2010). Western blotting and immunofluorescence analyses reveal that *PfATG8* localizes on subcellular membranes and appears as punctate structures in the parasite (Kitamura *et al.*, 2012). Additionally, a previous report from the lab has demonstrated that *PfATG8* levels can be regulated in response to autophagy induction and inhibition, indicating autophagy-like features of the protein (Joy *et al.*, 2018). The increase in the number of *PfATG8* labelled puncta and the expression levels of the protein upon parasite exposure to DHA indicates that autophagy is activated in response to ER stress. *PfATG18* has been shown to participate in both the canonical autophagy-like pathway and food vacuole fission in the parasite (Agrawal *et al.*, 2020). Increased expression of *PfATG18* in response to DHA treatment reaffirms that parasite autophagy underpins processes of ER homeostasis with regard to DHA induced ER stress. Further, our results validate our proposition that increased expression of parasite autophagy proteins upon DHA exposure is mediated directly through the UPR. Incubation of the parasites with GSK2606414, a mammalian PERK inhibitor which specifically blocks UPR/PERK activation (Axten *et al.*, 2012), leads to inhibition of the basal and DHA induced phosphorylation of *PfeIf2 α* , indicating inhibition of parasite PERK/*PfeIf2 α* mediated translational attenuation. GSK2606414 also leads to a significant reduction in the expression levels of *PfATG8* and *PfATG18*, suggesting their activation is through the UPR/PERK pathway in the malaria parasite.

In summary, our findings establish parasite autophagy as an ER stress response pathway in *P. falciparum* that is triggered by UPR. Induced autophagy likely mitigates parasite ER stress by sequestering and subsequently degrading excess ER containing misfolded protein aggregates formed as a consequence of ART mediated widespread protein alkylation.

4.2 Putative *PfATG1* (PF3D7_1450000) participates in the autophagy-like pathway in *P. falciparum*

Several new findings emerge from our characterization of the putative *PfATG1* like protein kinase. The gene with the accession number PF3D7_1450000 was predicted to be a *Plasmodium* homolog of the human ULK1 and yeast ATG1 (Hain and Bosch, 2013). Putative *PfATG1* is expressed throughout the intraerythrocytic stages of *P. falciparum* as punctate structures across the parasite cytoplasm and colocalizes partially with the autophagosome marker protein *PfATG8*, similar to yeast ATG1 which colocalizes with ATG8 on the PAS (Suzuki *et al.*, 2007). Putative *PfATG1* also partially localizes to the ER, which is known to provide membranes for autophagosome biogenesis (Shibutani and Yoshimori, 2014). Inhibition of the *PfATG1* kinase activity with MRT68921, a small molecule inhibitor of the human autophagy protein ULK1 (Petherick *et al.*, 2015), results in reduced expression of *PfATG8* and *PfATG18*, homologs of which are known to function downstream of ATG1 in yeast and other eukaryotes (Yin *et al.*, 2016). This suggests that putative *PfATG1* functions upstream of both *PfATG8* and *PfATG18*, and in conjunction with the similarity in localization to yeast ATG1, supports our hypothesis that this ATG protein participates in an autophagy-like process in *P. falciparum*.

Upon induction of autophagy in yeast and other eukaryotes, ATG1/ULK1 binds to ATG13, which is crucial for the assembly of other autophagy proteins to the PAS prior to autophagosome formation (Lin and Hurley, 2016). However, compared to the classical ATG1-ATG13 complex present in other organisms, there are a few differences in *P. falciparum*. *PfATG1* is about half the length of its yeast and mammalian counterparts. Although the amino acid sequence of putative *PfATG1* harbors a conserved kinase domain, the protein lacks the two microtubule interacting and transport (MIT) domains which facilitate its binding to ATG13 (Chew *et al.*, 2015; Lin and Hurley, 2016), suggesting that *PfATG1* might participate in the autophagy-like pathway irrespective of its association with ATG13 or be involved in other non-canonical roles in the parasite. Additionally, bioinformatic analyses suggest the absence of an ATG13 homolog in the *P. falciparum* genome (Hain and Bosch, 2013), which correlates with the lack of an ATG13 binding domain in the putative *PfATG1*. However, threonine at position 226 on *ScATG1*, which is required for proper autophagy induction (Yeh *et al.*, 2010), is replaced with another phosphorylatable serine residue (*PfATG1* S208), retaining the phosphorylation site in the

activation loop of putative *PfATG1*. Thus, the putative *PfATG1* sequence encodes both unique as well as conserved autophagy-like features in *P. falciparum*.

In the current study, putative *PfATG1* is found to be localized to cytoplasmic vesicular structures throughout the intraerythrocytic parasite stages, while in other systems, ATG1 is observed to interact with membranes only during autophagy (Suzuki *et al.*, 2007). One plausible explanation for this constitutive expression is that putative *PfATG1* is essential for the assembly of core autophagy proteins, including *PfATG8* to a PAS-like structure in the parasite, which is also the canonical role of the ATG1-ATG13 complex in other systems (Nakatogawa *et al.*, 2012; Yin *et al.*, 2016). Owing to the fact that *PfATG8* associates with subcellular membrane structures throughout the asexual blood stages of the parasite (Cervantes *et al.*, 2014), it is likely that *PfATG1* is required to enhance *PfATG8*'s interaction with membranes and hence contribute to basal autophagy (Joy *et al.*, 2018). Additionally, as putative *PfATG1* colocalizes with the key autophagosome marker protein *PfATG8*, even at basal levels, this suggests that *PfATG1* is associated with autophagosome-like structures in the parasite. In addition to autophagosome-like structures, putative *PfATG1* also partially colocalizes with the ER. Since the ER contributes membrane to the formation of autophagosomes in higher eukaryotes (Shibutani and Yoshimori, 2014; Suzuki *et al.*, 2007), this supports a role for parasite ER in autophagosome biogenesis in *P. falciparum*. There is mounting evidence which show that *PfATG1* homolog in mammalian cells can localize to membranes even in the absence of ATG13 through a putative lipid binding domain (Nishimura and Tooze, 2020). Additionally, ULK-mediated phosphorylation of the ER protein SEC16A regulates specific cargo trafficking from the ER to the Golgi, a process that is independent of the ATG1-ATG13 interaction (Joo *et al.*, 2016). In the absence of a ATG13 homolog in *P. falciparum*, it is likely that membrane association of putative *PfATG1* may occur in a similar way. In future, a detailed analysis of the *PfATG1* domain architecture will facilitate a better understanding of the protein's function in the context of *P. falciparum*.

Our results indicate that the putative *PfATG1* is essential for parasite survival even in nutrient-rich conditions. MRT68921 inhibits parasite growth dose-dependently (IC₅₀ = 761.1 nM), and cultures treated at concentrations greater than the IC₅₀ exhibit developmental abnormalities in the trophozoite and schizont stages, hence lowering the parasites' invasion ability during the subsequent developmental cycle. A previous report

from our lab demonstrates ability of MRT68921 to bind to and fit well inside the substrate binding groove of *PfATG1* as revealed by docking studies to simulate binding of the MRT68921 dihydrochloride on the homology model of *PfATG1* (Joy *et al.*, 2018), suggesting that the small molecule inhibitor can specifically bind to *PfATG1*. Additionally, MRT68921 inhibition of putative *PfATG1* kinase activity decreases both the baseline and starvation-induced expression levels of *PfATG8* and *PfATG18*, demonstrating a function for *PfATG1* upstream of *PfATG8* and *PfATG18* and comparable to its role in autophagy initiation in yeast and other eukaryotes.

Although putative *PfATG1* exhibits several features indicative of its role as an autophagy-like protein in the parasite, *PfATG1*-GFP was unable to participate in the autophagy pathway when expressed in *atg1Δ* yeast cells. This observation may be explained by the lack of crucial domains in *PfATG1* that enable its association with ATG13, which in turn facilitates the recruitment of downstream ATG proteins to the PAS, where autophagosome assembly is initiated. Due to the inability of putative *PfATG1* to localize to the PAS in *atg1Δ* cells, we hypothesize that *Plasmodium* ATG1 is unable to interact with yeast ATG13 and thus cannot complement autophagy in *atg1Δ* yeast.

In conclusion, our findings indicate that putative *PfATG1* is a component of the parasite's autophagy-like machinery and may be exploited as a biomarker for autophagosome formation in the parasite. However, further work is necessary to unravel *PfATG1*'s kinase activity and determine if MRT68921 affects the substrate binding ability of the kinase in *P. falciparum*.

4.3 *P. falciparum* autophagy underpins various mechanisms of artemisinin resistance

This work demonstrates that parasite autophagy underpins various mechanisms of ART resistance and advances the understanding of two recently proposed mechanisms for ART resistance involving the induced ER and cytoplasmic proteostasis mechanisms mitigating ART mediated proteopathy (Bhattacharjee *et al.*, 2018; Suresh and Haldar, 2018), and the *PfK13* C580Y mutation associated reduced hemoglobin endocytosis pathway (Birnbaum *et al.*, 2020). We show that basal expression levels of *PfATG8* and *PfATG18* are higher in the ART resistant isolate (K13^{C580Y}) compared to its isogenic (K13^{WT}) counterpart, which is further enhanced upon starvation. Resistant parasites, characterized by enhanced PI3P

vesiculation, also show increased colocalization of PI3P with *PfATG18* at the basal level and upon activation of autophagy through starvation. *K13^{C580Y}* parasites are more sensitive to the specific autophagy inhibitor MRT68921, indicating the involvement of autophagy in mediating various proteostasis mechanisms governing parasite survival. Additionally, the co-localization of *PfK13*, *PfATG18*, and PI3P on parasite hemoglobin trafficking vesicles suggests co-trafficking to the FV through the same subcellular vesicles.

Mammalian orthologs of *PfATG8*, the LC3, and of *PfATG18*, the WIPI1, participate in autophagy with an increase in mRNA levels indicating autophagy activation (Kabeya *et al.*, 2005; Proikas-Cezanne *et al.*, 2007; Tsuyuki *et al.*, 2014). Our results show increased expression of *PfATG8* and *PfATG18* at the mRNA and protein levels, as well as colocalization of *PfATG18* labelled puncta with *PfATG8*, in ART resistant parasites compared to their isogenic counterparts during the early ring and young trophozoite stages, indicating that parasite autophagy regulates the various proteostasis mechanisms underlying ART resistance. According to a recent report, *PfK13* mutations, in particular C580Y, result in decreased hemoglobin endocytosis, particularly in the early ring stage, hence decreasing ART activation and ultimately leading to ART resistance at the ring stage (Birnbaum *et al.*, 2020). Due to the low metabolic activity of rings, ART resistance is predicted at this stage, while the trophozoites and schizonts are more metabolically active and therefore vulnerable to ART mediated damage. We hypothesize that, as the primary source of amino acids, host hemoglobin endocytosis (Liu *et al.*, 2006) decreases during the ring stage, autophagy rescues the parasites from nutrient limiting conditions and is therefore responsible for survival through delayed progression to the trophozoite stage. This is reflected in the higher expression levels of *PfATG8* and *PfATG18* in early ring stage ART resistant parasites compared to the isogenic one. Due to the large proportion of heme in the FV during the trophozoite and schizont stages owing to more hemoglobin uptake (Elliott *et al.*, 2008), results in oxidative stress, which promotes autophagy in other eukaryotes (Filomeni *et al.*, 2015). Enhanced ER-PI3P vesiculation and the UPR chaperone *PfBiP* (Bhattacharjee *et al.*, 2018; Mok *et al.*, 2015), also contribute to autophagy induction, particularly during the trophozoite stage.

Previous studies suggest increased PI3P levels, even by transgenic methods, as the major proteostasis response of ART resistance (Mbengue *et al.*, 2015). PI3P induces autophagy in yeast and eukaryotes by providing a platform for the recruitment of multiple autophagy

proteins to the PAS. It is also believed to modulate the membrane curvature required for autophagosome assembly and maturation (Dall'Armi *et al.*, 2013; Devereaux *et al.*, 2013). PI3P interacts with one of its effector proteins, ATG18, through the conserved FRRG motif, and this interaction is regulated by the phosphorylation state of yeast ATG18 (Dove *et al.*, 2004; Tamura *et al.*, 2013). Additionally, due to ATG18 mediated vacuolar fission and fusion, vacuolar shape is also maintained, which is crucial in minimizing macromolecular crowding inside the vacuole, essential for the survival of organism (Desfougères *et al.*, 2016). *Pf*ATG18 also binds to PI3P with its FRRG motif, enabling membrane association for carrying out downstream functions (Bansal *et al.*, 2017). This is consistent with previous findings from our lab that demonstrate participation of *Pf*ATG18 in the parasite autophagy-like pathway and is also implicated in the FV fission process, as well as being trafficked to the food vacuole through HCv in a PI3P-dependent manner (Agrawal *et al.*, 2020). Here we show that in the *Pf*K13 mutant strain, PI3P bound *Pf*ATG18 vesicles are increased even at baseline levels, suggesting that autophagy is initiated in resistant parasites even in the absence of an external stress. This vesicle number increase further upon autophagy induction by starvation in both the resistant and isogenic parasites, establishing a conserved role of *Pf*ATG18 in parasite autophagy and demonstrating a functional autophagy-like pathway that responds to autophagy induction under starvation. Furthermore, autophagy activation is much higher in the resistant isolate than in the sensitive one, indicating the reliance on autophagy for parasite fitness.

Further, several recent reports highlight the importance of *Pf*K13 in regulating the amount of hemoglobin endocytosis by the cytostomes and its degradation in the FV (Birnbbaum *et al.*, 2020; Gnädig *et al.*, 2020; Yang *et al.*, 2019). Regardless of that, there is no experimental evidence suggesting the presence of *Pf*K13 on HCv, which are discrete vesicles transporting host derived hemoglobin to the parasite FV (Milani *et al.*, 2015). As *Pf*ATG18 is trafficked to the FV via HCv and this association is believed to be mediated by its interaction with PI3P (Agrawal *et al.*, 2020), we dwelled on whether the *Pf*K13 endocytic pathway vesicles are the same sub-cellular compartments on which *Pf*ATG18 and PI3P colocalize. We observe that *Pf*K13-PI3P and *Pf*K13-*Pf*ATG18 partially colocalize on these HCv. As other routes for hemoglobin delivery to the FV are also proposed, including processes involving phagotrophs and the microtubule assisted cytostomal tubes (Elliott *et al.*, 2008; Spielmann *et al.*, 2020), this explains the partial colocalization of *Pf*K13-*Pf*ATG18-PI3P with *Pf*FP2-decorated vesicles. Our results show

colocalization of *PfK13* and *PfATG18* increases towards the parasite periphery at the ring stage while being localized close to the FV in trophozoites, which we speculate is due to their enhanced co-trafficking to the FV in the trophozoite stage.

Genetic background has a profound effect on the acquisition and maintenance of ART resistance (Miotto *et al.*, 2015). The increased prevalence of *PfK13* C580Y mutation across Southeast Asia is partly attributed to epistatic interactions from background genetic mutations that compensate for the loss of fitness endured by parasites during resistance (Miotto *et al.*, 2015; Nair *et al.*, 2018; Straimer *et al.*, 2017). Additionally, nutrient unavailability severely impacts parasite fitness and reduces cell cycle maturation rate in ART resistant parasites (Bunditvorapoom *et al.*, 2018), further envisaging the importance of autophagy in resistance. Given that mutations in the autophagy genes encoding *PfATG18* and *PfATG7* have been identified in ART resistant subpopulations (Dwivedi *et al.*, 2017), and that the *PfATG18* T38I mutation confers a fitness advantage to parasites by enabling faster growth rates in nutrient limiting conditions (Breglio *et al.*, 2018; Wang *et al.*, 2016), we believe that the co-occurrence of *PfATG18* T38I mutation with major *PfK13* mutations identified in resistant parasites indicates possible compensation by autophagy. Dephosphorylation of ATG18 has been demonstrated to enhance its capacity to bind phosphoinositides in yeast, aiding the membrane association required for autophagosome formation (Tamura *et al.*, 2013). Although it is unclear if the mutation in T38 facilitates *PfATG18* dephosphorylation mediated membrane association (Breglio *et al.*, 2018), we hypothesize that this mutation facilitates the autophagy-like pathway in the parasite. Thus, polymorphisms in autophagy genes that increase parasite survival might be selected during resistance development to compensate for decreased parasite fitness.

However, ART resistance is not limited to *PfK13* and autophagy proteins alone, but is also associated with an enrichment of chaperones in the ER-PI3P vesicles of *in-vitro* resistant parasites, as well as the increased UPR pathway involving the *Plasmodium* reactive oxidative stress complex and TCP-1 ring complex (TRiC) chaperone complexes in *in-vivo* resistant clinical isolates (Bhattacharjee *et al.*, 2018; Mok *et al.*, 2015). These factors, together with our findings, which establish parasite autophagy as an ER stress response pathway activated by UPR, further highlight autophagy as a key player in the proteostatic processes underlying ART resistance.

Our findings collectively establish a unifying role for autophagy as a cellular process, interlinking various mechanisms of ART resistance. In addition, the inhibition of ART resistant parasites by a specific autophagy inhibitor, MRT68921, identifies this pathway as a novel target, which needs further efforts to develop novel and more effective therapeutics.

4.4 Conclusion and key findings

In this work, we investigated the role of *P. falciparum* autophagy in ER homeostasis processes in response to DHA induced ER stress, as well as its participation in mechanisms underlying ART resistance. We have demonstrated that ER stress activates UPR in the malaria parasite, resulting in autophagy induction. Our study establishes a previously unexplored crosstalk between ER stress, UPR and autophagy in *P. falciparum* and shows the participation of autophagy in facilitating ART resistance (Figure 4.1).

We find that upon DHA induced ER stress, parasites exhibit heightened expression levels of *PfATG8* and *PfATG18*, as well as increased *PfATG8* labelled autophagosome-like vesicles. The induction of autophagy is attributed to the activation of parasite UPR in response to DHA mediated ER stress. To further advance our understanding of how ER stress stimulates parasite autophagy, it is essential to investigate the protein complexes involved in autophagy initiation. ATG1/ULK1 is involved in the initiation of autophagosome in yeast and other eukaryotes by recruiting several autophagy proteins to the PAS and responds to ER stress by activating the autophagy pathway. Thus, functional characterization of putative *PfATG1* is necessary to fully understand the mechanisms by which the malaria parasite integrates the ER stress response with autophagy. Our findings demonstrate the presence of putative *PfATG1* throughout the intraerythrocytic parasite stages as discrete cytoplasmic puncta that colocalize with the autophagosome marker protein *PfATG8*. MRT68921 inhibits parasite growth and decreases the expression of autophagy proteins downstream of putative *PfATG1*, indicating that the kinase functions upstream of other autophagy proteins in the parasite, similar to its role in yeast and other eukaryotes in initiating autophagy.

Parasite autophagy underpins various mechanisms of ART resistance. Our results showing higher expression of *PfATG8* and *PfATG18*, and their increased colocalization in resistant parasites indicates activation of parasite autophagy, which may regulate various mechanisms of ART resistance. We show autophagy to be functional in the malaria

parasite, with both isogenic and resistant parasites responding to pathway activation through starvation. The colocalization of *Pf*ATG18-decorated vesicles with PI3P is significantly greater in resistant parasites than in sensitive parasites, indicating that the autophagy protein is associated with ER-PI3P vesicles that dissipate protein folding capacity throughout the parasite. Additionally, resistant parasites are shown to be more sensitive to autophagy inhibition than isogenic ones, indicating that the pathway plays a critical role in the survival of ART resistant parasites. The autophagy protein *Pf*ATG18 appears to associate with the major resistant marker protein *Pf*K13 on HCv, indicating co-trafficking to the FV through the same subcellular vesicles.

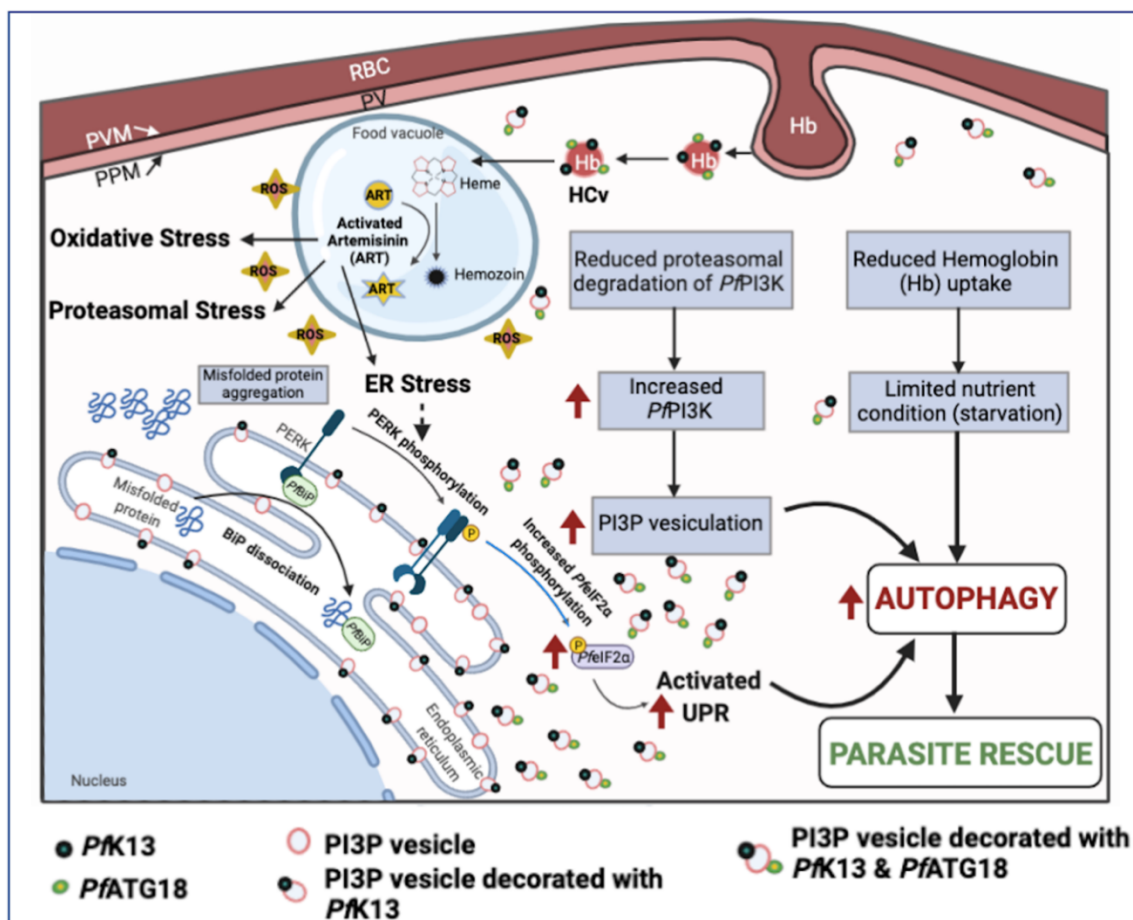


Figure 4.1 Model representing role of autophagy in mechanisms of ART resistance

Activated ART generates ROS and leads to alkylation and subsequent misfolding of proteins, activating the stress response pathways. The primary source of amino acid supply, host hemoglobin endocytosis, is diminished at the ring stage in *Pf*K13 mutants, leading to reduced ART activation and decreased protein misfolding. The reduced hemoglobin uptake in *Pf*K13 mutants results in limited nutrient conditions, which induces autophagy. Also, the decrease in PI3K ubiquitination

and degradation leads to increased PI3P vesiculation, which induces the parasite autophagy pathway. Our results reveal that *PfK13* mutants have increased levels of autophagy proteins indicating the role of autophagy in the survival of these resistant parasites.

Appendices

Appendix 1: Multiple sequence alignment between *Sc*ATG1, *Pf*ATG1 and *Hs*ULK1

ScATG1	1	MGDIKMKD.....HTTSVNHNLMASAGNYTAEKEIGKGSFATVYRGH
PfATG1	1	MGSTISKRRKNTDKNVKDESVENKQKKNEENDSNLEFIKYYKIINKIGDGNFSKVFCCR
HsULK1	1MEPG..RGGTEIVGKFE....ESRKDLIGHGAFVVFVFKGR
ScATG1	43	LTSDK SQHVAI KEVSRAKLKNKLLLENLEIEIA ILKKIKHPHIVGLIDCERSTST...DF
PfATG1	61	GENK K KCA MK LMCCPLKKTSHYN.CFKREL FIMKTINNKHPIV KILDYHEKIWKYYIV
HsULK1	35	HREKH DLEVAVKCINKKNLAKSQTL LGKEIKILKE..LKHENIVALYDFQEMAN...SV
ScATG1	99	YLIMEYCALGDLITFL LKRRKELMENHPLLRTVFEKYPPPS ENHNGLHRAFVLSYLQQLAS
PfATG1	120	KLILEYCEG NLF EYIK INGSCTH.....SEARV I I I K L T K
HsULK1	89	YL VMEYCN GDLADY LHAMRTLSE.....DTI IRLFLQQLIAG
ScATG1	159	ALKFLR SKNLVHRDIKPNL LLS TPLIGYHDSKSFHELGFVGIYNLP I LKTA DFG FARFL
PfATG1	156	TIQYINSLKIMHRDIKPNEN LLS RTKD.....NIKS VVLSDFGLAKIT
HsULK1	125	AMRL LHSKGI IHRDLKPNL LLS NPAGRR.....ANPNSIRVKIADFGFARYL
ScATG1	219	PN...TSLAE T LCGS PLYMAPEI LNYQKYNAKADLWSVGT VVFEMCCGTPPFRASNHLBL
PfATG1	198	PSNQSVVKSRSVCGSDFYLAPEI IKNKEYGIKIDIWSLGV LIFFIITGKV PFTGKNANBL
HsULK1	173	QS...NMMAA T LCGSPM YMAPEVI MSQHYD GKADLWSIGT I VYQCLTGKAPFQASSPQDL
ScATG1	276	FKKIKRANDV...ITFPSYCNIEPE LKE L ICS L LTFDPAQRIGFEFFANKV V NEDLSS
PfATG1	258	YNNI..LKANIP ELLSKEKSLNIQ PGLKNLLEN I L VHDPDQR FSCAD I L NHRW I RGT L T S
HsULK1	230	RLFYEKNKTLVPTI.PRET....SAPLRQL L L L Q R N H K D R M D F D E F F H H P F L D A S P S V
ScATG1	332	YELEDD.LPELESKSKGIVESNM FVSEYLSKQPKSPNSNLAGHQSMADNPAELSDALKNS
PfATG1	316	CEF K I F N S A S Y I K K.....LRLD
HsULK1	285	RKSPFPVPVPSYPSSGSGSSSSSSS.....TSHL.....ASPPSLGEMQQLQ
ScATG1	391	NILTAPAVKTDHTQAVDKKASNNKYHNSLVSDRSFER.....EYVVVEKKSVEV.
PfATG1	334	KK.....KASYDEE...A...KDN.QIKDKS FENEKDSFANKKKRYTFFLKKITN..
HsULK1	326	KTLASPADTAGFLHS....S....RDSGGSKDS SC..DTDDFVMVPAQF...PGDLVAEA
ScATG1	440NSLADEVAQAG.....FNP.....PI
PfATG1		
HsULK1	373	PSAKPPPDSL MCGSSLVASAGLESHGRTPSPSPPCSSSPSPSGRAGPFSSSRGASVPI
ScATG1	457	KHPTSTQNQNVLN.....EQFSPNNQYFQNGENPRLLRATSSSSSGSDGSRRPSLV D
PfATG1		
HsULK1	433	PVPTQVQNYQRIERNLQSPTQFQTPRSSAIRRSGSTSP L G F A R A S P S . P P A H A E H G G V L A

ScATG1 512 RRLSISLNPNSALS.....RALGIA.....STRLFGGANQQQQ.....
PfATG1
HsULK1 492 RKMSLGGGRPYTPSPQVGTIPERPGWSGTPSPQGAEMRGGRSRPRPGSSAPEHSPRTSGLG

ScATG1 546QQQITSSPPYSQT
PfATG1
HsULK1 552 CRLHSAPNLSDLHVVRPKLPKPPDPLGAVFSPPQASPPQPSHGLQSCRNLRGSPKLPDF

ScATG1 559 LLNSQLFHELTENIILRIDHLQHPETLKLNDNTNIVSILES LAAKAFVVYSYAEV...KFS
PfATG1
HsULK1 612 LQRN.PLPPILGSPTKAVPSFDFPKTPS..SQNLL...ALLARQGVVMTPPRNRTLPLDLS

ScATG1 616 QIVP.....LSTTLKGM....A....NFENRRSMDS..NAIAEEQDSDDAEEDETLKKY
PfATG1
HsULK1 666 EVGPFHGQPLGPGLRPGEDPKGPFGRSFSTSRLLTDLLLKAAFQTQAPDPG..STESLQEK

ScATG1 661 KEDCLSTKTFGKGRTLSATSQLSA.....T.....FNKLPRSEMI.....
PfATG1
HsULK1 724 PMEIAPSAGFGG..SLHPGARAGGTSSPSPVVFTVGSPPSGSTPPQGPRTRMFSAGPTGS

ScATG1 696LLCNEAIVLYMKALSILSKSMQVTSNWWYESQEKSCSLRVNVLVQ.....
PfATG1
HsULK1 782 ASSSARHLVPGPCSEAPE.....LPAPGHGCSFADPITANLEGAV

ScATG1 741 .WL.....REKFNECLEKADFLRLKINDLRFKHASEVAENQ..TLEEKGSSEEP.
PfATG1
HsULK1 824 TFEAPDLPEETLMEQEHETEILRGLRFT.....LLFVQHVLEIAALKGSASEAAGGPEYQL

ScATG1 787 ...V.....YLEK.LLYDRALEISK.....MAAHMELK
PfATG1
HsULK1 879 QESVVADQISLLSREWGFAEQVLVLYLKVAELLSSGLQSAIDQIRAGKLCLSSTVKQVRR

ScATG1 811 GENLYNCE.....LAYATSLWMLETSLDDDDFT
PfATG1
HsULK1 939 LNELYKASVVSCQGLSLRLQRFFLDKQRLLDRIHSITAERLIFSHAVQMVQSAALDEMFO

ScATG1 839 NAYGDYPFKTNIHLKSNDEVEDKEKYHSVLDENDRIIRKYIDSIANRLKILRQKMNHQ
PfATG1
HsULK1 999 HREGCVPRYHKALLLLEGL.....QHMLSDQADIENVTKCKLCIERRLSALLTGICA..

References

- Adjalley, S.H., Johnston, G.L., Li, T., Eastman, R.T., Ekland, E.H., Eappen, A.G., Richman, A., *et al.* (2011), “Quantitative assessment of *Plasmodium falciparum* sexual development reveals potent transmission-blocking activity by methylene blue”, *Proceedings of the National Academy of Sciences*, National Acad Sciences, Vol. 108 No. 47, pp. E1214–E1223.
- Agrawal, P., Manjithaya, R. and Surolia, N. (2020), “Autophagy-related protein PfATG18 participates in food vacuole dynamics and autophagy-like pathway in *Plasmodium falciparum*”, *Molecular Microbiology*, Wiley Online Library, Vol. 113 No. 4, pp. 766–782.
- Aman, Y., Schmauck-Medina, T., Hansen, M., Morimoto, R.I., Simon, A.K., Bjedov, I., Palikaras, K., *et al.* (2021), “Autophagy in healthy aging and disease”, *Nature Aging*, Nature Publishing Group, Vol. 1 No. 8, pp. 634–650.
- Anderson, T.J.C., Nair, S., McDew-White, M., Cheeseman, I.H., Nkhoma, S., Bilgic, F., McGready, R., *et al.* (2017), “Population parameters underlying an ongoing soft sweep in Southeast Asian malaria parasites”, *Molecular Biology and Evolution*, Oxford University Press, Vol. 34 No. 1, pp. 131–144.
- Ariey, F., Witkowski, B., Amaratunga, C., Beghain, J., Langlois, A.-C., Khim, N., Kim, S., *et al.* (2014), “A molecular marker of artemisinin-resistant *Plasmodium falciparum* malaria”, *Nature*, Nature Publishing Group, Vol. 505 No. 7481, pp. 50–55.
- Arstila, A.U. and Trump, B.F. (1968), “Studies on cellular autophagocytosis. The formation of autophagic vacuoles in the liver after glucagon administration.”, *The American Journal of Pathology*, American Society for Investigative Pathology, Vol. 53 No. 5, p. 687.
- Ashley, E.A., Dhorda, M., Fairhurst, R.M., Amaratunga, C., Lim, P., Suon, S., Sreng, S., *et al.* (2014), “Spread of artemisinin resistance in *Plasmodium falciparum* malaria”, *New England Journal of Medicine*, Mass Medical Soc, Vol. 371 No. 5, pp. 411–423.
- Aweeka, F.T. and German, P.I. (2008), “Clinical pharmacology of artemisinin-based combination therapies”, *Clinical Pharmacokinetics*, Springer, Vol. 47 No. 2, pp. 91–102.
- Axten, J.M., Medina, J.R., Feng, Y., Shu, A., Romeril, S.P., Grant, S.W., Li, W.H.H., *et al.* (2012), “Discovery of 7-methyl-5-(1-([3-(trifluoromethyl) phenyl] acetyl)-2, 3-

- dihydro-1 H-indol-5-yl)-7 H-pyrrolo [2, 3-d] pyrimidin-4-amine (GSK2606414), a potent and selective first-in-class inhibitor of protein kinase R (PKR)-like endoplasmic reticulum kinase”, *Journal of Medicinal Chemistry*, ACS Publications, Vol. 55 No. 16, pp. 7193–7207.
- Babbitt, S.E., Altenhofen, L., Cobbold, S.A., Istvan, E.S., Fennell, C., Doerig, C., Llinás, M., *et al.* (2012), “Plasmodium falciparum responds to amino acid starvation by entering into a hibernatory state”, *Proceedings of the National Academy of Sciences*, National Acad Sciences, Vol. 109 No. 47, pp. E3278–E3287.
- Bakar, N.A., Klonis, N., Hanssen, E., Chan, C. and Tilley, L. (2010), “Digestive-vacuole genesis and endocytic processes in the early intraerythrocytic stages of Plasmodium falciparum”, *Journal of Cell Science*, The Company of Biologists Ltd, Vol. 123 No. 3, pp. 441–450.
- Balint, G.A. (2001), “Artemisinin and its derivatives: an important new class of antimalarial agents”, *Pharmacology & Therapeutics*, Elsevier, Vol. 90 No. 2–3, pp. 261–265.
- Bannister, L.H., Hopkins, J.M., Fowler, R.E., Krishna, S. and Mitchell, G.H. (2000), “A brief illustrated guide to the ultrastructure of Plasmodium falciparum asexual blood stages”, *Parasitology Today*, Elsevier, Vol. 16 No. 10, pp. 427–433.
- Bansal, P., Tripathi, A., Thakur, V., Mohammed, A. and Sharma, P. (2017), “Autophagy-related protein ATG18 regulates apicoplast biogenesis in apicomplexan parasites”, *MBio*, American Society for Microbiology (ASM), Vol. 8 No. 5.
- Baton, L.A. (2005), *Comparative Infectivity of Plasmodium Falciparum to Anopheles Albimanus and Anopheles Stephensi*, University of Glasgow (United Kingdom).
- B’chir, W., Maurin, A.-C., Carraro, V., Averous, J., Jousse, C., Muranishi, Y., Parry, L., *et al.* (2013), “The eIF2 α /ATF4 pathway is essential for stress-induced autophagy gene expression”, *Nucleic Acids Research*, Oxford University Press, Vol. 41 No. 16, pp. 7683–7699.
- Becker, K., Tilley, L., Vennerstrom, J.L., Roberts, D., Rogerson, S. and Ginsburg, H. (2004), “Oxidative stress in malaria parasite-infected erythrocytes: host–parasite interactions”, *International Journal for Parasitology*, Elsevier, Vol. 34 No. 2, pp. 163–189.
- Bernales, S., McDonald, K.L. and Walter, P. (2006), “Autophagy counterbalances endoplasmic reticulum expansion during the unfolded protein response”, *PLoS Biol*, Public Library of Science, Vol. 4 No. 12, p. e423.

- Bertolotti, A., Zhang, Y., Hendershot, L.M., Harding, H.P. and Ron, D. (2000), “Dynamic interaction of BiP and ER stress transducers in the unfolded-protein response”, *Nature Cell Biology*, Nature Publishing Group, Vol. 2 No. 6, pp. 326–332.
- Bhattacharjee, S., Coppens, I., Mbengue, A., Suresh, N., Ghorbal, M., Slouka, Z., Safeukui, I., *et al.* (2018), “Remodeling of the malaria parasite and host human red cell by vesicle amplification that induces artemisinin resistance”, *Blood*, American Society of Hematology, Vol. 131 No. 11, pp. 1234–1247.
- Birnbaum, J., Scharf, S., Schmidt, S., Jonscher, E., Hoeijmakers, W.A.M., Flemming, S., Toenhake, C.G., *et al.* (2020), “A Kelch13-defined endocytosis pathway mediates artemisinin resistance in malaria parasites”, *Science*, American Association for the Advancement of Science, Vol. 367 No. 6473, pp. 51–59.
- Bommiasamy, H., Back, S.H., Fagone, P., Lee, K., Meshinchi, S., Vink, E., Sriburi, R., *et al.* (2009), “ATF6 α induces XBP1-independent expansion of the endoplasmic reticulum”, *Journal of Cell Science*, Company of Biologists, Vol. 122 No. 10, pp. 1626–1636.
- Borrmann, S., Straimer, J., Mwai, L., Abdi, A., Rippert, A., Okombo, J., Muriithi, S., *et al.* (2013), “Genome-wide screen identifies new candidate genes associated with artemisinin susceptibility in *Plasmodium falciparum* in Kenya”, *Scientific Reports*, Nature Publishing Group, Vol. 3 No. 1, pp. 1–10.
- Boya, P., Reggiori, F. and Codogno, P. (2013), “Emerging regulation and functions of autophagy”, *Nature Cell Biology*, Nature Publishing Group, Vol. 15 No. 7, pp. 713–720.
- Breglio, K.F., Amato, R., Eastman, R., Lim, P., Sa, J.M., Guha, R., Ganesan, S., *et al.* (2018), “A single nucleotide polymorphism in the *Plasmodium falciparum* atg18 gene associates with artemisinin resistance and confers enhanced parasite survival under nutrient deprivation”, *Malaria Journal*, Springer, Vol. 17 No. 1, pp. 1–16.
- Brennan, A., Gualdrón-López, M., Coppens, I., Rigden, D.J., Ginger, M.L. and Michels, P.A.M. (2011), “Autophagy in parasitic protists: unique features and drug targets”, *Molecular and Biochemical Parasitology*, Elsevier, Vol. 177 No. 2, pp. 83–99.
- Bridgford, J.L., Xie, S.C., Cobbold, S.A., Pasaje, C.F.A., Herrmann, S., Yang, T., Gillett, D.L., *et al.* (2018), “Artemisinin kills malaria parasites by damaging proteins and inhibiting the proteasome”, *Nature Communications*, Nature Publishing Group, Vol. 9 No. 1, pp. 1–9.

- Bunditvorapoom, D., Kochakarn, T., Kotanan, N., Modchang, C., Kümpornsin, K., Loesbanluechai, D., Krasae, T., *et al.* (2018), “Fitness loss under amino acid starvation in artemisinin-resistant *Plasmodium falciparum* isolates from Cambodia”, *Scientific Reports*, Nature Publishing Group, Vol. 8 No. 1, pp. 1–9.
- Calfon, M., Zeng, H., Urano, F., Till, J.H., Hubbard, S.R., Harding, H.P., Clark, S.G., *et al.* (2002), “IRE1 couples endoplasmic reticulum load to secretory capacity by processing the XBP-1 mRNA”, *Nature*, Nature Publishing Group, Vol. 415 No. 6867, pp. 92–96.
- Carreras-Sureda, A., Pihán, P. and Hetz, C. (2018), “Calcium signaling at the endoplasmic reticulum: fine-tuning stress responses”, *Cell Calcium*, Elsevier, Vol. 70, pp. 24–31.
- Cervantes, S., Bunnik, E.M., Saraf, A., Conner, C.M., Escalante, A., Sardu, M.E., Ponts, N., *et al.* (2014), “The multifunctional autophagy pathway in the human malaria parasite, *Plasmodium falciparum*”, *Autophagy*, Taylor & Francis, Vol. 10 No. 1, pp. 80–92.
- Chaharbakhshi, E. and Jemc, J.C. (2016), “Broad-complex, tramtrack, and bric-à-brac (BTB) proteins: Critical regulators of development”, *Genesis*, Wiley Online Library, Vol. 54 No. 10, pp. 505–518.
- Chaubey, S., Grover, M. and Tatu, U. (2014), “Endoplasmic reticulum stress triggers gametocytogenesis in the malaria parasite”, *Journal of Biological Chemistry*, ASBMB, Vol. 289 No. 24, pp. 16662–16674.
- Chawira, A.N. and Warhurst, D.C. (1987), “The effect of artemisinin combined with standard antimalarials against chloroquine-sensitive and chloroquine-resistant strains of *Plasmodium falciparum* in vitro.”, *The Journal of Tropical Medicine and Hygiene*, Vol. 90 No. 1, pp. 1–8.
- Chen, J.-J. and London, I.M. (1995), “Regulation of protein synthesis by heme-regulated eIF-2 α kinase”, *Trends in Biochemical Sciences*, Elsevier, Vol. 20 No. 3, pp. 105–108.
- Chen, M.Z., Moily, N.S., Bridgford, J.L., Wood, R.J., Radwan, M., Smith, T.A., Song, Z., *et al.* (2017), “A thiol probe for measuring unfolded protein load and proteostasis in cells”, *Nature Communications*, Nature Publishing Group, Vol. 8 No. 1, pp. 1–11.
- Cheong, H. and Klionsky, D.J. (2008a), “Dual role of Atg1 in regulation of autophagy-specific PAS assembly in *Saccharomyces cerevisiae*”, *Autophagy*, Taylor & Francis, Vol. 4 No. 5, pp. 724–726.
- Cheong, H. and Klionsky, D.J. (2008b), “Biochemical methods to monitor autophagy-related processes in yeast”, *Methods in Enzymology*, Elsevier, Vol. 451, pp. 1–26.

- Cheong, H., Nair, U., Geng, J. and Klionsky, D.J. (2008), “The Atg1 kinase complex is involved in the regulation of protein recruitment to initiate sequestering vesicle formation for nonspecific autophagy in *Saccharomyces cerevisiae*”, *Molecular Biology of the Cell*, Am Soc Cell Biol, Vol. 19 No. 2, pp. 668–681.
- Chew, L.H., Lu, S., Liu, X., Li, F.K., Yu, A.Y., Klionsky, D.J., Dong, M.-Q., *et al.* (2015), “Molecular interactions of the *Saccharomyces cerevisiae* Atg1 complex provide insights into assembly and regulatory mechanisms”, *Autophagy*, Taylor & Francis, Vol. 11 No. 6, pp. 891–905.
- Clark, S.L. (1957), “Cellular differentiation in the kidneys of newborn mice studied with the electron microscope”, *The Journal of Biophysical and Biochemical Cytology*, The Rockefeller University Press, Vol. 3 No. 3, pp. 349–362.
- Clarke, P.G.H. (1990), “Developmental cell death: morphological diversity and multiple mechanisms”, *Anatomy and Embryology*, Springer, Vol. 181 No. 3, pp. 195–213.
- Coronado, L.M., Nadovich, C.T. and Spadafora, C. (2014), “Malarial hemozoin: from target to tool”, *Biochimica et Biophysica Acta (BBA)-General Subjects*, Elsevier, Vol. 1840 No. 6, pp. 2032–2041.
- Cortés, G.T., Wiser, M.F. and Gómez-Alegría, C.J. (2020), “Identification of *Plasmodium falciparum* HSP70-2 as a resident of the *Plasmodium* export compartment”, *Heliyon*, Elsevier, Vol. 6 No. 6, p. e04037.
- Coulson, R.M.R., Hall, N. and Ouzounis, C.A. (2004), “Comparative genomics of transcriptional control in the human malaria parasite *Plasmodium falciparum*”, *Genome Research*, Cold Spring Harbor Lab, Vol. 14 No. 8, pp. 1548–1554.
- Cowman, A.F., Berry, D. and Baum, J. (2012), “The cellular and molecular basis for malaria parasite invasion of the human red blood cell”, *Journal of Cell Biology*, The Rockefeller University Press, Vol. 198 No. 6, pp. 961–971.
- Cowman, A.F. and Crabb, B.S. (2006), “Invasion of red blood cells by malaria parasites”, *Cell*, Elsevier, Vol. 124 No. 4, pp. 755–766.
- Cowman, A.F., Healer, J., Marapana, D. and Marsh, K. (2016), “Malaria: biology and disease”, *Cell*, Elsevier, Vol. 167 No. 3, pp. 610–624.
- Cox, F.E.G. (2010), “History of the discovery of the malaria parasites and their vectors”, *Parasites & Vectors*, BioMed Central, Vol. 3 No. 1, pp. 1–9.
- Crabb, B.S., Rug, M., Gilberger, T.-W., Thompson, J.K., Triglia, T., Maier, A.G. and Cowman, A.F. (2004), “Transfection of the human malaria parasite *Plasmodium falciparum*”, *Parasite Genomics Protocols*, Springer, pp. 263–276.

- Cui, L. and Su, X. (2009), “Discovery, mechanisms of action and combination therapy of artemisinin”, *Expert Review of Anti-Infective Therapy*, Taylor & Francis, Vol. 7 No. 8, pp. 999–1013.
- Cullinan, S.B., Zhang, D., Hannink, M., Arvisais, E., Kaufman, R.J. and Diehl, J.A. (2003), “Nrf2 is a direct PERK substrate and effector of PERK-dependent cell survival”, *Molecular and Cellular Biology*, Am Soc Microbiol, Vol. 23 No. 20, pp. 7198–7209.
- Dagen, M. (2020), “History of malaria and its treatment”, *Antimalarial Agents*, Elsevier, pp. 1–48.
- Dahl, E.L., Shock, J.L., Shenai, B.R., Gut, J., DeRisi, J.L. and Rosenthal, P.J. (2006), “Tetracyclines specifically target the apicoplast of the malaria parasite *Plasmodium falciparum*”, *Antimicrobial Agents and Chemotherapy*, Am Soc Microbiol, Vol. 50 No. 9, pp. 3124–3131.
- Dall’Armi, C., Devereaux, K.A. and Di Paolo, G. (2013), “The role of lipids in the control of autophagy”, *Current Biology*, Elsevier, Vol. 23 No. 1, pp. R33–R45.
- Das, A., Anvikar, A.R., Cator, L.J., Dhiman, R.C., Eapen, A., Mishra, N., Nagpal, B.N., *et al.* (2012), “Malaria in India: the center for the study of complex malaria in India”, *Acta Tropica*, Elsevier, Vol. 121 No. 3, pp. 267–273.
- Dasaradhi, P.V.N., Korde, R., Thompson, J.K., Tanwar, C., Nag, T.C., Chauhan, V.S., Cowman, A.F., *et al.* (2007), “Food vacuole targeting and trafficking of falcipain-2, an important cysteine protease of human malaria parasite *Plasmodium falciparum*”, *Molecular and Biochemical Parasitology*, Elsevier, Vol. 156 No. 1, pp. 12–23.
- Datta, G., Hossain, M.E., Asad, M., Rathore, S. and Mohammed, A. (2017), “*Plasmodium falciparum* OTU-like cysteine protease (PfOTU) is essential for apicoplast homeostasis and associates with noncanonical role of Atg8”, *Cellular Microbiology*, Wiley Online Library, Vol. 19 No. 9, p. e12748.
- Delorme-Axford, E., Guimaraes, R.S., Reggiori, F. and Klionsky, D.J. (2015), “The yeast *Saccharomyces cerevisiae*: an overview of methods to study autophagy progression”, *Methods*, Elsevier, Vol. 75, pp. 3–12.
- Demas, A.R., Sharma, A.I., Wong, W., Early, A.M., Redmond, S., Bopp, S., Neafsey, D.E., *et al.* (2018), “Mutations in *Plasmodium falciparum* actin-binding protein coronin confer reduced artemisinin susceptibility”, *Proceedings of the National Academy of Sciences*, National Acad Sciences, Vol. 115 No. 50, pp. 12799–12804.

- Denecke, J., de Rycke, R. and Botterman, J. (1992), “Plant and mammalian sorting signals for protein retention in the endoplasmic reticulum contain a conserved epitope.”, *The EMBO Journal*, Vol. 11 No. 6, pp. 2345–2355.
- Desfougères, Y., Neumann, H. and Mayer, A. (2016), “Organelle size control–increasing vacuole content activates SNAREs to augment organelle volume through homotypic fusion”, *Journal of Cell Science*, The Company of Biologists Ltd, Vol. 129 No. 14, pp. 2817–2828.
- Devereaux, K., Dall’Armi, C., Alcazar-Roman, A., Ogasawara, Y., Zhou, X., Wang, F., Yamamoto, A., *et al.* (2013), “Regulation of mammalian autophagy by class II and III PI 3-kinases through PI3P synthesis”, *PloS One*, Public Library of Science San Francisco, USA, Vol. 8 No. 10, p. e76405.
- Dhanao, B.S., Cogliati, T., Satish, A.G., Bruford, E.A. and Friedman, J.S. (2013), “Update on the Kelch-like (KLHL) gene family”, *Human Genomics*, BioMed Central, Vol. 7 No. 1, pp. 1–7.
- Dogovski, C., Xie, S.C., Burgio, G., Bridgford, J., Mok, S., McCaw, J.M., Chotivanich, K., *et al.* (2015), “Targeting the cell stress response of *Plasmodium falciparum* to overcome artemisinin resistance”, *PLoS Biology*, Public Library of Science San Francisco, CA USA, Vol. 13 No. 4, p. e1002132.
- Dondorp, A.M., Nosten, F., Yi, P., Das, D., Phyto, A.P., Tarning, J., Lwin, K.M., *et al.* (2009), “Artemisinin resistance in *Plasmodium falciparum* malaria”, *New England Journal of Medicine*, Mass Medical Soc, Vol. 361 No. 5, pp. 455–467.
- van Dooren, G.G., Marti, M., Tonkin, C.J., Stimmler, L.M., Cowman, A.F. and McFadden, G.I. (2005), “Development of the endoplasmic reticulum, mitochondrion and apicoplast during the asexual life cycle of *Plasmodium falciparum*”, *Molecular Microbiology*, Wiley Online Library, Vol. 57 No. 2, pp. 405–419.
- Dove, S.K., Piper, R.C., McEwen, R.K., Yu, J.W., King, M.C., Hughes, D.C., Thuring, J., *et al.* (2004), “Svp1p defines a family of phosphatidylinositol 3, 5-bisphosphate effectors”, *The EMBO Journal*, John Wiley & Sons, Ltd Chichester, UK, Vol. 23 No. 9, pp. 1922–1933.
- Duszenko, M., Ginger, M.L., Brennand, A., Gualdrón-López, M., Colombo, M.I., Coombs, G.H., Coppens, I., *et al.* (2011), “Autophagy in protists”, *Autophagy*, Taylor & Francis, Vol. 7 No. 2, pp. 127–158.

- De Duve, C., Pressman, B.C., Gianetto, R., Wattiaux, R. and Appelmans, F. (1955), “Tissue fractionation studies. 6. Intracellular distribution patterns of enzymes in rat-liver tissue”, *Biochemical Journal*, Portland Press Ltd, Vol. 60 No. 4, p. 604.
- De Duve, C., De Reuck, A.V.S. and Cameron, M.P. (1963), *Ciba Foundation Symposium: Lysosomes*, Little, Brown.
- Dwivedi, A., Reynes, C., Kuehn, A., Roche, D.B., Khim, N., Hebrard, M., Milanese, S., *et al.* (2017), “Functional analysis of *Plasmodium falciparum* subpopulations associated with artemisinin resistance in Cambodia”, *Malaria Journal*, BioMed Central, Vol. 16 No. 1, pp. 1–17.
- Eckstein-Ludwig, U., Webb, R.J., van Goethem, I.D.A., East, J.M., Lee, A.G., Kimura, M., O’Neill, P.M., *et al.* (2003), “Artemisinins target the SERCA of *Plasmodium falciparum*”, *Nature*, Vol. 424 No. 6951, pp. 957–961.
- Ellgaard, L., Molinari, M. and Helenius, A. (1999), “Setting the standards: quality control in the secretory pathway”, *Science*, American Association for the Advancement of Science, Vol. 286 No. 5446, pp. 1882–1888.
- Elliott, D.A., McIntosh, M.T., Hosgood, H.D., Chen, S., Zhang, G., Baevova, P. and Joiner, K.A. (2008), “Four distinct pathways of hemoglobin uptake in the malaria parasite *Plasmodium falciparum*”, *Proceedings of the National Academy of Sciences*, National Acad Sciences, Vol. 105 No. 7, pp. 2463–2468.
- Engelberg, D. (2004), “Stress-activated protein kinases—tumor suppressors or tumor initiators?”, *Seminars in Cancer Biology*, Vol. 14, Elsevier, pp. 271–282.
- Engelbrecht, D. and Coetzer, T.L. (2013), “Turning up the heat: heat stress induces markers of programmed cell death in *Plasmodium falciparum* in vitro”, *Cell Death & Disease*, Nature Publishing Group, Vol. 4 No. 12, pp. e971–e971.
- Fairhurst, R.M. and Dondorp, A.M. (2016), “Artemisinin-resistant *Plasmodium falciparum* malaria”, *Microbiology Spectrum*, Am Soc Microbiol, Vol. 4 No. 3, pp. 3–4.
- Farré, J.-C. and Subramani, S. (2016), “Mechanistic insights into selective autophagy pathways: lessons from yeast”, *Nature Reviews Molecular Cell Biology*, Nature Publishing Group, Vol. 17 No. 9, pp. 537–552.
- Feng, Y., He, D., Yao, Z. and Klionsky, D.J. (2014), “The machinery of macroautophagy”, *Cell Research*, Nature Publishing Group, Vol. 24 No. 1, pp. 24–41.
- Fennell, C., Babbitt, S., Russo, I., Wilkes, J., Ranford-Cartwright, L., Goldberg, D.E. and Doerig, C. (2009), “PfeIK1, a eukaryotic initiation factor 2 α kinase of the human

- malaria parasite *Plasmodium falciparum*, regulates stress-response to amino-acid starvation”, *Malaria Journal*, Springer, Vol. 8 No. 1, pp. 1–15.
- Fidock, D.A. and Wellems, T.E. (1997), “Transformation with human dihydrofolate reductase renders malaria parasites insensitive to WR99210 but does not affect the intrinsic activity of proguanil”, *Proceedings of the National Academy of Sciences*, National Acad Sciences, Vol. 94 No. 20, pp. 10931–10936.
- Filomeni, G., De Zio, D. and Cecconi, F. (2015), “Oxidative stress and autophagy: the clash between damage and metabolic needs”, *Cell Death & Differentiation*, Nature Publishing Group, Vol. 22 No. 3, pp. 377–388.
- Fumagalli, F., Noack, J., Bergmann, T.J., Cebollero, E., Pisoni, G.B., Fasana, E., Fregno, I., *et al.* (2016), “Translocon component Sec62 acts in endoplasmic reticulum turnover during stress recovery”, *Nature Cell Biology*, Nature Publishing Group, Vol. 18 No. 11, pp. 1173–1184.
- Furukawa, M., He, Y.J., Borchers, C. and Xiong, Y. (2003), “Targeting of protein ubiquitination by BTB–Cullin 3–Roc1 ubiquitin ligases”, *Nature Cell Biology*, Nature Publishing Group, Vol. 5 No. 11, pp. 1001–1007.
- Gardner, M.J., Hall, N., Fung, E., White, O., Berriman, M., Hyman, R.W., Carlton, J.M., *et al.* (2002), “Genome sequence of the human malaria parasite *Plasmodium falciparum*”, *Nature*, Nature Publishing Group, Vol. 419 No. 6906, pp. 498–511.
- Gelband, H., Panosian, C.B. and Arrow, K.J. (2004), “Saving lives, buying time: economics of malaria drugs in an age of resistance”, National Academies Press.
- Geng, J. and Klionsky, D.J. (2008), “The Atg8 and Atg12 ubiquitin-like conjugation systems in macroautophagy”, *EMBO Reports*, John Wiley & Sons, Ltd Chichester, UK, Vol. 9 No. 9, pp. 859–864.
- GILLOOLY, D.J., SIMONSEN, A. and STENMARK, H. (2001), “Cellular functions of phosphatidylinositol 3-phosphate and FYVE domain proteins”, *Biochemical Journal*, Portland Press Ltd., Vol. 355 No. 2, pp. 249–258.
- Gnädig, N.F., Stokes, B.H., Edwards, R.L., Kalantarov, G.F., Heimsch, K.C., Kuderjavy, M., Crane, A., *et al.* (2020), “Insights into the intracellular localization, protein associations and artemisinin resistance properties of *Plasmodium falciparum* K13”, *PLoS Pathogens*, Public Library of Science, Vol. 16 No. 4, p. e1008482.
- Goldberg, D.E. and Zimmerberg, J. (2020), “Hardly vacuous: The parasitophorous vacuolar membrane of malaria parasites”, *Trends in Parasitology*, Elsevier, Vol. 36 No. 2, pp. 138–146.

- Goldshmidt, H., Matas, D., Kabi, A., Carmi, S., Hope, R. and Michaeli, S. (2010), “Persistent ER stress induces the spliced leader RNA silencing pathway (SLS), leading to programmed cell death in *Trypanosoma brucei*”, *PLoS Pathogens*, Public Library of Science San Francisco, USA, Vol. 6 No. 1, p. e1000731.
- Gosline, S.J.C., Nascimento, M., McCall, L.-I., Zilberstein, D., Thomas, D.Y., Matlashewski, G. and Hallett, M. (2011), “Intracellular eukaryotic parasites have a distinct unfolded protein response”, *PLoS One*, Public Library of Science San Francisco, USA, Vol. 6 No. 4, p. e19118.
- Grumati, P., Dikic, I. and Stolz, A. (2018), “ER-phagy at a glance”, *Journal of Cell Science*, The Company of Biologists Ltd, Vol. 131 No. 17, p. jcs217364.
- Hain, A.U.P., Bartee, D., Sanders, N.G., Miller, A.S., Sullivan, D.J., Levitskaya, J., Meyers, C.F., *et al.* (2014), “Identification of an Atg8-Atg3 protein–protein interaction inhibitor from the medicines for Malaria Venture Malaria Box active in blood and liver stage *Plasmodium falciparum* parasites”, *Journal of Medicinal Chemistry*, ACS Publications, Vol. 57 No. 11, pp. 4521–4531.
- Hain, A.U.P. and Bosch, J. (2013), “Autophagy in *Plasmodium*, a multifunctional pathway?”, *Computational and Structural Biotechnology Journal*, Elsevier, Vol. 8 No. 11, p. e201308002.
- Hain, A.U.P., Miller, A.S., Levitskaya, J. and Bosch, J. (2016), “Virtual screening and experimental validation identify novel inhibitors of the *Plasmodium falciparum* Atg8-Atg3 protein-protein interaction”, *ChemMedChem*, John Wiley and Sons Ltd, Vol. 11 No. 8, pp. 900–910.
- Hain, A.U.P., Weltzer, R.R., Hammond, H., Jayabalasingham, B., Dinglasan, R.R., Graham, D.R.M., Colquhoun, D.R., *et al.* (2012), “Structural characterization and inhibition of the *Plasmodium* Atg8–Atg3 interaction”, *Journal of Structural Biology*, Elsevier, Vol. 180 No. 3, pp. 551–562.
- Haldar, K., Bhattacharjee, S. and Safeukui, I. (2018), “Drug resistance in *Plasmodium*”, *Nature Reviews Microbiology*, Nature Publishing Group, Vol. 16 No. 3, p. 156.
- Hallée, S., Thériault, C., Gagnon, D., Kehrer, J., Frischknecht, F., Mair, G.R. and Richard, D. (2018), “Identification of a Golgi apparatus protein complex important for the asexual erythrocytic cycle of the malaria parasite *Plasmodium falciparum*”, *Cellular Microbiology*, Wiley Online Library, Vol. 20 No. 8, p. e12843.
- Harbut, M.B., Patel, B.A., Yeung, B.K.S., McNamara, C.W., Bright, A.T., Ballard, J., Supek, F., *et al.* (2012), “Targeting the ERAD pathway via inhibition of signal peptide

- peptidase for antiparasitic therapeutic design”, *Proceedings of the National Academy of Sciences*, National Acad Sciences, Vol. 109 No. 52, pp. 21486–21491.
- Harding, H.P., Zhang, Y. and Ron, D. (1999), “Protein translation and folding are coupled by an endoplasmic-reticulum-resident kinase”, *Nature*, Nature Publishing Group, Vol. 397 No. 6716, pp. 271–274.
- Harding, H.P., Zhang, Y., Zeng, H., Novoa, I., Lu, P.D., Calton, M., Sadri, N., *et al.* (2003), “An integrated stress response regulates amino acid metabolism and resistance to oxidative stress”, *Molecular Cell*, Elsevier, Vol. 11 No. 3, pp. 619–633.
- Harding, T.M., Morano, K.A., Scott, S. V and Klionsky, D.J. (1995), “Isolation and characterization of yeast mutants in the cytoplasm to vacuole protein targeting pathway.”, *The Journal of Cell Biology*, Vol. 131 No. 3, pp. 591–602.
- Hempelmann, E. and Krafts, K. (2013), “Bad air, amulets and mosquitoes: 2,000 years of changing perspectives on malaria”, *Malaria Journal*, Springer, Vol. 12 No. 1, pp. 1–14.
- Henrici, R.C., van Schalkwyk, D.A. and Sutherland, C.J. (2020), “Modification of pfap2 μ and pfubp1 markedly reduces ring-stage susceptibility of Plasmodium falciparum to artemisinin in vitro”, *Antimicrobial Agents and Chemotherapy*, American Society for Microbiology (ASM), Vol. 64 No. 1.
- Heppner Jr, D.G., Kester, K.E., Ockenhouse, C.F., Tornieporth, N., Ofori, O., Lyon, J.A., Stewart, V.A., *et al.* (2005), “Towards an RTS, S-based, multi-stage, multi-antigen vaccine against falciparum malaria: progress at the Walter Reed Army Institute of Research”, *Vaccine*, Elsevier, Vol. 23 No. 17–18, pp. 2243–2250.
- Hiller, N.L., Bhattacharjee, S., van Ooij, C., Liolios, K., Harrison, T., Lopez-Estrano, C. and Haldar, K. (2004), “A host-targeting signal in virulence proteins reveals a secretome in malarial infection”, *Science*, American Association for the Advancement of Science, Vol. 306 No. 5703, pp. 1934–1937.
- Ho, C.-M., Beck, J.R., Lai, M., Cui, Y., Goldberg, D.E., Egea, P.F. and Zhou, Z.H. (2018), “Malaria parasite translocon structure and mechanism of effector export”, *Nature*, Nature Publishing Group, Vol. 561 No. 7721, pp. 70–75.
- Holcik, M. and Sonenberg, N. (2005), “Translational control in stress and apoptosis”, *Nature Reviews Molecular Cell Biology*, Nature Publishing Group, Vol. 6 No. 4, pp. 318–327.

- Høyer-Hansen, M. and Jäättelä, M. (2007), “Connecting endoplasmic reticulum stress to autophagy by unfolded protein response and calcium”, *Cell Death & Differentiation*, Nature Publishing Group, Vol. 14 No. 9, pp. 1576–1582.
- Imwong, M., Suwannasin, K., Kunasol, C., Sutawong, K., Mayxay, M., Rekol, H., Smithuis, F.M., *et al.* (2017), “The spread of artemisinin-resistant *Plasmodium falciparum* in the Greater Mekong subregion: a molecular epidemiology observational study”, *The Lancet Infectious Diseases*, Elsevier, Vol. 17 No. 5, pp. 491–497.
- Ismail, H.M., Barton, V.E., Panchana, M., Charoensutthivarakul, S., Biagini, G.A., Ward, S.A. and O’Neill, P.M. (2016), “A click chemistry-based proteomic approach reveals that 1, 2, 4-trioxolane and artemisinin antimalarials share a common protein alkylation profile”, *Angewandte Chemie International Edition*, Wiley Online Library, Vol. 55 No. 22, pp. 6401–6405.
- Jayabalasingham, B., Bano, N. and Coppens, I. (2010), “Metamorphosis of the malaria parasite in the liver is associated with organelle clearance”, *Cell Research*, Nature Publishing Group, Vol. 20 No. 9, pp. 1043–1059.
- Jogdand, P.S., Singh, S.K., Christiansen, M., Dziegiel, M.H., Singh, S. and Theisen, M. (2012), “Flow cytometric readout based on Mitotracker Red CMXRos staining of live asexual blood stage malarial parasites reliably assesses antibody dependent cellular inhibition”, *Malaria Journal*, Springer, Vol. 11 No. 1, pp. 1–11.
- Jonscher, E., Flemming, S., Schmitt, M., Sabitzki, R., Reichard, N., Birnbaum, J., Bergmann, B., *et al.* (2019), “PfVPS45 is required for host cell cytosol uptake by malaria blood stage parasites”, *Cell Host & Microbe*, Elsevier, Vol. 25 No. 1, pp. 166–173.
- Joo, J.H., Wang, B., Frankel, E., Ge, L., Xu, L., Iyengar, R., Li-Harms, X., *et al.* (2016), “The noncanonical role of ULK/ATG1 in ER-to-Golgi trafficking is essential for cellular homeostasis”, *Molecular Cell*, Elsevier, Vol. 62 No. 4, pp. 491–506.
- Joy, S., Thirunavukkarasu, L., Agrawal, P., Singh, A., Sagar, B.K.C., Manjithaya, R. and Surolia, N. (2018), “Basal and starvation-induced autophagy mediates parasite survival during intraerythrocytic stages of *Plasmodium falciparum*”, *Cell Death Discovery*, Nature Publishing Group, Vol. 4 No. 1, pp. 1–13.
- Joyce, B.R., Tampaki, Z., Kim, K., Wek, R.C. and Sullivan Jr, W.J. (2013), “The unfolded protein response in the protozoan parasite *Toxoplasma gondii* features translational and transcriptional control”, *Eukaryotic Cell*, Am Soc Microbiol, Vol. 12 No. 7, pp. 979–989.

- Kabeya, Y., Kamada, Y., Baba, M., Takikawa, H., Sasaki, M. and Ohsumi, Y. (2005), “Atg17 functions in cooperation with Atg1 and Atg13 in yeast autophagy”, *Molecular Biology of the Cell*, Am Soc Cell Biol, Vol. 16 No. 5, pp. 2544–2553.
- Kamada, Y., Funakoshi, T., Shintani, T., Nagano, K., Ohsumi, M. and Ohsumi, Y. (2000), “Tor-mediated induction of autophagy via an Apg1 protein kinase complex”, *Journal of Cell Biology*, The Rockefeller University Press, Vol. 150 No. 6, pp. 1507–1513.
- Kirkin, V. (2020), “History of the selective autophagy research: how did it begin and where does it stand today?”, *Journal of Molecular Biology*, Elsevier, Vol. 432 No. 1, pp. 3–27.
- Kitamura, K., Kishi-Itakura, C., Tsuboi, T., Sato, S., Kita, K., Ohta, N. and Mizushima, N. (2012), “Autophagy-related Atg8 localizes to the apicoplast of the human malaria parasite *Plasmodium falciparum*”, Public Library of Science San Francisco, USA.
- Klionsky, D.J. and Codogno, P. (2013), “The mechanism and physiological function of macroautophagy”, *Journal of Innate Immunity*, Karger Publishers, Vol. 5 No. 5, pp. 427–433.
- Klonis, N., Xie, S.C., McCaw, J.M., Crespo-Ortiz, M.P., Zaloumis, S.G., Simpson, J.A. and Tilley, L. (2013), “Altered temporal response of malaria parasites determines differential sensitivity to artemisinin”, *Proceedings of the National Academy of Sciences*, National Acad Sciences, Vol. 110 No. 13, pp. 5157–5162.
- Kruger, N.J. (2009), “The Bradford method for protein quantitation”, *The Protein Protocols Handbook*, Springer, pp. 17–24.
- Kumar, S., Bhardwaj, T.R., Prasad, D.N. and Singh, R.K. (2018), “Drug targets for resistant malaria: historic to future perspectives”, *Biomedicine & Pharmacotherapy*, Elsevier, Vol. 104, pp. 8–27.
- Lambros, C. and Vanderberg, J.P. (1979), “Synchronization of *Plasmodium falciparum* erythrocytic stages in culture”, *The Journal of Parasitology*, JSTOR, pp. 418–420.
- Lazarus, M.B., Novotny, C.J. and Shokat, K.M. (2015), “Structure of the human autophagy initiating kinase ULK1 in complex with potent inhibitors”, *ACS Chemical Biology*, ACS Publications, Vol. 10 No. 1, pp. 257–261.
- Lee, A.-H., Iwakoshi, N.N. and Glimcher, L.H. (2003), “XBP-1 regulates a subset of endoplasmic reticulum resident chaperone genes in the unfolded protein response”, *Molecular and Cellular Biology*, Am Soc Microbiol, Vol. 23 No. 21, pp. 7448–7459.
- Lee, A.S. (2005), “The ER chaperone and signaling regulator GRP78/BiP as a monitor of endoplasmic reticulum stress”, *Methods*, Elsevier, Vol. 35 No. 4, pp. 373–381.

- Lee, M.C.S., Moura, P.A., Miller, E.A. and Fidock, D.A. (2008), “Plasmodium falciparum Sec24 marks transitional ER that exports a model cargo via a diacidic motif”, *Molecular Microbiology*, Wiley Online Library, Vol. 68 No. 6, pp. 1535–1546.
- Levine, B. and Kroemer, G. (2008), “Autophagy in the pathogenesis of disease”, *Cell*, Elsevier, Vol. 132 No. 1, pp. 27–42.
- Li, S.C. and Kane, P.M. (2009), “The yeast lysosome-like vacuole: endpoint and crossroads”, *Biochimica et Biophysica Acta (BBA)-Molecular Cell Research*, Elsevier, Vol. 1793 No. 4, pp. 650–663.
- Lin, M.G. and Hurley, J.H. (2016), “Structure and function of the ULK1 complex in autophagy”, *Current Opinion in Cell Biology*, Elsevier, Vol. 39, pp. 61–68.
- Liu, J., Istvan, E.S., Gluzman, I.Y., Gross, J. and Goldberg, D.E. (2006), “Plasmodium falciparum ensures its amino acid supply with multiple acquisition pathways and redundant proteolytic enzyme systems”, *Proceedings of the National Academy of Sciences*, National Acad Sciences, Vol. 103 No. 23, pp. 8840–8845.
- Livak, K.J. and Schmittgen, T.D. (2001), “Analysis of relative gene expression data using real-time quantitative PCR and the 2⁻ΔΔCT method”, *Methods*, Elsevier, Vol. 25 No. 4, pp. 402–408.
- Lu, F., He, X.-L., Richard, C. and Cao, J. (2019), “A brief history of artemisinin: Modes of action and mechanisms of resistance”, *Chin J Nat Med*, Vol. 17 No. 5, pp. 331–336.
- Lynch-Day, M.A. and Klionsky, D.J. (2010), “The Cvt pathway as a model for selective autophagy”, *FEBS Letters*, Elsevier, Vol. 584 No. 7, pp. 1359–1366.
- Malhotra, J.D. and Kaufman, R.J. (2007), “The endoplasmic reticulum and the unfolded protein response”, *Seminars in Cell & Developmental Biology*, Vol. 18, Elsevier, pp. 716–731.
- Mamidi, A.S., Ray, A. and Surolia, N. (2019), “Structural analysis of PfSec62-Autophagy Interacting Motifs (AIM) and PfAtg8 interactions for its implications in recover- phagy in Plasmodium falciparum”, *Frontiers in Bioengineering and Biotechnology*, Frontiers, Vol. 7, p. 240.
- Marciniak, S.J., Yun, C.Y., Oyadomari, S., Novoa, I., Zhang, Y., Jungreis, R., Nagata, K., *et al.* (2004), “CHOP induces death by promoting protein synthesis and oxidation in the stressed endoplasmic reticulum”, *Genes & Development*, Cold Spring Harbor Lab, Vol. 18 No. 24, pp. 3066–3077.

- Marti, M., Good, R.T., Rug, M., Knuepfer, E. and Cowman, A.F. (2004), “Targeting malaria virulence and remodeling proteins to the host erythrocyte”, *Science*, American Association for the Advancement of Science, Vol. 306 No. 5703, pp. 1930–1933.
- Massey, A., Kiffin, R. and Cuervo, A.M. (2004), “Pathophysiology of chaperone-mediated autophagy”, *The International Journal of Biochemistry & Cell Biology*, Elsevier, Vol. 36 No. 12, pp. 2420–2434.
- Mbengue, A., Bhattacharjee, S., Pandharkar, T., Liu, H., Estiu, G., Stahelin, R. V, Rizk, S.S., *et al.* (2015), “A molecular mechanism of artemisinin resistance in *Plasmodium falciparum* malaria”, *Nature*, Nature Publishing Group, Vol. 520 No. 7549, pp. 683–687.
- Meister, S., Plouffe, D.M., Kuhen, K.L., Bonamy, G.M.C., Wu, T., Barnes, S.W., Bopp, S.E., *et al.* (2011), “Imaging of *Plasmodium* liver stages to drive next-generation antimalarial drug discovery”, *Science*, American Association for the Advancement of Science, Vol. 334 No. 6061, pp. 1372–1377.
- Ménard, D., Khim, N., Beghain, J., Adegnika, A.A., Shafiul-Alam, M., Amodu, O., Rahim-Awab, G., *et al.* (2016), “A worldwide map of *Plasmodium falciparum* K13-propeller polymorphisms”, *New England Journal of Medicine*, Mass Medical Soc, Vol. 374 No. 25, pp. 2453–2464.
- Mijaljica, D., Prescott, M. and Devenish, R.J. (2011), “Microautophagy in mammalian cells: revisiting a 40-year-old conundrum”, *Autophagy*, Taylor & Francis, Vol. 7 No. 7, pp. 673–682.
- Mijaljica, D., Prescott, M., Klionsky, D.J. and Devenish, R.J. (2007), “Autophagy and vacuole homeostasis: a case for self-degradation?”, *Autophagy*, Taylor & Francis, Vol. 3 No. 5, pp. 417–421.
- Milani, K.J., Schneider, T.G. and Taraschi, T.F. (2015), “Defining the morphology and mechanism of the hemoglobin transport pathway in *Plasmodium falciparum*-infected erythrocytes”, *Eukaryotic Cell*, Am Soc Microbiol, Vol. 14 No. 4, pp. 415–426.
- Miotto, O., Amato, R., Ashley, E.A., MacInnis, B., Almagro-Garcia, J., Amaratunga, C., Lim, P., *et al.* (2015), “Genetic architecture of artemisinin-resistant *Plasmodium falciparum*”, *Nature Genetics*, Nature Publishing Group, Vol. 47 No. 3, pp. 226–234.
- Mishra, P., Dauphinee, A.N., Ward, C., Sarkar, S., Gunawardena, A.H. and Manjithaya, R. (2017), “Discovery of pan autophagy inhibitors through a high-throughput screen highlights macroautophagy as an evolutionarily conserved process across 3 eukaryotic kingdoms”, *Autophagy*, Taylor & Francis, Vol. 13 No. 9, pp. 1556–1572.

- Mita, T., Venkatesan, M., Ohashi, J., Culleton, R., Takahashi, N., Tsukahara, T., Ndounga, M., *et al.* (2011), “Limited geographical origin and global spread of sulfadoxine-resistant dhps alleles in Plasmodium falciparum populations”, *The Journal of Infectious Diseases*, Infectious Diseases Society of America, Vol. 204 No. 12, pp. 1980–1988.
- Mitchell, G.H., Thomas, A.W., Margos, G., Dluzewski, A.R. and Bannister, L.H. (2004), “Apical membrane antigen 1, a major malaria vaccine candidate, mediates the close attachment of invasive merozoites to host red blood cells”, *Infection and Immunity*, Am Soc Microbiol, Vol. 72 No. 1, pp. 154–158.
- Mizushima, N. (2007), “Autophagy: process and function”, *Genes & Development*, Cold Spring Harbor Lab, Vol. 21 No. 22, pp. 2861–2873.
- Mizushima, N. (2010), “The role of the Atg1/ULK1 complex in autophagy regulation”, *Current Opinion in Cell Biology*, Elsevier, Vol. 22 No. 2, pp. 132–139.
- Mizushima, N. (2018), “A brief history of autophagy from cell biology to physiology and disease”, *Nature Cell Biology*, Nature Publishing Group, Vol. 20 No. 5, pp. 521–527.
- Mizushima, N., Yoshimori, T. and Levine, B. (2010), “Methods in mammalian autophagy research”, *Cell*, Elsevier, Vol. 140 No. 3, pp. 313–326.
- Mok, S., Ashley, E.A., Ferreira, P.E., Zhu, L., Lin, Z., Yeo, T., Chotivanich, K., *et al.* (2015), “Population transcriptomics of human malaria parasites reveals the mechanism of artemisinin resistance”, *Science*, American Association for the Advancement of Science, Vol. 347 No. 6220, pp. 431–435.
- Mueller, P.P. and Hinnebusch, A.G. (1986), “Multiple upstream AUG codons mediate translational control of GCN4”, *Cell*, Elsevier, Vol. 45 No. 2, pp. 201–207.
- Murtha-Riel, P., Davies, M. V., Scherer, B.J., Choi, S.Y., Hershey, J.W. and Kaufman, R.J. (1993), “Expression of a phosphorylation-resistant eukaryotic initiation factor 2 alpha-subunit mitigates heat shock inhibition of protein synthesis”, *Journal of Biological Chemistry*, Elsevier, Vol. 268 No. 17, pp. 12946–12951.
- Nagaraj, V.A., Sundaram, B., Varadarajan, N.M., Subramani, P.A., Kalappa, D.M., Ghosh, S.K. and Padmanaban, G. (2013), “Malaria parasite-synthesized heme is essential in the mosquito and liver stages and complements host heme in the blood stages of infection”, *PLoS Pathogens*, Public Library of Science San Francisco, USA, Vol. 9 No. 8, p. e1003522.
- Nair, S., Li, X., Arya, G.A., McDew-White, M., Ferrari, M., Nosten, F. and Anderson, T.J.C. (2018), “Fitness costs and the rapid spread of kelch13-C580Y substitutions

- conferring artemisinin resistance”, *Antimicrobial Agents and Chemotherapy*, American Society for Microbiology (ASM), Vol. 62 No. 9.
- Nakatogawa, H., Ohbayashi, S., Sakoh-Nakatogawa, M., Kakuta, S., Suzuki, S.W., Kirisako, H., Kondo-Kakuta, C., *et al.* (2012), “The autophagy-related protein kinase Atg1 interacts with the ubiquitin-like protein Atg8 via the Atg8 family interacting motif to facilitate autophagosome formation”, *Journal of Biological Chemistry*, ASBMB, Vol. 287 No. 34, pp. 28503–28507.
- Navale, R., Allanki, A.D. and Sijwali, P.S. (2014), “Characterization of the autophagy marker protein Atg8 reveals atypical features of autophagy in *Plasmodium falciparum*”, *PLoS One*, Public Library of Science San Francisco, USA, Vol. 9 No. 11, p. e113220.
- “NCVBDC, 2021”. (n.d.), available at: <https://nvcvdc.gov.in/index1.php?lang=1&level=1&sublinkid=5784&lid=3689>.
- Nie, T., Yang, S., Ma, H., Zhang, L., Lu, F., Tao, K., Wang, R., *et al.* (2016), “Regulation of ER stress-induced autophagy by GSK3 β -TIP60-ULK1 pathway”, *Cell Death & Disease*, Nature Publishing Group, Vol. 7 No. 12, pp. e2563–e2563.
- Nishimura, T. and Tooze, S.A. (2020), “Emerging roles of ATG proteins and membrane lipids in autophagosome formation”, *Cell Discovery*, Nature Publishing Group, Vol. 6 No. 1, pp. 1–18.
- Noedl, H., Se, Y., Schaefer, K., Smith, B.L., Socheat, D. and Fukuda, M.M. (2008), “Evidence of artemisinin-resistant malaria in western Cambodia”, *New England Journal of Medicine*, Mass Medical Soc, Vol. 359 No. 24, pp. 2619–2620.
- Novikoff, A.B. (1959), “The proximal tubule cell in experimental hydronephrosis”, *The Journal of Cell Biology*, Rockefeller University Press, Vol. 6 No. 1, pp. 136–138.
- Ogata, M., Hino, S., Saito, A., Morikawa, K., Kondo, S., Kanemoto, S., Murakami, T., *et al.* (2006), “Autophagy is activated for cell survival after endoplasmic Reticulum Stress”, *Molecular and Cellular Biology*, Am Soc Microbiol, Vol. 26 No. 24, pp. 9220–9231.
- Ohsumi, Y. (2014), “Historical landmarks of autophagy research”, *Cell Research*, Nature Publishing Group, Vol. 24 No. 1, pp. 9–23.
- O’neill, P.M., Barton, V.E. and Ward, S.A. (2010), “The molecular mechanism of action of artemisinin—the debate continues”, *Molecules*, Molecular Diversity Preservation International, Vol. 15 No. 3, pp. 1705–1721.

- Organization, W.H. (2016), *Artemisinin and Artemisinin-Based Combination Therapy Resistance: Status Report*, World Health Organization.
- Organization, W.H. (2018), *First Malaria Vaccine in Africa: A Potential New Tool for Child Health and Improved Malaria Control*, JSTOR.
- Organization, W.H. (2020), “World malaria report 2020: 20 years of global progress and challenges”, World Health Organization.
- Organization, W.H. (2021a), *WHO Guidelines for Malaria, 16 February 2021*, World Health Organization.
- Organization, W.H. (2021b), *World Malaria Report 2021*, World Health Organization.
- Pang, Y., Yamamoto, H., Sakamoto, H., Oku, M., Mutungi, J.K., Sahani, M.H., Kurikawa, Y., *et al.* (2019), “Evolution from covalent conjugation to non-covalent interaction in the ubiquitin-like ATG12 system”, *Nature Structural & Molecular Biology*, Nature Publishing Group, Vol. 26 No. 4, pp. 289–296.
- Parzych, K.R. and Klionsky, D.J. (2014), “An overview of autophagy: morphology, mechanism, and regulation”, *Antioxidants & Redox Signaling*, Mary Ann Liebert, Inc. 140 Huguenot Street, 3rd Floor New Rochelle, NY 10801 USA, Vol. 20 No. 3, pp. 460–473.
- Percário, S., Moreira, D.R., Gomes, B.A.Q., Ferreira, M.E.S., Gonçalves, A.C.M., Laurindo, P.S.O.C., Vilhena, T.C., *et al.* (2012), “Oxidative stress in malaria”, *International Journal of Molecular Sciences*, Multidisciplinary Digital Publishing Institute, Vol. 13 No. 12, pp. 16346–16372.
- Perkins, S.L. (2014), “Malaria’s many mates: past, present, and future of the systematics of the order Haemosporida”, *Journal of Parasitology*, American Society of Parasitologists, Vol. 100 No. 1, pp. 11–25.
- Petherick, K.J., Conway, O.J.L., Mpamhanga, C., Osborne, S.A., Kamal, A., Saxty, B. and Ganley, I.G. (2015), “Pharmacological inhibition of ULK1 kinase blocks mammalian target of rapamycin (mTOR)-dependent autophagy”, *Journal of Biological Chemistry*, Elsevier, Vol. 290 No. 18, pp. 11376–11383.
- Phillips, M.A., Burrows, J.N. and Manyando, C. (2017), “Nature reviews disease primers”, *Malaria*, Vol. 3, p. 17050.
- Phillips, M.A., Burrows, J.N., Manyando, C., van Huijsduijnen, R.H., Van Voorhis, W.C. and Wells, T.N.C. (2017), “Malaria”, *Nature Reviews Disease Primers*, Vol. 3 No. 1, p. 17050.

- Phyo, A.P., Ashley, E.A., Anderson, T.J.C., Bozdech, Z., Carrara, V.I., Sriprawat, K., Nair, S., *et al.* (2016), “Declining efficacy of artemisinin combination therapy against *P. falciparum* malaria on the Thai–Myanmar border (2003–2013): the role of parasite genetic factors”, *Clinical Infectious Diseases*, Oxford University Press, Vol. 63 No. 6, pp. 784–791.
- Van Der Pluijm, R.W., Imwong, M., Chau, N.H., Hoa, N.T., Thuy-Nhien, N.T., Thanh, N.V., Jittamala, P., *et al.* (2019), “Determinants of dihydroartemisinin-piperaquine treatment failure in *Plasmodium falciparum* malaria in Cambodia, Thailand, and Vietnam: a prospective clinical, pharmacological, and genetic study”, *The Lancet Infectious Diseases*, Elsevier, Vol. 19 No. 9, pp. 952–961.
- Poinar, G. (2005), “*Plasmodium dominicana* n. sp.(Plasmodiidae: Haemospororida) from Tertiary Dominican amber”, *Systematic Parasitology*, Springer, Vol. 61 No. 1, pp. 47–52.
- Preston, M.D., Campino, S., Assefa, S.A., Echeverry, D.F., Ocholla, H., Amambua-Ngwa, A., Stewart, L.B., *et al.* (2014), “A barcode of organellar genome polymorphisms identifies the geographic origin of *Plasmodium falciparum* strains”, *Nature Communications*, Nature Publishing Group, Vol. 5 No. 1, pp. 1–7.
- Proikas-Cezanne, T., Ruckerbauer, S., Stierhof, Y.-D., Berg, C. and Nordheim, A. (2007), “Human WIPI-1 puncta-formation: a novel assay to assess mammalian autophagy”, *FEBS Letters*, Elsevier, Vol. 581 No. 18, pp. 3396–3404.
- Project, M.P. *falciparum* C. (2016), “Genomic epidemiology of artemisinin resistant malaria”, *Elife*, eLife Sciences Publications Limited, Vol. 5, p. e08714.
- Proud, C.G. (2005), “eIF2 and the control of cell physiology”, *Seminars in Cell & Developmental Biology*, Vol. 16, Elsevier, pp. 3–12.
- Rieter, E., Vinke, F., Bakula, D., Cebollero, E., Ungermann, C., Proikas-Cezanne, T. and Reggiori, F. (2013), “Atg18 function in autophagy is regulated by specific sites within its β -propeller”, *Journal of Cell Science*, The Company of Biologists Ltd, Vol. 126 No. 2, pp. 593–604.
- Rigden, D.J., Michels, P. and Ginger, M.L. (2009), “Autophagy in protists: Examples of secondary loss, lineage-specific innovations, and the conundrum of remodeling a single mitochondrion”, *Autophagy*, Taylor & Francis, Vol. 5 No. 6, pp. 784–794.
- Ron, D. and Walter, P. (2007), “Signal integration in the endoplasmic reticulum unfolded protein response”, *Nature Reviews Molecular Cell Biology*, Nature Publishing Group, Vol. 8 No. 7, pp. 519–529.

- Roper, C., Pearce, R., Nair, S., Sharp, B., Nosten, F. and Anderson, T. (2004), “Intercontinental spread of pyrimethamine-resistant malaria”, *Science*, American Association for the Advancement of Science, Vol. 305 No. 5687, p. 1124.
- Rosenthal, M.R. and Ng, C.L. (2020), “Plasmodium falciparum artemisinin resistance: the effect of heme, protein damage, and parasite cell stress response”, *ACS Infectious Diseases*, ACS Publications, Vol. 6 No. 7, pp. 1599–1614.
- Rubinsztein, D.C., Mariño, G. and Kroemer, G. (2011), “Autophagy and aging”, *Cell*, Elsevier, Vol. 146 No. 5, pp. 682–695.
- Ryter, S.W., Cloonan, S.M. and Choi, A.M.K. (2013), “Autophagy: a critical regulator of cellular metabolism and homeostasis”, *Molecules and Cells*, Springer, Vol. 36 No. 1, pp. 7–16.
- Sakai, Y., Koller, A., Rangell, L.K., Keller, G.A. and Subramani, S. (1998), “Peroxisome degradation by microautophagy in *Pichia pastoris*: identification of specific steps and morphological intermediates”, *The Journal of Cell Biology*, The Rockefeller University Press, Vol. 141 No. 3, pp. 625–636.
- Saralamba, S., Pan-Ngum, W., Maude, R.J., Lee, S.J., Tarning, J., Lindegårdh, N., Chotivanich, K., *et al.* (2011), “Intrahost modeling of artemisinin resistance in *Plasmodium falciparum*”, *Proceedings of the National Academy of Sciences*, National Acad Sciences, Vol. 108 No. 1, pp. 397–402.
- Schröder, M. and Kaufman, R.J. (2005), “The mammalian unfolded protein response”, *Annu. Rev. Biochem.*, Annual Reviews, Vol. 74, pp. 739–789.
- Shibutani, S.T. and Yoshimori, T. (2014), “A current perspective of autophagosome biogenesis”, *Cell Research*, Nature Publishing Group, Vol. 24 No. 1, pp. 58–68.
- Siddiqui, F.A., Boonhok, R., Cabrera, M., Mbenda, H.G.N., Wang, M., Min, H., Liang, X., *et al.* (2020), “Role of *Plasmodium falciparum* Kelch 13 protein mutations in *P. falciparum* populations from northeastern Myanmar in mediating artemisinin resistance”, *MBio*, Am Soc Microbiol, Vol. 11 No. 1, pp. e01134-19.
- Siddiqui, F.A., Liang, X. and Cui, L. (2021), “*Plasmodium falciparum* resistance to ACTs: Emergence, mechanisms, and outlook”, *International Journal for Parasitology: Drugs and Drug Resistance*, Elsevier.
- Slomianny, C. (1990), “Three-dimensional reconstruction of the feeding process of the malaria parasite.”, *Blood Cells*, Vol. 16 No. 2–3, pp. 369–378.
- Smith, M. and Wilkinson, S. (2017), “ER homeostasis and autophagy”, *Essays in Biochemistry*, Portland Press Ltd., Vol. 61 No. 6, pp. 625–635.

- Song, S., Tan, J., Miao, Y. and Zhang, Q. (2018), “Crosstalk of ER stress-mediated autophagy and ER-phagy: Involvement of UPR and the core autophagy machinery”, *Journal of Cellular Physiology*, Wiley Online Library, Vol. 233 No. 5, pp. 3867–3874.
- Spielmann, T., Gras, S., Sabitzki, R. and Meissner, M. (2020), “Endocytosis in Plasmodium and Toxoplasma parasites”, *Trends in Parasitology*, Elsevier.
- Stogios, P.J., Downs, G.S., Jauhal, J.J.S., Nandra, S.K. and Privé, G.G. (2005), “Sequence and structural analysis of BTB domain proteins”, *Genome Biology*, Springer, Vol. 6 No. 10, pp. 1–18.
- Stokes, B.H., Dhingra, S.K., Rubiano, K., Mok, S., Straimer, J., Gnädig, N.F., Deni, I., *et al.* (2021), “Plasmodium falciparum K13 mutations in Africa and Asia impact artemisinin resistance and parasite fitness”, *Elife*, eLife Sciences Publications Limited, Vol. 10, p. e66277.
- Straimer, J., Gnädig, N.F., Stokes, B.H., Ehrenberger, M., Crane, A.A. and Fidock, D.A. (2017), “Plasmodium falciparum K13 mutations differentially impact ozonide susceptibility and parasite fitness in vitro”, *MBio*, Am Soc Microbiol, Vol. 8 No. 2, pp. e00172-17.
- Straimer, J., Gnädig, N.F., Witkowski, B., Amaratunga, C., Duru, V., Ramadani, A.P., Dacheux, M., *et al.* (2015), “K13-propeller mutations confer artemisinin resistance in Plasmodium falciparum clinical isolates”, *Science*, American Association for the Advancement of Science, Vol. 347 No. 6220, pp. 428–431.
- Sudhakar, A., Ramachandran, A., Ghosh, S., Hasnain, S.E., Kaufman, R.J. and Ramaiah, K.V.A. (2000), “Phosphorylation of serine 51 in initiation factor 2 α (eIF2 α) promotes complex formation between eIF2 α (P) and eIF2B and causes inhibition in the guanine nucleotide exchange activity of eIF2B”, *Biochemistry*, ACS Publications, Vol. 39 No. 42, pp. 12929–12938.
- Suresh, N. and Haldar, K. (2018), “Mechanisms of artemisinin resistance in Plasmodium falciparum malaria”, *Current Opinion in Pharmacology*, Elsevier, Vol. 42, pp. 46–54.
- Surolia, N. and Surolia, A. (2001), “Triclosan offers protection against blood stages of malaria by inhibiting enoyl-ACP reductase of Plasmodium falciparum”, *Nature Medicine*, Nature Publishing Group, Vol. 7 No. 2, pp. 167–173.
- Sutherland, C.J., Henrici, R.C. and Artavanis-Tsakonas, K. (2021), “Artemisinin susceptibility in the malaria parasite Plasmodium falciparum: propellers, adaptor proteins and the need for cellular healing”, *FEMS Microbiology Reviews*, Oxford University Press, Vol. 45 No. 3, p. fuaa056.

- Suzuki, K., Kubota, Y., Sekito, T. and Ohsumi, Y. (2007), “Hierarchy of Atg proteins in pre-autophagosomal structure organization”, *Genes to Cells*, Wiley Online Library, Vol. 12 No. 2, pp. 209–218.
- Tamura, N., Oku, M., Ito, M., Noda, N.N., Inagaki, F. and Sakai, Y. (2013), “Atg18 phosphoregulation controls organellar dynamics by modulating its phosphoinositide-binding activity”, *Journal of Cell Biology*, The Rockefeller University Press, Vol. 202 No. 4, pp. 685–698.
- Tanida, I., Ueno, T. and Kominami, E. (2008), “LC3 and Autophagy”, in Deretic, V. (Ed.), *Autophagosome and Phagosome*, Humana Press, Totowa, NJ, pp. 77–88.
- Tarning, J., Rijken, M.J., McGready, R., Physo, A.P., Hanpithakpong, W., Day, N.P.J., White, N.J., *et al.* (2012a), “Population pharmacokinetics of dihydroartemisinin and piperazine in pregnant and nonpregnant women with uncomplicated malaria”, *Antimicrobial Agents and Chemotherapy*, Am Soc Microbiol, Vol. 56 No. 4, pp. 1997–2007.
- Tarning, J., Rijken, M.J., McGready, R., Physo, A.P., Hanpithakpong, W., Day, N.P.J., White, N.J., *et al.* (2012b), “Population pharmacokinetics of dihydroartemisinin and piperazine in pregnant and nonpregnant women with uncomplicated malaria”, *Antimicrobial Agents and Chemotherapy*, Am Soc Microbiol, Vol. 56 No. 4, pp. 1997–2007.
- Tawk, L., Chicanne, G., Dubremetz, J.-F., Richard, V., Payrastre, B., Vial, H.J., Roy, C., *et al.* (2010), “Phosphatidylinositol 3-phosphate, an essential lipid in Plasmodium, localizes to the food vacuole membrane and the apicoplast”, *Eukaryotic Cell*, Am Soc Microbiol, Vol. 9 No. 10, pp. 1519–1530.
- Tilley, L., Straimer, J., Gnädig, N.F., Ralph, S.A. and Fidock, D.A. (2016), “Artemisinin action and resistance in Plasmodium falciparum”, *Trends in Parasitology*, Elsevier, Vol. 32 No. 9, pp. 682–696.
- Tomlins, A.M., Ben-Rached, F., Williams, R.A.M., Proto, W.R., Coppens, I., Ruch, U., Gilberger, T.W., *et al.* (2013), “Plasmodium falciparum ATG8 implicated in both autophagy and apicoplast formation”, *Autophagy*, Taylor & Francis, Vol. 9 No. 10, pp. 1540–1552.
- Tonkin, C.J., van Dooren, G.G., Spurck, T.P., Struck, N.S., Good, R.T., Handman, E., Cowman, A.F., *et al.* (2004), “Localization of organellar proteins in Plasmodium falciparum using a novel set of transfection vectors and a new immunofluorescence

- fixation method”, *Molecular and Biochemical Parasitology*, Elsevier, Vol. 137 No. 1, pp. 13–21.
- Torggler, R., Papinski, D. and Kraft, C. (2017), “Assays to monitor autophagy in *Saccharomyces cerevisiae*”, *Cells*, Multidisciplinary Digital Publishing Institute, Vol. 6 No. 3, p. 23.
- Trager, W. and Jensen, J.B. (1976), “Human malaria parasites in continuous culture”, *Science*, American Association for the Advancement of Science, Vol. 193 No. 4254, pp. 673–675.
- Travers, K.J., Patil, C.K., Wodicka, L., Lockhart, D.J., Weissman, J.S. and Walter, P. (2000), “Functional and genomic analyses reveal an essential coordination between the unfolded protein response and ER-associated degradation”, *Cell*, Elsevier, Vol. 101 No. 3, pp. 249–258.
- Tsukada, M. and Ohsumi, Y. (1993), “Isolation and characterization of autophagy-defective mutants of *Saccharomyces cerevisiae*”, *FEBS Letters*, Elsevier, Vol. 333 No. 1–2, pp. 169–174.
- Tsuyuki, S., Takabayashi, M., Kawazu, M., Kudo, K., Watanabe, A., Nagata, Y., Kusama, Y., *et al.* (2014), “Detection of WIPI1 mRNA as an indicator of autophagosome formation”, *Autophagy*, Taylor & Francis, Vol. 10 No. 3, pp. 497–513.
- Vaid, A., Ranjan, R., Smythe, W.A., Hoppe, H.C. and Sharma, P. (2010), “PfPI3K, a phosphatidylinositol-3 kinase from *Plasmodium falciparum*, is exported to the host erythrocyte and is involved in hemoglobin trafficking”, *Blood, The Journal of the American Society of Hematology*, American Society of Hematology Washington, DC, Vol. 115 No. 12, pp. 2500–2507.
- Vattem, K.M. and Wek, R.C. (2004), “Reinitiation involving upstream ORFs regulates ATF4 mRNA translation in mammalian cells”, *Proceedings of the National Academy of Sciences*, National Acad Sciences, Vol. 101 No. 31, pp. 11269–11274.
- Vaughan, A.M. and Kappe, S.H.I. (2017), “Malaria parasite liver infection and exoerythrocytic biology”, *Cold Spring Harbor Perspectives in Medicine*, Cold Spring Harbor Laboratory Press, Vol. 7 No. 6, p. a025486.
- Vembar, S.S. and Brodsky, J.L. (2008), “One step at a time: endoplasmic reticulum-associated degradation”, *Nature Reviews Molecular Cell Biology*, Nature Publishing Group, Vol. 9 No. 12, pp. 944–957.

- Venugopal, K., Hentzschel, F., Valkiūnas, G. and Marti, M. (2020), “Plasmodium asexual growth and sexual development in the haematopoietic niche of the host”, *Nature Reviews Microbiology*, Nature Publishing Group, Vol. 18 No. 3, pp. 177–189.
- Verdrager, J. (1986), “Epidemiology of emergence and spread of drug-resistant falciparum malaria in Southeast Asia.”, *The Southeast Asian Journal of Tropical Medicine and Public Health*, Vol. 17 No. 1, pp. 111–118.
- Vinayak, S., Alam, M.T., Mixson-Hayden, T., McCollum, A.M., Sem, R., Shah, N.K., Lim, P., *et al.* (2010), “Origin and evolution of sulfadoxine resistant Plasmodium falciparum”, *PLoS Pathogens*, Public Library of Science San Francisco, USA, Vol. 6 No. 3, p. e1000830.
- Vonlaufen, N., Kanzok, S.M., Wek, R.C. and Sullivan Jr, W.J. (2008), “Stress response pathways in protozoan parasites”, *Cellular Microbiology*, Wiley Online Library, Vol. 10 No. 12, pp. 2387–2399.
- Voss, C., Ehrenman, K., Mlambo, G., Mishra, S., Kumar, K.A., Sacci Jr, J.B., Sinnis, P., *et al.* (2016), “Overexpression of Plasmodium berghei ATG8 by liver forms leads to cumulative defects in organelle dynamics and to generation of noninfectious merozoites”, *MBio*, Am Soc Microbiol, Vol. 7 No. 3, pp. e00682-16.
- Walczak, M., Ganesan, S.M., Niles, J.C. and Yeh, E. (2018), “ATG8 is essential specifically for an autophagy-independent function in apicoplast biogenesis in blood-stage malaria parasites”, *MBio*, Am Soc Microbiol, Vol. 9 No. 1, pp. e02021-17.
- Walter, P. and Ron, D. (2011), “The unfolded protein response: from stress pathway to homeostatic regulation”, *Science*, American Association for the Advancement of Science, Vol. 334 No. 6059, pp. 1081–1086.
- Wang, J., Xu, C., Wong, Y.K., Li, Y., Liao, F., Jiang, T. and Tu, Y. (2019), “Artemisinin, the magic drug discovered from traditional Chinese medicine”, *Engineering*, Elsevier, Vol. 5 No. 1, pp. 32–39.
- Wang, J., Zhang, C.-J., Chia, W.N., Loh, C.C.Y., Li, Z., Lee, Y.M., He, Y., *et al.* (2015), “Haem-activated promiscuous targeting of artemisinin in Plasmodium falciparum”, *Nature Communications*, Nature Publishing Group, Vol. 6 No. 1, pp. 1–11.
- Wang, Z., Cabrera, M., Yang, J., Yuan, L., Gupta, B., Liang, X., Kemirembe, K., *et al.* (2016), “Genome-wide association analysis identifies genetic loci associated with resistance to multiple antimalarials in Plasmodium falciparum from China-Myanmar border”, *Scientific Reports*, Nature Publishing Group, Vol. 6 No. 1, pp. 1–12.

- Ward, P., Equinet, L., Packer, J. and Doerig, C. (2004), “Protein kinases of the human malaria parasite *Plasmodium falciparum*: the kinome of a divergent eukaryote”, *BMC Genomics*, BioMed Central, Vol. 5 No. 1, pp. 1–19.
- Wek, R.C., Jiang, H.-Y. and Anthony, T.G. (2006), “Coping with stress: eIF2 kinases and translational control”, *Biochemical Society Transactions*, Portland Press Ltd., Vol. 34 No. 1, pp. 7–11.
- Wek, S.A., Zhu, S. and Wek, R.C. (1995), “The histidyl-tRNA synthetase-related sequence in the eIF-2 alpha protein kinase GCN2 interacts with tRNA and is required for activation in response to starvation for different amino acids”, *Molecular and Cellular Biology*, Am Soc Microbiol, Vol. 15 No. 8, pp. 4497–4506.
- White, N.J., Pukrittayakamee, S., Hien, T.T., Faiz, M.A., Mokuolu, O.A. and Dondorp, A.M. (2014), “Malaria”, *The Lancet*, Elsevier, Vol. 383 No. 9918, pp. 723–735.
- Wilson, R.J.M.I. (2005), “Parasite plastids: approaching the endgame”, *Biological Reviews*, Cambridge University Press, Vol. 80 No. 1, pp. 129–153.
- Witkowski, B., Amaratunga, C., Khim, N., Sreng, S., Chim, P., Kim, S., Lim, P., *et al.* (2013), “Novel phenotypic assays for the detection of artemisinin-resistant *Plasmodium falciparum* malaria in Cambodia: in-vitro and ex-vivo drug-response studies”, *The Lancet Infectious Diseases*, Elsevier, Vol. 13 No. 12, pp. 1043–1049.
- Wu, H., Ng, B.S.H. and Thibault, G. (2014), “Endoplasmic reticulum stress response in yeast and humans”, *Bioscience Reports*, Portland Press Ltd., Vol. 34 No. 4, p. e00118.
- Wu, J., Rutkowski, D.T., Dubois, M., Swathirajan, J., Saunders, T., Wang, J., Song, B., *et al.* (2007), “ATF6 α optimizes long-term endoplasmic reticulum function to protect cells from chronic stress”, *Developmental Cell*, Elsevier, Vol. 13 No. 3, pp. 351–364.
- Xie, S.C., Ralph, S.A. and Tilley, L. (2020), “K13, the cytosome, and artemisinin resistance”, *Trends in Parasitology*, Elsevier.
- Yamamoto, K., Sato, T., Matsui, T., Sato, M., Okada, T., Yoshida, H., Harada, A., *et al.* (2007), “Transcriptional induction of mammalian ER quality control proteins is mediated by single or combined action of ATF6 α and XBP1”, *Developmental Cell*, Elsevier, Vol. 13 No. 3, pp. 365–376.
- Yang, T., Yeoh, L.M., Tutor, M. V, Dixon, M.W., McMillan, P.J., Xie, S.C., Bridgford, J.L., *et al.* (2019), “Decreased K13 abundance reduces hemoglobin catabolism and proteotoxic stress, underpinning artemisinin resistance”, *Cell Reports*, Elsevier, Vol. 29 No. 9, pp. 2917–2928.

- Yang, Y., Hu, L., Zheng, H., Mao, C., Hu, W., Xiong, K., Wang, F., *et al.* (2013), “Application and interpretation of current autophagy inhibitors and activators”, *Acta Pharmacologica Sinica*, Nature Publishing Group, Vol. 34 No. 5, pp. 625–635.
- Yeh, Y.-Y., Shah, K.H. and Herman, P.K. (2011), “An Atg13 protein-mediated self-association of the Atg1 protein kinase is important for the induction of autophagy”, *Journal of Biological Chemistry*, ASBMB, Vol. 286 No. 33, pp. 28931–28939.
- Yeh, Y.-Y., Wrasman, K. and Herman, P.K. (2010), “Autophosphorylation within the Atg1 activation loop is required for both kinase activity and the induction of autophagy in *Saccharomyces cerevisiae*”, *Genetics*, Oxford University Press, Vol. 185 No. 3, pp. 871–882.
- Yin, Z., Pascual, C. and Klionsky, D.J. (2016), “Autophagy: machinery and regulation”, *Microbial Cell*, Shared Science Publishers, Vol. 3 No. 12, p. 588.
- Yorimitsu, T. and Klionsky, D.J. (2005), “Autophagy: molecular machinery for self-eating”, *Cell Death & Differentiation*, Nature Publishing Group, Vol. 12 No. 2, pp. 1542–1552.
- Yorimitsu, T., Nair, U., Yang, Z. and Klionsky, D.J. (2006), “Endoplasmic reticulum stress triggers autophagy”, *Journal of Biological Chemistry*, ASBMB, Vol. 281 No. 40, pp. 30299–30304.
- Yoshida, H., Matsui, T., Yamamoto, A., Okada, T. and Mori, K. (2001), “XBP1 mRNA is induced by ATF6 and spliced by IRE1 in response to ER stress to produce a highly active transcription factor”, *Cell*, Elsevier, Vol. 107 No. 7, pp. 881–891.
- Yuan, W., Tuttle, D.L., Shi, Y.-J., Ralph, G.S. and Dunn, W.A. (1997), “Glucose-induced microautophagy in *Pichia pastoris* requires the alpha-subunit of phosphofructokinase”, *Journal of Cell Science*, Company of Biologists The Company of Biologists, Bidder Building, 140 Cowley ..., Vol. 110 No. 16, pp. 1935–1945.
- Zhang, M., Fennell, C., Ranford-Cartwright, L., Sakthivel, R., Gueirard, P., Meister, S., Caspi, A., *et al.* (2010), “The Plasmodium eukaryotic initiation factor-2 α kinase IK2 controls the latency of sporozoites in the mosquito salivary glands”, *Journal of Experimental Medicine*, The Rockefeller University Press, Vol. 207 No. 7, pp. 1465–1474.
- Zhang, M., Gallego-Delgado, J., Fernandez-Arias, C., Waters, N.C., Rodriguez, A., Tsuji, M., Wek, R.C., *et al.* (2017), “Inhibiting the Plasmodium eIF2 α kinase PK4 prevents artemisinin-induced latency”, *Cell Host & Microbe*, Elsevier, Vol. 22 No. 6, pp. 766–776.

Zhang, M., Mishra, S., Sakthivel, R., Rojas, M., Ranjan, R., Sullivan, W.J., Fontoura, B.M.A., *et al.* (2012), “PK4, a eukaryotic initiation factor 2 α (eIF2 α) kinase, is essential for the development of the erythrocytic cycle of Plasmodium”, *Proceedings of the National Academy of Sciences*, National Acad Sciences, Vol. 109 No. 10, pp. 3956–3961.